AN INVESTIGATION OF
SOLVATED ELECTRONS IN HEXAMETHYLPHOSPHORAMIDE

BY

GARRY JOHN FLYNN
B.Sc., University of British Columbia, 1969

A THESIS SUBMITTED IN PARTIAL FULFILMENT OF
THE REQUIREMENTS FOR THE DEGREE OF
DOCTOR OF PHILOSOPHY

in the Department
of
CHEMISTRY

We accept this thesis as conforming to the
required standard

THE UNIVERSITY OF BRITISH COLUMBIA
February, 1975

In presenting this thesis in partial fulfilment of the requirements for an advanced degree at the University of British Columbia, I agree that the Library shall make it freely available for reference and study. I further agree that permission for extensive copying of this thesis for scholarly purposes may be granted by the Head of my Department or by his representatives. It is understood that copying or publication of this thesis for financial gain shall not be allowed without my written permission.

Department of CHEMISTRY

The University of British Columbia
Vancouver 8, Canada

Date Feb. 13, 1975

ABSTRACT

This thesis is concerned with a detailed investigation of the nature, yield, stability, and reactivity of solvated electrons in hexamethylphosphoramide (HMPA). Evidence is presented for their formation by radiolysis and for their comparatively long-lived existence in this highly polar aprotic solvent in which ordinary anions are particularly weakly solvated. By means of microsecond pulse radiolysis methods it was shown that the solvated electron in HMPA has a intense broad structureless absorption band with a band maximum at 2200 $\pm$ 100 nm, a band half-width of 3600 cm^{-1} and maximum molar absorptivity of (3.2 $\pm$ 0.5) X 10^4 M^{-1} cm^{-1}. The spectrum is similar to that found in solutions of sodium metal dissolved in HMPA.

Radiolysis studies provided a value of 2.2 $\pm$ 0.2 for the free-ion yield of solvated electrons. This was established by both pulse and steady-state methods and is approximately what one would expect on the basis of the liquid's dielectric constant when compared with other solvents. An interesting deduction from the steady-state γ-radiolysis results was that N_2O does not scavenge electrons on a one-to-one basis in this solvent; but rather produced more than one N_2 molecule per electron scavenged. The yields of N_2 from N_2O scavenging of electrons in HMPA/water mixtures are also reported for the full composition range. Electron decays were studied spectrophotometrically and its rate of reaction with N_2O, pyrene,

anthracene and other additives are reported in the thesis. When stable solutions of solvated electrons in HMPA (alkali metal solutions) were themselves irradiated, a net decrease in electron concentration occurred, indicating that e^-_{HMPA} reacts not only with its concomitant positive ion but also with other radiolysis products.

Pure HMPA produces hydrogen and methane when irradiated, with yields of 3.3 $\pm$ 0.3 and 0.29 $\pm$ 0.03 respectively. The H_2 yield was shown to comprise a non-scavengable molecular process (whose yield is 1.4 $\pm$ 0.1) and a scavengable part (yield 1.9 $\pm$ 0.2) that clearly involved solvated electrons.

TABLE OF CONTENTS

LIST OF TABLES

LIST OF FIGURES

ACKNOWLEDGEMENTS

The author would like to express his gratitude to Dr. D. C. Walker for his invaluable guidance and continued encouragement throughout the course of this study.

Sincere appreciation is extended to Dr. L. M. Dorfman and his group at The Ohio State University, Columbus, Ohio. Their co-operation in the use of the pulse radiolysis facilities at that institution greatly enhanced this work. Special thanks are due to Dr. E. A. Shaede for his expert operation of the linear accelerator, many invaluable discussions, and innumerable long hours of additional work. The author is indebted to Dr. F. Y. Jou for obtaining absorption data pertaining to HMPA/EDA mixtures.

Gratitude for financial support of this work is expressed to the National Research Council of Canada for postgraduate scholarships and to the U. S. Atomic Energy Commission (at The Ohio State University).

To dear Jennifer

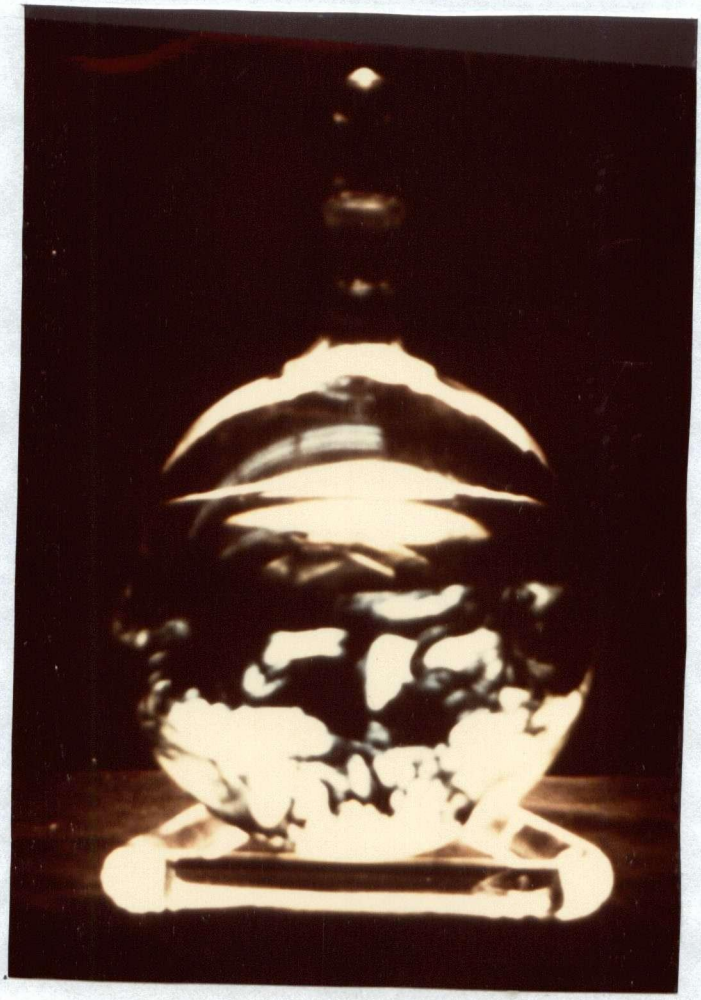

e^-_{HMPA}

CHAPTER I

INTRODUCTION

A. HEXAMETHYLPHOSPHORAMIDE

Hexamethylphosphoramide (HMPA), $[(CH_3)_2N]_3PO$, is a most remarkable polar aprotic solvent! It is a liquid at room temperature of moderately high dielectric constant (30 at 20°C), has a large dipole moment (5.3D at 20°C), and is completely miscible with both polar and -- with the exception of saturated hydrocarbons -- non-polar liquids. This solvent derives a number of extraordinary properties from its peculiar structure and charge distribution.

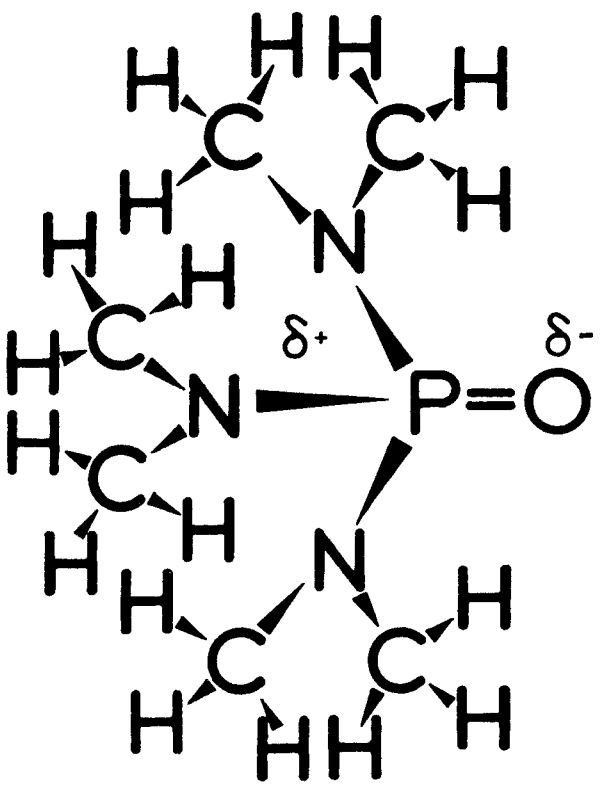

Figure I-1. Hexamethylphosphoramide.

As shown in Figure I-1, the HMPA molecule has a general pyramidal shape. The phosphoryl group is considered to be about 50% ionic which accounts for the molecule's large dipole moment. In addition, the resulting high electron density localized at the oxygen atom imparts to the molecule an unusually high basicity. The positive end of the dipole, on the other hand, is symmetrically dispersed over the phosphorus and three nitrogen atoms and is thereby sterically screened from the surroundings by six methyl groups. In terms of its dielectric arrangement then, the HMPA molecule is a sort of "mushroom" shaped dipole having a well defined negative "stock" but an extremely diffuse positive "head". As a result, HMPA solvates positive ions extremely strongly but negative ions only very weakly. This, combined with its basicity, renders dissolved anions exceptionally reactive. For example, fluoride and chloride ions are especially strong bases in HMPA. Some reactions that are known to involve the formation of intermediate anions (carbanions for instance) are greatly accelerated in this solvent.

Equally remarkable is the innate stability exhibited by HMPA towards many types of highly reactive species. Probably because of the steric screening of its positive region, HMPA is essentially inert with respect to nucleophilic attack. All its hydrogen atoms are β to the polar group and rather unreactive. The solvent does not undergo hydrolysis in the presence of alkaline media, and only those reagents

which can attack the exposed negative region of the molecule, i.e., the oxygen atom, react to any great extent with HMPA. Thus both Brönsted and Lewis acids act vigorously on HMPA. While such reactions ultimately lead to the replacement of one or more dimethylamino groups by the anion (A^- from say, reagent H^+A^-), it is likely that the initial attack occurs at the oxygen. Subsequent heating of the resultant complex no doubt gives rise to the observed substitution product -- probably via reaction (1.1).

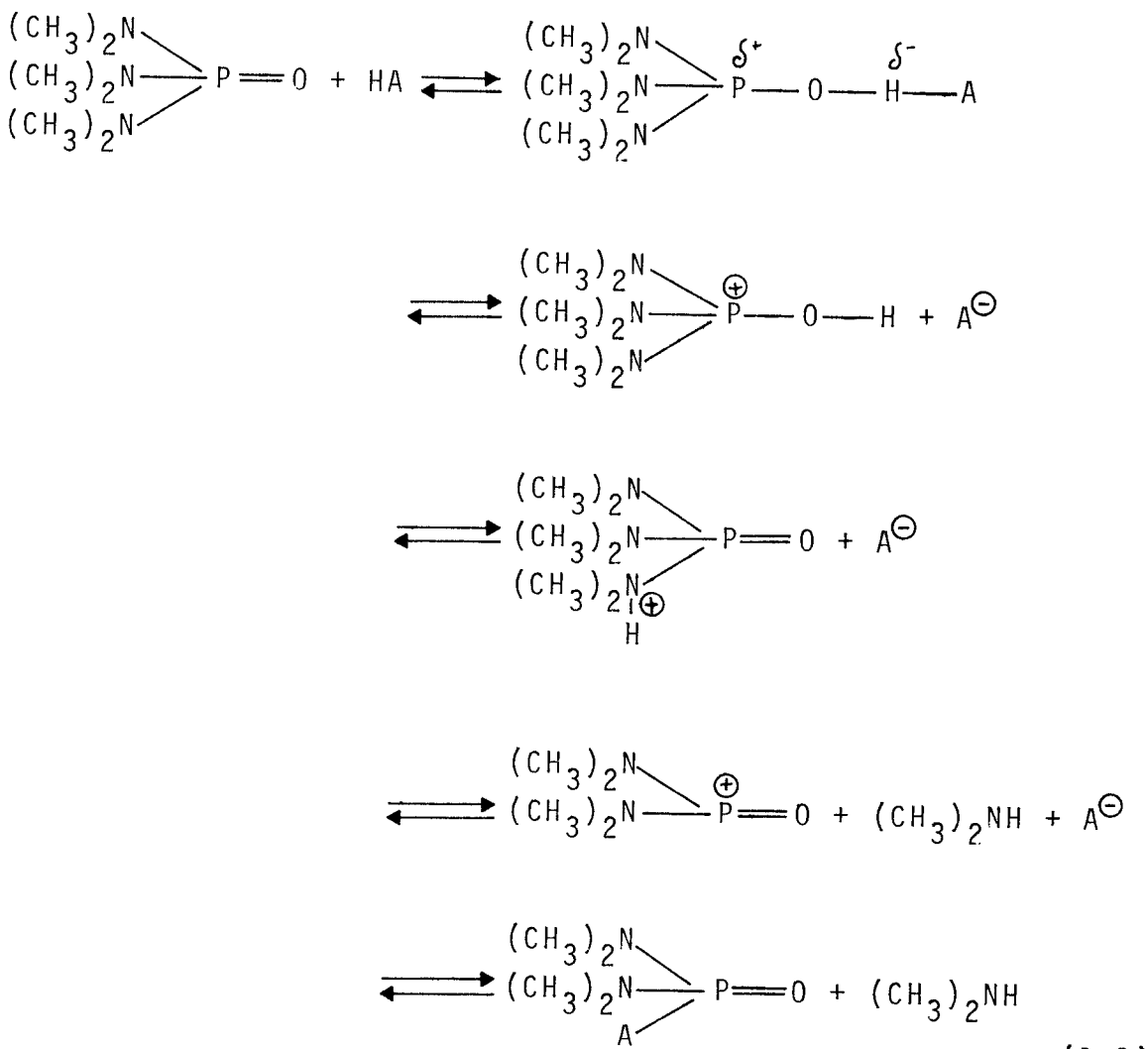

(1.1)

Normant[1] in a comprehensive review of the physical and chemical properties of HMPA, concluded that from all points of view it is the best polar aprotic solvent.

An undergraduate student, J. P. Matanovich[2] noticed that alkali metals dissolved in HMPA to yield stable blue reducing solutions. Such solutions have subsequently been shown to contain electrons in solution. This thesis explores the possible occurrence of radiation produced solvated electrons in HMPA.

B. ALKALI METAL SOLUTIONS

1. Liquid Ammonia

More than a century ago, in 1864, Weyl[3] reported the preparation of intensely coloured solutions from the dissolution of sodium or potassium in liquid ammonia. He found that by boiling away the ammonia he could recover the pure metals, so the intense colour was attributed to ordinary chemical compounds such as $NaH_3 \cdot N$. Some thirty years later, an undergraduate student named H. P. Cady found that the electrical conductivity of the metal-ammonia solutions was higher than that found for solutions of simple salts in ammonia. It was Kraus[4] however who was first to realize the true significance of this result. He meticulously studied the "metal ammoniums" over a period of more than twenty-five years and showed conclusively that dilute solutions consisted principally of ammoniated metal ions and

and ammoniated electrons (1.2).

$$M_{am} \overset{NH_3}{\rightleftharpoons} M^+_{am} + e^-_{am} \qquad (1.2)$$

Ogg[5] described the ammoniated electron as an electron trapped in a solvent cavity formed as a result of the surrounding solvent dipoles having all their protons directed inward. The resulting net positive charge at the cavity center acts to stabilize the electron. Solvation of the metal cation occurs similarily, but in that case the solvent dipoles are reversed -- the nitrogen atoms being directed to the cavity center. There is probably little tendency for a simple NH_3^- anion to be formed. One can easily envisage electron capture by aromatic molecules because they have low-lying unfilled molecular π orbitals available with which to stabilize the excess electron. For the NH_3^- anion, however, the excess electron must occupy an antibonding orbital -- an energetically unfavorable arrangement.

Now, the close orientation of several ammonia molecules in the solvent cage, each having the positive end of its dipole directed inward, would lead to mutual repulsions. Such forces would result in the expansion of the cavity which should be accompanied by a decrease in the density of the solution. In point of fact, a saturated solution of lithium in liquid ammonia has a density of only 0.477 gm/cm^3 at room temperature[6] and is the least dense liquid known at that temperature. Since lithium and ammonia have densities of 0.534 gm/cm^3 at 20°C and 0.68 gm/cm^3 at -30°C respectively, cavity expansion appears evident

in metal-ammonium solutions. Lipscomb[7] made calculations which showed the electron cavity in liquid ammonia being about 3.2 Å in radius or roughly three times the volume of ammonia molecules themselves. If one assumes cubic-close-packing of solvent molecules however, this vacancy corresponds to the complete removal of only a single NH_3 molecule. In this regard then, the solvated electron in ammonia resembles an electron trapped in a crystal defect (i.e. an F centre).

Kraus[8] has shown that the mobility of the ammoniated electron is about eight times that of a sodium ion. This observed mobility is much smaller than would be expected for a free electron, but is sufficiently high to require an electron-jump mechanism rather than migration of the entire cavity. In a more recent conductivity study, Arnold and Patterson[9] have shown that electron mobility is concentration dependent and may partly involve an electron tunnelling mechanism. Indeed, the uncertainty principle requires that the electron not be localized in the trap but move freely in the region of the cavity. Calculations[10] indicate that the electron in fact spends much of its time outside the cavity.

Regardless of the alkali metal dissolved, the ammonia solutions exhibit a broad asymmetric absorption in the infra-red. This band, associated with the ammoniated electron, has a maximum at 1500 nm and a width at half-height of about 650 nm. The question arises as to whether the band results from transition between bound electronic levels, or simply a transition from the trap to a conduction band. Stairs[12] refined the calculations of

Lipscomb and concluded that only a single bound state existed. Attempts to detect photoconductivity from these solutions were unsuccessful.[13] To date, many attempts have been made to describe these systems. Perhaps the most successful theoretical description of the optical properties of alkali metal/ammonia solutions is that formulated by Copeland, Kestner, and Jortner.[14] Kestner[15] extended the calculations to predict the location of the first excited state of the ammoniated electron. The overall consensus of opinion is reflected in a recent publication on the subject;[16] that the absorption band associated with the ammoniated electron arises from a single ($2p \leftarrow 1s$) electronic transition between bound states. A study of the photoelectron emission spectrum from solvated electrons in ammonia by Delahey et al.[17] adds practical support to this conjecture. Their observations were consistent with a bound-bound electronic transition (similar to the β band for F centres) followed by auto-ionization.

In dilute metal/ammonia solutions, the ions interact only very weakly with the result that their behavior resembles species in the gas phase. More concentrated solutions take on a bronze-like luster, become even less dense, and in some cases separate into two liquid phases.[10] Pohler and Thompson,[18] by simply treating the concentration solutions as liquid metals, were able to quite accurately predict their electrical conductivity. In fact, solutions containing more than 9 mol % metal have since been shown to behave in most respects as liquid metals.[19] Clearly then, additional species are present at the higher concentrations.

It is known that the total spin paramagnetism of the solutions decreases markedly with increasing metal concentration.[20] Hustler[21] proposed an equilibrium between ionic species and diamagnetic metal atom dimers (1.3).

$$2M^{+}_{am} + 2e^{-}_{am} \rightleftharpoons M_{2\ am} \qquad (1.3)$$

Jolly and co-workers[11] were first to attempt to distinguish spectroscopically e^{-}_{am}, M^{+}_{am}, M_{am} and $M_{2\ am}$ species or evaluate the equilibrium constants:

$$K_{1.2} = \frac{\left[M^{+}_{am}\right]\left[e^{-}_{am}\right]}{\left[M_{am}\right]} \qquad (i)$$

$$K_{1.3} = \frac{\left[M_{2\ am}\right]}{\left[M^{+}_{am}\right]^{2}\left[e^{-}_{am}\right]^{2}} \qquad (ii)$$

Unfortunately, they were only able to suggest that the deviation from Beer's Law at 2100 nm exhibited by solutions containing greater than 0.05 M metal in ammonia arose from dimer or polymer formation. Becker, Lindquist and Alder[22] proposed a monomeric species M_{am}, or $(M^{+}_{am} \cdot e^{-}_{am})$ consisting of an alkali metal cation surrounded by approximately six oriented ammonia molecules with an electron circulating around the ion on the protons. The discovery of nuclear hyperfine splitting by the metal from EPR studies of the solutions[23] has demonstrated unequivocally the presence of a monomeric metal species. However, that work showed

that the species was not responsible for the visible absorption band and that its most likely structure was that proposed by Becker et al.

Arnold and Patterson[24] studied the proposed models carefully and found serious discrepancies between the theories and experiment -- particularly for some electrical and magnetic properties of the solutions. It became apparent that at least two different species containing paired electrons were required. They proposed the addition of an M'_{am} centre in addition to the neutral $M_{2\ am}$ centre: an M'_{am} centre being an electron trapped in the field of the monomeric M_{am} species as depicted by reaction (1.4).

$$M_{am} + e^-_{am} \rightleftharpoons M'_{am} \text{ (or } M^-_{am}) \qquad (1.4)$$

Finally, Golden, Guttman and Tuttle[25] assembled all the known data and were able to quantitatively account for the properties of metal ammonium solutions in terms of the following equilibria:

$$M_{am} \rightleftharpoons M^+_{am} + e^-_{am} \qquad (1.2)$$

$$M^+_{am} + 2e^- \rightleftharpoons M^-_{am} \qquad (1.5)$$

$$M^+_{am} + M^-_{am} \rightleftharpoons M_{2\ am} \qquad (1.6)$$

2. Amines & Ethers

Possibly for historical reasons, the major portion of the work with alkali metal solutions has been conducted with liquid ammonia. The solvated electron is an extremely reactive species and seems to react with many solvents and their trace impurities. However, a number of amines and ethers have been proven capable of forming stable solutions of the active metals.[26] The pre-requisites for solvent suitability appear to include an inherent permanent dipole and a resistance to reduction. Most of the compounds are in fact "better" solvents for alkali metals than is liquid ammonia in so far as ease of handling and solution stability is concerned. These advantages have had their price however as the amine systems have proven to be the more complicated. In the amines, even in the dilute solution, the alkali metal appears to play a more active role than simply being the counter-ion to the solvated electron. In contrast to the alkali metal/ammonia systems in which only a single broad asborption is observed, when amines are used as a solvent the solutions generally exhibited at least three distinct absorption bands[27] -- called the IR, R, and V bands. The IR band in the infra-red near 1300 nm was nearly independent of the metal used both in shape and position. That band was attributed to the solvated electron. The R band occurred at higher energy but the position of the maximum was dependent upon the metal dissolved. The V band, found around 660 nm, was not dependent upon the alkali metal used. This discovery of a second stable species apparently involving

only electrons and/or solvent molecules stimulated a great deal of research. A number of species were proposed to account for the V band, among them the dielectron;[28] e_2^{2-}. However, there was a disconcerting lack of agreement among various groups pertaining to the relative intensity of the absorption.[29] Then, Hurley, Tuttle and Golden[27] offered a very rational explanation. They proposed that the absorption was simply the R band of sodium in the solution. That is, in amine solutions containing alkali metals other than sodium, the sodium R band appeared as a result of sodium ions being leached from pyrex vessels. They went on to demonstrate that potassium/ethylamine solutions prepared and contained solely in quartz apparatus did not exhibit the 660 nm band. However, the addition of sodium salts or contact with pyrex glassware resulted in the immediate formation of the V band, confirming their suspicions.

The position of the R band maximum in amine solution was dependent upon the alkali metal dissolved. The species responsible then, call it Xm, was clearly a "metallic" species and was probably analogous to one of the species (M_s^+, M_s, M_s^-, or $M_{2\ s}$) postulated for the alkali metal/liq. ammonia system. Now, there was evidence that the species were diamagnetic[23] which rules out the atomic species M_s. The relative intensity of the R band with respect to the IR (e_s^-) band tended to decrease upon dilution. This, along with the fact that photolysis of the R band yielded an increase in the IR band indicates a metallic species having "excess" electrons which was probably in equilibrium with solvated electrons and some other metallic ion. These facts taken together

tend to eliminate the possibility of Xm being the positive ion, M_s^+.

DeBecker and Dye[30] managed to measure the oscillator strength of the V band transition (i.e. the R band of sodium). They found that cesium solutions in ethylenediamine showed only the IR (e_s^-) band. The addition of excess sodium ions removed the IR band completely, replacing it with the V band. By using intermediate concentrations of sodium salts, they obtained both spectra and calculated a value for the V band extinction coefficient of 8.2×10^4 M^{-1} cm^{-1} assuming one sodium ion per absorbing species. This value enabled integration of the V band spectra and calculation of the oscillator strength for the transition -- a value $f = 1.9 \pm 0.2$ being obtained. Notice that if the species contained two sodium nuclei this value would have been doubled. An oscillator strength of 2 required that at least two equivalent electrons be involved in the transition. These calculations indicate rather convincingly that the species (Xm) responsible for the R bands of sodium in amine solution is the metal anion, Na_s^-. Dye also showed from fast kinetic studies of the reaction between Na^+ and e_s^- in ethylenediamine that both the decay of the electron and the growth of the R band were second order in e_s^-, consistent with the other calculations.

Actually, Mantalon, Golden and Ottolenghi[31] had earlier concluded (although from much less conclusive work) that metal anions were responsible for the R bands. They had noticed that the Xm species was easily photolyzed and that the R band spectra

itself exhibited a marked blue shift when the solutions were cooled. Since these properties are characteristic of charge-transfer-to-solvent (CTTS) spectra, Mantalon et al. decided to examine the amine spectra in this light.

In CTTS spectra the solvent plays an integral part in determining the transition energy. Generally, visible and ultraviolet absorptions of molecules involve electronic excitations from ground to excited molecular states -- i.e. intramolecular transitions. The excited electron remains bound to the molecule and its absorption spectra often details the vibrational properties of the molecule. CTTS spectra on the other hand arise from the transfer of an electron from some solute species, X, to a molecule of its solvation shell, S (1.7).

$$X^{-} \cdot S \longrightarrow X \cdot S^{-} \qquad (1.7)$$

The ground state species is regenerated by thermal degradation of the excited state. Because the electron is only weakly bound to the solute, CTTS species readily undergo autoionization. The halide ions in water are typical examples. CTTS spectra are smooth and structureless, usually occurring in the ultraviolet. They usually obey Beer's Law. Because of the direct involvement of solvent structure in the transitions, the absorption maximum, λ_{max}, is very sensitive to changes in solvent temperature, pressure, and composition.

With these considerations in mind then, Mantalon, Golden and Ottolenghi[31] carefully studied solutions of sodium metal

in ethylamine/ammonia. They concluded that the species Xm was the metal anion (Na^- in that case) and that it produced a typical CTTS spectrum.

As was the case with metal/ammonia solutions, extensive spectroscopic[32] and electron spin studies[33,34,35] of metal/amine solutions led to the discrimination of at least six distinct species.

That is, in general solutions of alkali metals involve the stability, interaction and reactivity of the following solvated species:

S, solvent molecules

M_s, neutral metal monomers or atoms

M_s^+, metal cations

e_s^-, electrons

M_s^-, metal anions

$M_{2\ s}$, neutral metal dimers

Of these species, the solvated electron is particularly interesting and important.

3. Water - The Hydrated Electron

The addition of alkali metals to pure water leads not to the formation of stable solutions but instead to rather violent reaction. Classically, the process has been described in terms

of the formation of hydrogen atoms (1.8) which combine to produce molecular hydrogen (1.9).

$$M + H_2O \longrightarrow M^+ + OH^- + H \qquad (1.8)$$

$$H + H \longrightarrow H_2 \qquad (1.9)$$

As the solvated electron became more and more established as a species of major importance in metal solutions of ammonia and the amines, people began to suspect that it might also play a role in the aqueous system. That is, hydrated electrons might be formed initially (1.10) which then go on to produce hydrogen (1.11).

$$M + H_2O \longrightarrow M^+_{aq} + e^-_{aq} \qquad (1.10)$$

$$e^-_{aq} \xrightarrow{H_2O} \longrightarrow \tfrac{1}{2}H_2 + OH^- \qquad (1.11)$$

Shaede and Walker[36] attempted to interrupt such a process by reacting sodium with water containing scavenger solutes that could distinguish between hydrated electrons and hydrogen atoms as intermediates. Initial experiments with sodium mirrors and water showed that the presence of 0.02 moles/litre scavenger had little effect upon hydrogen formation. Thus, either the process was too fast to be interrupted, or else didn't involve the intermediates proposed. They subsequently "diluted" the

sodium by making an amalgam with an excess of mercury. Dilution made it possible to extend the reaction time from less than a second to several hours. Shaede and Walker were then able to scavenge the hydrogen precursor. Even in the presence of an excess of methanol which is known to efficiently scavenge hydrogen atoms (1.12), hydrogen formation could be prevented.

$$H + CH_3OH \xrightarrow{k_{1.12}} CH_2OH + H_2 \qquad (1.12)$$

where $k_{1.12} = 2 \times 10^6\ M^{-1}\ sec^{-1}$ [37]

However, at low pH where hydrated electrons would quickly be converted by protons to hydrogen atoms (1.13), hydrogen production was unaffected by the presence of additional solutes.

$$e^-_{aq} + H^+ \longrightarrow H \qquad (1.13)$$

That study proved conclusively that hydrogen atoms are <u>not</u> produced during the sodium amalgam/water reaction and strongly indicated that the hydrated electron is the reactive intermediate. Similar investigations,[38] in which reaction rate ratio studies were conducted, corroborated that conclusion. As can be seen, solvated electrons were becoming a species of increasing chemical importance.

C. RADIATION CHEMISTRY AND SOLVATED ELECTRONS

When matter is subjected to radiation of sufficiently high energy, some of its molecules are ionized and electrons ejected. In a liquid, the excess energy of such electrons is quickly lost to the surrounding solvent molecules. However, before it is thermalized (reduced to thermal energy, kT) an electron may have travelled quite some distance from the ionized molecule (now a positive ion). Therefore, the distinct possibility exists that such an electron might become solvated and thus stabilized in the medium rather than returning to its parent ion and being immediately neutralized. After all, aside from its tendency for neutralization, the thermal electron should not appear to the solvent to be very different to an electron from a dissolved sodium atom. Therefore, in solvents where the species are already known to be stable one might well expect to find a radiation produced solvated electron. The implications of such a species on the reactions associated with an irradiated medium (i.e. its radiation chemistry) may be enormous. In addition, such phenomena might facilitate detailed studies of the species itself.

Without doubt, studies of water or aqueous systems have dominated the field of radiation chemistry. This is not suprising when one considers that water is the most common solvent; can easily be highly purified; and makes up the bulk of biological systems.

Prior to 1950, radiation chemical studies of aqueous systems

were apparently well explained in terms of the production and reactions of hydrogen atoms, H, and hydroxyl radicals, OH. The formation of these reducing and oxidizing species following irradiation was proposed by Weiss[39] to occur via the following mechanism:

$$H_2O \xrightarrow{\text{radiation}} H_2O^+ + e^- \qquad (1.14)$$

$$H_2O^+ + H_2O \longrightarrow H_3O^+ + OH \qquad (1.15)$$

$$e^- + H_2O \longrightarrow OH^- + H \qquad (1.16)$$

where e^- and H_2O^+ were extremely short lived species ($\tau < 10^{-11}$ sec). Over the next decade, it became increasingly apparent that more than one reducing species is produced during the radiolysis of water. In 1952, Stein[40] found that CO_2 inhibited the bleaching (reduction) of aqueous methylene blue during irradiation, yet CO_2 is unreactive towards hydrogen atoms. Platzman had been making theoretical calculations on water based on knowledge of the ammoniated electron in alkali metal solutions. At a conference in 1953[41] he made the rather profound remark: "I think irradiated water turns blue and we just don't see it". His postulation was that a short-lived solvated electron absorbing in the red region of the spectrum should exist in irradiated water. The great reduction in hydrogen yield from irradiated acidified aqueous methanol solutions observed in the

presence of ferric ion by Baxendale and Hughes[42] in 1958 could not be satisfactorily explained in terms of a competition for hydrogen atoms, (1.12) and (1.17).

$$H + CH_3OH \longrightarrow \dot{C}H_2OH + H_2 \qquad (1.12)$$

$$H + Fe^{3+} \longrightarrow Fe^{2+} + H^+ \qquad (1.17)$$

Reaction (1.17) would not be expected to be able to compete with reaction (1.12). But, if a hydrated electron were the precursor of H in acid solution (1.13), then ferric ions might well be efficiently reduced by such a species (1.18).

$$e^-_{aq} + H^+ \longrightarrow H \qquad (1.13)$$

$$e^-_{aq} + Fe^{3+} \longrightarrow Fe^{2+} \qquad (1.18)$$

The following year, Hayon and Weiss[43] confirmed the suspicions by chemically distinguishing two reducing species. They did so by studying a system in which the two reducing species reacted to give different observable products. Aqueous solutions of monochloroacetic acid yielded hydrogen as the predominant product in acid solution but at pH > 4, chloride ion formation was favoured. These results are consistent with the following mechanism.

$$H_2O \xrightarrow{\sim\sim\sim} e^-_{aq} + \text{other products} \qquad (1.19)$$

$$e^-_{aq} + H^+ \longrightarrow H \qquad (1.13)$$

$$e^-_{aq} + ClCH_2CO_2H \longrightarrow \underline{Cl}^- + \dot{C}H_2CO_2H \qquad (1.20)$$

$$H + ClCH_2CO_2H \longrightarrow \underline{H_2} + Cl\dot{C}HCO_2H \qquad (1.21)$$

That is, radiolysis leads to the formation of hydrated electrons (1.19) which react at neutral or high pH with monochloroacetic acid to give chloride ions (1.20). As the pH is lowered, hydrated electrons are scavenged by protons producing the second reducing species, hydrogen atoms (1.13), which upon reaction with monochloroacetic acid produce a different product, molecular hydrogen (1.21). These conclusions were echoed by Barr and Allen[44] who studied the problem by a totally different approach. Instead of trying to prove the existence of two reducing species by looking for different products from a single reactant under different conditions, they studied the reaction of "hydrogen atoms" produced by different methods. They found that hydrogen atoms produced from the free radical oxidation of molecular hydrogen (1.22) reacted much more quickly with oxygen than with hydrogen peroxide.

$$H_2 + OH \longrightarrow H + H_2O \qquad (1.22)$$

However, the rate constants for the reaction of "hydrogen atoms" produced from aqueous irradiation with oxygen and peroxide were essentially equal. This again implies the presence of a reducing species other than the hydrogen atom. Proof that the second reducing species is in fact the hydrated electron was nearly complete when in 1962 Czapski and Schwarz[45] determined from kinetic ionic strength effects that the species carries -1 unit of charge. Finally, that same year, when sufficiently fast detection equipment had become available, Hart and Boag[46] observed a transient absorbing species in water immediately following a short radiation pulse. Although the species lived for less than 10 μsec, Hart and Boag determined its visible spectrum and identified it as the hydrated electron, e^-_{aq}. Since that time, the hydrated electron has been the subject of countless investigations.

D. THE INTERACTION OF HIGH ENERGY RADIATION WITH MATTER

In order to properly investigate the formation, properties, reactivity and exact nature of radiation produced solvated electrons, it is imperative to understand something about the way in which the high energy radiation from the sources used interacts with matter.

1. Gamma Radiolysis

The intensity, I, of electromagnetic radiation passing through matter is governed by the relationship:

$$I = I_0 e^{-\mu x} \qquad \text{(iii)}$$

where I_0 is the intensity of the incident radiation, and μ is the total linear absorption coefficient of the medium of thickness x. For X or γ-rays, the overall linear absorption coefficient is the sum of contributions from the four principle mechanisms whereby energy is transferred to the medium[47]. They are the photoelectric effect, the Compton process, pair production, and photonuclear reactions. The relative importance of these interactions depends primarily upon the energy of the incident photons and to a lesser extent upon the atomic number, Z, of the absorbing medium.

a) The Photoelectric Effect

When all the energy of a photon is completely absorbed by a single atomic electron, the electron is ejected from the atom with an energy, E_e, equal to the difference between the photon energy, E_o, and the binding energy, E_b, of the electron in the atom (iv). This is the photoelectric effect.

$$E_e = E_o - E_b \qquad \text{(iv)}$$

Momentum conservation is made possible through atom recoil, so that photoelectric interaction is not possible with single particles. The absorption cross section for the photoelectric effect, τ_p, is governed by equation (v).

$$\tau_p \propto Z^4/E_o^3 \qquad \text{(v)}$$

Thus this process is important only for high atomic number materials and low photon energies.

b) The Compton Process

At energies > 0.1 MeV, photons can undergo elastic collisions with free or loosely bound electrons which result in the transfer of only part of the incident photon energy. Interaction of this type is called the Compton process and is depicted in Figure I-2.

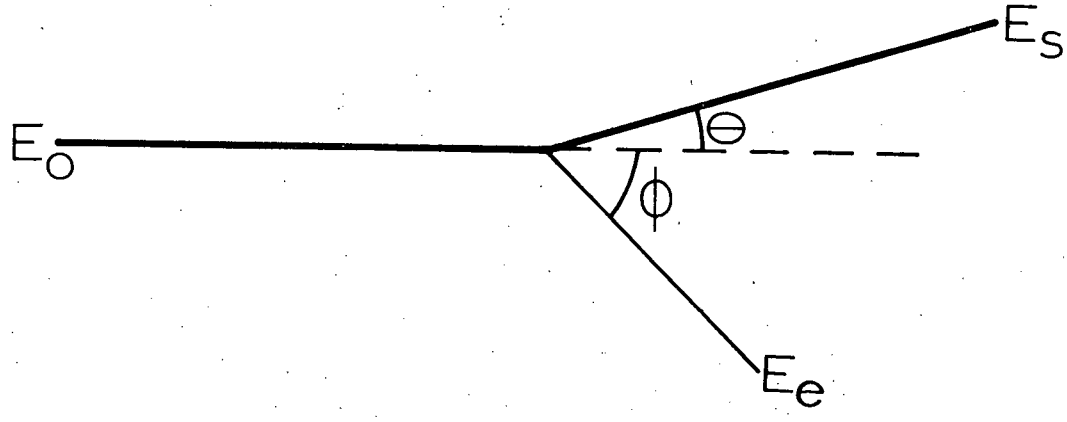

Figure I-2. The Compton Process.

Upon collision, the photon is scattered at an angle θ, with energy E_s. The electron recoils with energy E_e, at an angle ϕ. As a consequence of the laws of conservation of energy and momentum, the angular relations are dependent upon the energies involved. For example, the energy of the scattered photon is given by (vi):

$$E_s = \frac{E_o}{1 + (E_o/m_oC^2)\ (1 - \cos\ \theta)} \qquad \text{(vi)}$$

where m_oC^2 is the rest mass energy of the electron. Neglecting its binding energy, the recoil of Compton electron has energy, E_e, given by (vii).

$$E_e = E_o - E_s \qquad \text{(vii)}$$

It can be seen from equations (vi) and (vii) that the Compton electron will have maximum energy when the photon is scattered 180°.

c) Pair Production and Photonuclear Reactions

These are high energy processes which intimately involve the atomic nucleus. Pair production occurs when a high energy photon is annihilated near a nucleus, accompanied by the concomitant production of an electron/position pair. The reaction

can only occur with photons having sufficient energy to produce two electron rest masses ($2m_oC^2$ = 1.02 MeV). A recoil nucleus is required to conserve momentum. Energies in excess of 10 MeV are usually required. Even more energetic photons are required to bring about photonuclear reactions which involve the ejection of neutrons or protons from atomic nuclei.

The relative importance of the various interactions of electromagnetic radiation with water is easily seen in Figure I-3 which shows the total absorption coefficient as a function of photon energy. It can be seen that for ^{60}Co radiolysis (γ-rays at 1.17 and 1.33 MeV), interaction with water occurs almost exclusively via the Compton process which essentially converts high energy photons to high energy electrons. It is thus necessary to consider the consequences of interactions between these species and matter.

2. High Energy Electrons

High speed particles, particularly charged species, interact much more strongly with matter than does electromagnetic radiation. As a consequence, such particles have rather short, finite ranges in an absorbing material. A charged particle passing close to an atom is decelerated by the electric field of the nucleus. According to classical physics, such interaction must be accompanied by the emission of electromagnetic radiation (bremsstrahlung). The rate of energy loss, -dE/dx, is proportional to $e^2Z_n^2/m^2$ where e and Z_n are the electron and

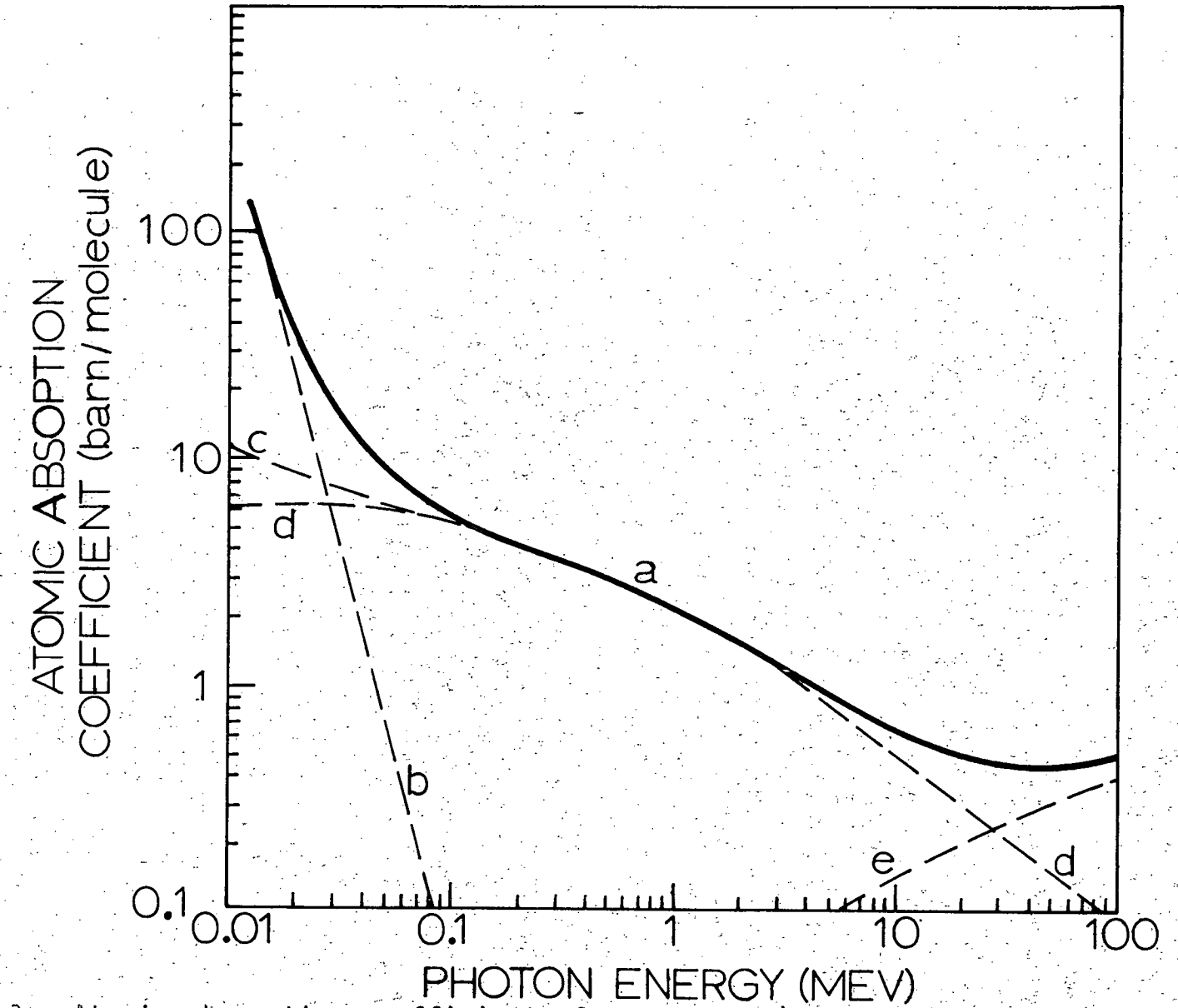

Figure I-3. Atomic absorption coefficients for water. a) Total absorption coefficient; b) Photoelectric absorption coefficient; c) Compton coefficient (with coherent scattering); d) Compton coefficient (without coherent scattering); e) Pair-production coefficient. 1 barn = 10^{-24} cm^2.

nuclear charges respectively and m the electron mass. Bremsstrahlung emission is most efficient for materials of high atomic number, thus lead and tungsten are generally used in X-ray production systems. The process is negligible for electron energies below 100 KeV, becomes significant above 1 MeV, and predominates above 100 MeV. Note that this electromagnetic radiation can subsequently interact further with the medium as discussed previously.

Electrons possessing energies below 1 MeV can undergo coulombic interactions with the electrons of the medium. Such inelastic collisions lead to excitation and ionization of the molecules of the medium and are ultimately responsible for the observed chemical changes in the system. The linear rate of energy transfer (LET), -dE/dx, for an electron having velocity v is given by the Bethe equation (viii).

$$\frac{-dE}{dx} = \frac{2\pi Ne^4 Z}{m_o v^2}\left[\ln\frac{m_o v^2 E}{2I^2(1-\beta^2)} - (2\sqrt{1-\beta^2} - 1 + \beta^2)\ln 2 + 1-\beta^2 + 1/8\,(1-\sqrt{1-\beta^2})^2\right] \text{ ergs cm}^{-1} \qquad \text{(viii)}$$

where, N is the number of atoms per cubic centimeter,

e is the charge on the electron,

Z is the atomic number of the absorber,

m_o is the rest mass of the electron,

E is the kinetic energy of the electron in ergs,

β equals v/c where c is the velocity of light in vacuo and I is the average excitation potential of the absorber. The energy deposited (dose) in a sample irradiated by parallel beams of electrons can be calculated from this expression. Figure I-4 shows the dose distribution as a function of depth for some moderate electron energies.[48] Notice that except for very small or thin samples, irradiation leads on the macro scale to an inhomogeneous distribution of species.

The relative importance of bremsstrahlung interactions and collisions in the energy transfer scheme is approximated by expression (ix).

$$\frac{(dE/dx)_{brem}}{(dE/dx)_{coll}} \sim \frac{EZ}{1600\ m_o c^2} \qquad \text{(ix)}$$

where E, Z, m_o, c^2 are as before.
For electrons in the 1 - 3 MeV range, bremsstrahlung radiation accounts for less than 5% of the energy loss.

The average specific ionization brought about by gamma rays is only one tenth to one hundredth that caused by a β particle (high energy electron) of the same energy. Therefore, gamma rays have a much greater range in a given medium. However, it is still possible to estimate the LET for electromagnetic radiation from the Bethe equation provided one sums over the spectrum of Compton electrons produced. In attempts to relate different types of irradiations, an average linear energy transfer ($\overline{LET}$) is often discussed. $\overline{LET}$ is obtained simply by dividing

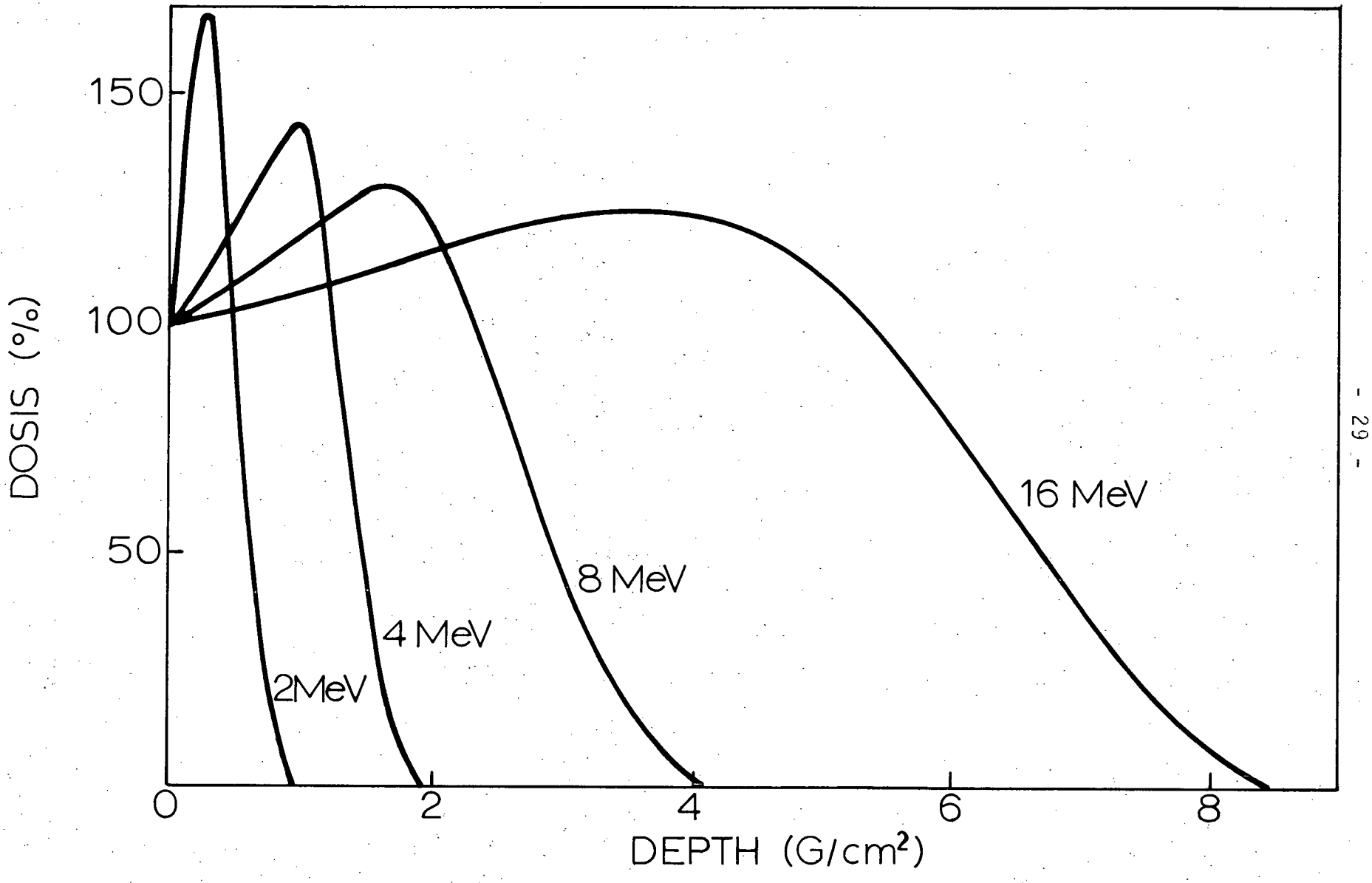

Figure I-4. Dose distribution from high energy electrons as a function of depth and energy.

the initial energy of the particle by its range. It should be pointed out that the $\overline{LET}$ values for 3 MeV electrons and ^{60}Co gamma rays are comparable.

As electrons interact with matter by the processes discussed they are constantly being deflected in random directions. The result of this scattering is that the total distance travelled by the electron (its path length) will far exceed its depth of penetration (range) in the medium. The distribution of electron ranges in the substance as expressed by some number/distance relationship falls off fairly linearily and is not simply reflected by the dose distribution which shows a maximum.

It has been stated that it is the coulombic interactions between high energy electrons and the electrons of the medium which give rise to chemical effects. However, these inelastic collisions do not give rise to a homogenous distribution of excited or ionized species, nor even to continuous cylinders of such species. Instead, the "track" of an incident particle (be it a primary or Compton electron) consists of a series of collisions or "primary events" occurring at irregular intervals. Primary ionization events leading to the production of secondary electrons having sufficient energy to escape immediate recombination with their positive parent ion produce one of several types of energized regions.

Secondary electrons with energies less than 100 eV have a high LET value and consequently quickly initiate a rapid succession of tertiary excitations and ionizations. This leads

to the formation of roughly sperical "spurs" containing a relatively small number of low energy electrons, positive ions and excited molecules.

More energetic secondary electrons (>100 eV) have sufficient range to produce their own short tracks, called δ-rays. Further ionizations and spur formation can occur and if the secondary electron is only moderately energetic (100 - 500 eV) the spurs will overlap to produce elongated "blobs". Higher energy secondary or δ-electrons (500 eV - 5 keV) form a true track of their own -- a "short track".

In water for example spurs of perhaps 20Å diameter are separated by thousands of Angstrom units when produced by a 1 MeV electron. Also, as the primary electron loses its energy its LET increases and primary events begin to converge. The process is not unlike a three dimensional analogue of the disturbance pattern produced when a flat stone is skipped across a calm water surface. ^{60}Co gamma rays give rise to secondary electrons having a mean energy of about 440 keV.[49] This energy is mainly dissipated in the form of spurs (∿64%) with the remaining energy deposited as short tracks (∿25%) and blobs (∿11%). Further, it may be stated that, in general, energy deposited by ionizing radiation seems to be about equally divided between ionic and excited species.

Thus it can be seen that the physical effect of radiation on matter is to produce a grossly inhomogenous distribution of species on both the micro and macro scales. The subsequent reactions and interactions of these species must ultimately

govern the observed chemical changes.

E. THE CHEMICAL CONSEQUENCES OF RADIATION ABSORPTION

Upon subjection to ionizing radiation, matter undergoes changes which are best described in terms of three stages. The Physical stage encompasses that period of time (usually less than 10^{-15} sec) during which radiant energy is dissipated in the system. The next stage, lasting for perhaps 10^{-11} sec, is called the Physicochemical stage. Excited state and photophysical reactions, geminate ion recombinations and proton transfer or fragmentation reactions occur during this stage as the system attains thermal equilibrium. Finally, surviving reactive intermediate species begin to diffuse into the bulk of the medium where the decay or react through normal chemical reactions. This, the Chemical stage, occurs during a period of 10^{-8} sec or longer until such time as chemical equilibrium is re-established.

When the radiolysis of a substance results in the formation of some measurable product, the radiation chemist discusses the process in terms of a radiolytic yield. For convenience, the yield or "G value" of such a product is defined as the number of molecules changed or produced for each 100 eV of radiant energy absorbed by the medium. This value was arbitrarily chosen so as to give typical G values near unity. Recall however, that this energy is about that generally associated with the average

spur.

During the early days of radiation chemistry, ion neutralization in condensed media was considered so rapid that only radical species were considered long enough lived to be capable of initiating chemical reaction. In a theoretical treatment of aqueous systems for example, Samuel and Magee[50] accounted for the observed product yields solely in terms of the diffusion kinetics of H and OH radicals.

Molecular product yields, in general, were found to be highly dependent upon the LET properties of the ionizing radiation. This was considered to be a consequence of the inhomogenous distribution of the reactive species. For example, molecular hydrogen is thought to be formed in irradiated water when diffusion allows spurs to overlap enabling interspur combination of hydrogen atoms. As discussed earlier, ^{60}Co γ-irradiation produces a series of well isolated spurs in water. Heavy helium nuclei (α particles) on the other hand interact strongly with matter -- i.e. have a high LET value and produce a short series of overlapping spurs equivalent to a cylinder of excited and ionized species. Thus, as one might expect, in water, the molecular hydrogen yield from γ-radiolysis $G(H_2)_\gamma = 0.42$ is much less than that from α-radiolysis where $G(H_2)_\alpha = 1.57$.[51]

F. SOLVATED ELECTRONS

1. Formation

As more data became available it was becoming increasingly obvious to the theoreticians that radical diffusion kinetic considerations alone were not sufficient to describe the observations. The presence of ionic and electron scavengers had significant effects on product yields so the fate of the electrons on thermalization had to be reconsidered. Furthermore, scavenger data pointed to electron species having lifetimes considerably longer than one would associate with free electrons. Indications were that electrons were being stabilized or "solvated" in liquid media.

Normal anions become solvated in polar liquids by attracting the positive ends of nearby solvent molecules thereby forming a solvent sheath. Generally, this first layer of solvent molecules is tightly bound to the ion and moves with it through the solution thereby decreasing the ion mobility. On the other hand, an electron can move much more rapidly than bulky solvent molecules. During the time required for the solvent dipoles to rotate and point towards the electron ($\sim 10^{-11}$ sec, the dipolar relaxation time) the electron moves on. As a result, the solvent dipoles can only orient themselves towards the average position of the electron. This however gives us a clue as to a possible mechanism which could lead to electron stabilization. Figure I-5 illustrates the process. In (a)

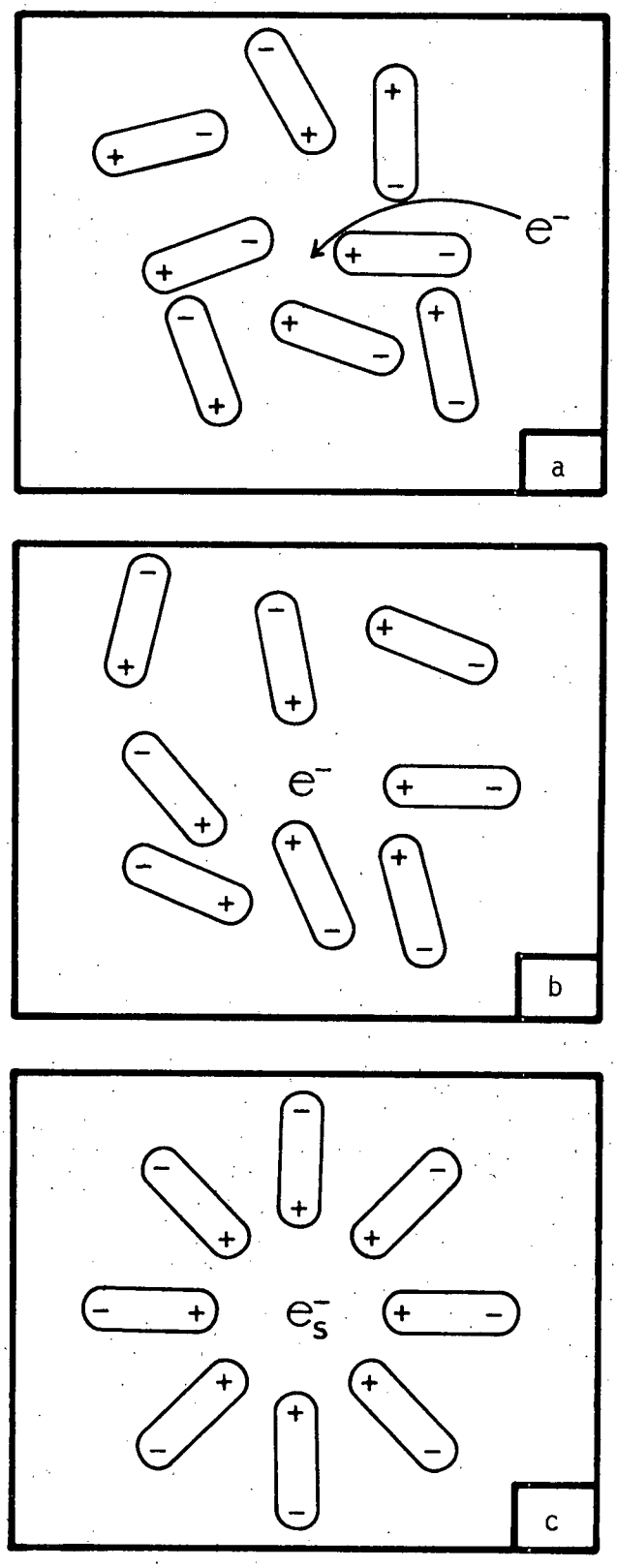

Figure I-5. A possible mechanism for electron solvation in polar liquids. The scheme is outlined in the text.

random thermal motion of polar solvent molecules has created a region of accidental polarization. A nearby thermal electron is attracted to this region and thus spends a greater proportion of its time in its vicinity. In (b) the positive ends of solvent dipoles in the region are now attracted by the electron and the polarization is enhanced. Through this feedback process the mutual attraction increases until a fully formed trap (c) is capable of stabilizing the electron. This process of producing a solvated electron could occur in about 10^{-10} sec. Notice that as the solvent dipoles begin to align themselves with their positive ends all pointing inwards, they will mutually repel one another to create an enlarged cavity devoid of solvent molecules. Also, it is interesting to think about the solvent cavity that would remain if the electron were suddenly completely removed. The remaining positive "hole" might in fact not be very different energetically from the 1s orbital of a proton. From this view, it is perhaps understandable that solvated electrons behave very much like, and were long mistaken for, hydrogen atoms. Indeed, as Hart commented;[52] "Our understanding of the chemical reactions of the solvated electron will be much improved if we think of it as an element having nuclear mass 0, atomic number 0 and electric charge -1".

Another way in which the process of solvating a thermal electron could be initiated is as follows. The presence of an electron could quickly induce electronic polarization in nearby solvent molecules. The shallow trap thus produced might well

serve to stabilize the electron long enough to allow dipolar relaxation (i.e. rotation of the permanent dipoles) of the media leading to true solvation. The electron, retarded as a result of the polarizability of the medium, (we might call it a "dry" electron) may well itself initiate the solvation process or "dig its own grave".

In order to demonstrate that electron solvation was indeed energetically favourable, Baxendale[53] calculated its hydration energy from the cycle given in Figure I-6. Using all energy values for the reactions given in kcal/mole he obtained a free energy of -38.2 kcal/mole (1.66 eV) for the process.

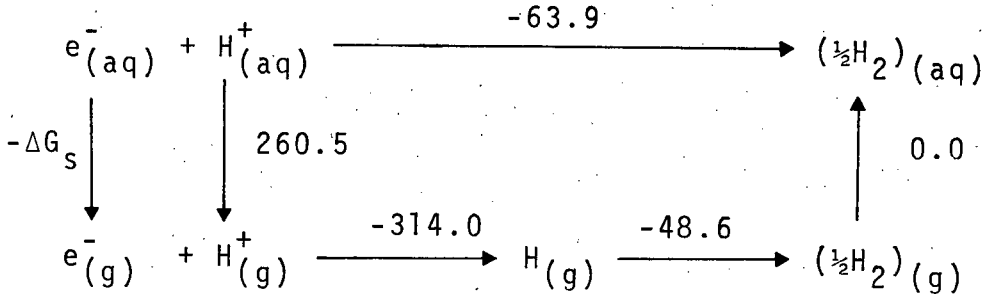

Figure I-6. Determination of the free energy of solvation (ΔG_s) for the hydrated electron. All free energy values are in kcal/mole.

Solvated electrons exhibit intense absorption spectra. The absorption usually takes the form of a single broad asymetric and structureless band in the visible or near infra-red region

of the spectrum. The position of the band maximum is dependent on the medium (environment) but apparently independent of the phase of a given medium. Solutions of solvated electrons are highly conductive, indicating the presence of ionic species. Studies indicate an electron mobility higher than that of simple anions but much lower than that generally associated with so-called "free" electrons. Minday and co-workers[54] concluded that even in non-polar hydrocarbons electron transport appeared to involve short-lived traps in fluid. Further, they suggest that the traps must be a collective property of the fluid rather than being associated with individual molecules. The paramagnetic nature of stabilized electrons tends to corroborate these conclusions. Solvated electrons exhibit electron spin resonance spectra characterized by a single narrow line with a gyromagnetic factor g = 2.0022, very near that of the free electron, g_f = 2.0023. The absence of any proton hyperfine splitting and the line sharpness indicate that there is no strong magnetic interaction between the electron and the solvent molecules of an ordered solvation sheath. That is, the solvent molecule forming the cavity must be very loosely bound, and the overlap of electron density with specific protons very weak.

While radiolysis techniques offer a direct method for generating solvated electrons, the production of this species in many other ways has been confirmed. Solvated electron formation upon the dissolution of alkali metals has already been discussed in detail. Walker[55] has presented evidence to

suggest that the species is also an intermediate in the reduction of water by U^{3+} salts (1.23).

$$U^{3+} \xrightarrow{H_2O} U^{4+}_{aq} + e^-_{aq} \qquad (1.23)$$

Photoionization of a number of aqueous ions has been achieved by conventional flash photolysis techniques. Such reaction often leads to the production of the hydrated electron. Those ions which exhibit charge-transfer-to-solvent spectra (the iodide ion for example) seem particularly suitable for such reaction (1.24).

$$I^-_{aq} \xrightarrow{h\nu} I + e^-_{aq} \qquad (1.24)$$

A number of studies have shown that solvated electrons can be prepared electrolytically. In an early study, Walker[56] looked for and found evidence for e^-_{aq} from the electrolysis of water. Also, it may well be that the hydrated electron is an important intermediate of many photochemical reactions (photosynthesis for example) in which it has not been considered.

Regardless of the method whereby they were produced, the solutions containing solvated electrons exhibited identical spectra. Further, many of the reactions of the species were also independent of its origin. These facts suggest that the solvation mechanism does not involve the counter-ion to any significant extent. This is a very important finding, for it

allows one to study solvated electrons by whichever technique is convenient and still be able to relate the results with research performed by other means.

2. Theoretical Models

Many attempts have been made to quantitatively account for the observed chemical and physical properties of solvated electrons. Particular attention has been paid to theoretical models which could account for the shape and position of their absorption spectra. Ogg[57] proposed that the ammoniated electron be considered trapped in a spherical cavity. The electron was taken to be confined by an infinitely steep potential well produced by the electric polarization of the surrounding solvent molecules. A simple electron-in-a-box calculation gave values roughly approximating experimental data. Jortner[58a,b] applied the polaron idea of Landau[58c] and Pekar[58d] to e_s^- and calculated the energy by means of a dielectric-continuum model in which long-range interactions were considered. That is, the polarization potential on the electron was treated as constant within the cavity (zero as the first approximation) and as coulombic outside. As a consequence of the energy levels of that model being determined by long-range interactions, the lowest observable transition was related to the quantity $(1/D_{op} - 1/D_s)$ -- where D_{op} and D_s are the high frequency and static dielectric constants respectively. The potential energy function as a function of distance r, P(r), for a solvated

electron in a cavity of radius R was taken as:

$$P(r) = -\beta e^2/R \qquad \text{for } r \leq R$$

$$= -\beta e^2/r \qquad \text{for } r > R \qquad \text{(x)}$$

where $\beta = (1/D_{op} - 1/D_s)$ and e is the unit electric charge.

Considering an electronic transition involving hydrogenic-like 1s and 2p states, Jortner was able to match experimental values of the absorption band maxima for many solvents. However, since the cavity radius, R, was an adjustable parameter in his calculations, Jortner's model was still semi-empirical at best.

A major flaw of the early theoretical models is that they provided no information about -- in fact ignored -- short-range interactions. Clearly, the electrostatic potential gradient in the immediate vicinity of the solvated electron would be large. Fueki[59] attempted to account for the short-range interactions in terms of dielectric constant, D, through the use of expression (xi) in his calculations.

$$D = D_{op} \qquad \text{for } 0 \leq r \leq r_1$$

$$= (r/r_2)D_s \qquad \text{for } r_1 \leq r \leq r_2$$

$$= D_s \qquad \text{for } r_2 \leq r \qquad \text{(xi)}$$

where $r_1 = (D_{op}/D_s)r_2$ and r_2 was taken to be 9 A.

Jortner, Copeland and Kestner[60] presented a semi-continuum dielectric model utilizing an even more complete potential expression. Electron stabalization was subdivided into short-range attractions, long-range polarizations and short-range repulsions. Those interactions were expressed in terms of various specific distances associated with the cavity that can be seen in Figure I-7 which depicts the physical implications of the model.

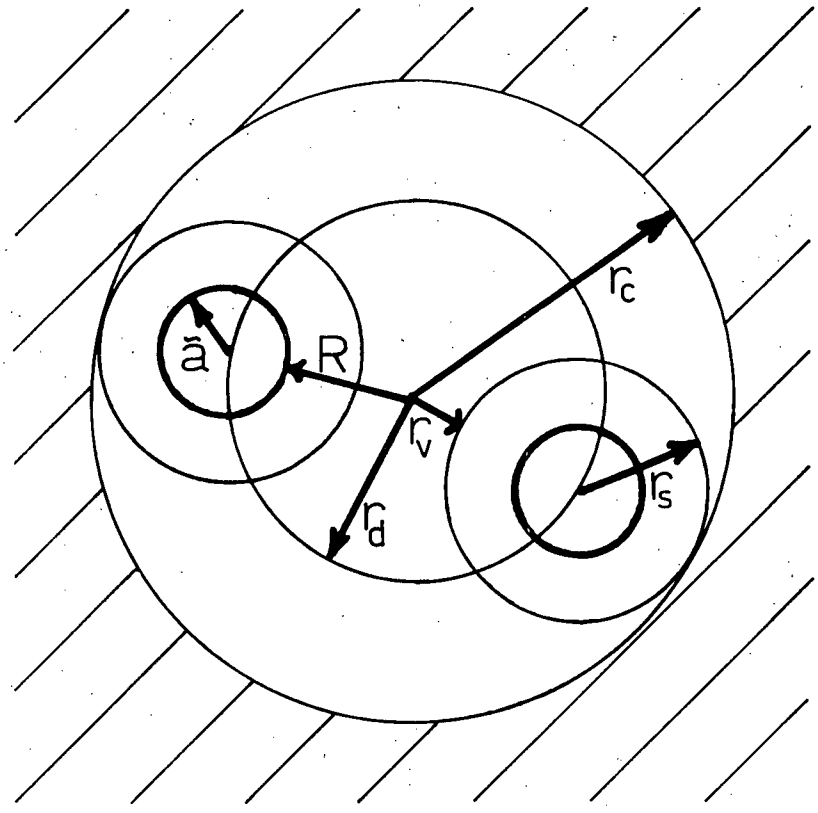

Figure I-7. Definition of cavity distances in Jortner's semi-continuum model for solvated electrons.

The distances utilized in the model are namely:

r_v, the actual void radius of the cavity

r_s, the effective solvent molecule radius

$\tilde{a}$, the effective hard core of the molecules

r_d, the distance of the solvent molecules from the cavity center

r_c, the distance from the cavity centre to the beginning of the continuum and

R, the normal or mean cavity radius

Jortner et al. showed that the electron/medium interaction potential, P(r), for this model takes the form of equation (xii).

$$\begin{aligned} P(r) &= -N\mu e/r_d^2 - \beta e^2/r_c && \text{for } 0 < r < R \\ &= -N\mu e/r_d^2 - \beta e^2/r_c + V_o && \text{for } R < r < r_d \\ &= -\beta e^2/r + V_o && \text{for } r_d < r \end{aligned} \qquad \text{(xii)}$$

where e and β are as defined for equation (x). N is number of nearest molecules of the electron, V_o is the energy of the quasifree (conduction) electron state and μ is the effective dipole moment of the nearest molecules.

The effective dipole term μ takes into account the specific orientation of the actual dipole moment vector, μ_o, with respect to the radius vector,

$$\mu = \mu_o \langle \cos\theta \rangle \qquad \text{(xiii)}$$

The important feature of this detailed inclusion of short-range interactions and orientations in the model is that the configuration stability of the energy states can be established so that a unique cavity radius corresponding to a minimum in the total energy of the system can be calculated. Thus, the semi-continuum model is not plagued by the necessity of the earlier models to include an empirical cavity radius parameter and is thereby inherently more useful for predicting physical properties. For example, Jortner showed that for the ammoniated electron system, the model correctly predicts volume expansion, co-ordination number, heat of solution and many spectroscopic properties.

To date, additional improvements and approaches to solvation models have been made[61] which when taken in total enable one to more readily think of solvated electrons in terms of ordinary, discrete chemical species.

3. Reactions

In early steady-state ^{60}Co γ-radiolysis studies, measurements of product yields from solute mixtures enabled rate constant ratios for electron reactions to be determined. With the advent in the early '60's of pulse radiolysis and fast kinetic analysis equipment it became possible to monitor the electrons (and other reactive intermediates) to determine reaction rates

directly. For example, in 1967, Anbar and Neta[37] compiled a list containing published rate constants for reaction between hydrated electrons and more than 600 solutes.

Several experimenters noticed that the presence of large concentrations of electron scavengers in water resulted in a decreased molecular hydrogen yield upon radiolysis. The Draganics for example[62] observed this effect whether they used a cation (Cu^{2+}), an anion (NO_3^-) or neutral species (H_2O_2, acetone) as electron scavenger. This effect has been attributed to the interruption of a neutralization reaction which ordinarily leads ultimately to hydrogen atom formation (1.25).

$$e^-_{aq} + H_2O^+_{aq} \text{ (or } H_3O^+_{aq}) \longrightarrow \longrightarrow H + OH \text{ (or } H_2O) \qquad (1.25)$$

Indeed, there has even been evidence to suggest that the intermediate ionic species could be scavenged <u>prior</u> to solvation. Hamill[63] claimed that the "dry hole" in water (H_2O^+) could be scavenged by halogen anions at high concentration (1.26).

$$H_2O^+ + X^- \longrightarrow H_2O + X \qquad (1.26)$$

Now, since the "dry hole" is thought to react rapidly with a nearby solvent molecule to produce a hydroxyl radical (1.18) it is possible that reaction of the anion with that radical (1.27) could easily be mistaken for hole scavenging.

$$OH + X^- \longrightarrow OH^- + X \qquad (1.27)$$

However, chloride ion cannot be oxidized by OH in neutral solution so a distinction was easily made and that possibility excluded. Suggestions have also been made that "dry" electrons can also be scavenged. It could not be shown conclusively however whether the effects were not simply a consequence of the time dependent rate constants (inhomogenous kinetics) possible at large solute concentrations.[64] In any event it is apparent that charge neutralization must be a major source of excited and fragmented species during radiolysis. Schuler et al.[65] for instance have estimated that about 70% of the molecular hydrogen from cyclohexane radiolysis arises in that way.

4. Yield

It became readily apparent that the yields of free ions (i.e. those ions escaping geminate recombination) were much larger from those solvents possessing a high dielectric constant or permanent dipole moment. While highly polar molecules might be expected to solvate an electron more strongly than weakly polar molecules, there is no aspect of the solvation process itself as discussed that could account for a higher yield of solvated electrons. Also, recall that the initial ionization yield depends only on the electron density of the medium as a whole, not on the properties of individual molecules. Clearly then, the effect of molecular polarization (or

polarizability) must be to increase the probability for an ionized electron to escape geminate recombination and thereby survive long enough to be solvated.

The ejected electron is, on thermalization, subject to motion of two types. Firstly, due to coulombic attraction, the electron moves towards its counter-ion with velocity, v^-. The magnitude of this velocity being inversly proportional to the ion-electron distance. Secondly, simply as a consequence of its small mass and thermal energy, the electron is subject to diffusive motion. This diffusion, being a random process akin to Brownian motion, may well have a non-zero component directed away from the counter-ion (v^+). At some ion-electron distance, r_c, these two opposite virtual velocities would be equal. If the actual distance is greater than r_c the electron escapes; if it is less the electron returns to the ion. This critical distance, r_c, called the escape radius, has been shown[66] to be given by equation (xiv),

$$r_c = e^2/3\varepsilon kT \qquad \text{(xiv)}$$

where e is the elementary charge, ε is the dielectric constant of the solvent, k is the Boltzmann constant and T the absolute temperature.

Onsager[67] in a statistical treatment showed that for an electron thermalized at a distance R from its geminate ion the probability that it would escape recombination $P(R)_{esc}$, is given by (xv):

$$P(R)_{esc} = \exp(-e^2/\varepsilon RkT) \qquad (xv)$$

Thus in media of high dielectric constant the solvated electron yield would be expected to be higher because polarized solvent molecules act to screen the electron from its parent ion, thereby increasing its chance to escape geminate recombination.

The relationship between dielectric constant and free ion yields from the radiolysis of various liquids has been examined by a number of investigators.[68] Figure I-8 shows that while a general trend exists, there are a number of exceptional cases and it is clear that other factors are important. It has been suggested[69] that electrons are less readily localized when the solvent molecules are more nearly spherical. Thus a secondary electron would probably travel further from its parent ion before becoming localized in, say, neopentane than n-pentane although both compounds possess indentical dielectric constants. The free ion yields of 0.9 and 0.1 respectively tend to support such considerations. Even when carried to the extreme case of liquid argon, which does <u>not</u> form a localized electron state, the free ion yield is about 5 indicating that the electrons are thermalized at great distance from their parent ions.

In addition to their yield, the position of the absorption maximum of solvated electrons appears to be dependent upon the dielectric properties of the media. Sauer et al.[70] have shown for example that the absorption maximum for the alcohols exhibits a red shift with a decreasing dielectric constant. It

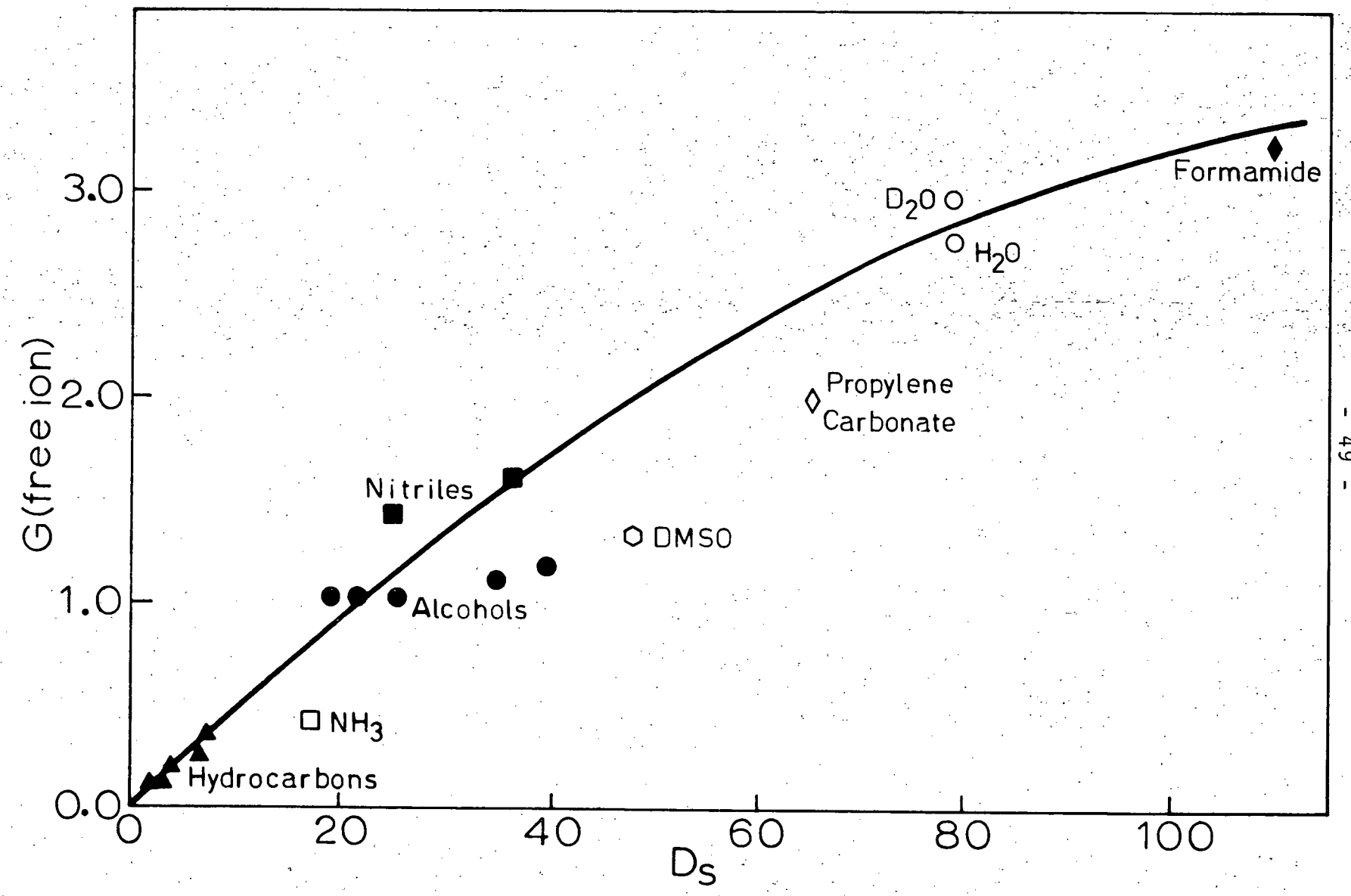

Figure I-8. Free ion yield plotted as a function of static dielectric constant for a variety of solvents.

should be possible to test the theoretical models, especially regarding the involvement of bulk properties, through studies of mixed solvents. One could vary dielectric constant for example and observe its effect on results. If, as postulated, the electrons are truely delocalized and thus sample their average environment their yield and optical properties will be dependent upon such macroscopic properties of mixtures.

Binary mixtures of alcohols and water were studied by Arai and Sauer.[71] They found that, indeed, the electron absorption exhibited a single band intermediate between those for the two pure substances. The position of the maximum was dependent upon the actual mixture composition. Similar results have been found with mixture of water with ammonia and ethylenediamine.[72] However, attempts were made to study a mixture containing molecules of vastly different polarity[73] (ethanol, D_s = 25.7 and n-hexane D_s = 1.8), the band maximum remained at the position for pure ethanol throughout. In that case, its magnitude and the free ion yield were both directly proportional to the ethanol concentration. However, since the lifetime of the electron species was independent of mixture composition it seems more likely that it formed only in cavities formed by clusters of ethanol molecules. Similar results have been obtained for mixtures of methanol in tetrahydrofuran and cyclohexane[73] as well as for 3-methylhexane in ethanol and methanol.[74]

These investigations tend to indicate that while solvated electrons are certainly not strongly associated with individual

solvent molecules it is the first shell or perhaps the first few layers of solvent that have the most influence on the properties of the species. This has been particularly well demonstrated in a rather elegant investigation by Vannikov and Marevtsev.[75] These authors measured the absorption spectra of solvated electrons in monoethanolamine (MEA), $HOCH_2CH_2NH_2$, and an equimolar mixture of ethanol, $HOCH_2CH_3$, and monobutylamine, $CH_3CH_2CH_2CH_2NH_2$, (ETOH-MBA). These two systems have similar macroscopic chemical composition but vastly different dielectric properties. The dielectric constant of MEA is 57.7 and that of the ETOH-MBA mixture, 10.5. As is shown in Figure I-9, despite their five-fold difference in dielectric constant, the systems were found to exhibit nearly identical solvated electron spectra, each with absorption maxima intermediate between that of pure ethanol and ethylamine. Vannikov and Marevtsev attributed no particular importance to the fact that the solvated electron band in the ETOH-MBA mixture is much broader than that in MEA. To the contrary, this result is most significant for it affords further evidence of the influence of the explicit solvent cavity structure. Consider for simplicity that these cavities consisted of a tetrahedral arrangement of four solvent molecules. In MEA, the molecules forming the traps are equivalent so that the potential experienced by stabilized electrons in different cavities will be similar. As a result, the absorption band for electronic transitions should be relatively narrow. On the other hand, in the ETOH-MBA mixture, solvent cages would contain molecules of two types.

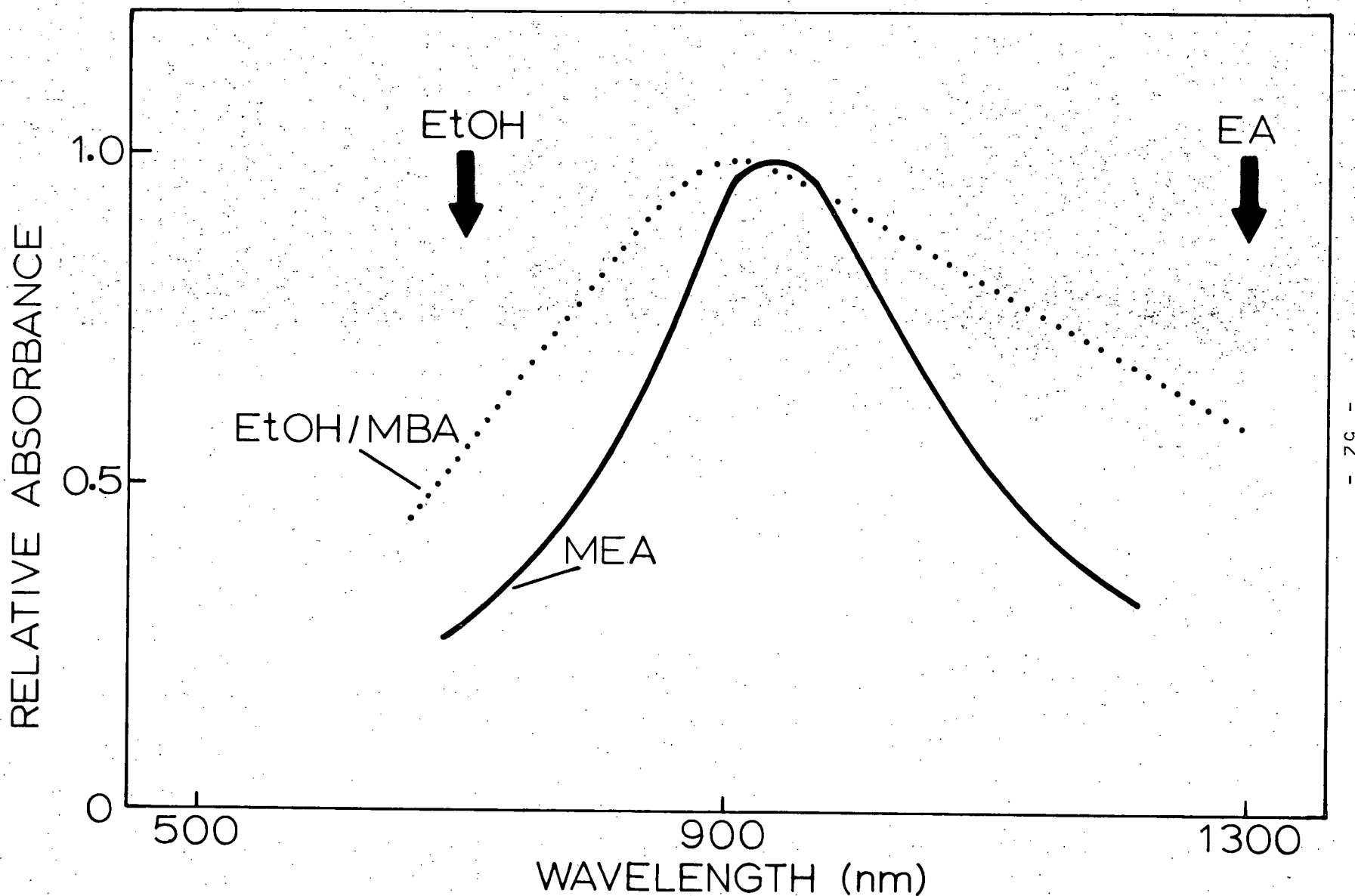

Figure I-9. Absorption spectra of e_s^- in monoethanolamine (——) and in an equimolar mixture of ethanol and monobutylamine (·····) reported by Vannikov and Morevtsev. Arrows indicate positions of λ_{max} for e_s^- in pure ethanol and ethylamine.

Simple statistical considerations dictate that randomly formed tetrahedral traps exhibit a predictable distribution of structure compositions. Table I lists the number of permutations possible for each of the five combinations of two objects taken four at a time.

TABLE I

Combination	Number of Permutations
AAAA	1
AAAB	4
AABB	6
ABBB	4
BBBB	1

Electronic transitions involving such a distribution of cavities would be expected to produce a much broader absorption band compared to a system in which the traps are all similar. This was precisely the observed result. Clearly, these experiments confirm that the microscopic properties of media are very important in determining many of the physical properties of solvated electrons. Kenney-Wallace and Hentz[68c] had concluded for example that local solvent structure and packing were much more important than bulk dielectric properties.

G. THE PRESENT STUDY - SOLVATED ELECTRONS IN HMPA

Thus, Matanovich's[2] discovery that alkali metals dissolve in HMPA to produce stable blue reducing solutions becomes very significant. That is, despite its very poor anion solvating power, HMPA appears capable of accomodating solvated electrons.

A number of investigations have been carried out on solutions of alkali metals in HMPA. A broad, asysmetric, infra-red absorption band,[76] a single, narrow e.s.r. absorption,[77] and electrical conductivity[78a] all characteristic of solvated electrons, have been reported for such solutions. In addition, Sternberg et al.[78b] have observed the formation of dark blue globules at a platinum cathode when a solution of lithium chloride in HMPA was electrolyzed. Alpatrova and Grishina,[79] using e.s.r. spectroscopic techniques, attributed this colouration to solvated electrons.

All of the HMPA studies for which stable solutions of solvated electrons have been proposed contain large concentrations of foreign cations (usually one of the alkali metals). Thus it is not clear whether or not it is the presence of such cations which is in fact responsible for the electron stabilization in those systems.

It was proposed to study by means of radiolysis techniques the ability of HMPA to accommodate and stabilize solvated electrons. Preliminary steady-state radiolysis studies[80] utilizing competitive scavenger techniques demonstrated the feasibility of the project. That work was developed further

and in conjunction with studies of Na solutions in HMPA the yield, stability and reactivity of e^-_{HMPA} were fairly well established. Finally, the work was extended to pulse radiolysis techniques which facilitated direct observation of the species, its spectrum, and reactions along with an independent measurement of its yield.

CHAPTER II

EXPERIMENTAL

A. STEADY STATE EXPERIMENTS

1. Materials

Hexamethylphosphoramide was purified in the following manner. Freshly cut pieces of sodium metal were added to several liters of Fisher Scientific technical grade HMPA in a vacuum distillation apparatus. The samples were agitated at atmospheric pressure by means of a helium gas purge until a stable blue solution of sodium in HMPA was attained. This solution was fractionally distilled under vacuum. The middle two-thirds (that which boiled at 87 °C for about one torr pressure) was retained. The purification technique was then repeated with that sample as starting material, the middle fraction being collected and stored until required. When sodium metal was added to the singly distilled sample of HMPA prior to the second distillation, the solution became stable blue almost immediately indicating that few oxidizing impurities remained.

Water used as scavenger and for HMPA/water mixture studies was triply distilled. Singly distilled water was refluxed from an acidified dichromate solution, gamma irradiated overnight (0.5 Mrad) to remove trace organic impurities, then refluxed

from an alkaline permaganate solution.

Nitrous oxide, carbon dioxide, oxygen and argon were purified in the vacuum system by conventional "trap-to-trap" distillations involving multiple freeze-pump-thaw cycles. These gases were stored on the vacuum line in stopped bulbs until required.

Sodium metal was purified and prepared for addition to liquid samples as amalgams with mercury. Small weighed slugs of freshly cut sodium metal were sealed into a long pyrex tube which was subsequently evacuated. The metal was distilled through a number of constrictions in the tube. The residue chamber from each distillation was sealed-off and removed with the result that the last chamber contained a bright sodium mirror. "Clean" mercury was distilled onto this mirror and the resulting amalgam stored under vacuum.

Other chemicals used as scavengers were analytical grade or better and were not subjected to further purification.

Special care was taken to ensure that glassware was scrupulously clean. Vessels were washed with permanganic acid; rinsed with distilled water; washed with a solution of hydrogen peroxide in nitric acid; and finally rinsed with singly and triply distilled water. Glassware was usually dried in a 120 °C oven and on occasion annealed overnight in a glassblower's oven.

2. Radiation Source

An Atomic Energy of Canada Gammacell 220 was used as a

source of gamma rays. This machine, which had a nominal activity of 3800 curies, uses ^{60}Co as its source. ^{60}Co has a half-life of 5.26 years and decays with the emission of gamma rays of 1.173 MeV and 1.333 MeV. ^{60}Co also emits 0.32 MeV beta particles (electrons) but in the Gammacell 220 those are absorbed before they reach the sample irradiation chamber.

3. Dosimetry

In order to be able to discuss the experimental effects of radiation quantitatively in terms of G values, it is necessary to determine the radiation energy absorbed by a given sample. Absorbed dose is usually expressed in rads - one rad being the absorption of 100 ergs gm^{-1} or 6.24×10^{13} eV gm^{-1}. Since the dose rate in the radiation chamber of the Gammacell is not spatially uniform, care was taken to ensure reproducible placement of the irradiation cells. In addition, dosimetry measurements were made utilizing a pseudo-cell which accurately reproduced sample positioning. Chemical dosimetry was performed which monitored the oxidation of ferrous ions. Known as Fricke dosimetry, the technique is a universally accepted standard technique.[81] An air saturated solution of triply distilled water containing 1×10^{-3}M ferrous ammonium sulphate, 1×10^{-3}M sodium chloride, and 4×10^{-1}M sulphuric acid was prepared. Irridation of such a solution is thought to lead to the following processes:

$$nH_2O \wwwarrow e^-_{aq} + H + OH + H_2O_2 + H_2 \qquad (2.1)$$

$$e^-_{aq} + H^+ \longrightarrow H \qquad (1.13)$$

$$H + O_2 \longrightarrow HO_2 \qquad (2.2)$$

$$HO_2 + Fe^{2+} + H^+ \longrightarrow Fe^{3+} + H_2O_2 \qquad (2.3)$$

$$H_2O_2 + Fe^{2+} + H^+ \longrightarrow Fe^{3+} + OH + H_2O \qquad (2.4)$$

$$OH + Fe^{2+} + H^+ \longrightarrow Fe^{3+} + H_2O \qquad (2.5)$$

From these reactions, it can be seen that:

$$G(Fe^{3+}) = 3\left[G(e^-_{aq}) + G(H)\right] + G(OH) + 2G(H_2O_2) \qquad (xvi)$$

Based on direct colorimetric measurements the ferric ion yield $G(Fe^{3+}) = 15.5$ molec $(100\ eV)^{-1}$ has been measured with great precision.[8,1] Clearly, the ferric ion yield is very sensitive to a number of intermediate species in the radiolysis of water. In particular, the oxidation of organic impurities (RH) by hydroxyl radicals (2.6) and the subsequent reaction with oxygen (2.7) can produce organic peroxides.

$$OH + RH \longrightarrow R + H_2O \qquad (2.6)$$

$$R + O_2 \longrightarrow RO_2 \qquad (2.7)$$

Such peroxides could then react with ferrous ions in a reaction scheme analagous to (2.3, 2.4, 2.5). The result would be to increase the ferric ion yield. However, the presence of chloride ions in the Fricke solution serves to suppress such a process by scavenging the hydroxyl radicals (2.8).

$$OH + Cl^- \longrightarrow OH^- + Cl \qquad (2.8)$$

The chlorine atom then oxidizes a ferrous ion (2.9) so that the ferric ion yield is preserved.

$$Cl + Fe^{2+} \longrightarrow Fe^{3+} + Cl^- \qquad (2.9)$$

Fricke solutions were irradiated for various periods of time. The resulting ferric ion concentration in each sample was measured spectrophotometrically using a Beckman DU spectrophotometer which had been calibrated with a known potassium chromate solution. Figure II-1 shows that the observed optical density at 304 nm (from Fe^{3+} ion) was a linear function of the Gammacell timer setting. The positive intercept to be seen in that figure reflects a peculiarity of the Gammacell operation. That is, because the timer mechanism is only activated when the cavity drawer is at its lowermost position, samples are subjected to an untimed but constant residual dose of radiation during the periods of descent from

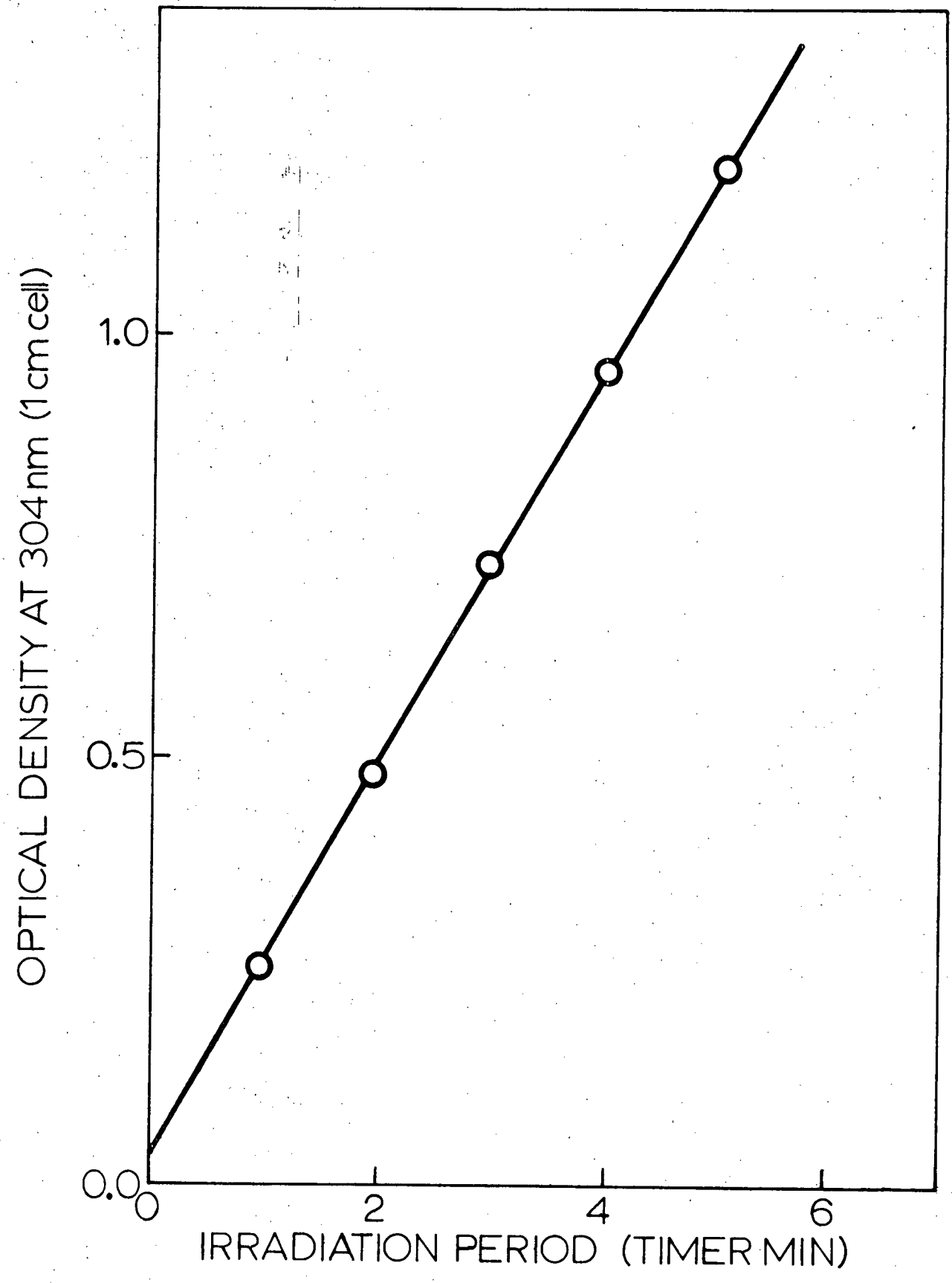

Figure II-1. Fricke Dosimetry. Results from the ^{60}Co γ-irradiation of appropriate solutions in the radiolysis cell.

and ascent to the upper loading position. As can be seen, the residual dose was equivalent to an irradiation of about 5 sec as measured by the timer.

The absorbed dose rate, R_o, for the Fricke dosimeter solution is given by equation (xvii):

$$R_o = \frac{9.65 \times 10^8 \, \Delta O.D./\Delta t \text{ rad min}^{-1}}{\varepsilon_{304}^{Fe^{3+}} \cdot l \cdot \rho \cdot G(Fe^{3+})} \qquad \text{(xvii)}$$

where $\varepsilon_{304}^{Fe^{3+}}$ is the molar absorptivity of Fe^{3+} at 304 nm (2174 M^{-1} cm^{-1}), l is the optical path length of the cell (1 cm), ρ is the density of the Fricke solution (1.024 ± 0.001 at 20 °C) and $G(Fe^{3+})$ = 15.5 molec $(100 \text{ eV})^{-1}$.

For the data of Figure II-1 a dose rate, R_o = 6580 rad min^{-1} was calculated.

Now, the major energy transfer mechanism -- the Compton process -- depends on the electron density of the absorbing medium. Therefore, the corresponding radiation dose rate for HMPA samples in the same physical position in radiation chamber is given by (xviii).

$$R_{HMPA} = R_o \frac{(Z/A)_{HMPA}}{(Z/A)_{FRICKE}} \qquad \text{(xviii)}$$

where Z and A are the atomic numbers and weights of the two media.

In addition to the physical influences on dose rate, ^{60}Co itself is subject to an inherent natural decay. The activity of radioactive material at time t, A_t, is related to some initial activity, A_o, by the expression (xix).

$$A_t = A_o\, e^{-\lambda t} \qquad \text{(xix)}$$

where λ is the decay constant (xx)

$$\lambda = \frac{0.693}{\tau_{1/2}} \qquad \text{(xx)}$$

and $\tau_{1/2}$ is the radioactive half-life (5.27 years for ^{60}Co).

The dose rate, R_t, for a sample irradiated t days after dosimetry was performed would be given by the expression (xxi):

$$R_t = R_o\, e^{-(0.693t/1925)} \qquad \text{(xxi)}$$

A simple computer program was written that took into account sample electron density, cell position, irradiation time, residual dose, time since dosimetry measurements, dosimetry results, and ^{60}Co decay and returned a value representing the

actual absorbed dose for a given experiment.

4. Experimentation

a) ^{60}Co Gamma Radiolysis

Figure II-2 depicts the reaction cell used in the steady-state radiolysis studies. That pyrex vessel could be reproducibly placed in the Gammacell radiation chamber. Its construction facilitated the rapid introduction, homogeneous solution formation, and quantitative retrieval of gaseous substances. The four-way stopcock was removed and known amounts of liquid solutions introduced into the cell through the vent. The stopcock was sparingly lubricated with inert Apiezon N and held firmly in place with a aluminum retainer which could withstand the pressures required for analysis. Samples were then deoxygenated by flushing with argon for 15 minutes. Turning the stopcock 45° to a fully closed position retained the liquid above the fritted glass disk. At this point the sample (generally HMPA with or without scavengers) was either irradiated or attached to a vacuum line for the addition of gaseous scavengers.

The vacuum apparatus enabled one to introduce measured amounts of gas or a mixture of gases directly into the reaction vessel. Figure II-3 gives schematic details of the equipment. Various pure gases (N_2O, CO_2, O_2, Ar) were stored in large flasks A, B, or C. Flask A was generally reserved for the

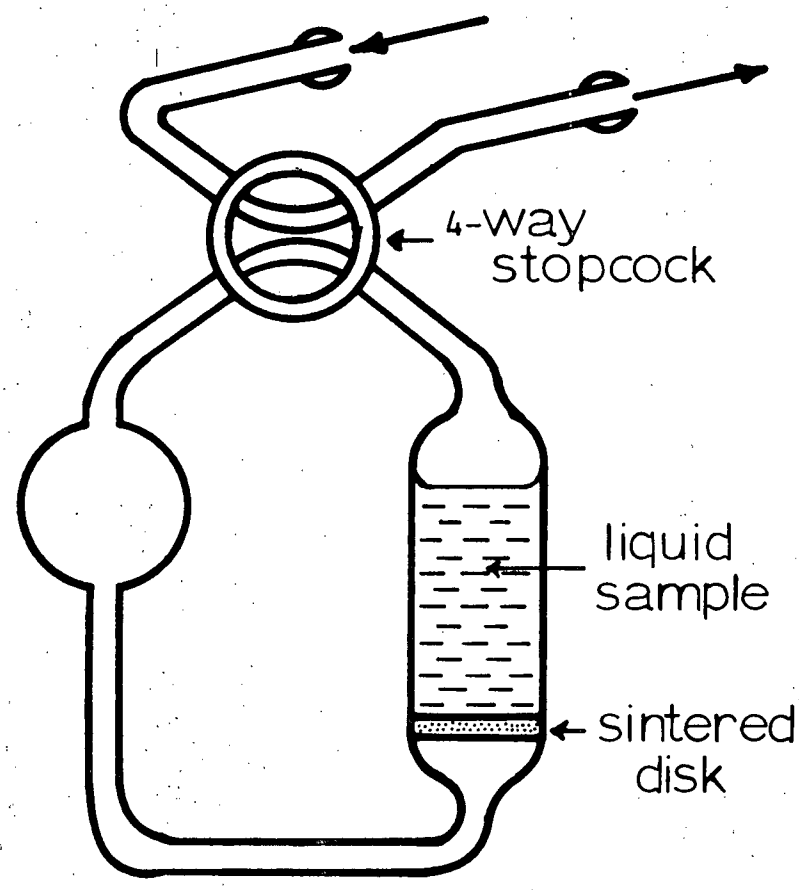

Figure II-2. Gamma radiolysis reaction vessel.

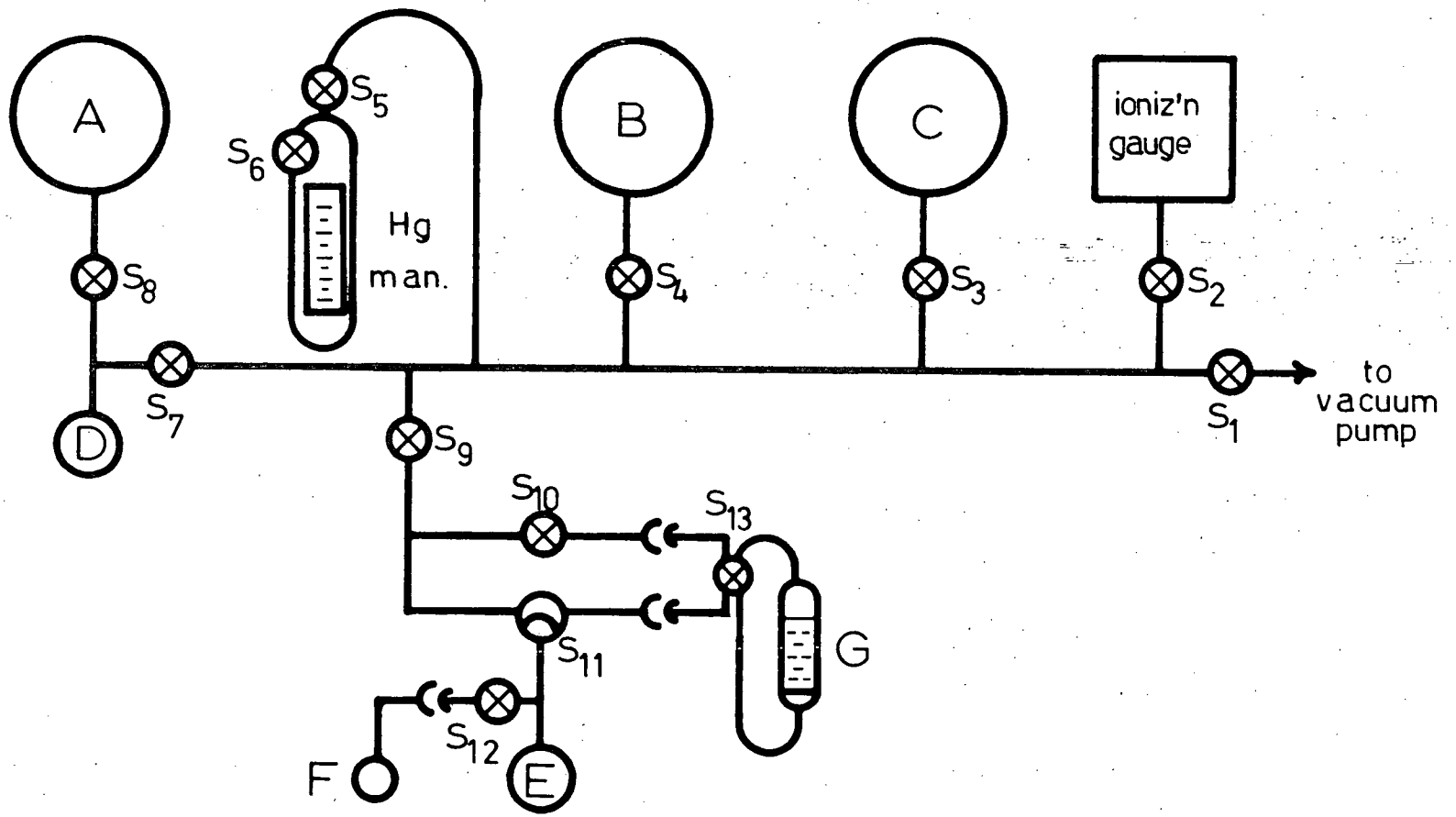

Figure II-3. Schematic diagram of vacuum line used for the preparation and addition of gaseous scavengers to HMPA solutions in the radiolysis vessel, G.

major gaseous scavenger, N_2O. Through the use of a liquid nitrogen bath and bulb D, N_2O samples could be conveniently recovered from other regions of the line, purified, and returned to storage bulb A. The reaction cell G, containing the HMPA solution being studied, was attached to the vacuum line by means of two ball and socket joints. Since at room temperature the vapour pressure of HMPA is negligible, samples of the liquid could be readily degassed by evacuating the reaction cell. This was accomplished by opening stopcocks S_1, S_2, S_5, S_9, S_{10}, S_{11} (between S_9 and S_{13}) and slowly, S_{13}. When equilibrium was established S_{13} was closed isolating the cell. S_{11} was rotated so that addition bulb E would be evacuated. If two gaseous scavengers were to be added to the reaction vessel S_{12} would be opened so as to allow evacuation of bulb F as well. These bulbs were attached by means of cone and socket joints and could be replaced with a number of bulbs of various known capacities. Gaseous scavengers to be added to the reaction cell were transferred to bulb E and/or F at a known pressure and temperature. Two scavengers could be independently metered, the first going into bulb F and the second into bulb E. Stopcock S_{11} was opened between S_9 and S_{13} and the line evacuated as before. At the same time stopcock S_{12} would be opened to allow thorough mixing of scavengers when two were being used. The scavenger or mixture was introduced into the reaction cell and monitored by closing S_1 (as well as S_3, S_4, S_6, S_7) and opening S_2, S_5, S_9, S_{10}, S_{13}, S_{12} and slowly S_{11} (between S_{12} and S_{13}). When bubbling had ceased

and equilbrium attained, the temperature and pressure of residual scavenger gases measured. Since all relevent volumes in the system were accurately known and assuming ideal gas behavior it was possible to calculate the concentration of gaseous scavenger (or scavengers) dissolved in the liquid.

Measurements were made to determine the solubility of each of the gaseous scavengers in HMPA. Figure II-4 shows the variation of concentration with the observed equilibrium partial pressures of N_2O, O_2 and CO_2. It can be seen that in each of those cases the scavenger concentration was a linear function of its equilibrium partial pressure. Table II gives solubilities for the gases in HMPA at 23 °C as determined from the slopes of the plots in Figure II-4.

TABLE II

Gas	Solubility in HMPA at 23 °C as a function of equilibrium partial pressure (M/mm Hg)
N_2O	$1.85 \pm 0.05 \times 10^{-4}$
O_2	$4.2 \pm 0.4 \times 10^{-5}$
CO_2	$2.4 \pm 0.2 \times 10^{-4}$

It should be noted that extrapolation of the plots of Figure II-4 lead to constant but non-zero intercepts. This appears to arise as consequence of the particular experimental set up. That is,

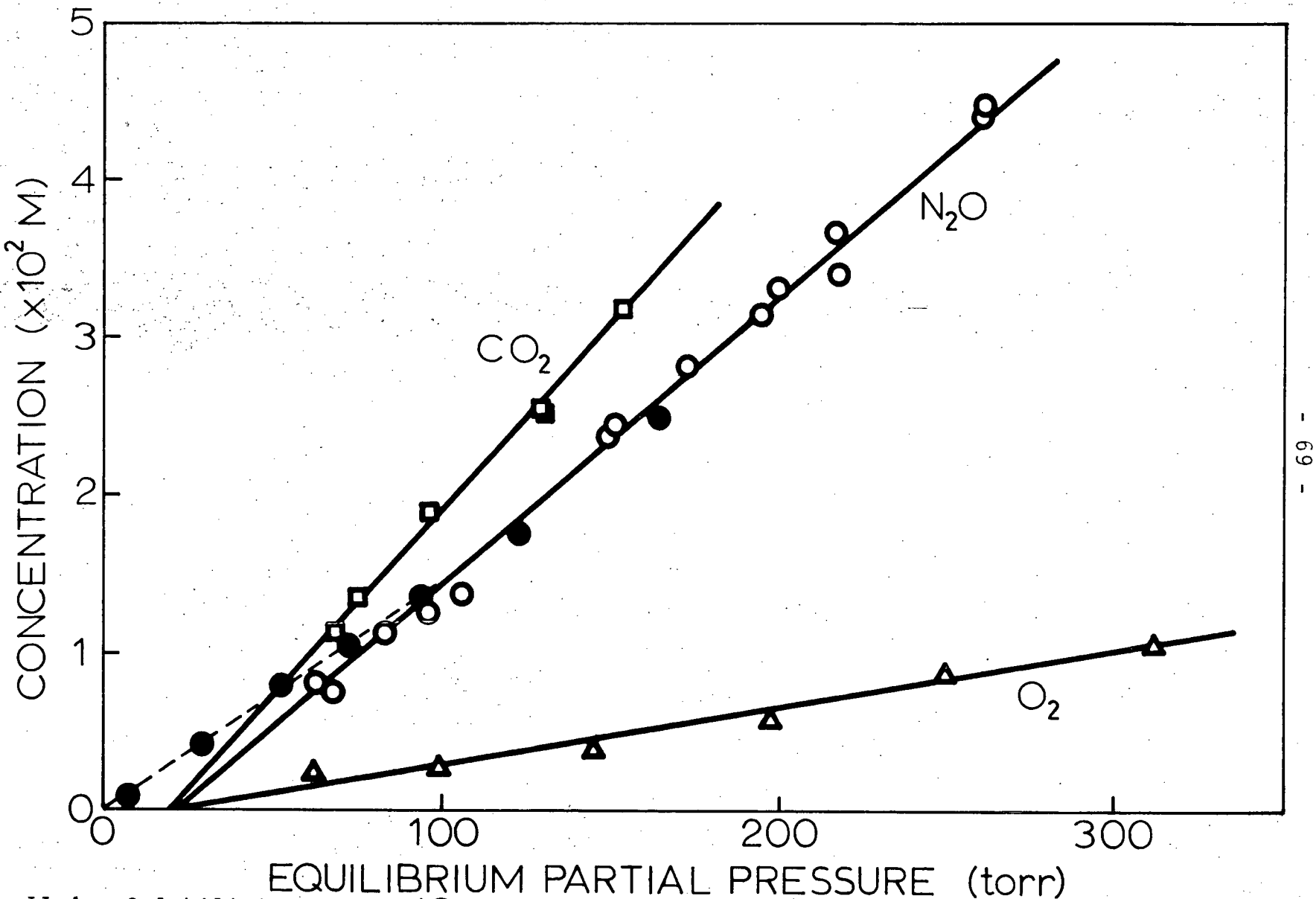

Figure II-4. Solubilities of N_2O (○), CO_2 (□), and O_2 (△) at 23 °C in HMPA measured in the reaction vessel. Filled circles indicate N_2O samples using Ar as diluent.

because of a large pressure drop across the sintered disk in the reaction cell, a gas pressure of at least 100 torr was required to initiate bubbling. Presumably this pressure was essential to force liquid out of the disk so that the gas itself could pass through.

Unfortunately, the initial pressure requirement of 100 torr tended to place a lower limit on the concentration of scavenger that one could obtain. This was especially a problem with N_2O because it was highly desirable to produce solutions of very low but known concentrations of that scavenger. The problem was somewhat overcome by limiting the total amount of scavenger through the use of a small bulb at E. To achieve very low concentrations of N_2O, argon gas was mixed with the scavenger to provide the required initial pressure. That is, very small amounts of N_2O were transferred to bulb F, then sufficient argon transferred to bulb E to ensure the mixture of gases in E and F could initiate bubbling. Argon itself was found to be essentially insoluble in HMPA. The N_2O pressures were still of sufficient magnitude so as to allow ideal gas calculations. The filled circles and the dashed line in the figure show the solubility relationship obtained for N_2O in HMPA at 23 °C when used in conjunction with constant amount of argon "carrier" gas. In that case, the slope gives a value for the N_2O solubility $S_{N_2O/Ar} = 1.47 \pm 0.05 \times 10^{-4}$ M/mm for low N_2O pressures which should be compared to the value for N_2O along at higher pressure of $S_{N_2O} = 1.85 \pm 0.05 \times 10^{-4}$ M/mm.

It must be emphasized that this is a purely empirical relationship applying to a particular experimental arrangement. Where extremely low concentrations ($<10^{-3}$M) of N_2O were desired, ideal gas calculations were impractical, so the N_2O composition was obtained from an extrapolation of the data of Figure II-4. Admittedly this was pushing the system beyond reasonable limits and undoubtedly led to large uncertainties in the actual N_2O concentrations. However, the method appeared to give sensible and consistent results and certainly one could expect the proportionality between N_2O additions to be preserved.

It was desired to compare experiments in which equal concentrations of N_2O were added to various mixtures of water and HMPA. Solubility data was obtained for a number of mixtures and the results are shown in Figure II-5.

When samples containing the desired concentrations of scavengers were prepared, S_{13} was closed, the cell removed from the vacuum line and the sample irradiated with an appropriate dose of gamma radiation in the Gammacell.

b) Sodium Metal Solutions

The reaction cell used in the study of the effects of the dissolution of sodium metal in HMPA solutions is depicted in Figure II-6. Though somewhat different in design from the radiolysis vessel, this cell possessed similar capabilities. HMPA containing various materials introduced directly into the cell (including sodium metal) could be degassed with an

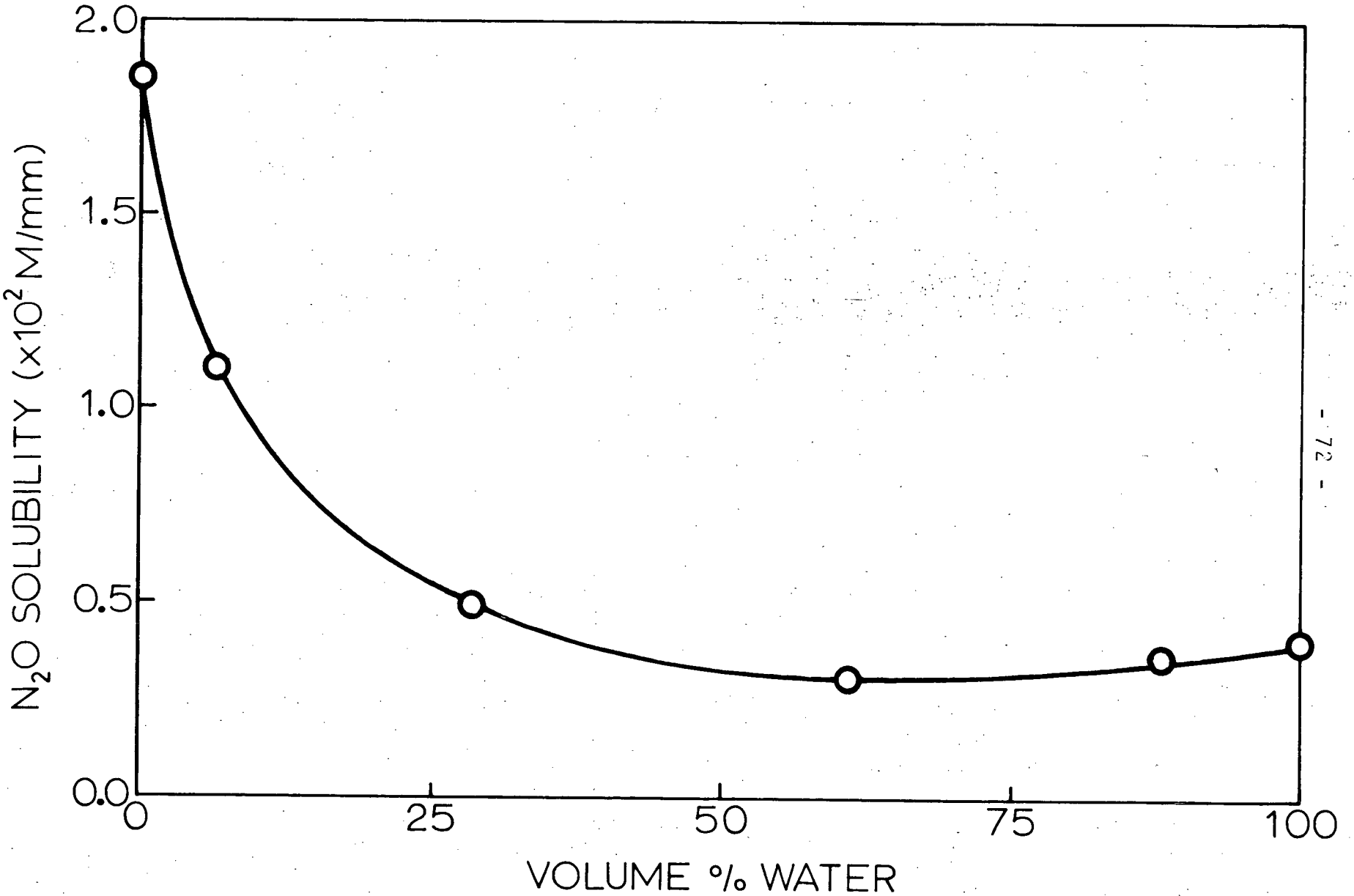

Figure II-5. Solubility at 23 °C of N_2O in H_2O/HMPA mixtures.

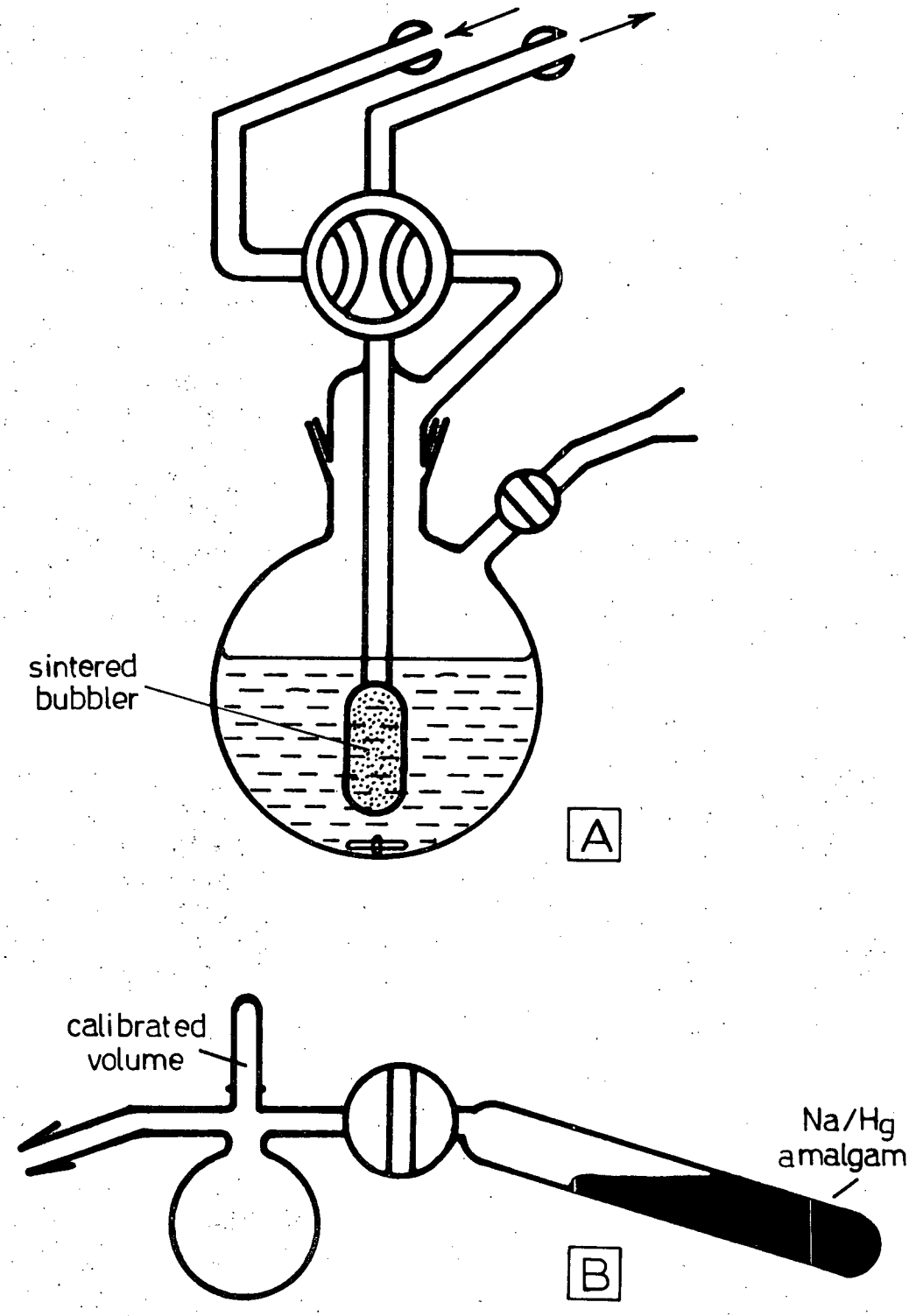

Figure II-6. A. Reaction vessel for sodium metal solutions.
B. Sodium/mercury amalgam preparation and addition accessory.

inert gas purge via the sintered bubbler. The outlets were compatible with the vacuum system leads so that the vessel could be evacuated and gaseous scavengers added. A side arm provided access for introduction of measured aliquots of prepared sodium/mercury amalgams. Transfer could be performed in vacuo or, if the reaction vessel contained volatile materials, the amaglam quickly forced into the cell by means of an excess pressure of argon. A small Teflon stirring magnet was used in the reaction vessel to agitate the amalgam thereby increasing its reactive surface area. Upon completion of reactions, the bubbler facilitated quantitative recovery of gaseous materials for analytical purposes.

5. Analysis

Sample analysis was performed using a Varian Aerograph Series 1700 Chromatograph with dual 20 foot by ¼ inch stainless steel columns. The columns, containing 13X molecular sieve material, were maintained at 50 °C. Argon carrier gas with a flowrate of 30 ml min^{-1} was eluted through WX thermal conductivity detectors. These detectors, maintained at 110 °C, were operated at a filament current of 100 mA. Output was monitored via a Westronics chart recorder. Figure II-7 gives a schematic diagram of the external sample and standard inlet arrangements.

Following radiolysis or reaction with sodium metal or amalgam the cell in question was attached to the chromatograph

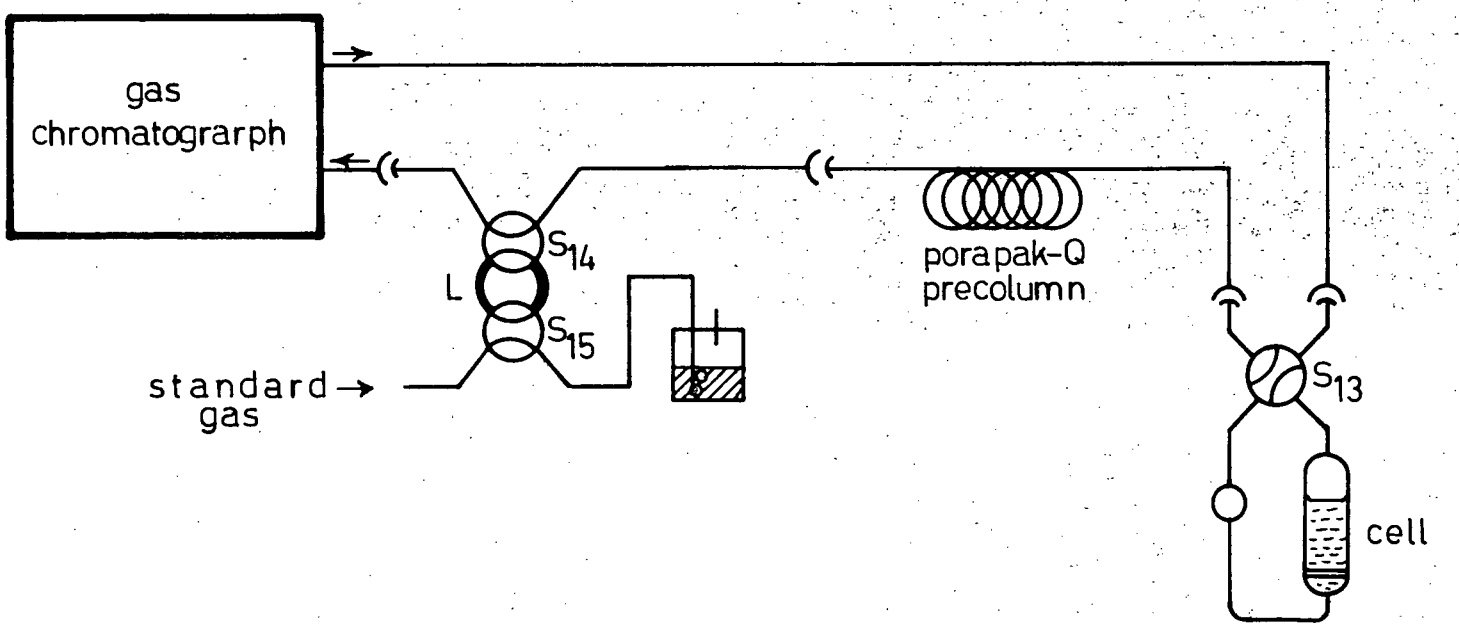

Figure II-7. Schematic diagram of chromatographic gas standard and sample injection system.

as shown in Figure II-7. The various stopcocks were turned so as to flush the air from the external line and cell leads. When the air slug had eluted, the cell stopcock S_{13} was rotated 90° which flushed gases from the cell into the chromatograph. Various standard gases were introduced at atmospheric pressure via S_{15} into the calibrated standard loop L. When it was convenient, such standards were injected through S_{14} into the chromatograph. Interchanging loop L and the reaction cell (and pre-column) allowed one to inject known amounts of various gases into the reaction cell immediately prior to analysis. Products were identified by comparing their retention time with known standards. Over the range studied, the detector response was linear for the gases monitored thus quantitative results were obtained by triangular integration of the recorder output peaks. Table III lists typical values for the response time and detector sensitivity of a number of gases for the conditions outlined. A typical chromatogram is shown in Figure II-8.

TABLE III

GAS	Retention Time (min)	Detector Sensitivity (cm^2/μmole)
H_2	8	58.1
O_2	13	6.6
N_2	23	5.2
CH_4	35	15.2
C_2H_2	>60	12.7

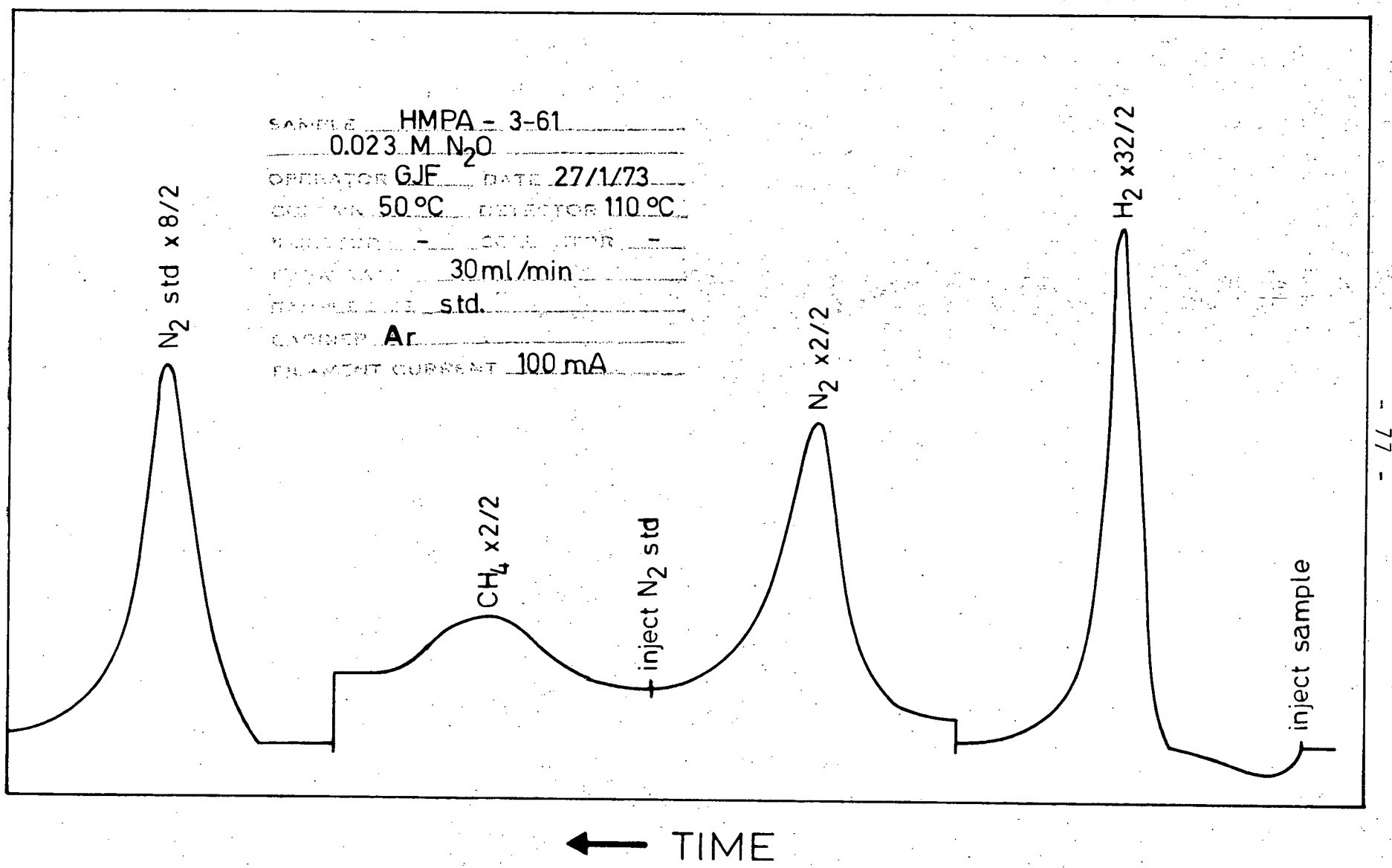

Figure II-8. Typical chromatogram obtained from an irradiated sample of HMPA containing N_2O.

B. PULSE RADIOLYSIS

1. General Outline of the Technique

Pulse radiolysis studies of HMPA were conducted during brief visits to the Ohio State University. The radiation facilities at the establishment were particularily well suited to the types of experiments that might remove many of the ambiguities inherent with indirect steady-state ^{60}Co γ-radiolysis studies. The pulse radiolysis equipment allows one to directly observe transient absorptions produced by short bursts of ionizing radiation. Figure II-9 is a simplified schematic diagram showing the layout of the various components. A portion of the electron beam from the linear accelerator was absorbed in an irradiation cell containing the sample under study. Any transient species formed as a result of such interaction which absorbed between 300 and 2300 nm were monitored by means of a beam of analyzing light passing through the sample cell at right angles to the electron beam. Through the judicious selection of the sample, filters, detector and settings of the monochromator and oscilloscope, spectral and kinetic information was obtained for a number of transient species.

2. Sample Preparation

Dow Chemical Company "Dorcol" brand HMPA was purified by

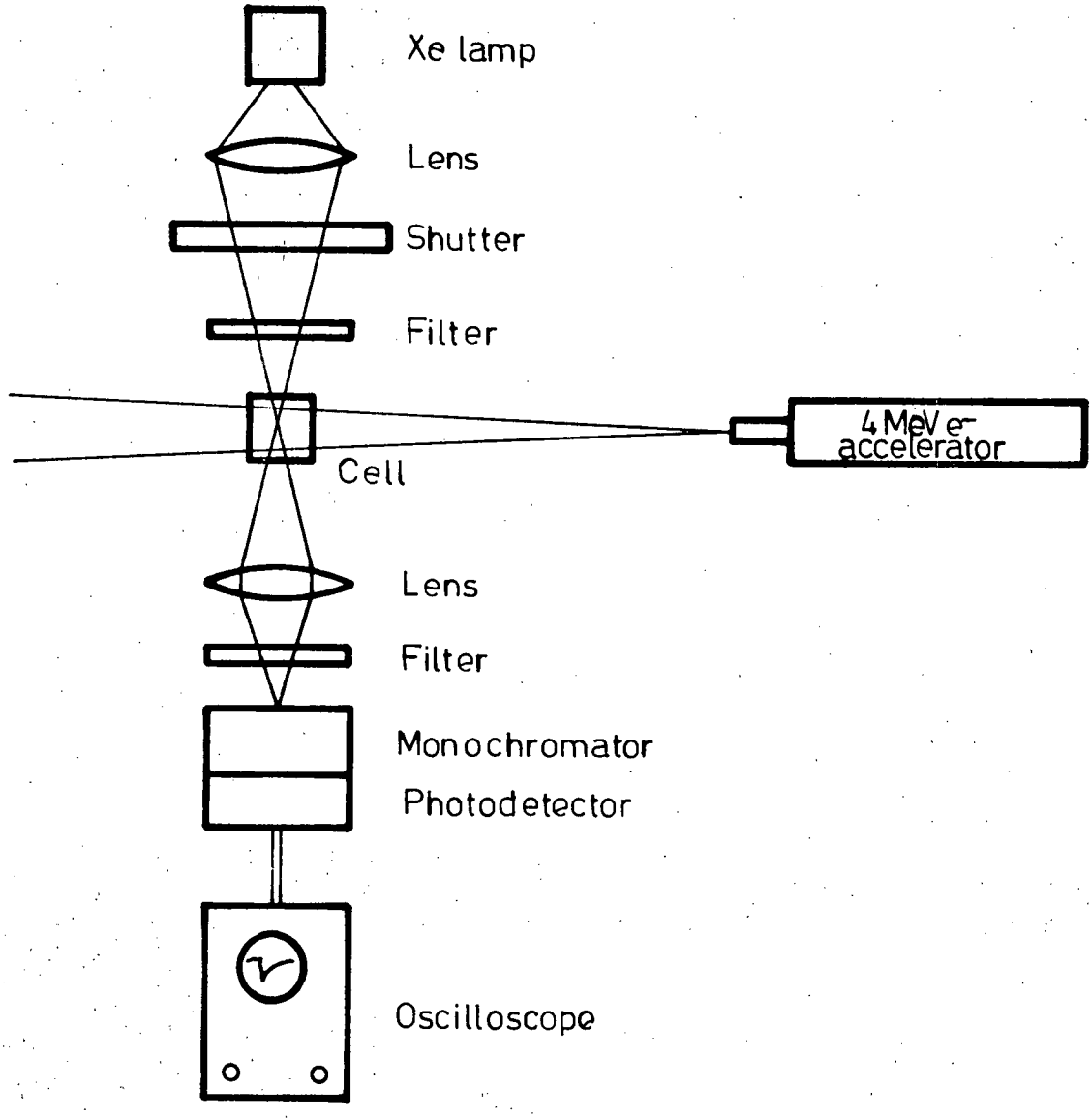

Figure II-9. Simplified schematic of the pulse radiolysis apparatus at The Ohio State University.

stirring with metallic sodium under vacuum until a stable dark blue solution of solvated electrons was formed. This sodium solution was then fractionally distilled under vacuum, the middle portion being collected in a scrupulously clean evacuated flask equipped with a Teflon stopcock. Samples for irradiation were prepared by re-distilling HMPA from this storage bulb directly into radiolysis cells. A typical cell is shown in Figure II-10. Again, only Teflon stopcocks were employed, and attachment of the cell to the vacuum system was achieved through the use of Solv-Seal glass and Teflon joints. Each cell included a large heart-shaped chamber which facilitated the removal of traces of dissolved gases through a multiple freeze-pump-thaw procedure. A long side arm terminated by a precision optical cell provided a means whereby small portions of the bulb sample could be irradiated and observed. Optical cells were either Suprasil quartz with an optical path of 20 mm or thin Vitrosil (3 mm path length). The path of radiation through the cell was at right angles to the optical path and was 10 mm in length. The cell shown in the diagram had a small chamber between two Teflon stopcocks which could be used to introduce under vacuum, small known amounts of solutes.

Chemicals used as scavengers were analytical reagent grade or better. Anthracene and pyrene, used in the solvated electron yield determination, were Aldrich "Gold Label" zone-refined (99.9+% purity) grade. Gaseous scavengers were purified by multiple trap-to-trap distillation on the vacuum line.

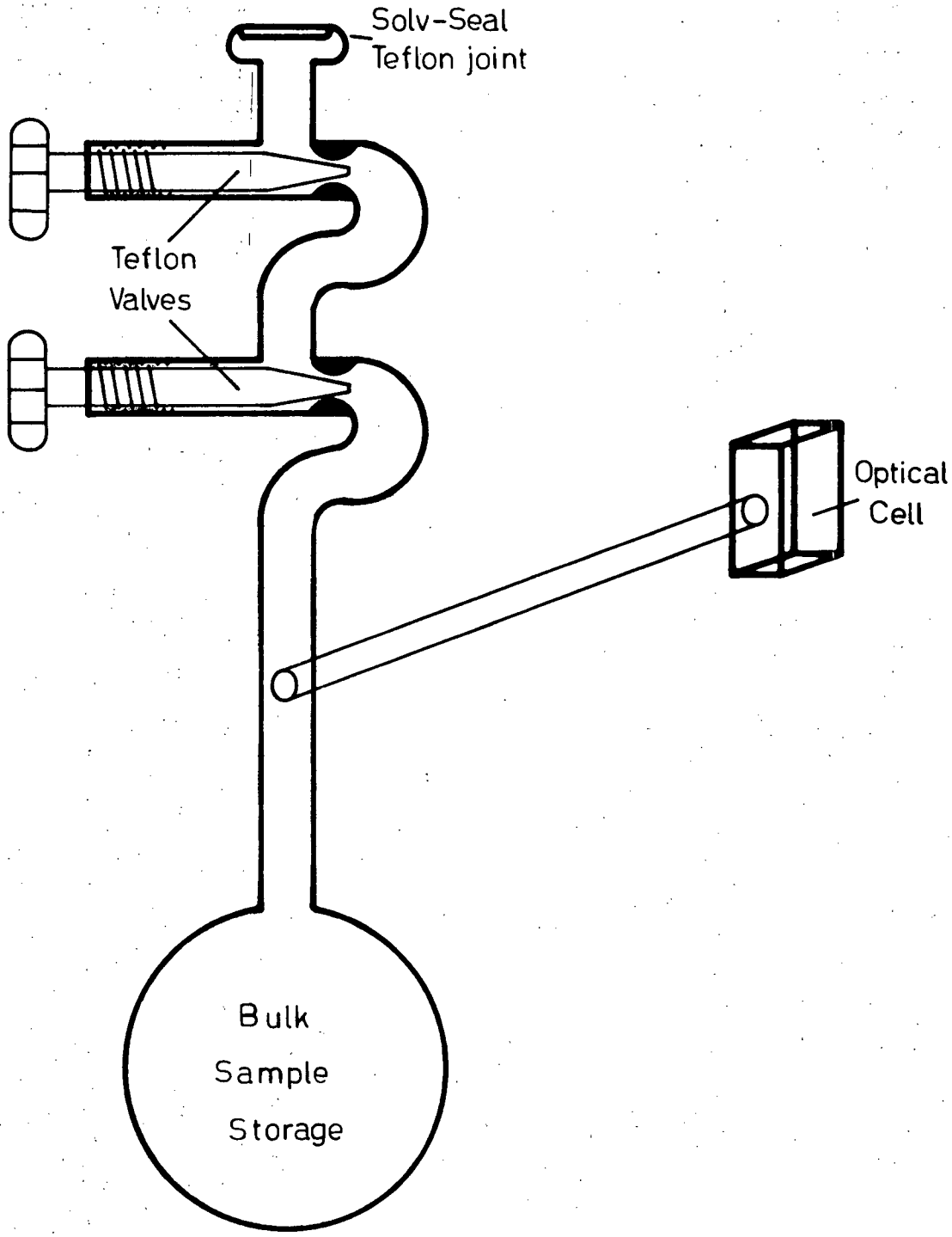

Figure II-10. Pulse radiolysis sample preparation and irradiation vessel. The optical cell (20 X 10 X 5 mm) has Spectrosil windows.

Samples of HMPA containing very small amounts of nitrous oxide were prepared by quantitatively freezing measured amounts of the gas directly into the radiolysis cell. The resulting scavenger concentration could then be calculated from known parameters. That is, assuming ideal gas behavior, the number of moles, n, of nitrous oxide transferred from a small bulb on the vacuum line is given by (xxii).

$$n = \frac{P_I V_I}{RT_I} \qquad \text{(xxii)}$$

where P_I = N_2O pressure in bulb (mm Hg)
V_I = bulb volume (l)
T_I = bulb temperature (°K)
R = 62.3 mm Hg $°K^{-1}$ $mole^{-1}$

After quantative transfer to a radiolysis cell containing a known amount of HMPA, the nitrous oxide has components in both the liquid and gas phases (xxiii).

$$n = \frac{P_F V_G}{RT_F} + SP_F V_L \qquad \text{(xxiii)}$$

where P_F = pressure of nitrous oxide (mm Hg) above HMPA
V_G = volume of gas space in radiolysis cell (l)
V_L = volume of HMPA liquid (l)
S = solubility of N_2O in HMPA (1.85×10^{-4} M/mm Hg)

T_F = radiolysis cell temperature (°K)

Assuming the temperature of the two bulbs were equal (i.e. allowed to reach ambient room temp.), one can combine equations (xxii) and (xxiii) obtaining the final equilibrium pressure of N_2O in the radiolysis cell (xxiv),

$$P_F = \frac{V_I P_I}{(V_G + V_L SRT)} \qquad \text{(xxiv)}$$

and therefore the concentration of N_2O in solution, $\left[N_2O\right]_{HMPA}$, by equation (xxv).

$$\left[N_2O\right]_{HMPA} = P_F S \qquad \text{(xxv)}$$

For 100 mm N_2O in a 13.37 ml bulb transferred to a cell containing 86.0 ml HMPA and having a gas space of 20.1 ml the final concentration of N_2O in HMPA was calculated to be $(7.9 \pm 0.2) \times 10^{-4}$M.

3. Pulse Radiation Source

A Varian V-7715A microwave linear accelerator (linac) was used as a source of high energy electrons. This machine produced electron pulses in the energy range 2 - 6 MeV with pulse width continuously variable from 0.005 to 1.6 μsec. Most of the present experiments utilized single pulses of 4 MeV

electrons at a pulse current of 300 mA, corresponding to a dose rate of about 10^{10} rad sec^{-1}. Pulse to pulse reproducibility of the accelerator was generally better than ±5% of the mean.

Through the use of a ferroelectric device, it was possible to examine in detail the shape, intensity, and duration of radiation pulses. That device made from a ceramic material containing lead zirconate titanate (PZT) has a large pyroelectric coefficient. Incident radiation produces an instantaneous small temperature increase in the device which delivers an electrical impulse corresponding to the time rate of temperature change. The device was particularly useful for monitoring the linac pulses because it had a rise time of less than two nsec and responded linearily to even very intense energy fluxes. Figure II-11 depicts the response of the PZT device to a 600 nsec electron pulse. As can be seen, the linac produces remarkably near-rectangular pulses of electrons.

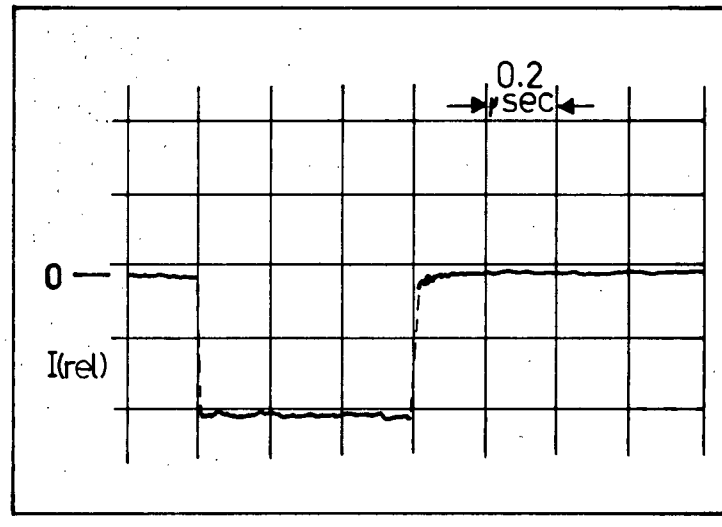

Figure II-11. Shape of linac electron pulse.

4. Optical Detection

a) Analysing Light Source

Transient species produced in the sample were studied by observing their optical absorption spectrophotometrically. A 500 watt Osram xenon-arc lamp, type XBO, was used as white light source. The lamp could be operated in either constant intensity or flashed modes. When a pulsed current of 150A was added to the continuous operation current of 20A, the lamp intensity was increased by a factor of 25 to 40 depending on wavelength. The resulting light pulse lasted several milliseconds and had a usable constant intensity portion of about 100 µsec which could be sychronized with the accelerator electron beam. Figure II-12 shows the profile of a typical flash.

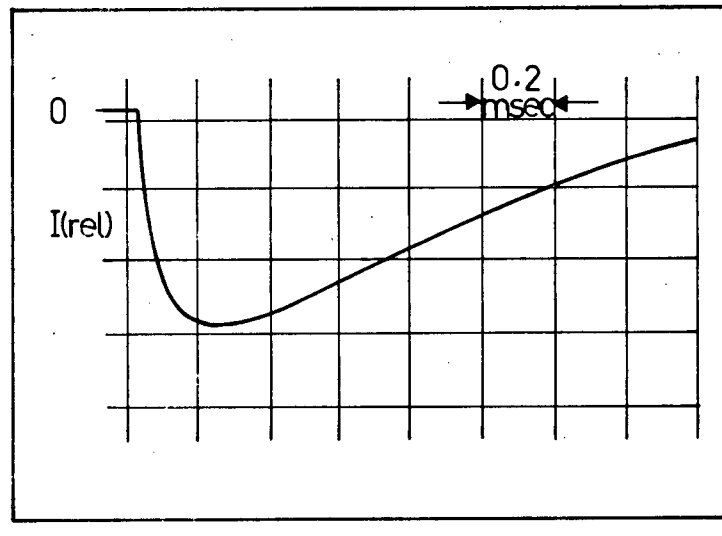

Figure II-12. Profile of the output from the Xenon-arc lamp used in pulse mode.

The output from the lamp was focussed onto the reaction cell and again on the monochromator entrance slit. Until just prior to each radiation pulse, the shutter was closed to prevent heating and photolysis of samples by the lamp -- operating in its constant intensity mode.

b) Wavelength Selection

A Bausch and Lomb f/3.5 grating monochromator, type 33-86-26 was used in conjunction with a number of gratings. Table IV lists pertinent information for the gratings.

TABLE IV Bausch and Lomb Gratings used in the pulse radiolysis experiments.

Grating Type	Spectral Region (nm)	Dispersion (nm/mm)
33-86-02	350 - 800	6.4
33-86-03	700 - 1600	12.8
33-86-04	1400 - 3200	25.6

Each grating was calibrated in the monochromator with reference to line emissions from a lamp containing Hg, Ar, Xe, and He.

Appropriate Corning glass filters were placed in the optical path -- before the radiolysis cell to prevent sample photolysis -- and before the monochromator to eliminate second-order components (especially from Cerenkov radiation) and the

effects of scattered light.

c) Detection

Transient absorptions below 1200 nm were measured through the use of one of several photomultiplier tubes (RCA 7200, 7102, 1P28 or HTV 196). For wavelengths between 800 and 2300 nm an indium-antimonide photodiode was employed. This device was mounted behind a sapphire window on a cold finger of a liquid nitrogen dewar. It had a sensitive area of about 0.04 cm^2 and was connected directly to the input of a high-speed solid state operational amplifier.[82] The 10 - 90% rise-time of this infra-red detector was about 100 nsec. Experiments generally utilized a Tektronix 545 dual beam oscilloscope. For some studies, where faster time resolution was particularly desirable, a photomultiplier system with a 2 nsec rise-time (RCA 1P28) was used with a Fairchild 777V oscilloscope. A resolution time of 5 nsec was attained with this arrangement. Permanent records of the transient signals were captured on Polaroid speed 3000 or 10,000 film. In addition, the various shutters and pulses were timed such that traces from signals representing zero and 100 percent transmission of the analyzing light through the reaction mixture were also recorded on each photograph. Figure II-13 is a tracing of a typical photograph in which these features can be seen.

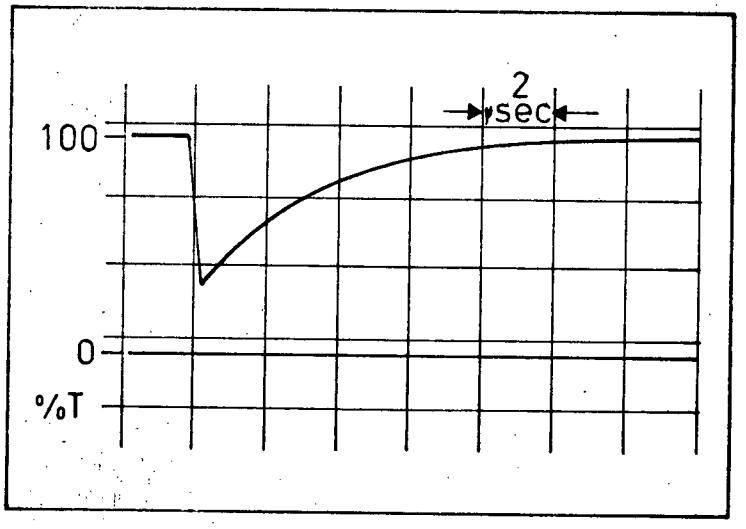

Figure II-13. Typical oscilloscope trace showing a transient absorption in HMPA following a 400 nsec radiation pulse.

It can be seen that through the judicious selection of experimental parameters one could obtain a detailed history of the formation and decay of transient species following irradiation.

d) Dosimetry

Measurement of the energy absorbed by the samples per radiation pulse was performed through the use of aqueous potassium thiocyanate as a chemical dosimeter. Dosimetry was carried out in cells of the same type and dimensions as those containing the samples. Measurements were made just prior to investigations on various samples. After completion of a series of experiments (or periodically during long

experiments) dose measurements were again made to ensure that the accelerator conditions had not changed.

Radiolysis of aqueous KCNS solutions gives rise to a long lived species having an absorption maximum at 475 nm. Curve A in Figure II-14 shows the spectrum obtained from a solution of 0.1 M KCNS saturated with nitrous oxide. The absorption had been assigned[83] to the thiocyanate radical formed from reaction of hydroxyl radicals (2.10).

$$\dot{OH} + CNS^- \longrightarrow \dot{CNS} + OH^- \qquad (2.10)$$

Later, Adams et al.[84] reported a value for the molar absorptivity $\varepsilon_{500} = 7.1 \times 10^3\ M^{-1}\ cm^{-1}$ and conceeded that the data was also consistent with the transient being a dimeric species, $(CNS)_2^-$ (2.11).

$$\dot{CNS} + CNS^- \longrightarrow (CNS)_2^- \qquad (2.11)$$

Baxendale et al.[85] confirmed the formation of this dimeric species. Behar and co-workers[86] observed two transient intermediate precursors of $(CNS)_2^-$ with maxima at 330 nm and 390 nm. The former was attributed to the thiocyanate radical, $\dot{CNS}$ and the later was assigned to a new intermediate species, $CNSOH^-$ (2.12, 2.13).

$$\dot{OH} + CNS^- \longrightarrow CNSOH^- \qquad (2.12)$$

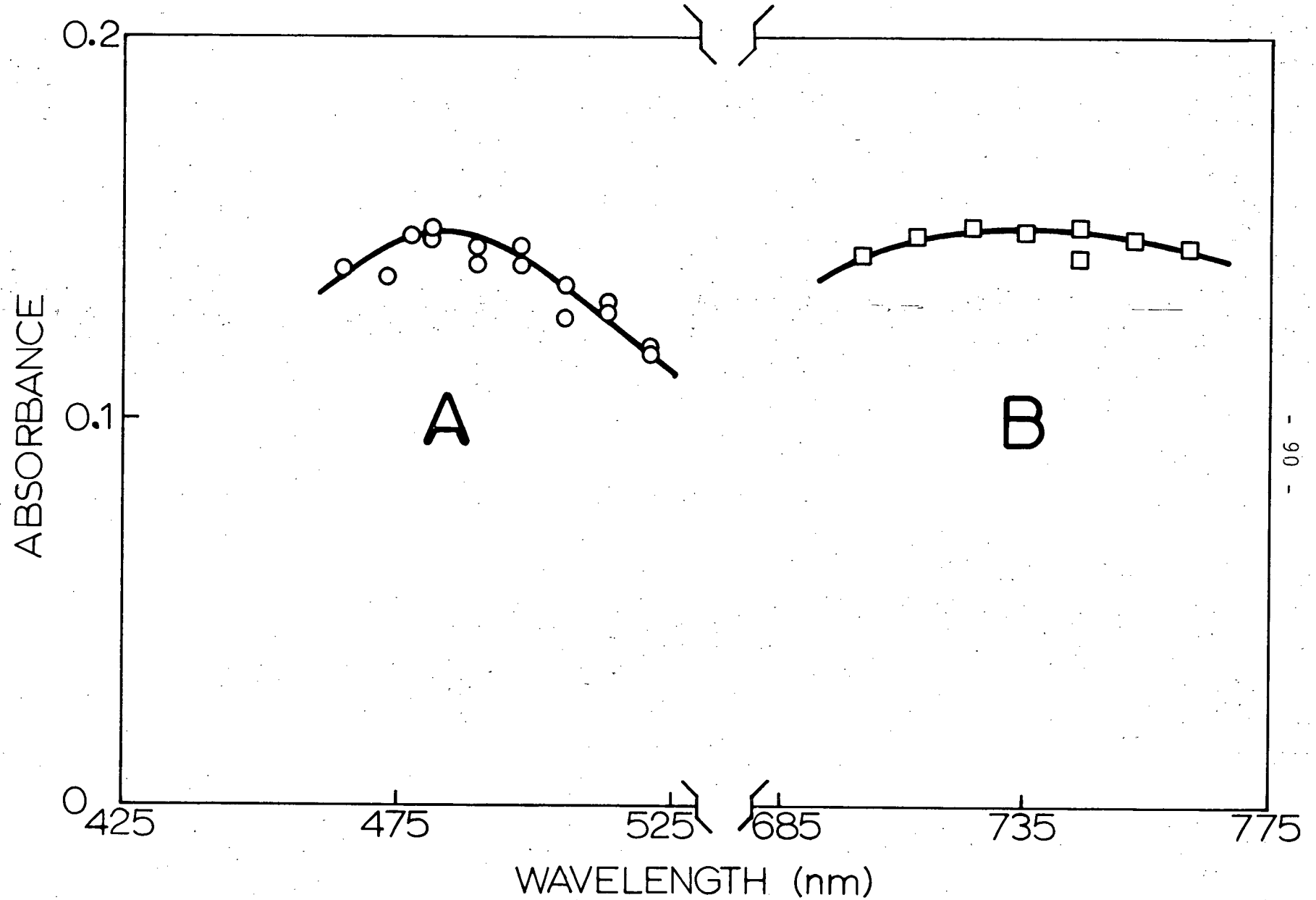

Figure II-14. Radiation Dosimetry. Transient absorptions resulting from 100 nsec pulses of 4 MeV electrons observed in a cell having an optical path length of 20 mm and containing A, aqueous KCNS solution and B, triply distilled water.

$$CNSOH^- \longrightarrow \dot{C}NS + OH^- \qquad (2.13)$$

In neutral water, $G(\dot{O}H) = 2.9$ and for solutions containing greater than about 5×10^{-3}M CNS^-, all reactions of hydroxyl radicals save (1.10) are suppressed. For such solutions $G\left((CNS)_2^-\right) = G(\dot{O}H) = 2.9$.

In the presence of a saturated solution of nitrous oxide, hydrated electrons are converted to hydroxyl radicals (2.14).

$$e_{aq}^- + N_2O \longrightarrow \left[N_2O^-\right] \xrightarrow{H_2O} \dot{O}H + OH^- + N_2 \qquad (2.14)$$

Under those conditions, the $(CNS)_2^-$ yield is given by (xxvi).

$$G\left((CNS)_2^-\right) = G(\dot{O}H) + G(e_{aq}^-) = 5.7 \qquad (xxvi)$$

where the hydrated electron yield is taken as 2.8.

For a species of known G value and molar absorptivity, absorbed dose, D, is given by (xxvii).

$$\dot{D}(eV\ l^{-1}) = \frac{AN_o}{\varepsilon l G} \qquad (xxvii)$$

where A = absorbance of dosimeter species

N_o = Avagadro's number (molec $mole^{-1}$)

ε = molar absorptivity of dosimeter species ($mole^{-1}$ l cm^{-1})

l = optical path length (cm)

G = G value of dosimeter species (molec $(100\ eV)^{-1}$)

The dose absorbed by the HMPA samples was obtained by correcting for the relative electron densities of HMPA and water. The absorbed dose from a 400 nsec pulse was typically 4×10^{20} eV/l. Pulse to pulse reproducibility of the accelerator was usually better than ±5% of the mean.

As a check, a second dosimeter -- pure water -- was employed. Curve B in Figure II-14 shows the spectra obtained in the region near 715 nm from the radiolysis of triply distilled water. A value of $G\varepsilon^{e^-_{aq}}_{715} = 5.0 \times 10^4\ M^{-1}\ cm^{-1}$ molec $(100\ eV)^{-1}$ was taken for the hydrated electron at 715 nm.[87] Because the hydrated electron is relatively short-lived, the results were corrected to account for decay during the pulse. The two dosimetry techniques gave results within about 10% of each other. The results of the thiocyanate dosimeter, by virtue of the stability of its absorbing species, were averaged and used in the calculations.

CHAPTER III

RESULTS AND DISCUSSION

A. RESULTS: STEADY STATE EXPERIMENTS

1. Gamma Radiolysis Studies

a) Pure HMPA

Gamma radiolysis of samples of HMPA at 23 ± 2 °C yielded hydrogen and methane as gaseous products. Figure III-1 shows the yields of these products obtained from four different samples of HMPA as a function of accumulated dose. The methane yield was independent of dose up to at least 1.5×10^6 rads (9.4×10^{19} eV g^{-1}). From the slope of the line the yield of methane, $G(CH_4)$, expressed as molecules per 100 eV of energy absorbed, was calculated to be:

$$G(CH_4) = 0.29 \pm 0.03$$

As can be seen in the figure, the hydrogen yield dependence was more complex. The curves were different for the samples, but each exhibited a final linear portion corresponding to $G(H_2) = 3.3 \pm 0.3$. The effect can be seen more clearly in Figure III-2. There, hydrogen and methane yields (calculated from the slope d(product)/d(Dose)) for each irradiation are

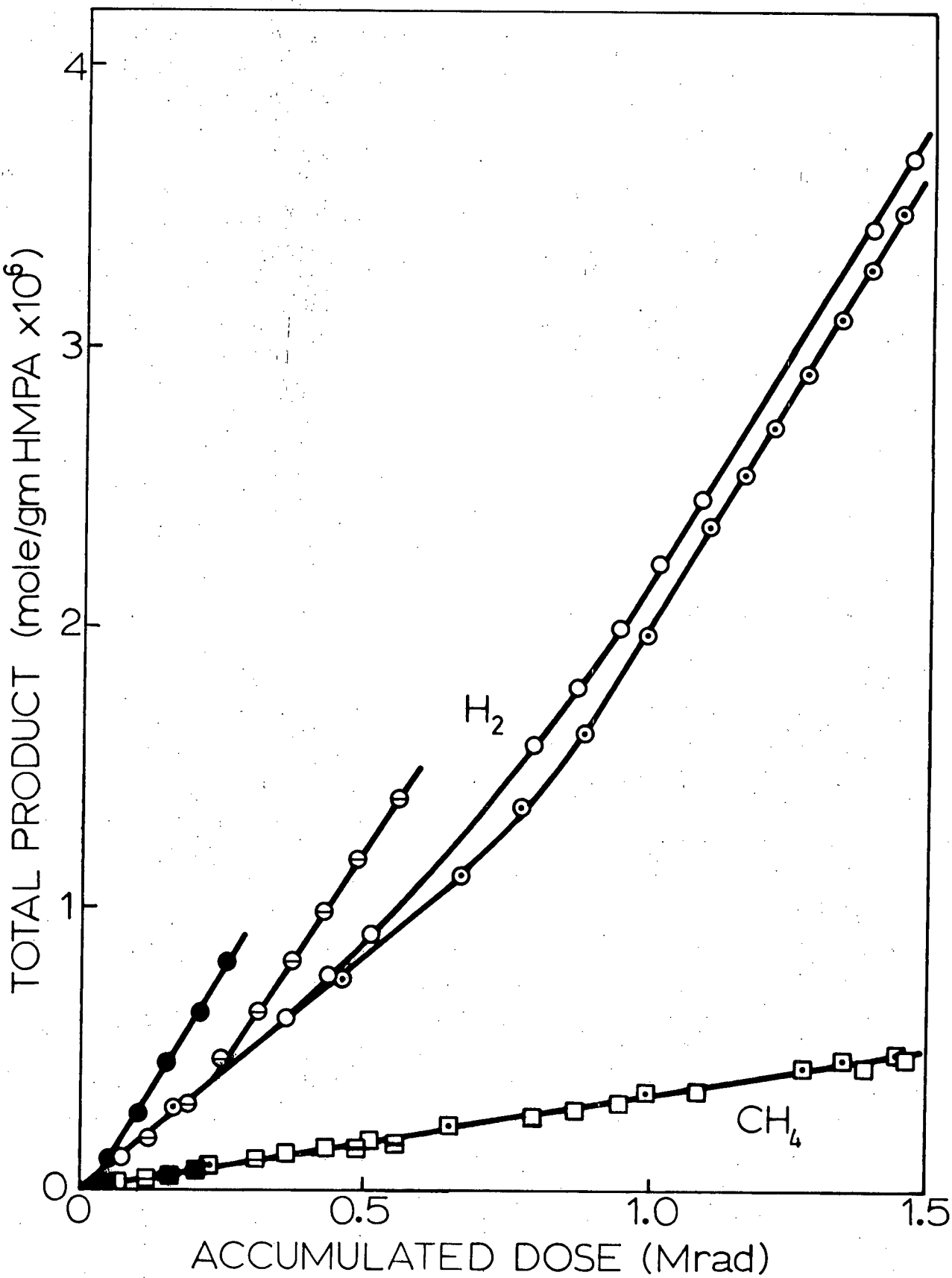

Figure III-1. Total production of hydrogen (O) and methane (□) as a function of total absorbed dose from the radiolysis of four different samples of HMPA.

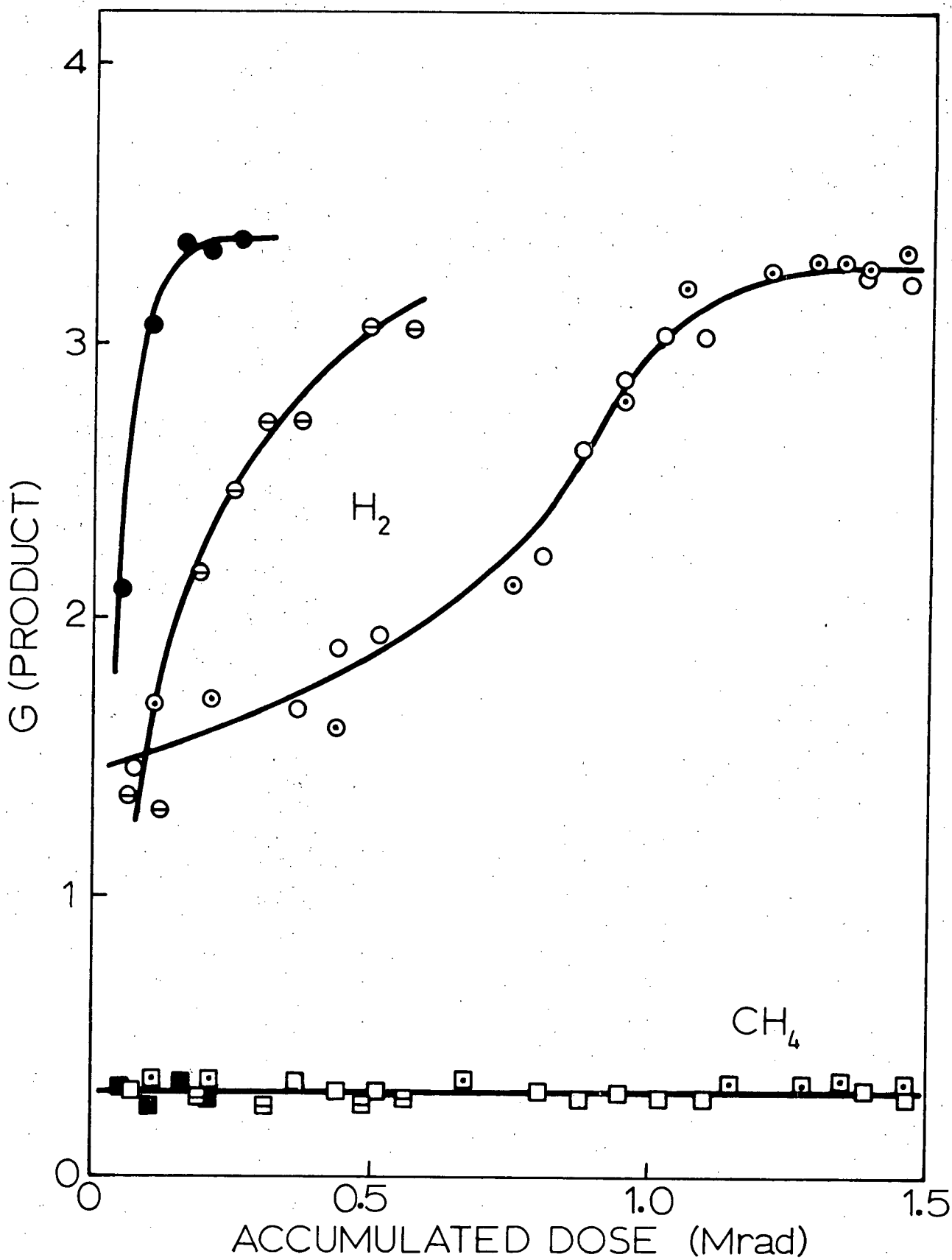

Figure III-2. Actual yields of hydrogen (O) and methane (□) as a function of total absorbed dose for the data of Figure III-1.

plotted as a function of total absorbed dose. The results suggest that the samples initially contained low concentrations of impurity which reacted with a precursor of molecular hydrogen and was consumed in the process. The samples were prepared from different batches of technical grade HMPA. Special care was taken in the preparation of sample four. That sample was subjected to several additional stages of distillation from sodium. In addition, it was stored and transferred under vacuum. The hydrogen yield data shown in Figure III-2 supports the "impurity" theory as that sample quickly attained the plateau hydrogen yield value. Radiolysis of the technical grade HMPA gave a constant low hydrogen yield $G(H_2) = 1.3 \pm 0.2$ for a total dose up to 2 Mrad.

One could not expect to subject samples of HMPA to unlimited doses of radiation without affecting the primary processes. Indeed, the production of hydrogen and methane gave evidence that molecular degradation occurs. Obviously other liquid products were also produced in conjunction with those monitored. Therefore, when it was clear that a "pure" sample condition had been obtained, various scavengers were added prior to subsequent irradiation so as to facilitate much more informative studies of the system and its reactions. After a number of experiments in which scavengers were used, the samples were once again irradiated with no added solutes. Return of the "plateau" hydrogen yield indicated that impurity build-up was probably unimportant.

b) Scavenger Studies

i) Nitrous Oxide

Nitrous oxide was used extensively in this study for the purpose of determining the yield and nature of the reducing species formed during the radolysis of HMPA. Following irradiation, samples of HMPA containing dissolved N_2O were found to contain significant amounts of molecular nitrogen. For a given concentration of N_2O, the nitrogen yield was independent of dose and total absorbed dose.

Methane gas production from HMPA radiolysis was unaffected by the presence of N_2O. The hydrogen yield on the other hand was reduced from an initial value of $G(H_2) = 3.3 \pm 0.3$ to a constant value of $G(H_2) = 1.4 \pm 0.1$ for any solution containing greater than about 10^{-3}M N_2O. Evidently N_2O reacts efficiently with a precursor of some of the hydrogen.

Figure III-3 shows a plot of the observed nitrogen yield as a function of N_2O concentration. The filled circles represent those experiments in which argon "carrier gas" was used to ensure thorough mixing of small amounts of N_2O. The nitrogen yield increased rapidly to $G(N_2)>3$ for N_2O up to about 1×10^{-2}M and then increased more slowly to $G(N_2) > 4.5$ at 1.3×10^{-1}M N_2O.

For very low concentrations of N_2O it is somewhat misleading to refer to "yields" of molecular products that are affected by the presence of that scavenger. For the HMPA sample size and

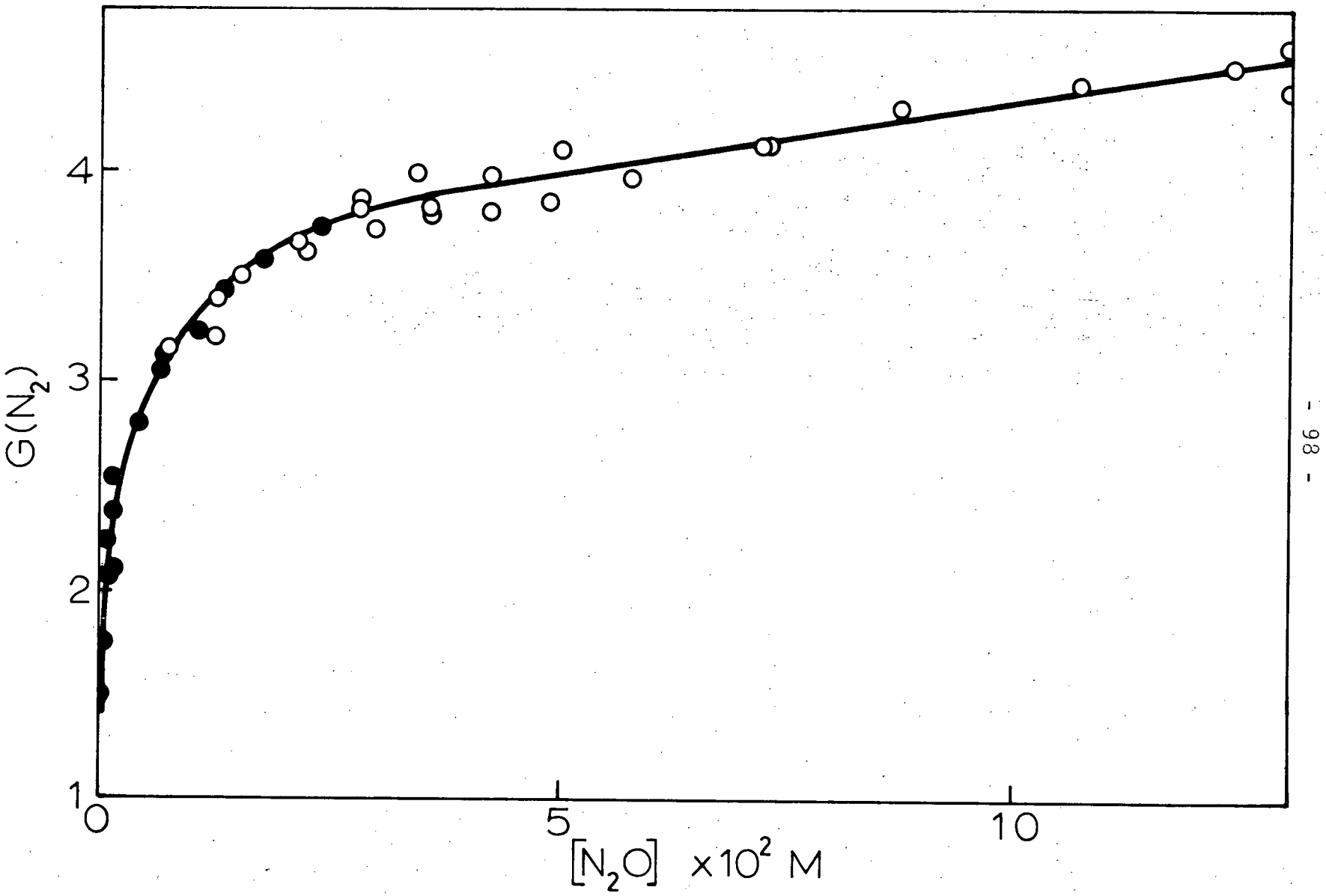

Figure III-3. Nitrogen yield from irradiated samples of HMPA as a function of nitrous oxide concentration.

radiation doses employed in these experiments, approximately 5×10^{-4}M reducing species (with a yield of 2) would be formed during the radiolysis. A scavenging reaction with N_2O could result in a substantial decrease -- possible depletion -- of scavenger from samples initially containing small amounts of N_2O. Product "yields" from such solutions are denoted as pseudo-yields, $G'(X)$, so as to differentiate them from yields obtained under constant scavenger concentration.

Figure III-4 details the pseudo-yields of nitrogen and hydrogen obtained from the radiolysis of solutions initially containing less than 1×10^{-3}M N_2O. Between 0 and 5×10^{-4}M N_2O, the hydrogen pseudo-yield decreased from $G'(H_2) = 3.4 \pm 0.3$ to $G'(H) = 1.4 \pm 0.1$. Over this same range, nitrogen formation increased from 0 to $G'(N_2) = 2.2 \pm 0.2$. It is worthy of attention that the sum of the two "yields" remained fairly constant throughout, with $G'(H_2 + N_2) = 3.4 \pm 0.3$ to 3.7 ± 0.3. These results were more suggestive of the expected "depletion" effect.

To confirm this suspicion, samples of very pure HMPA containing a constant low initial concentration of N_2O ($\sim 7 \times 10^{-5}$M) were irradiated for different lengths of time. That concentration corresponded to only one or two micromoles of N_2O in the samples. The observed effect of dose on product "yields" is given in Table V.

As one would expect, the absolute amounts of methane, hydrogen and nitrogen formed during radiolysis increased with dose. Nitrogen, however, reached a limiting value of 1.2

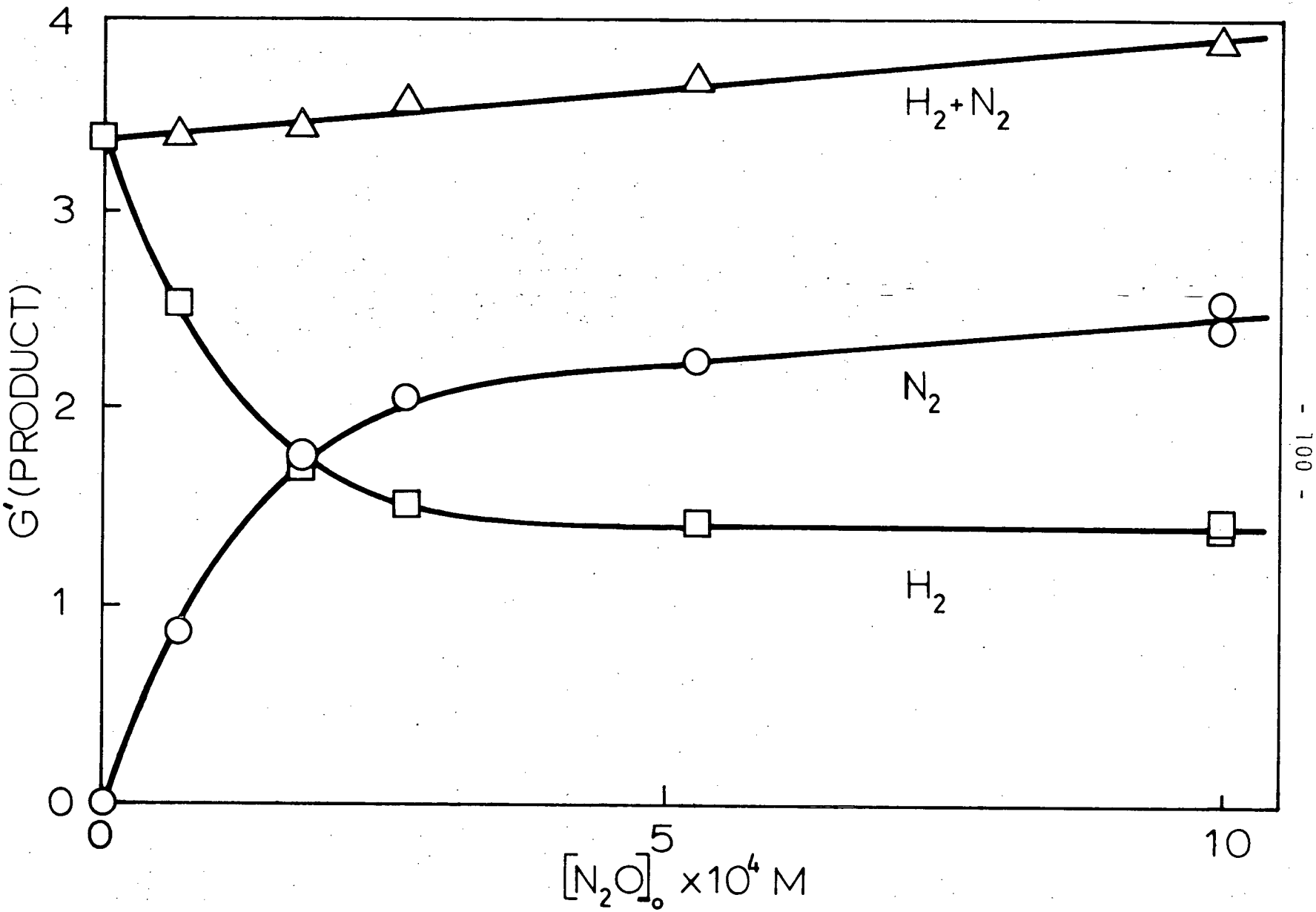

Figure III-4. Observed hydrogen (□) and nitrogen (○) "yields" from irradiated samples of HMPA containing very low initial N_2O concentrations.

TABLE V Effect of dose on gaseous product "yield" in HMPA samples initially containing 7 X 10^{-5}M nitrous oxide.

Dose (rads X 10^4)	Product Formation (μmoles)			Product "Yield"			
	CH_4	N_2	H_2	$G'(CH_4)$	$G'(N_2)$	$G'(H_2)$	$G'(N_2 + H_2)$
1.74	0.1	0.7	0.9	0.3	1.5	1.9	3.4
3.45	0.2	0.9	2.0	0.3	1.0	2.2	3.2
5.16	0.4	1.2	3.4	0.3	0.9	2.5	3.4
6.87	0.5	1.2	4.8	0.3	0.6	2.7	3.3

micromoles for the larger doses -- a value within experimental error of the total estimated initial N_2O content. Product yields (product formed per unit dose) from studies utilizing high concentrations of scavenger were independent of dose and total absorbed dose. Here, only the methane "yield" was independent of dose. The nitrogen "yield" decreased with dose while that of H_2 increased. Again, the sum of the H_2 and N_2 pseudo-yields remained constant at $G'(H_2 + N_2) = 3.3 \pm 0.1$.

The facts are consistent with a scheme in which nitrous oxide scavenges a precursor of some of the hydrogen, and that as nitrous oxide is depleted the hydrogen formation reaction predominates. Note that hydrogen formation is not precluded by the N_2O scavenging reaction but rather a simple competition for a precursor exists. Two facts from the table point to this conclusion. Firstly, in the lower dose experiments (where N_2O was not depleted) the hydrogen pseudo-yield still increased with dose. Secondly, even for the smallest dose studied (1.7×10^4 rads) the hydrogen yield $G'(H_2) = 1.9$ was higher than the plateau $G(H_2) = 1.4 \pm 0.1$ obtained from samples containing $> 10^{-3}$M N_2O.

ii) Nitrous Oxide Plus a Second Scavenger

In order to elucidate the nature of the N_2 precursor the effect of the addition of a second scavenger on gaseous product yields in HMPA and solutions of N_2O in HMPA was investigated. Several known radical and electron scavengers were employed.

Some of the data are summarized in Table VI. Silver nitrate, and sulphuric acid were unsuitable as second scavengers, as the addition of these substances led to decomposition of HMPA.

Small amounts of galvinoxyl (Gv), a stable free radical, or iodine in HMPA yielded solutions having absorption spectra characteristic of known ionic species, suggestive of interaction with solvent or impurities.

The visible absorption spectra of galvinoxyl in HMPA exhibited intense bands at 430 nm and 580 nm as shown in Figure III-5. The bands were similar in position and shape to those attributed to the galvinoxyl free radical ($\dot{G}v$) in iso-octanol and the galvinoxyl radical anion ($\dot{G}v^-$) in alkaline ethanol.[88] The species have reported extinction coefficients of 1.8×10^{-5} M^{-1} cm^{-1} and 2.2×10^{5} M^{-1} cm^{-1} respectively in those solutions. Also shown in the figure is the spectra obtained for a solution of galvinoxyl in cyclohexane, where only the free radical band was observed. It would appear that in HMPA, galvinoxyl reacted with the solvent (3.1) or some impurity, Im, (3.2) to form the galvinoxyl anion.

$$\dot{G}v + HMPA \longrightarrow HMPA^+ + \dot{G}v^- \qquad (3.1)$$

$$\dot{G}v + Im \longrightarrow Im^+ + \dot{G}v^- \qquad (3.2)$$

Examination of the absorption spectra of HMPA samples containing different amounts of galvinoxyl would tend to favour reaction with impurity (3.2). From the observed absorbances,

TABLE VI Molecular product yields from the irradiation of HMPA samples containing known amounts of N_2O and a second scavenger.

Second Scavenger	$[S_2]$(M)	$[N_2O]$(M)	$G(N_2)$	$G(H_2)$	$G(CH_4)$
NIL	-	-	-	3.2[a]	0.29
(only N_2O)	-	0.0005	2.2	1.4	0.28
		0.001	2.5	1.4	0.27
		0.01	3.4	1.4	0.29
		0.10	4.4	1.4	0.26
Water	0.22	-	-	1.4	0.27
	0.22	0.016	3.3	1.4	0.27
	0.22	0.030	3.6	1.4	0.27
	0.22	0.045	3.8	1.4	0.25
	1.0	0.045	3.8	1.4	0.24
Methanol	0.10	-	-	1.4	0.27
	0.10	0.015	3.3	1.4	0.28
	0.10	0.030	3.7	1.4	0.27
	0.10	0.044	3.9	1.4	0.26
	1.0	0.030	3.4	1.4	0.27
Acetone	0.03	-	-	1.3	0.31
	0.03	0.015	3.5	1.3	0.26
	0.03	0.030	4.2	1.4	0.28
	0.03	0.044	4.2	1.3	0.29

TABLE VI (continued)

Second Scavenger	$[S_2]$(M)	$[N_2O]$(M)	$G(N_2)$	$G(H_2)$	$G(CH_4)$
Acetone (con't)	0.27	0.013	3.8	1.3	0.28
	0.27	0.05	4.6	1.4	0.26
	0.27	0.11	5.1	1.4	0.28
$CHCl_3$	0.015	0.015	1.5	1.4	0.25
	0.015	0.029	2.2	1.4	0.26
	0.015	0.043	2.6	1.4	0.26
	0.045	0.015	0.8	1.3	0.22
	0.045	0.029	1.2	1.3	0.24
	0.045	0.044	1.6	1.3	0.24
CCl_4	0.015	0.015	1.4	1.3	0.25
	0.015	0.029	2.2	1.3	0.25
	0.015	0.043	2.6	1.4	0.25
	0.030	0.015	0.9	1.4	0.24
	0.030	0.020	1.2	1.3	0.25
	0.030	0.029	1.4	1.3	0.26
	0.030	0.044	1.8	1.3	0.26
	0.045	0.016	0.6	1.3	0.22
	0.045	0.029	1.1	1.3	0.22
	0.045	0.044	1.5	1.3	0.24
I_2	0.10	0.011	0.5	1.1	0.12
	0.10	0.018	0.7	1.2	0.11

TABLE VI (continued)

Second Scavenger	$[S_2]$(M)	$[N_2O]$(M)	$G(N_2)$	$G(H_2)$	$G(CH_4)$
I_2 (con't)	0.10	0.028	1.0	1.2	0.13
	0.10	0.051	1.5	1.1	0.12
	0.10	0.133	2.6	1.1	0.10
Galvinoxyl	0.0001	0.014	3.2	1.4	0.25
	0.0025	-	-	1.4	0.26
	0.0025	0.008	2.5	1.4	0.26
	0.0025	0.014	2.8	1.4	0.26
	0.0025	0.024	3.1	1.4	0.25
	0.0025	0.053	3.6	1.4	0.26
	0.046	0.011	0.7	1.2	0.12
	0.046	0.014	0.8	1.2	0.13
	0.046	0.025	1.2	1.2	0.11
	0.046	0.050	1.9	1.2	0.12
	0.046	0.124	2.7	1.2	0.11
O_2	0.002	0.014	3.3	1.4	0.24
	0.002	0.026	3.4	1.4	0.24
	0.002	0.042	3.9	1.5	0.25
	0.002	0.059	4.3	1.5	0.24
	0.011	0.014	3.1	1.4	0.21
CO_2	0.001	0.014	3.2	1.4	0.27
	0.015	0.014	3.3	1.4	0.25

TABLE VI (continued)

Second Scavenger	$[S_2]$(M)	$[N_2O]$(M)	$G(N_2)$	$G(H_2)$	$G(CH_4)$
CO_2 (con't)	0.034	0.014	3.3	1.5	0.26
	0.011	-	-	1.3	0.24
LiBr	0.20	-	-	1.3	0.28
	0.20	0.014	3.6	1.4	0.25
	0.20	0.028	3.8	1.4	0.23
	0.20	0.044	4.1	1.4	0.24
	0.20	0.060	4.3	1.4	0.23
	0.20	0.12	4.5	1.4	0.25

[a] data accuracy estimated to be ± (5 to 10)%.

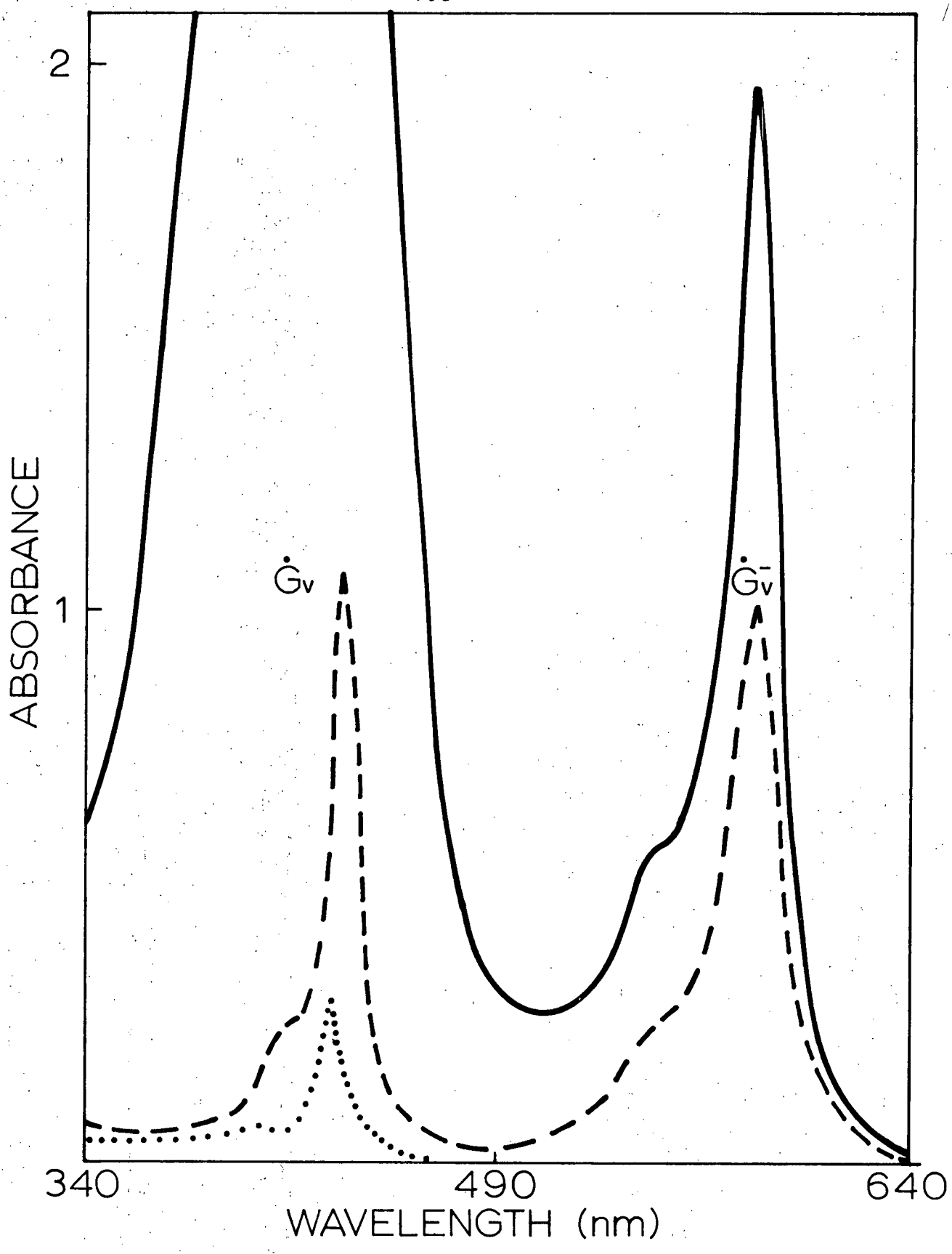

Figure III-5. Spectra obtained from a 1 mm cell containing: 2.5 X 10^{-3} M Gv in HMPA (——); 1.1 X 10^{-4} Gv in HMPA (— —); 1.4 X 10^{-5} M Gv in cyclohexane (····).

and assuming that the extinction coefficients for the radical and ionic galvinoxyl species in HMPA are identical to those reported for the other solvents, one calculates that 1.1 X 10^{-4}M galvinoxyl in HMPA produces a solution containing 5 X 10^{-5}M radical species ($G\dot{v}$) and 5 X 10^{-5}M ionic species ($G\bar{v}$).

For a more concentrated solution (containing 2.5 X 10^{-3}M galvinoxyl in HMPA) the anion band intensity increased only two fold, representing the presence of only 1.0 X 10^{-4}M galvinoxyl anion. The radical band intensity on the other hand increased many times as would be expected if most of the galvinoxyl were in its radical form i.e., 2.4 X 10^{-3}M galvinoxyl radical in the 1 mm spectrophotometer cell used, would have an absorbance at 430 nm greater than fifty. These results suggest that galvinoxyl in HMPA reacts with impurity to yield small amount of galvinoxyl anion but that for concentrations greater than 10^{-3}M the bulk of the galvinoxyl in HMPA is in its free radical form.

Iodine also showed unusual behavior when dissolved in HMPA. Figure III-6 shows the spectrum obtained for a solution of 7.6 X 10^{-4}M iodine in HMPA. This spectra, with peaks at 295 nm and 360 nm, is compared in the figure to that attributed to I_3^- observed in a solution of iodine and iodide ion in water. Buckles et al. reported the spectra of I_2, I^- and I_3^- obtained from solutions of iodine, tetramethyl ammonium monoiodide and tetramethyl ammonium triiodide in ethylene chloride.[89] They found the iodine absorption to be centered at 500 nm, the iodide ion absorption below 280 nm and the triiodide absorption with peaks at 295 nm and 365 nm similar to Figure III-6.

From its absorption spectra, 7.6 X 10^{-4}M I_2 in HMPA would appear to be present entirely as the triiodide anion, implying reaction with solvent or impurity, Im. Possible reactions might be:

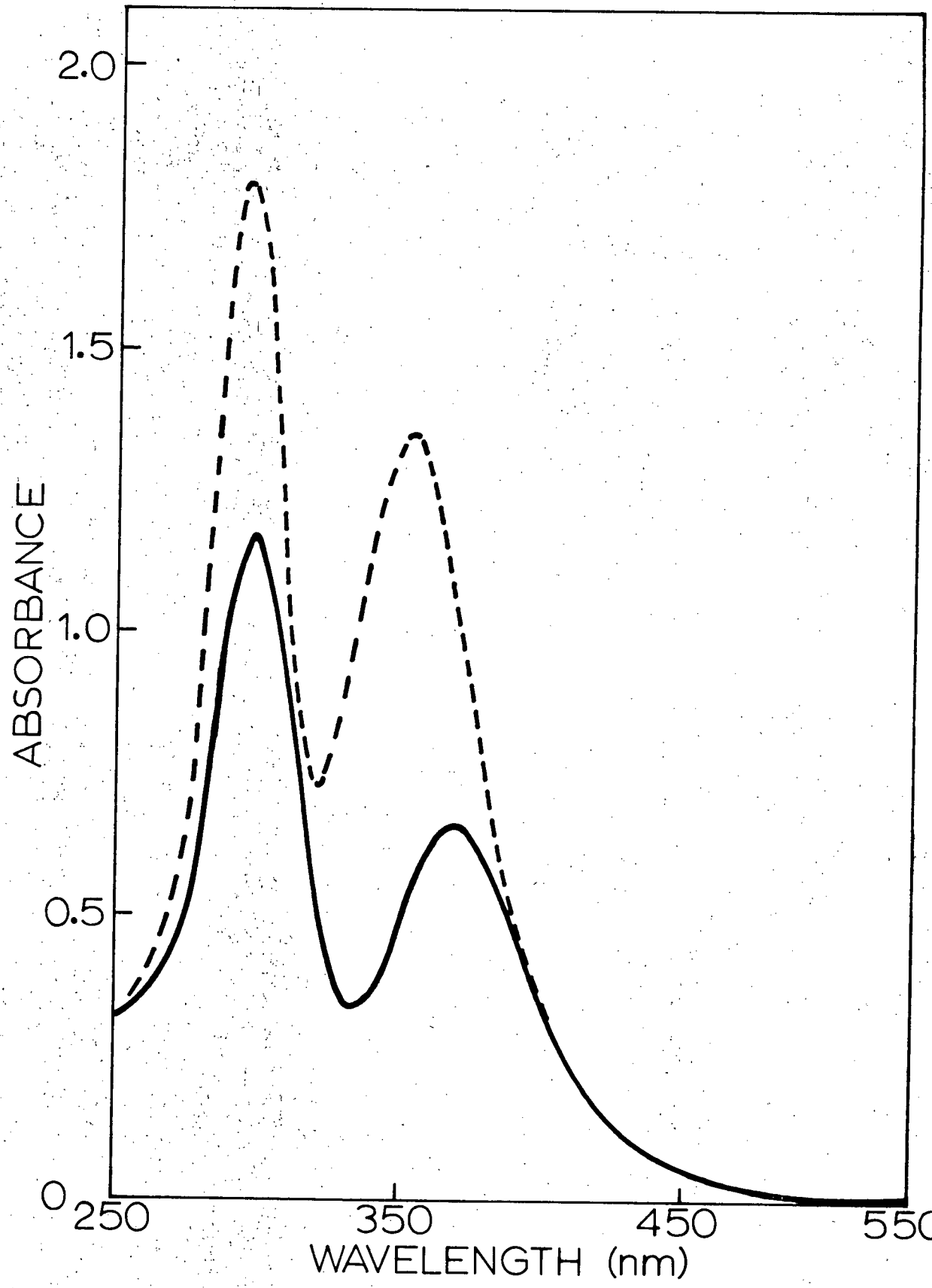

Figure III-6. Spectra obtained from a 1 mm cell containing: 7.6×10^{-3}M I_2 in HMPA (——); $\sim 10^{-3}$M KI and I_2 in water (— — —).

$$I_2 + Im \rightleftharpoons Im^+ + I_2^- \quad (3.3)$$

$$I_2 + Im^+ \rightleftharpoons ImI + I^- \quad (3.4)$$

$$I_2 + HMPA \rightleftharpoons HMPA^+ I_2^- \quad (3.5)$$

$$I_2 + HMPA^+ \rightleftharpoons HMPA^+ I + I^- \quad (3.6)$$

$$I_2^- \rightleftharpoons I + I^- \quad (3.7)$$

$$I_2^- + I_2 \rightleftharpoons I_3^- + I \quad (3.8)$$

$$I_2^- + I \rightleftharpoons I_3^- \quad (3.9)$$

$$I + I \rightleftharpoons I_2 \quad (3.10)$$

$$I^- + I_2 \rightleftharpoons I_3^- \quad (3.11)$$

Similar formation of polyiodide anions has been observed in pyridine by Andrews et al.[90] They attributed the conductivity of solutions of iodine in pyridine to IPy^+, I^-, and I_3^- ions.

Solutions of iodine in HMPA up to 0.1M showed strong absorption below 500 nm (presumably due to I_3^-) but little absorption above 500 nm where I_2 would be expected to absorb. Thus, unlike for galvinoxyl, impurity reaction with I_2 is insufficient to account for the observed formation of the polyiodide ions.

The suitability of iodine and galvinoxyl as scavengers in the HMPA system was vigorously pursued. This was because these scavengers offered a hope of obtaining independent yield data from spectrophotometric means. Unfortunately, as can be seen, both systems were too complicated for practical purposes. Both iodine and galvinoxyl possess large electron affinities. Perhaps this combined with the high basicity and unusual solvation properties of HMPA account for the observed results.

The methane yield from irradiated HMPA was little affected

by the presence of most scavengers. Iodine at 0.10M and galvinoxyl at 0.046M, both efficient electron and radical scavengers, reduced the methane yield by about 60% from $G(CH_4) = 0.29 \pm 0.03$ to 0.12 ± 0.02. The hydrogen yield was reduced from $G(H_2) = 3.3 \pm 0.3$ to a constant value of $G(H_2) = 1.4 \pm 0.1$ in the presence of most of the scavengers over a large concentration range. Exception to this were iodine at 0.10M and galvinoxyl at 0.046M which reduced the hydrogen further to values of $G(H_2) = 1.1 \pm 0.1$ and 1.2 ± 0.1 respectively.

The yield of nitrogen from solutions containing nitrous oxide and a second scavenger varied considerably. Water, methanol and carbon dioxide had little effect on $G(N_2)$. Oxygen lowered the nitrogen yield slightly when present at a concentration comparable to nitrous oxide. Iodine, galvinoxyl, carbon tetrachloride and chloroform all reduced the nitrogen yield substantially. Finally the presence of lithium bromide or acetone resulted in an increase in the nitrogen yield.

c) HMPA - Water Mixtures

Extensive studies of the radiolysis of water have fairly well established the processes which occur in that solvent. HMPA and water being totally miscible in all proportions, it was proposed that a study of HMPA/H_2O mixtures might help elucidate the mechanisms of the present study.

Of particular interest was the scavenging mechanism of N_2O in irradiated HMPA. In order to assess the situation properly,

mixtures of various HMPA/H_2O compositions were all made 0.02M in N_2O. This was achieved by determining the solubility of N_2O for each mixture and then introducing the gas at the appropriate partial pressure. The yields of nitrogen, hydrogen and methane obtained from the radiolysis of such solutions as a function of mixture composition is detailed in Figure III-7.

2. Na/HMPA Studies

a) Na Metal Solutions

Small amounts of sodium metal were added to degassed samples of HMPA. The metal dissolved slowly at room temperature to give relatively stable intensely blue coloured solutions. If left standing for several hours, the solutions slowly decayed to give stable yellow-orange solutions. The decomposition was monitored by gas chromatography and was found to proceed in part through the constant production of small amounts of hydrogen and methane. The production of these gases ceased as the last of the blue colour dissappeared -- the total yield of each representing only about 3% of the number of moles of Na metal used to prepare the solution.

The addition of excess N_2O to a sodium solution in HMPA resulted in the immediate removal of its blue colouration. The reaction was studied in more detail by passing equal amounts (27.0 μmoles) of N_2O through both blue and orange sodium metal solutions in HMPA. For calibration purposes, equivalent amounts

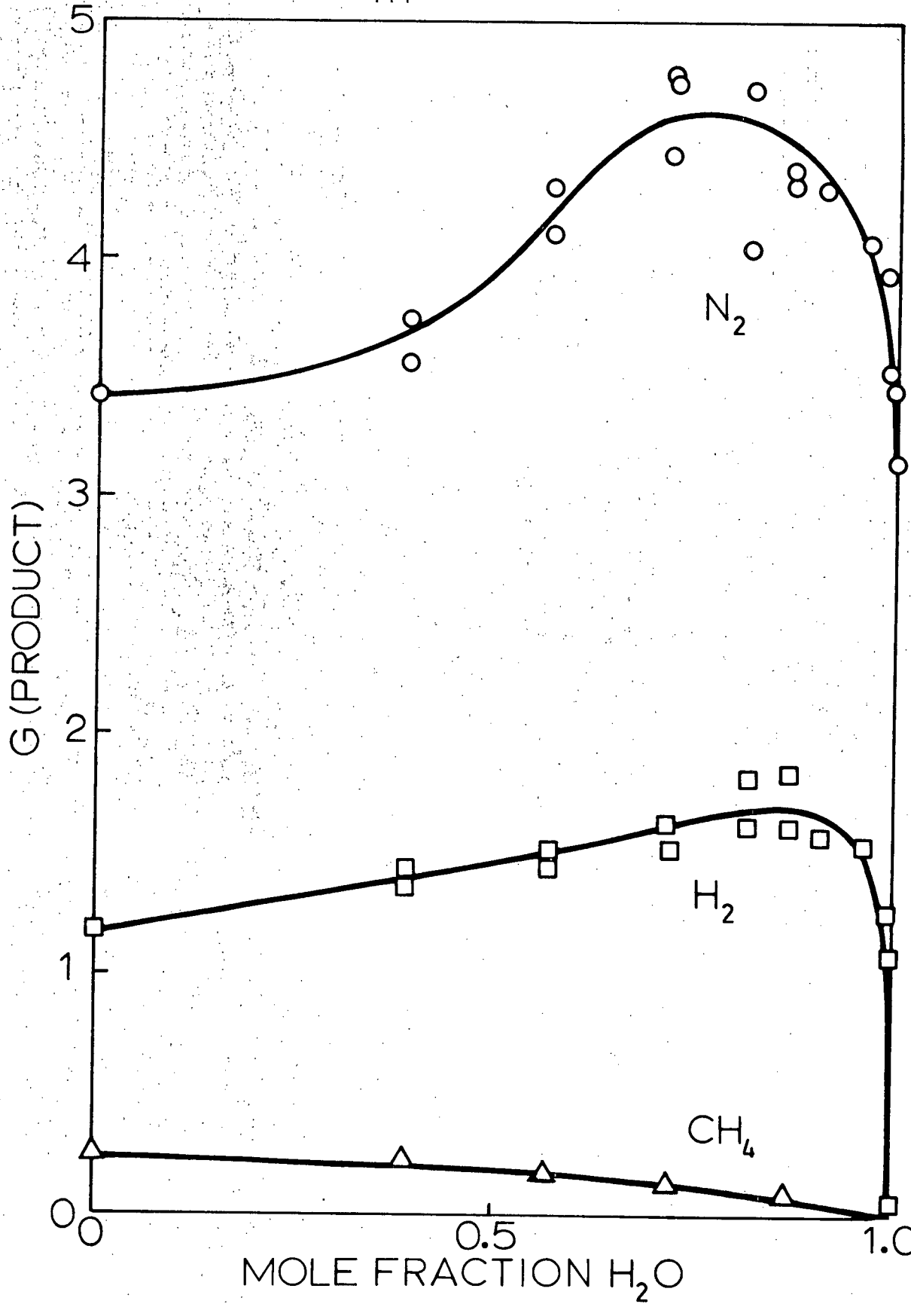

Figure III-7. Product yields from various mixtures of HMPA and H_2O containing 0.02M N_2O as a function of mole fraction H_2O.

of nitrogen gas were also passed through the two solutions. Table VII lists the amount of nitrogen gas recovered from each of the gas additions. The addition of 27 μmoles N_2O into the blue solution also resulted in the formation of 0.3 ± 0.1 μmoles of hydrogen. None was evolved when N_2O was injected into the orange sodium solution. No methane was produced in the Na solutions upon treatment with N_2O.

TABLE VII

Sample	N_2 observed (μmoles) following the injection of 27.0 μmole samples of: N_2	N_2O
Blue solution of Na in HMPA	27.3 ± 0.5	27.2 ± 0.5
Orange (decayed) solution of Na in HMPA	27.7 ± 0.5	0.0 ± 0.5

b) Sodium Amalgams in Solution

Because of their inherent reactivity, it is extremely difficult to prepare stable solutions of sodium metal in amines which will contain known, reproducible concentrations of solvated electrons. Furthermore, investigations have

suggested that N_2O molecules are involved in more than one step of the scavenging reaction. Therefore, even if "known" metal solutions could be prepared, this possibility requires that homogenous N_2O solutions of known composition exist initially. That is, Na must be added to a solution already containing nitrous oxide. In order to introduce a known amount of pure sodium and to retard its rate of dissolution (and hence its reaction), liquid amalgams of sodium in mercury were employed.

Equal aliquots of a given amalgam were transferred from an evacuated reservoir to an intermediate cell chamber.

They were then forced quickly into the reaction solution by means of a high backpressure of inert gas. This method was employed for two reasons. Firstly, the technique prevented the loss of volatile scavengers from the reaction chamber. Secondly, it limited possible reaction with amalgam prior to its entry into the solution being studied.

Experiments were conducted using HMPA, water, or mixtures of the two -- both with and without N_2O. No blue colouration was ever observed following the addition of amalgam to any of the samples.

Subsequent to the completion of reaction in solution, the samples were analyzed by means of atomic absorption spectroscopy for sodium ion content. These analyses confirmed that all aliquots did indeed contain the same expected amounts of sodium metal. For example, a piece of sodium metal weighing 0.14 ± 0.01 gm was sublimed in vacuo several times then mixed with

34.76 ± 0.01 gm of purified mercury. Aliquots of this amalgam produced solutions containing a mercury residue weighing 2.23 ± 0.02 gm. Based simply on the fraction of the total amalgam used (assuming that the sodium metal slug was 100% pure and that no loss occurred during its purification) the sodium content of each aliquot would be given by equation (xxviii).

Theoretical aliquot Na content

$$= \frac{2.24 \pm 0.02 \text{ gm Hg residue} \times 0.14 \pm 0.01 \text{ gm Na}}{34.76 \pm 0.01 \text{ gm Hg total} \times 2.30 \times 10^{-6} \text{ gm Na/}\mu\text{mole}}$$

$$= 393 \pm 32 \ \mu\text{moles Na} \qquad \text{(xxviii)}$$

However, since the sodium metal was cut in air it would be covered with an oxide layer initially and each sublimation prior to the amalgam formation left a small residue. Therefore, the actual sodium content of the aliquots would be expected to be somewhat less than this estimated value. Indeed, analysis of the spent solutions by atomic absorption techniques revealed the presence of 360 ± 20 μmoles of Na^+ ions in each case -- a value indicating excellent accord with expectations.

The gaseous products resulting from the addition of sodium amalgam to the various solutions were measured by gas chromatography. Typical results are given in Table VIII. In addition, one amalgam aliquot containing 360 ± 20 μmoles Na was introduced

TABLE VIII Yields of gaseous products obtained from various solvent mixtures upon the addition of amalgams containing 360 ± 20 μmoles of sodium metal. $[N_2O] \sim 6 \times 10^{-2}$M.

Mole Fraction		N_2O Present?	Gaseous Products (μmoles)	
HMPA	H_2O		H_2	N_2
1.00	0.00	x	4 ± 2[a]	0
		✓	2 ± 1	165 ± 15
0.67	0.33[b]	x	13 ± 3[a]	0
		✓	12 ± 3	100 ± 10
0.29	0.71	x	8 ± 2	0
		✓	19 ± 4	45 ± 5
0.03	0.97	x	92 ± 10	0
0.00	1.00	x	195 ± 15	0
		✓	2 ± 1	200 ± 15

a amalgam essentially stable in this solution. Addition of excess water resulted in reaction.

b 1 ml H_2O in 20 ml HMPA.

into the empty and evacuated reaction cell. Nitrous oxide at one atmosphere pressure was subsequently added to the cell. Immediately after the N_2O addition, the surface properties of the amalgam changed and it tended to stick to the cell walls. Analysis of any gases produced showed that some nitrogen ($\sim$ 25 μmoles) had been formed -- presumably by a direct surface reaction between sodium in the amalgam and gaseous nitrous oxide.

Several important results are immediately obvious from the data of Table VIII. Firstly, the amalgams were stable in pure HMPA or HMPA containing moderate amounts of water. Even in a solution having 0.33 mole fraction of water (1 ml H_2O in 20 ml HMPA or > 5 X 10^4 μmoles H_2O), the amalgam containing 360 μmoles of Na atoms was unreactive. The amalgam reacted with pure water to give 195 ± 15 μmoles of H_2. When 6 X 10^{-2}M N_2O was present in water, the hydrogen reaction was surpressed and 200 ± 15 μmoles of N_2 produced instead. That is, one mole of H_2 was produced from the reaction of two moles of Na but also only one mole of N_2 was produced from 2 moles of Na. From solutions of HMPA containing 6 X 10^{-2}M N_2O, slightly less (165 ± 15 μmoles) nitrogen was produced, but little hydrogen was produced in any predominately HMPA solution. Again the production of one mole of nitrogen from N_2O reaction required at least two moles of Na unless alternate reactions occurred which did not lead to gaseous product formation.

B. DISCUSSION: STEADY STATE EXPERIMENTS

HMPA was studied with the objective of investigating the role of solvated electrons in that solvent. In so-called steady state radiolysis experiments one cannot in general observe reactive intermediates directly. Therefore, one must make indirect investigations by observing stable reaction products and studying the effects of various solutes on their yields. In this way one can often deduce valuable information about intermediate species. It was with these considerations in mind that results of HMPA experiments were interpreted.

1. Gamma Radiolysis Studies

a) Processes Leading to Molecular Products Formation

The radiolysis of pure HMPA yielded hydrogen and methane as gaseous molecular products. The presence of known electron scavengers such as acetone, carbon tetrachloride, chloroform, and nitrous oxide had little effect on the methane yield. This would tend to rule out ionic processes in the formation of that product. Galvinoxyl which is a stable free radical, would be expected to scavenge radical species and has been shown to do so in 2,2,4-trimethylpentane?[91] Iodine is also known to efficiently scavenge radicals in many systems. In the presence of either of these substances, the methane yield was reduced indicating that a precursor is a radical species -- probably

the methyl radical. Although, as discussed, iodine in HMPA probably exists as the triiodide ion that species would also be expected to act as a radical scavenger. Since 0.10M iodine or 0.046M galvinoxyl in HMPA reduced the methane yield by only 60% it is apparent that methane is also formed through unscavengable radiation-induced molecular processes. Such processes could include spontaneous dissociation of electronically excited solvent molecules, intraspur reactions or "hot atom" (radical) reactions.

Since the presence of any of several electron scavengers over a large concentration range reduced the hydrogen yield from $G(H_2) = 3.3 \pm 0.3$ to a constant value of $G(H_2) = 1.4 \pm 0.1$, hydrogen must be formed via at least two processes, one of which involved a comparatively long-lived reducing species scavengable by N_2O. That this species was unlikely to be the hydrogen atom was shown from data for samples containing methanol or oxygen in addition to N_2O.

Methanol is known to react rapidly with hydrogen atoms in many solvents via reaction (1.12) to produce molecular hydrogen.[92]

$$\dot{H} + CH_3OH \longrightarrow H_2 + \dot{C}H_2OH \qquad (1.12)$$

Therefore, if the reducing species were hydrogen atoms, the addition of methanol to HMPA should have had no effect on or increased hydrogen yield upon radiolysis. As can be seen from the data of Table VII, the hydrogen yield from a solution

containing 0.1M methanol was reduced to $G(H_2) = 1.4 \pm 0.1$. Furthermore it has been reported that nitrous oxide does not react with hydrogen atoms during the radiolysis of liquid methanol[93] or cyclopentane.[94] In general, the scavenging of hydrogen atoms by N_2O is accepted as occuring with a relatively low rate constant.[95,96] For example, in aqueous solution methanol and oxygen react with hydrogen atoms some 20 and 10^5 times faster respectively than does N_2O.[37] From solutions of HMPA containing 10^{-2} to 10^{-1}M N_2O, the observed nitrogen yield was little affected by the presence of even 0.1M methanol or 0.01 M oxygen. Now, while this data cannot rule out the involvement of hydrogen atoms in a later stage of the process leading to molecular hydrogen formation, it does strongly preclude the possibility of the initial reducing species being the hydrogen atom. This suggests that the long-lived reducing species is probably a negative ion, X_s^-, either a solvated electron (e_s^-) or a molecular anion (A_s^-).

If the reducing species, X_s^-, were anionic in nature then it should be readily scavenged by protons. Furthermore, such reaction might distinguish between molecular anions and solvated electrons by producing different products, according to reactions (3.12) and (3.13).

$$H^+ + e_s^- \longrightarrow H \xrightarrow{\text{HMPA}} H_2 \qquad (3.12)$$

$$H^+ + A_s^- \longrightarrow MH \longrightarrow \text{products} \qquad (3.13)$$

Unfortunately, HMPA is attacked by electrophiles so that protons are unstable in this solvent[1]. The introduction of 10^{-2}M H_2SO_4 into a sample of HMPA produced a cloudy suspension indicating that decomposition had occurred.

Hydrogen atoms do appear to be involved to some extent in a second hydrogen forming process since high concentrations of efficient radical scavengers reduced the hydrogen yield below the plateau value of $G(H_2) = 1.4 \pm 0.1$. Galvinoxyl at 0.046M and "iodine" at 0.1M reduced $G(H_2)$ to 1.2 ± 0.1 and 1.1 ± 0.1 respectively. At these concentrations the radical scavengers would have been expected to pick up all the radical species produced during the radiolysis. Thus, as was the case for methane formation, molecular hydrogen also appears to arise through unscavengable molecular processes.

From the observed molecular product yields and the effects of scavengers on those yields, one can deduce possible mechanisms for the processes occuring during radiolysis. The following scheme would account for the observed results in pure HMPA. For convenience, the formula for HMPA, $((CH_3)_2N)_3PO$, is expressed as $CH_3(MPA)$. The wavy arrow denotes radiation induced processes, square brackets indicate processes occurring within the spurs and an asterisk signifies electronically excited species.

$$CH_3(MPA) \rightsquigarrow [CH_3(MPA)^*, CH_3(MPA)^+, e^-, H_2, CH_4] \qquad (3.14)$$

$$[CH_3(MPA)^*] \longrightarrow [\cdot(MPA), \cdot CH_3, \cdot H, \cdot CH_2(MPA), CH_3(MPA)] \qquad (3.15)$$

$$\left[\cdot CH_3 + CH_3(MPA)\right] \longrightarrow \left[CH_4 + \cdot CH_2(MPA)\right] \quad (3.16)$$

$$\left[\cdot H + CH_3(MPA)\right] \longrightarrow \left[H_2 + \cdot CH_2(MPA)\right] \quad (3.17)$$

$$\left[e^- + CH_3(MPA)\right] \longrightarrow \left[CH_3(MPA)^-\right] \quad (3.18)$$

$$\left[e^- + CH_3(MPA)^+\right] \longrightarrow \left[CH_3(MPA)^*\right] \quad (3.19)$$

$$\left[\cdot(MPA), \cdot CH_2(MPA)\right] \longrightarrow \longrightarrow \text{Products} \quad (3.20)$$

$$\left[\cdot CH_3\right] \longrightarrow \cdot CH_3 \quad (3.21)$$

$$\left[\cdot H\right] \longrightarrow \cdot H \quad (3.22)$$

$$\left[e^-\right] \longrightarrow e_s^- \quad (3.23)$$

$$\left[CH_3(MPA)^+\right] \longrightarrow CH_3(MPA)_s^+ \quad (3.24)$$

$$\left[CH_3(MPA)^-\right] \longrightarrow A_s^- \quad (3.25)$$

$$\cdot CH_3 + CH_3(MPA) \longrightarrow CH_4 + \cdot CH_2(MPA) \quad (3.26)$$

$$\cdot H + CH_3(MPA) \longrightarrow H_2 + \cdot CH_2(MPA) \quad (3.27)$$

$$e_s^- + CH_3(MPA)_s^+ \longrightarrow CH_3(MPA)^* \longrightarrow H + \cdot CH_2(MPA) \quad (3.28)$$

$$A_s^- + CH_3(MPA)_s^+ \longrightarrow \longrightarrow H + \cdot CH_2(MPA) + CH_3(MPA) \quad (3.29)$$

$$\cdot CH_2(MPA) \longrightarrow \text{Products} \quad (3.30)$$

It was not supposed that this mechanism represented the actual processes, but it simply served as a basis which suggested

reasonable investigative lines for the later experiments.

The observed one-to-one correspondence between $\Delta G(N_2)$ and $\Delta G(H_2)$ in the nitrous oxide depletion experiments and the fact that no ethane was observed implies that radical-radical reactions such as (1.9), (3.31) and (3.32) are not important.

$$\cdot H + \cdot H \longrightarrow H_2 \qquad (1.9)$$

$$\cdot H + \cdot CH_3 \longrightarrow CH_4 \qquad (3.31)$$

$$\cdot CH_3 + \cdot CH_3 \longrightarrow C_2H_6 \qquad (3.32)$$

This is probably a reflection of the efficiency of the molecular processes (3.16), (3.17) and the hydrogen abstraction processes (3.26), (3.27).

b) Free Ion Yield

Of all the species that arise as a result of the radiolysis of HMPA, the highly reactive reducing species X_s^-, is most important. Because of the strong possibility that X_s^- is a solvated electron, and therefore a free ion, determination of its yield is of paramount importance to an understanding of HMPA radiolysis. Here, the term free ion refers to any comparatively long-lived ionic species that has escaped geminate recombination and as such is free to diffuse through the medium and react in the normal chemical sense.

The anionic reducing species X_s^- is readily scavenged by nitrous oxide. Based on the nitrogen yield from solutions of up to 0.13M nitrous oxide in HMPA, as shown in Figure III-3, X_s^- is produced with a yield of $G(X_s^-) \geq 4.5 \pm 0.3$. This assumes of course that nitrous oxide scavenges only X_s^- and that each such reaction ultimately leads to the formation of a single nitrogen molecule according to reaction (3.33).

$$X_s^- + N_2O \xrightarrow{k_{N_2O}} N_2 + \text{products} \qquad (3.33)$$

In the absense of nitrous oxide, X_s^- must react with its counter positive ion, impurity, the solvent, or itself. If such alternate fates can be represented by a single reaction (3.34) where S represents a species other than N_2O, then the data of Figure III-3 can be analyzed on the basis of a simple competition between reactions (3.33) and (3.34).

$$X_s^- + S \xrightarrow{k_s} \text{products} \qquad (3.34)$$

That is, for this competition,

$$G(N_2) = G(X_s^-) \cdot \left[\frac{k_{N_2O} \left[N_2O\right]\left[X_s^-\right]}{k_{N_2O} \left[N_2O\right]\left[X_s^-\right] + k_s \left[S\right]\left[X_s^-\right]} \right] \qquad (xxix)$$

or rearranging,

$$\frac{1}{G(N_2)} = \frac{1}{G(X_s^-)} \cdot \left[1 + \frac{k_s [S]}{k_{N_2O} [N_2O]} \right] \qquad \text{(xxx)}$$

A plot of $1/G(N_2)$ versus $1/[N_2O]$ should be a straight line having a slope equal to $k_s[S]/k_{N_2O}G(X_s^-)$ and an intercept equal to $1/G(X_s^-)$ if this mechanism holds. Figure III-8 shows such a plot for the data of Figure III-3 for 5×10^{-4}M to 1.3×10^{-1}M nitrous oxide in HMPA. The filled circles represent those experiments for which the argon dilution technique was employed in order to attain low concentrations of nitrous oxide. The data for samples initially containing less than about 5×10^{-4}M nitrous oxide were not included because of probable nitrous oxide depletion during radiolysis. While the uncertainty in the data for low nitrous oxide concentrations may be large, the plot appears to be non-linear. However, for the high concentration range, 10^{-2} to 10^{-1}M nitrous oxide, a near linear relationship was obtained as shown in Figure III-9 and from the intercept a value of $G(X_s^-) = 4.3 \pm 0.3$ was calculated. It could be noted that this value is obtained at nitrous oxide concentrations very much higher than would be required to scavenge free ions with lifetimes of at least μsec. Further, the yield is much larger than the free ion yield that one would expect from a liquid having a dielectric constant of 30.[68,97,98]

Thus the simple competition mechanism represented by reactions (3.33) and (3.34) probably does not adequately describe the HMPA system and it is concluded that the high nitrogen yield obtained at high N_2O does not represent the "free-ion" yield.

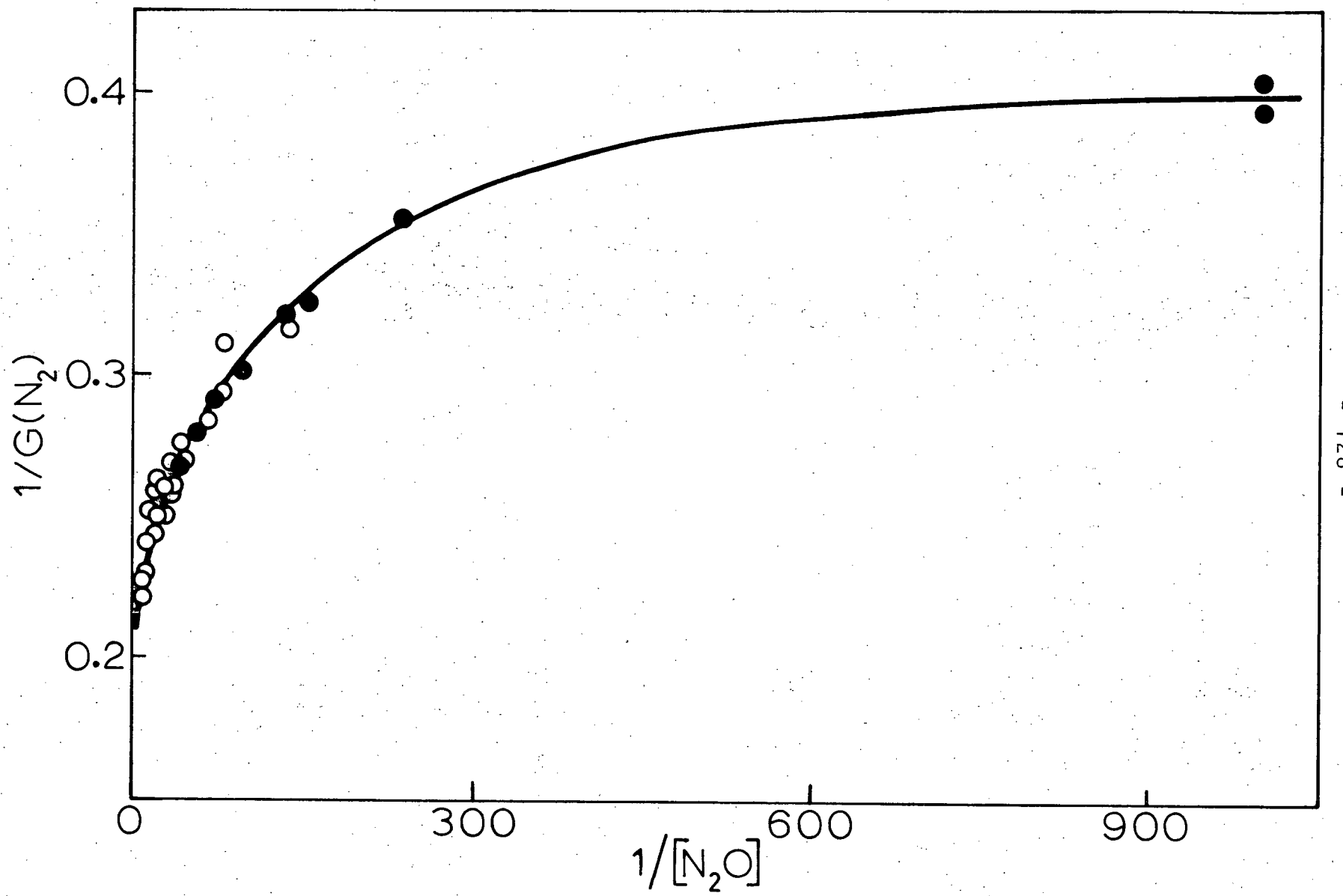

Figure III-8. Plot of the data of Figure III-3 utilizing equation (xxx).

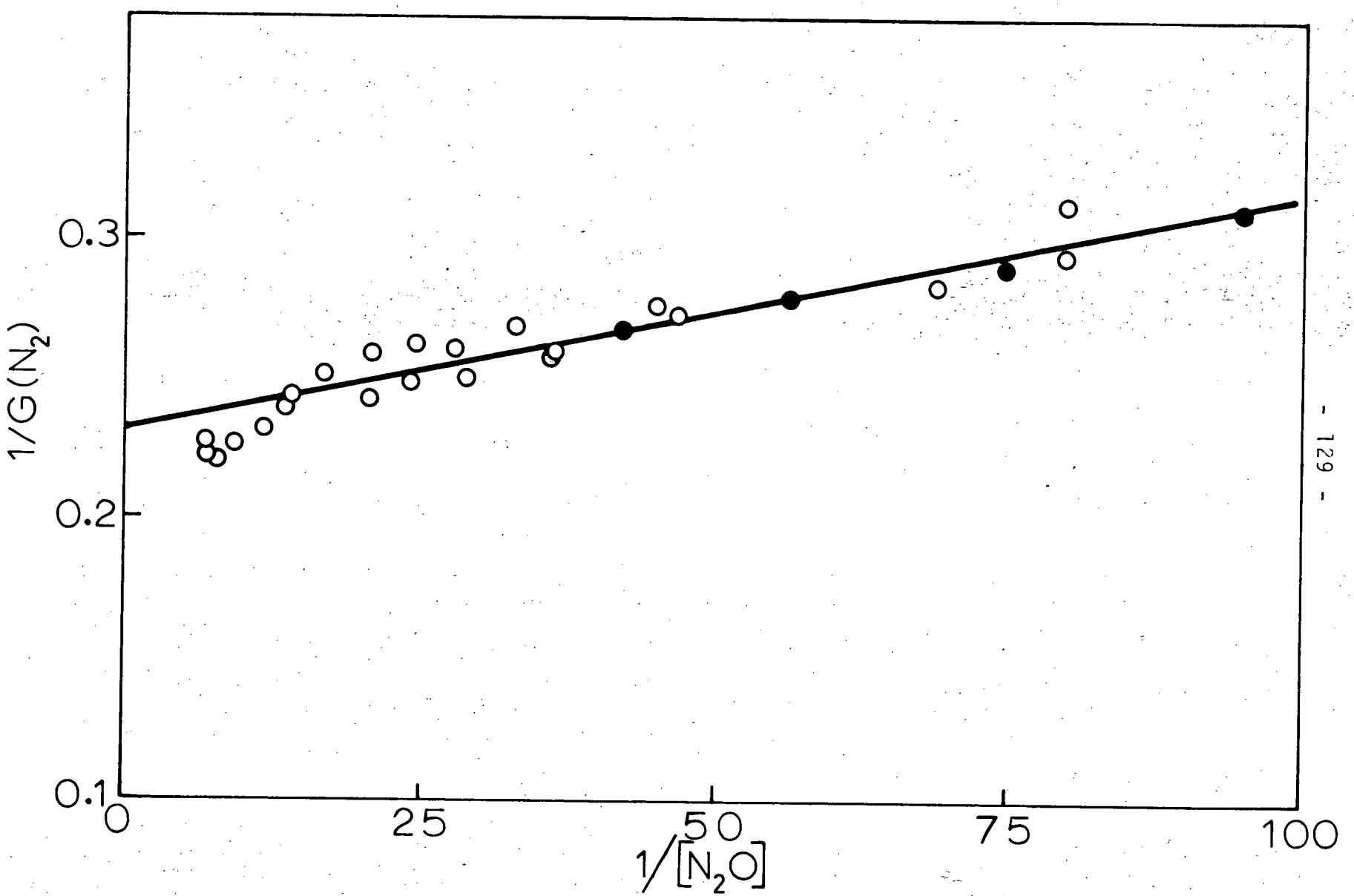

Figure III-9. Plot of the data of Figure III-8 for large concentrations (10^{-2} to 10^{-1}M) of N_2O.

Nitrogen yields from irradiated N_2O solutions have been found to be much larger than "free-ion" yields obtained by other methods for several systems. Table IX shows typical results which compare $G(N_2)$ from N_2O with G(free ion) measured independently. Similarly, Table X shows data from the vapour phase radiolysis of some nitrous oxide/hydrocarbon mixtures. For low concentrations of nitrous oxide in several systems, the nitrogen yield is comparable to the free ion yield. Indeed, in some cases such as water, methane, and neopentane, a plot of $G(N_2)$ versus low nitrous oxide concentration exhibits a plateau region where $G(N_2) \sim G(\text{free ion})$. This behavior would be expected if the reducing species were in fact a comparatively long lived free ion.

In the absence of scavengers, the fate of the reducing anion, X_s^-, must ultimately be neutralization recombination with a cation. In HMPA, such a process appears to lead at least in part to the formation of molecular hydrogen -- possibly via reactions (3.35) and (3.27).

$$X_s^- + CH_3(MPA)_s^+ \longrightarrow CH_3(MPA)^* \longrightarrow \cdot H + \cdot CH_2(MPA) \qquad (3.35)$$

$$\cdot H + CH_3(MPA) \longrightarrow H_2 + \cdot CH_2(MPA) \qquad (3.27)$$

That X_s^- is indeed a free ion is evidenced by the fact that very low concentrations of electron scavengers (even trace impurities) efficiently surpress the above mechanism to give only the low plateau hydrogen yield of $G(H_2) = 1.4 \pm 0.1$.

TABLE IX Nitrogen yields for low and high concentrations of nitrous oxide in various liquids compared to the free ion yields determined independently.

Solvent	Free Ion Yield G(f.i.)	N_2O (M)	$G(N_2)$	Plateau Exhibited	References
Ethane	0.13	0.0004 0.20	0.6 5.4	?	99
Propane	0.08	0.0004 1.5	0.3 5.4	?	99
Neopentane	0.9	0.0001 1.7	0.95 4.7	Yes	100
2,2,4 Trimethylpentane	0.3-0.4	0.001 0.7	0.8 5.5	?	101, 91
Cyclopropane	0.04	0.0004 1.8	~0.1 5.0	Yes	100

TABLE IX (continued)

Solvent	Free Ion Yield G(f.i.)	N_2O (M)	$G(N_2)$	Plateau Exhibited	References
Cyclopentane	0.16	0.001 1.1	0.9 5.5	No	94, 102
Cyclohexane	0.17	0.0009 0.4	0.5 5.4	No	103, 98, 91, 104
Ethylene	0.02	0.0004 2.0	0.2 4.2	Yes	99
Propylene	0.04	0.0003 1.6	<0.1 4.2	Yes	99
Benzene	0.06	0.04 4.6	0.7 6.7	No	104, 91
Methanol	1.1,1.9	0.003 1.0	2.0 4.5	Yes	93, 105

TABLE IX (continued)

Solvent	Free Ion Yield G(f.i.)	N_2O (M)	$G(N_2)$	Plateau Exhibited	References
Ethanol	1.0,1.7	0.00001 0.0001 0.4	0.2 1.3 4.5	Yes?	106, 98
2-Propanol	1.0,1.2	0.00001 0.001 1.0	0.3 1.1 3.5	No	107
Diethyl Ether	0.2-0.4	0.0003 0.29	0.6 4.0	No	108, 102
1,4 Dioxane	0.1,2.2	<0.001 0.21	<1 3.1	No	109, 110, 98
Water	2.7	0.00004 0.20	2.5 3.9	Yes	111, 112, 113

TABLE IX (continued)

Solvent	Free Ion Yield G(f.i.)	N_2O (M)	$G(N_2)$	Plateau Exhibited	References
Liq. Xenon	4.6,7.1	0.001 1.0	~4 ~12	No	114, 115
Formamide	>0.7	0.01 0.05	1.9 3.2	No	116, 98
Dimethyl Sulphoxide	1.3,1.6	~0.005 0.02	0.4 1.0 1.8	?	117, 98
Propylene Carbonate	2.3	0.001 0.10	0.2 2.0	No	118, 98

TABLE X Nitrogen yields from the gas phase radiolysis of various compounds in the presence of nitrous oxide.

Compound	Ion Yield $G(e^-)$	$G(N_2)$	N_2O Mole %	Reference
ethane	4.2	5.6	∿4	119, 120
propane	4.3	6.3	∿4	119, 120
n-butane	4.4	7.0	∿4	119, 120
isobutane	4.4	7.1	∿4	119, 120
1-butene	4.1	8.0	∿4	119, 120
cis-2-butene	4.1	8.2	∿4	119, 120
trans-2-butene	4.2	8.1	∿4	119, 120
propylene	4.0	4.2	∿4	119, 120
isobutene	4.1	4.1	∿4	119, 120
methyl cyclohexane	4.4	22.0	2-10	121
acetylene	3.9	6.0-18.2	1-20	122
isopropanol	3.5	12.5	2	123

Based on these considerations, the nitrogen yield from irradiated HMPA containing very low concentrations of N_2O should more accurately reflect the free ion yield. As explained however, suitable solutions were most difficult to prepare -- and those obtained subject to scavenger depletion. Fortunately, the alternate fate of the reducing species also resulted in the formation of an observable product, namely molecular hydrogen. Thus, those experiments in which N_2O depletion was significant were easily distinguishable. That is, the nitrogen yield from the sample containing the lowest initial N_2O concentration which gave no evidence for scavenger depletion (i.e. increased H_2 yield) should represent the free ion yield. As detailed in Figure III-4, the hydrogen yield increases from samples of HMPA initially containing less than about 3×10^{-4}M N_2O. From solutions containing $> 3 \times 10^{-4}$M N_2O, the hydrogen yield exhibited a plateau value 1.4 ± 0.1. Over the concentration range 3 to 10×10^{-4}M N_2O, the nitrogen yield was $G(N_2) = 2.2 \pm 0.2$.

The H_2 and N_2 yield data over the "N_2O depletion region" from 0 to $\sim 3 \times 10^{-4}$M N_2O provided additional consistant evidence. As shown in Figure III-4, the sum of H_2 and N_2 yields was constant, $G(N_2 + H_2) = 3.5 \pm 0.3$. This implies a simple competition for the reducing species. Over that concentration range N_2 production must reflect the scavenging of a <u>single</u> species by N_2O. Also, the fact that above 3×10^{-4}M N_2O, a three fold increase in N_2O concentration resulted in only a slight increase in N_2 yield implies that neutralization recombination

represents the only alternate fate of the free ions under those conditions.

In addition, the one-to-one relationship between H_2 or N_2 production means that the yield of reducing species would also be given by the difference in H_2 yields from pure HMPA in the presence and absence of N_2O, $\Delta G(H_2) = (3.4 \pm 0.3 - 1.4 \pm 0.1) = 2.0 \pm 0.4$.

On the basis of these experiments the free ion yield in irradiated HMPA was thus determined to be G(free ion) = 2.2 ± 0.2. Similar mechanisms have been proposed to account for the dependence of hydrogen yield on nitrous oxide concentration in several other systems.[93,94,124,125]

c) Free Ion Lifetime

If one makes certain assumptions about the rate constants involved, the experiments conducted at low nitrous oxide concentration allow an estimation of the free ion lifetime to be calculated.

If N_2O depletion is insignificant, reaction (3.33) becomes pseudo - first order. Assuming the reaction to be diffusion controlled (i.e. $k_{3.33} \sim 2 \times 10^{10}$ M^{-1} sec^{-1}), one calculates the mean lifetime τ (given by $(k_{3.33} [N_2O])^{-1}$) to be ~ 700 nsec for $[N_2O] = 7 \times 10^{-5}$M.

From Table VI it can be seen from the H_2 and N_2 data for solutions initially containing 7×10^{-5}M N_2O that neutralization (3.35) and free ion scavenging (3.33) occurred at comparable

rates. Therefore, the ion lifetime, τ, as calculated above should represent the free ion lifetime in the absence of scavenger. Indeed, since from the table it is evident that scavenger depletion was occurring in those solutions the value is at best a lower limit. The result does imply that the reducing species lives at least microseconds and is therefore justifiably labelled a free ion, since in general, species undergoing spur reactions have lifetimes $<10^{-8}$ sec. Indeed, as will be detailed later, there is considerable evidence from the present study to identify the primary reducing species in HMPA as a solvated electron, e^-_{HMPA}.

d) Nitrogen Yield From the Solutions Containing High Concentrations of Nitrous Oxide: Other Sources

It can be seen from Figure III-3 that the radiolysis of HMPA containing $> 10^{-1}$M nitrous oxide produced nitrogen with a yield $G(N_2) > 4.5 \pm 0.2$, much higher than the free ion yield G(free ion) = 2.2 ± 0.2 estimated in the previous section. There are three possible processes besides free ion scavenging which could lead to nitrogen formation from nitrous oxide solutions. They are:

i) Direct radiolysis of nitrous oxide.

ii) Reaction of nitrous oxide with other species produced either directly or indirectly from solvent radiolysis.

iii) Secondary ionic reactions of nitrous oxide.

i) Direct Radiolysis of N_2O

Direct radiolysis of N_2O leads to the formation of nitrogen according to the general reaction (3.36).

$$N_2O \xrightarrow{\wedge\wedge\wedge\wedge\wedge} N_2 + \text{products} \qquad (3.36)$$

The nitrogen yields from gaseous N_2O at room temperature and liquid N_2O at 185 °K are reported to be 10 and 13 respectively.[126,127,128]

However, despite those large yields, calculations reveal that direct radiolysis of N_2O in the HMPA studies could account for at the most two percent of the nitrogen observed. This is because the radiation energy absorbed directly by any component of a system is proportional to that component's electron (density) fraction. By far, the solvent represented the major bulk of the absorbing medium in the present study.

ii) Reaction of N_2O With Other Species Produced Either Directly or Indirectly From Solvent Radiolysis

The radiolysis of HMPA can be expected to produce a variety of excited, radical and ionic species. The interaction of all of these with N_2O must be considered as possible precursors of molecular nitrogen.

ii.1) Excited Species

The interaction of HMPA with ionizing radiation undoubtedly leads to the formation of highly excited solvent molecules in which bond dissociation occurs and the molecules are fragmented (predissociation). Evidence for this comes from the observed unscavengable yield of molecular hydrogen and methane produced by so-called "molecular processes". In this way a number of radical and possible ionic species could be formed. Of concern here, however, is the fate of excited solvent molecules that do not themselves dissociate. Such species are probably short-lived but might undergo energy transfer processes with solutes. However, there seems to be little evidence to suggest that nitrous oxide is capable of scavenging such excited neutral solvent molecules. Dainton and Logan[113] observed the nitrogen yield from the radiolysis of aqueous solutions of nitrous oxide and nitrite ion. They suggested that some of the nitrogen obtained from solutions of high nitrous oxide concentration (up to 0.2M) was a result of the scavenging of excited water molecules. Russell and Freeman[129] obtained similar results from aqueous nitrous oxide solutions containing ethanol. However, they attributed the increased nitrogen yield from concentrated solutions of nitrous oxide to nonhomogenous scavenging of ionic species within the spurs (geminate ion scavenging).

Holroyd[130] studied and compared the scavenging of species produced by the photolysis and radiolysis of alkanes. He concluded that at concentrations greater than 10^{-2}M, nitrous

oxide scavenged excited solvent molecules in cyclohexane, but not in 2,2,4-trimethylpentane. However, as has been pointed out,[131] Holroyd's observations may have been an artifact of his experimental arrangement which could have allowed direct photolysis of N_2O near the optical windows.

Salmon and co-workers[132] examined directly the fluorescence from excited states of aromatic solutes in cyclohexane and benzene. They found for benzene solutions that the triplet yields of naphthalene and 2,5-diphenyloxazole were little affected by the presence of large amounts of nitrous oxide (> 0.1M). In cyclohexane solutions, the aromatic solute triplet yields were reduced, but their fluorescence lifetimes were unaffected. Salmon et al. concluded that aromatic triplets were formed directly by energy transfer from excited solvent molecules in benzene but from ion neutralization processes in cyclohexane where excited solvent states would be expected to be short lived. In the latter case, nitrous oxide competed for the ionic precursors and thus reduced the observed triplet yield. In any event, the observations clearly indicate that nitrous oxide did not react with solvent or solute excited states in those systems.

The only system in which there may be some evidence of reaction between excited solvent molecules and N_2O is dioxane.[133] However, other radiolysis studies[103,110,134] have shown that system to be particularly "messy". In order to explain observations it was usually necessary to invoke mechamisms in which a large number of excited and ionized species underwent

rather specialized reactions.

Mayer and Baxendale[135] observed the emission from benzene and toluene in the pulse radiolysis of cyclohexane. They concluded that the upper limit for the yields of cyclohexane excited states was only $G(RH^*) \leq 0.3$, which is probably typical for the hydrocarbons. HMPA, with its many methyl groups, is probably not very different from the hydrocarbons in this respect.

Thus, the evidence from most systems studied seems to indicate that reaction of nitrous oxide with excited species in HMPA is unlikely. Even if such a process did occur the results of Mayer and Baxendale suggest that only a small yield of nitrogen would be produced.

ii.2) Radical Species

Radical species most likely to be produced during the radiolysis of HMPA are hydrogen atoms, H, and methyl radicals, $\dot{C}H_3$. The observed yields of molecular hydrogen and methane from pure HMPA and the effects of various electron and radical scavengers on these yields confirmed the presence of these radicals. As no ethane was observed among the radiolysis products, ethyl radicals were probably not produced during the solvent radiolysis. The existence of other radical species, $\dot{R}$, which would not lead to the formation of volatile molecular products was not investigated.

The reaction of nitrous oxide with these radical species

might lead to nitrogen formation according to reactions (3.37), (3.38) and (3.39).

$$N_2O + H \longrightarrow N_2 + OH \qquad (3.37)$$

$$N_2O + \dot{C}H_3 \longrightarrow N_2 + CH_3O \qquad (3.38)$$

$$N_2O + R \longrightarrow N_2 + OR \qquad (3.39)$$

As discussed earlier, nitrogen formation through hydrogen atom scavenging (3.37) can be ruled out in HMPA from the data obtained from samples containing oxygen or methanol as second scavenger. Seki and Imamura[93] showed that reaction (3.37) was unimportant in liquid methanol. They found that as the pH of a solution of nitrous oxide in methanol was lowered, the nitrogen yield decreased. At pH $\sim$ 1 where reaction with protons would convert all the solvated electrons to hydrogen atoms (1.13), little or no nitrogen was observed. Since acidic solutions of HMPA are unstable, the analogous reactions in HMPA could not be investigated directly.

Scavenging of methyl radicals by nitrous oxide (3.38) in HMPA can also be eliminated as an additional source of nitrogen. The presence of 0.1M nitrous oxide had little effect upon the yield of methane gas, while known radical scavengers (iodine and galvinoxyl) reduced the methane yield substantially. Indeed, the data for the competitions between nitrous oxide and iodine or galvinoxyl would tend to rule out the involvement of any radical

scavenging process (3.39) in the nitrogen formation mechanism.

ii.3) Ionic Species

In order to investigate the possible involvement of more than one ionic species in the nitrogen formation mechanism, additional scavengers were introduced into nitrous oxide solutions to compete for the precursors of nitrogen. To 10^{-2}M to 10^{-1}M nitrous oxide solutions, comparable concentrations of the known electron scavengers carbon tetrachloride, chloroform, galvinoxyl, iodine and acetone were added. With the exception of acetone, the nitrogen yield was considerably reduced in the presence of these second scavengers as shown in Table VII. The data were analyzed in terms of a simple competition between nitrous oxide and a second scavenger, S, for an undefined nitrogen precursor, P, according to reactions (3.40) and (3.41).

$$N_2O + P \xrightarrow{k_{3.40}} N_2 + \text{products} \qquad (3.40)$$

$$S + P \xrightarrow{k_{3.41}} \text{products} \qquad (3.41)$$

A steady state treatment of this mechanism (similar to that done for reaction (3.33) and (3.34) leads to the kinetic expression (xxxi).

$$\frac{1}{G(N_2)} = \frac{1}{G(P)}\left(1 + \frac{k_{3.41}\left[S\right]}{k_{3.40}\left[N_2O\right]}\right) \qquad (xxxi)$$

Figure III-10 shows the results of plots of $1/G(N_2)$ versus $[S]/[N_2O]$ for nitrous oxide in competition with carbon tetrachloride, chloroform, galvinoxyl, iodine and acetone. The fact that linear relationships were found indicates that the second scavengers were competing for the nitrogen precursors. Also, the linearity indicates that all the nitrogen comes from the same source.

Table XI lists the yield and rate constant ratio, $k_{3.41}/k_{3.40}$, for the nitrogen precursors in HMPA obtained from the slopes and intercepts of the competition plots of Figure III-10.

TABLE XI Nitrogen precursor yield and rate constant ratios calculated for competition between N_2O and second solutes in irradiated HMPA.

Second Scavenger	G(P)	$k_{3.41}/k_{3.40}$	$k_{3.41}/k_{3.40}$ (For e^-_{aq}, From Data of Ref. 37)
Carbon Tetrachloride	4.2±0.4	1.8±0.3	5.4
Chloroform	3.9±0.4	1.4±0.3	3.6
Galvinoxyl	3.9±0.4	1.1±0.2	-
Iodine	4.5±0.4	1.0±0.2	9.1
Acetone	4.2±0.4	<0.01	1.1

The calculated reducing species yield of $G(P) \sim 4$ is much higher than the proposed free ion yield, implying a mechanism involving

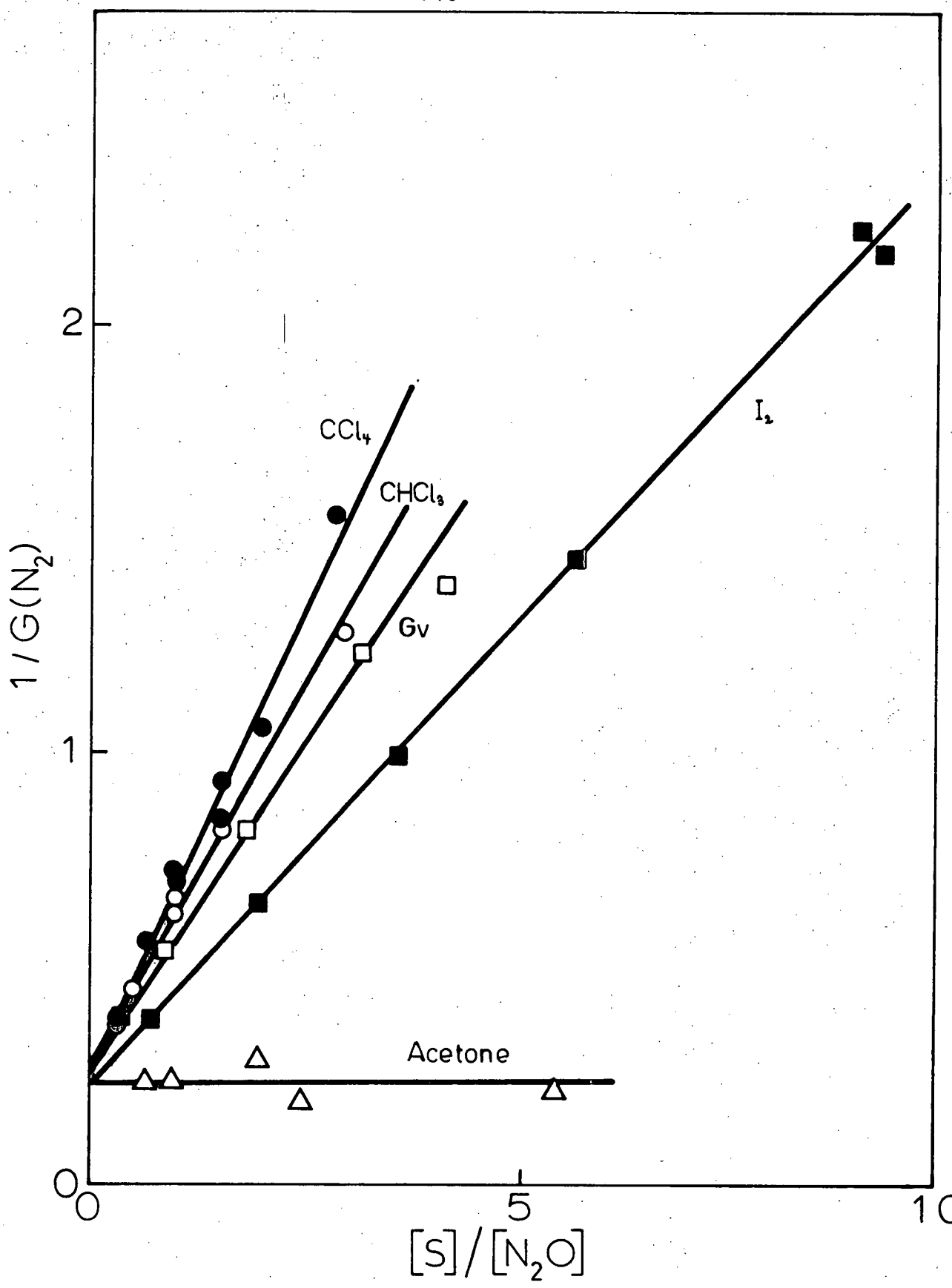

Figure III-10. Plot for the nitrogen yield data utilizing equation (xxxi) from competitions between N_2O and CCl_4 (●), $CHCl_3$ (○), galvinoxyl (□), I_2 (■), and acetone (△).

additional species. The relative scavenging rates of N_2O compared to the other electron scavengers (as determined from the rate constant ratios) were smaller than have been reported for e^-_{aq} in the radiolysis of aqueous solutions.[38] This again could indicate that species other than solvated electrons are involved. More likely, the observations suggest that since electrons are not expected to be strongly solvated in HMPA, their scavenging reactions may well be diffusion controlled. As such, the rates would tend to be independent of solute.

The results from acetone/N_2O mixtures in irradiated HMPA samples were unique. In HMPA, acetone (known to be an efficient electron scavenger in other systems)[136] did not appear to compete with N_2O for nitrogen precursors. Indeed, the nitrogen yield was substantially increased from samples containing N_2O and high concentrations of acetone.

A possible explanation for these results is that nitrous oxide undergoes a charge transfer reaction with the acetone anion formed from the initial competition for the nitrogen precursor, P, according to the following sequence:

$$N_2O + P \longrightarrow N_2 + \text{products} \qquad (3.40)$$

$$CH_3COCH_3 + P \longrightarrow (CH_3COCH_3)^- \qquad (3.42)$$

$$(CH_3COCH_3)^- + N_2O \longrightarrow N_2 + \text{products} \qquad (3.43)$$

If this were the case, the increase in the nitrogen yield is

simply a reflection of the increase in the total scavenger concentration. Vidyarthi[137] found that acetone quickly scavenges hydrated electrons ($k \sim 10^9\ M^{-1}\ sec^{-1}$). More important, he showed that the resulting acetone anion could subsequently be photolyzed, regenerating hydrated electrons with a yield of $\sim$ unity. This result suggests that the acetone anion is fairly long-lived (in water at least) and that it readily gives up its excess electron. Indeed, Chaudhri and Asmus[138] found that the acetone anion could act as a reducing species by transferring an electron to other solutes. And, more pertinent to the present consideration, Burchill and Wollner[139] presented strong evidence to suggest just such a transfer reaction to nitrous oxide from studies of the radiation-induced oxidation of 2-propanol by N_2O in alkaline aqueous solution. In HMPA then, the analogous electron transfer reaction (3.43) might easily be energetically favourable, accounting for the observed results. A similar mechanism has been proposed to explain the results of a nitrous oxide/acetone competition for radiolysis products in dimethylsulphoxide.[140]

ii.3i) Geminate Ions - A Historical Background

Gamma irradiation of media in the gaseous phase produces a uniform distribution of free electrons and positive ions which can be collected upon the application of an electric field. For hydrocarbons, the yield of these free ions is found to be $G(f.i.)_{gas} \sim 4.0$. The radiation-induced ionization processes

are not considered to depend upon the density of the medium, but, conductivity measurements on liquid hydrocarbons indicate a much lower free ion yield $G(f.i.)_{liq.} \sim 0.1$. Electrons injected into liquid media would undergo inelastic collisions with nearby molecules and quickly become thermalized. Apparently, in the hydrocarbons, most of these electrons are not sufficiently removed from their concomitant positive ion to escape its coulombic attraction and rapid geminate recombination occurs. Thus, in liquids, only a few electrons escape recapture and ultimately become uniformly distributed as free ions.

Calculations based on a model suggested by Samuel and Magee[141] indicate a reaction time for geminate recombination of $\sim 10^{-13}$ sec. Such short-lived geminate ions would not be expected to react with added solutes. However, for many systems and scavengers, it has been found that the yield of products attributable to electron scavenging was often much greater than the free ion yield. That is, many solutes, S, appear able to intercept the ion recombination process (3.44) by scavenging the geminate electrons (3.45).

$$\left[e^- + R^+\right] \longrightarrow R^* \qquad (3.44)$$

$$\left[e^-\right] + S \longrightarrow S^- \qquad (3.45)$$

Also, Khorana and Hamill[142] showed that halide ions, X^-, could do likewise by scavenging the oxidizing geminate species. They reported that from aqueous solutions of high halide concentrations

the solvated electron yield was increased and species identified as dihalide ions, X_2^-, observed. Similar results have been reported for alcoholic solutions of halide salts.[143] These groups attributed their observations to geminate ion reactions. They concluded that halide ions, which have low electron detachment energies ($\sim$ 5 eV for I^-_{aq}), readily underwent electron transfer reaction with the oxidizing geminate species (3.46), i.e., either the positive geminate ion or its oxidizing decomposition product.

$$\left[S^+\right] + X^- \longrightarrow X + S \qquad (3.46)$$

The resulting halide atom then reacted with a second halide ion (3.47) to produce the observed dihalide ions.

$$X + X^- \longrightarrow X_2^- \qquad (3.47)$$

Scavenging of positive ions by halide would produce neutral species, ending the coulombic attraction for the concomitant geminate electrons and thereby lessening their likelihood of geminate reaction. Reaction between the electrons and neutral halide atoms (3.48).

$$\left[e^-\right] + X \longrightarrow X^- \qquad (3.48)$$

would not be expected to compete with dihalide ion formation (3.47) because of the huge excess of halide ions at the

concentrations employed and the relative stability of the dihalide ion. Therefore, in the presence of high concentrations of halide ions, electrons that would have undergone geminate recombination are spared rapid neutralization and become free ions, resulting in the observed increased solvated electron yields.

The possibility of geminate ion scavenging means that the reaction time for geminate recombination must be longer than was originally thought. Freeman and Fayadh[68] stated that since trapped or solvated electrons have been found to have mobilities comparable to ordinary ions, most ion pairs that undergo geminate recombination would do so in about $10^{-(10\pm1)}$ sec. Thus in order for a scavenger, S, to appreciably intercept neutralization, the following relation (xxxii) must be satisfied:

$$k_{3.45}\left[S\right] > 10^{10\pm1}\ \text{sec}^{-1} \qquad \text{(xxxii)}$$

If geminate electron scavenging were correctly described in terms of a simple competition between ion recombination and electron capture by scavenger then the yield of a product, P, would be given by (xxxiii).

$$G(P) = \frac{G(g.i.)}{1 + \dfrac{1}{\tau\, k_{3.45}\left[S\right]}} \qquad \text{(xxxiii)}$$

where G(g.i.) is the geminate ion yield and $\tau = 1/k_{3.46}$ is the characteristic geminate ion lifetime.

However, the neutralization reaction does not take place randomly between uniformly distributed species but between isolated pairs of ions which are constrained by their mutual coulombic potential. The lifetime for recombination of such ion pairs therefore depends upon the individual charge separation distances. Electron thermalization would be expected to produce a whole spectrum of ion pair separations reflecting the initial electron energy spectrum. Therefore, no single characteristic lifetime could be assigned to the recombination process (3.44) and the dependence of product yield on scavenger would not in fact be expected to obey the relationship of equation (xxxiii). At low scavenger concentrations in hydrocarbons, a product yield $G(P) \sim 0.1$ is obtained corresponding nicely with the free ion yield determined from conductivity measurements. Schuler et al.[144] showed that as the scavenger concentration was increased, the experimentally observed dependence of product yields arising specifically from electron scavenging reactions deviated considerably from equation (xxx).

Several attempts have been made to derive an expression capable of describing the solute concentration dependence on ion scavenging.[145-148] Unfortunately, due to uncertainties in the initial relative spatial distribution of ions, their motions, encounter radii and efficiencies for reaction, all of these models failed to provide an explicit expression describing the product

yield of scavenging as a function of solute concentration. Schuler[144] reported a purely empirical relationship (xxxiv) that would correctly describe experimental results for a wide range of solute concentrations.

$$G(P) = G(f.i.) + \frac{G(g.i.)}{1 + \frac{1}{(\alpha_s [S])^{\frac{1}{2}}}} \qquad \text{(xxxiv)}$$

The quantity, α_s, called the reactivity, is proportional to the rate constant for the reaction of solute, S, with the geminate electrons. α_s was found experimentally to have a value from 10 - 15 M^{-1} for good electron scavengers. At low solute concentrations equation (xxxiv) reduces to (xxxv) which predicts a simple square root relationship between solute concentration and product yield.

$$G(P) = G(f.i.) + G(g.i.)\,(\alpha_s [S])^{\frac{1}{2}} \qquad \text{(xxxv)}$$

This expression is similar in form to that obtained by Hummel[147] using a mathematical model to describe ion scavenging at low solute concentrations (xxxvi),

$$G(P) = G(f.i.) + G(g.i.)\cdot K\cdot(k_{3.45} [S])^{\frac{1}{2}} \qquad \text{(xxxvi)}$$

where $k_{3.45}$ was the rate constant for reaction of ions with solute and K was a constant involving the appropriate

integrals over the spatial parameters.

These expressions are both in accord with a square root dependence observed earlier by Williams.[149]

Schuler has been able to describe other aspects of geminate ion reactions by simply extending the empirical relationship of equation (xxxiv). Through the inclusion of suitable terms into the equation, the reactivity of scavengers that produce no measurable product upon capture of geminate electrons have been determined from observations of the effect of such solutes on the hydrogen yield. Also, equations to describe competitive scavenging have been presented. The consistency with which equations based on the simple empirical relationship describe and correctly predict experimental observations greatly enhances the model's veracity.

Recently, in a rigorous mathematical treatment, Abell and Funabashi[150] formulated a "diffusion" model for geminate ion reactions. It is significant that their calculations predict that Schuler's empirical expression (xxxiv) should quite accurately describe the process.

ii.3ii) Geminate Ions in HMPA

The reaction between electrons and nitrous oxide in aqueous solution is close to the diffusion controlled limit, i.e., the rate constant for electron capture is $k \sim 10^{10}\ M^{-1}\ sec^{-1}$. If this applies for the N_2O/HMPA system as well, condition (xxxii)

would be satisfied for large nitrous oxide concentrations in HMPA and geminate electron scavenging could be significant. According to Schuler's empirical phenomenological model, the nitrogen yield in excess of the free ion yield in HMPA should then follow a square root dependence on solute concentration. Rearranging equation (xxiv) to a linear form gives the following equation (xxxvii) to describe the HMPA/N_2O system for N_2O concentrations where $G(N_2) > G(f.i.)$.

$$\frac{1}{(G(N_2) - G(f.i.))} = \frac{1}{G(g.i.)}\left(1 + \frac{1}{(\alpha_{N_2O}\left[N_2O\right])^{\frac{1}{2}}}\right) \qquad \text{(xxxvii)}$$

A plot of $1/(G(N_2) - G(f.i.))$ versus $1/\left[N_2O\right]^{\frac{1}{2}}$ should be a straight line with slope $1/\alpha_{N_2O}^{\frac{1}{2}}\ G(g.i.)$ and intercept $1/G(g.i.)$. Figure III-11 shows such a plot for the data of concentrations of nitrous oxide where the argon dilution technique was employed (filled circles), it is difficult to tell whether this deviation is real or simply a reflection of systematic errors. In any event, the non-linearity suggests that a mechanism involving geminate ion scavenging by N_2O does not apply to the HMPA system.

From the slope and intercept of the "best" line through the points, one calculates a geminate ion yield $G(g.i.) = 4.2 \pm 0.6$ and a reactivity of N_2O towards geminate electron, $\alpha_{N_2O} = 11 \pm 3\ M^{-1}$. The latter value is comparable to $\alpha_{N_2O} = 8 - 10\ M^{-1}$ reported for cyclohexane solutions. However, when combined with the free ion yield of $G(f.i.) = 2.2 \pm 0.2$, a geminate ion yield $G(g.i.) = 4.2 \pm 0.6$ would indicate a total ion yield of $G(t.i.) = 6.4 \pm 0.8$.

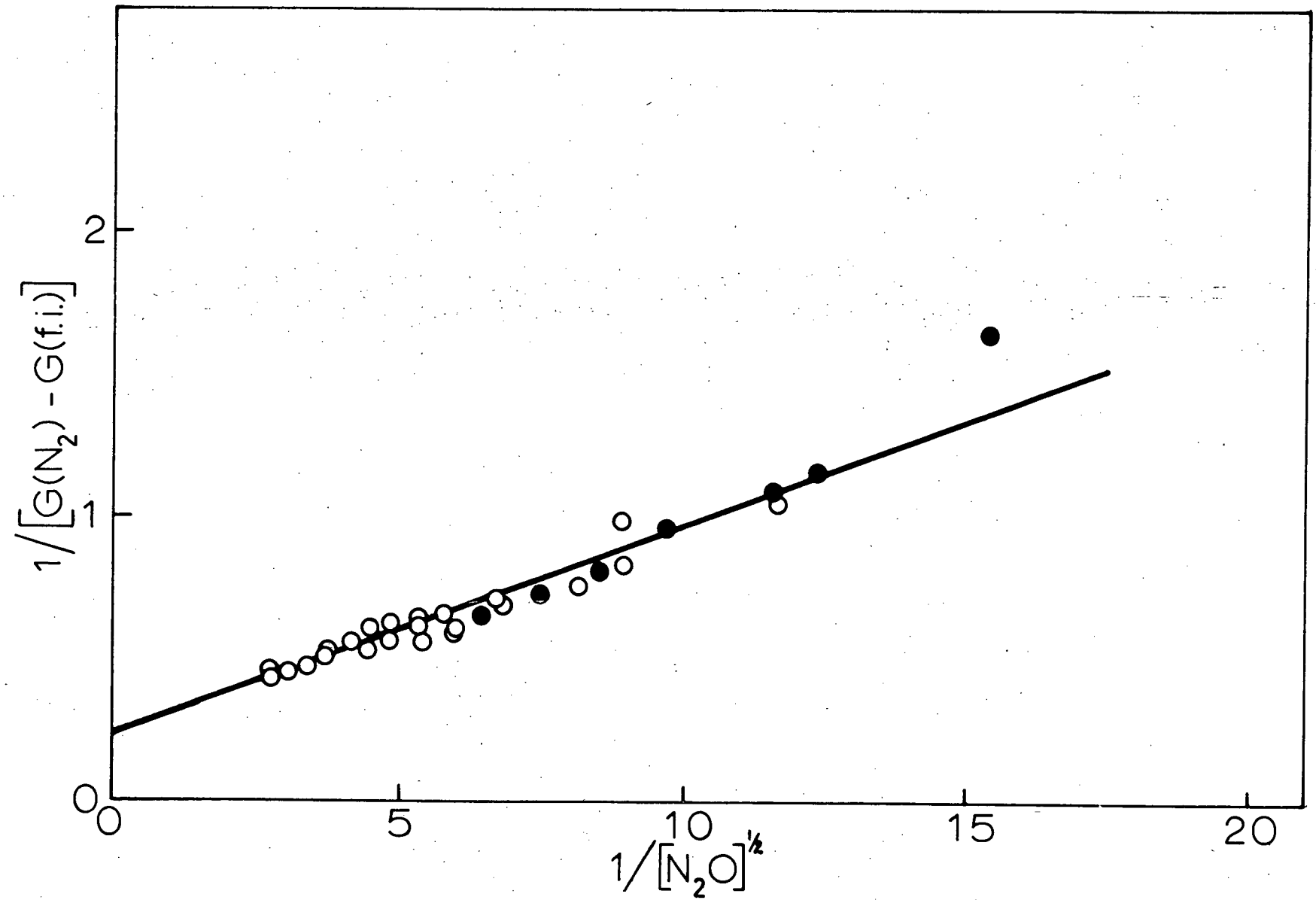

Figure III-11. Plot of the data for nitrogen yield in excess of the free ion yield from irradiated N_2O solutions of HMPA utilizing equation (xxxvii).

In terms of the initial ionization process, HMPA should not be much different from the hydrocarbons for which total ionization yields of about four are generally acknowledged. This fact along with the general non-linearity of Figure III-11 leads this author to reject the mechanism.

Results from several experiments in which multiple solutes were employed tend to corroborate this conclusion. Figure III-12 shows the effect of the presence of 0.2 M LiBr on the nitrogen yield from N_2O/HMPA solutions. The solid line in the figure represents the yield of nitrogen in the absence of bromide ion. As can be seen, the nitrogen yield was little affected.

At 0.2M, Br^- would be expected to scavenge positive geminate ions in HMPA and thereby increase the free anion yield and lifetime. If the extra yield of nitrogen above the free ion yield (G(f.i.) = 2.2) arose from geminate electron scavenging one would have expected a marked increase in the nitrogen yield in those solutions -- especially for the lower concentrations of N_2O. This was clearly not the case. Consequently there is the implication that geminate scavenging is <u>not</u> responsible for nitrogen yields up to two times the free ion yield in HMPA.

Experiments in which acetone was used as a second solute also lead to this conclusion. As has been described, acetone appears to scavenge electrons in HMPA to produce an intermediate species (probably the acetone anion) which can go on to reduce N_2O to nitrogen. Now, a large concentration of acetone would be expected to react with any "scavengeable" geminate electrons in

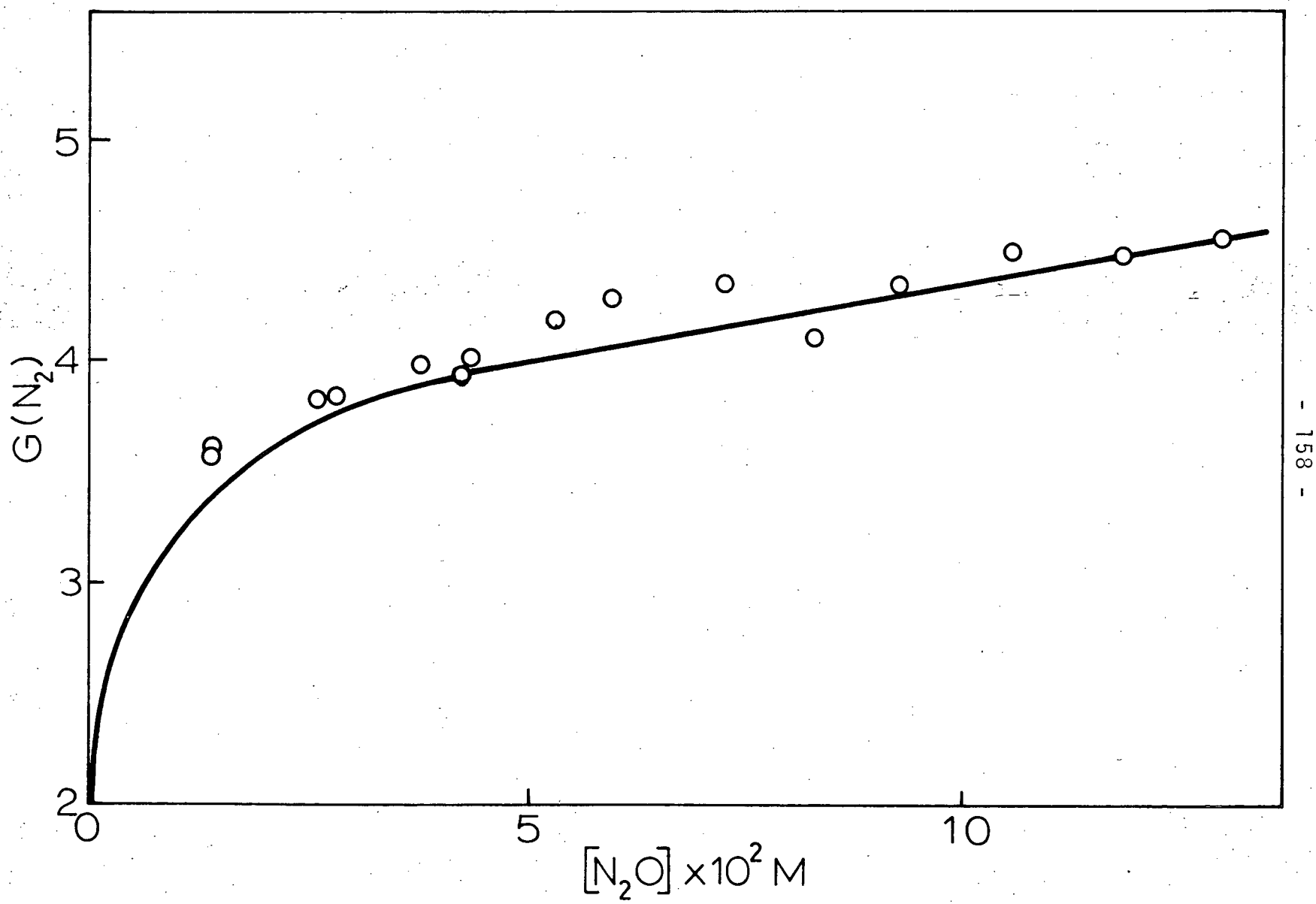

Figure III-12. The effect of 0.2M Br^- on nitrogen yield from N_2O in HMPA. The solid line represents the nitrogen yield in the absence of Br^-.

HMPA. Hunt[151] has shown this to be the case in water for instance. Thus, a large acetone concentration would serve to convert short-lived geminate electrons into relatively long-lived acetone anions which could in turn be scavenged by a much lower concentration of nitrous oxide. In this way, the contribution of geminate electrons to the total yield of scavengeable reducing species would be revealed.

Figure III-13 reveals that the presence of 0.27M acetone in N_2O/HMPA solutions resulted in a near uniform increase in nitrogen yield of about $\Delta G(N_2) \sim 0.7$. Clearly the results are not consistent with geminate scavenging processes being responsible for the high nitrogen yields observed from large concentrations of N_2O alone.

The high ionization potential of nitrous oxide (12.9 eV in the gas phase)[152] makes reaction with positive ions (3.49) to produce nitrogen unlikely.

$$R^+ + N_2O \longrightarrow N_2 + \text{products} \qquad (3.49)$$

The presence of known positive ion scavengers in HMPA supports this supposition. Water or bromide ions at >0.2M concentrations had little or no effect on $G(N_2)$.

Rzad et al.[153] found that in cyclohexane, the addition of N_2O (or other electron scavengers) resulted in an increase of positive ion scavenging by cyclopropane.

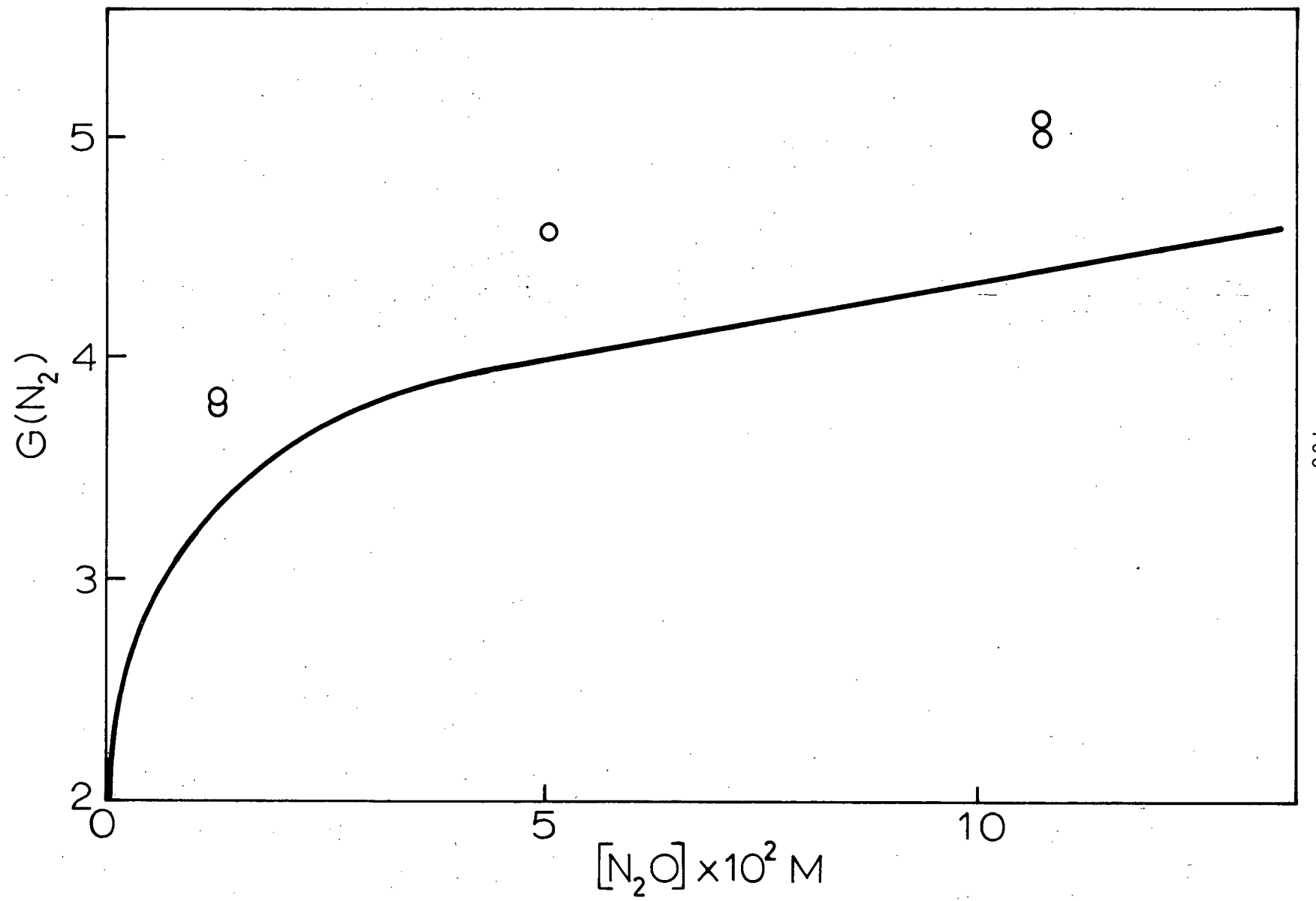

Figure III-13. The effect of 0.27M acetone on nitrogen yield from N_2O in HMPA. The solid line represents the nitrogen yield in the absence of acetone.

iii) Secondary Ionic Reactions of Nitrous Oxide

iii.1) Possible Mechanisms for N_2O Scavenging

In spite of the large number of investigations utilizing nitrous oxide as an electron scavenger there remains considerable uncertainty as to the nature of the intermediates involved.

Wentworth et al.[154] have shown that the attachment of thermal electrons to nitrous oxide in the gas phase takes place dissociatively via a two body process (3.50).

$$e_g^- + N_2O \longrightarrow N_2 + O^- \qquad (3.50)$$

However, they predicted from their observations that the species N_2O^- should also be stable. Other groups studied electron attachment reactions in nitrous oxide at much higher pressure. By monitoring the electron decay they found that a three-body process, probably (3.51), was indicated.[155,156]

$$e^- + N_2O + N_2O \longrightarrow N_2O^- + N_2O \qquad (3.51)$$

Paulson,[157] using a double mass spectrometer system, has observed N_2O^- formed via electron transfer from NO^- (3.52) thereby confirming that it has appreciable stability.

$$NO^- + N_2O \longrightarrow N_2O^- + NO \qquad (3.52)$$

Nitrous oxide used as an electron scavenger in the radiolysis of gaseous systems would therefore be expected to produce O^- or N_2O^- ions as intermediates. Johnson and Warman[125] in some early work on gaseous propane radiolysis proposed a mechanism including a secondary reaction between nitrous oxide and the oxide ion (3.53) to account for a nitrogen yield twice the electron yield.

$$e^- + N_2O \longrightarrow N_2 + O^- \qquad (3.50)$$

$$O^- + N_2O \longrightarrow N_2 + O_2^- \qquad (3.53)$$

Warman[119] later showed that the addition of CO_2 to N_2O/propane mixtures resulted in a decrease in the nitrogen yield to a limiting value near the electron yield. CO_2 does not appear to scavenge thermal electrons in the gas phase. Paulson[158] has in fact calculated that the electron affinity of gaseous CO_2 is negative. Nor is CO_2 known to react with other radical or ionic species produced in gaseous hydrocarbon radiolysis. However, a rapid reaction with the oxide ion (3.54) has been observed.[159]

$$O^- + CO_2 \longrightarrow CO_3^- \qquad (3.54)$$

Thus, Warman's CO_2/N_2O/propane gas phase data could be explained in terms of a simple competition between CO_2 and N_2O for

intermediate oxide ions.

Warman studied a number of alkane and alkene gases and observed nitrogen yields between one and two times the electron yield. He suggested that oxide ions might react with the various hydrocarbons, R, to produce ionic species (3.55) which could subsequently react with N_2O to produce secondary nitrogen (3.56).

$$O^- + R \longrightarrow RO^- \qquad (3.55)$$

$$RO^- + N_2O \longrightarrow N_2 + \text{products} \qquad (3.56)$$

Involvement of such reactions to various extents could account for his findings, and competition with CO_2 tended to support this conjecture. Warman further suggested that an alternate path for the secondary reaction between O^- and N_2O (3.57) could also result in intermediate nitrogen yields.

$$O^- + N_2O \longrightarrow NO^- + NO \qquad (3.57)$$

Indeed, mass spectrometric;[160] drift tube;[161] and ion cyclotron resonance[162] experiments have shown that reaction (3.57) is the dominant process when O^- is reacted with N_2O in the gas phase. Ferguson[163] pointed out that since the electron affinity of NO was very small (< 0.1 eV) the NO^- ion would readily undergo collisional detachment (3.58).

$$NO^- + M \longrightarrow NO + M + e^- \qquad (3.58)$$

Regeneration of electrons in this way would undoubtedly lead to a chain reaction formation of nitrogen and thus such a mechanism could not account for the somewhat depressed nitrogen yields observed.

More recently, Johnson[164] examined the radiolysis of propane, nitrous oxide and hydrogen chloride mixtures. It was expected that HCl would react with O^- by reaction (3.59),

$$O^- + HCl \longrightarrow OH + Cl^- \qquad (3.59)$$

and thereby reduce the nitrogen yield to the electron yield. Such was indeed the case as the addition of HCl decreased $G(N_2)$ rapidly to a value near the electron yield while the hydrogen yield remained unaffected. However, as the concentration of HCl was increased, the nitrogen yield slowly decreased further while the hydrogen yield increased. Gaseous HCl is known to react with electrons via reaction (3.60).

$$e^- + 2HCl \longrightarrow H_2 + \text{products} \qquad (3.60)$$

These results supported the earlier conjecture that the excess nitrogen arose from secondary reaction with an ionic intermediate. That is, at low concentration, HCl interfers with the secondary ionic reaction and at higher concentration competes with N_2O for electrons directly. However, Johnson found that at low concen-

trations of HCl, the nitrogen yield depression was <u>independent</u> of N_2O concentration. Upon re-investigating the CO_2-N_2O-propane system, he found a similar independence. Under these circumstances, the data were <u>not</u> consistent with O^- being the reactive intermediate. Therefore, it was suggested that electron capture by N_2O proceeded via the three body associative mechanism (3.51) and resulted in the formation of the $N_2O_2^-$ ion.

$$e^- + N_2O + N_2O \longrightarrow N_2O^- + N_2O \qquad (3.51)$$

$$N_2O^- + N_2O \longrightarrow N_2O_2^- + N_2 \qquad (3.61)$$

Johnson proposed that it was the subsequent secondary decay of the $N_2O_2^-$ ion (3.62) (possibly by neutralization) that accounted for the excess nitrogen.

$$N_2O_2^- \xrightarrow{(RH^+)} N_2 + \text{products} \qquad (3.62)$$

The effects of HCl and CO_2 would then be explained in terms of a competition for the $N_2O_2^-$ ion (3.63), (3.64), and reaction (3.62).

$$N_2O_2^- + HCl \longrightarrow N_2O + OH + Cl^- \qquad (3.63)$$

$$N_2O_2^- + CO_2 \longrightarrow N_2O + CO_3^- \qquad (3.64)$$

The $N_2O_2^-$ ion has in fact been identified as a stable species both in the gas phase[161,162] and in aqueous solution.[165,166]

The oxide ion, O^-, has been postulated as an important intermediate formed from electron scavenging by nitrous oxide in the radiolysis of gaseous methylcyclohexane;[121] acetylene;[122] and benzene.[167] In these systems, nitrogen yields of greater than 18 have been attributed to chain reactions involving reaction between O^- and the hydrocarbon, followed by electron transfer to N_2O. In the acetylene study, the addition of CO_2 to N_2O/acetylene mixtures resulted in a reduction in the nitrogen yield, tending to a lower limit around the electron yield. This was taken as evidence for the involvement of O^- ions in the chain mechanism. However, since these experiments were conducted at relatively high pressures (near atmospheric pressure in some cases), electron capture would be expected to produce the N_2O^- ion via the three body process (3.51). Therefore, the involvement of O^- ions would depend upon the lifetime of N_2O^- with respect to dissociation (3.65).

$$N_2O^- \longrightarrow N_2 + O^- \qquad (3.65)$$

From a kinetic study of the competition between dissociation and its reaction with deuterium iodide, a lifetime of $\geq 10^{-4}$ sec has been estimated for the N_2O^- ion in gaseous hydrocarbons.[168] Thus it seems likely that N_2O^- (or $N_2O_2^-$) ions were the intermediate reactive species.

Bailey and Dixon[123] suggested that these species were

responsible for their results from the vapour phase radiolysis of nitrous oxide in water/isopropanol mixtures. They found the nitrogen yield from N_2O about equal to the electron yield in water vapour but greater than three times the electron yield in isopropanol vapour. For water/alcohol mixtures the results indicated a competition for some intermediate species. Complete reaction of either N_2O^- or $N_2O_2^-$ with water (3.66, 3.67) would lead to an overall nitrogen yield equal to the electron yield.

$$e^- + N_2O + M \longrightarrow N_2O^- + M \qquad (3.51)$$

$$N_2O^- + N_2O \longrightarrow N_2 + N_2O_2^- \qquad (3.60)$$

$$N_2O^- + H_2O \longrightarrow N_2 + OH + OH^- \qquad (3.66)$$

$$N_2O_2^- + H_2O \longrightarrow N_2O + OH + OH^- \qquad (3.67)$$

In liquid phase radiolysis studies, the mechanisms whereby nitrogen is formed from electron scavenging by nitrous oxide appear even less well understood. The very nature of liquid radiolysis leads to inhomogenous distributions of radiolytic products and the solvation properties of liquids undoubtedly affect the stability of the various ionic intermediates. For example, the nitrogen yield obtained from the radiolysis of nitrous oxide in liquid benzene was only about one fifth that obtained from a gas phase study.[167] Sato et al.[104] were first to

propose secondary ionic reactions of nitrous oxide in liquid phase radiolysis from studies of cyclohexane. By analogy with gas phase work, the oxide ion was proposed as the reactive intermediate. Since that time a number of authors have proposed secondary nitrogen formation in many liquid systems.[93,101,108,114,115,169,170,171]

It is particularly interesting that Schuler's group[170] arrived at such a conclusion. Unlike most solutes, data from N_2O studies in cyclohexane could not be predicted from their empirical phenomenological model (based on equation (xxxiv)). Forced to conclude that secondary ionic reaction must occur in N_2O solutions they modified their model. The changes resulted in a much more complex (but logical) expression which then allowed correct predictions to be made for the cyclohexane solutions.

iii.2) Secondary Ionic Reactions in HMPA

It seems quite possible then that in the present investigation of HMPA radiolysis, the high nitrogen yields from N_2O solutions might arise from secondary ionic reactions involving N_2O. Electron capture by N_2O must lead, at least initially, to the formation of N_2O^- (3.68).

$$e_s^- + N_2O \longrightarrow N_2O^- \qquad (3.68)$$

The intermediate might more generally be denoted as $(N_2O)^-$ which represents the N_2O^- ion itself, or some daughter ion formed from decay or dissociation. Such an ion might then undergo any of several processes leading to the formation of a single molecule of nitrogen as represented by the pseudo-first order process (3.69).

$$(N_2O)^- \xrightarrow{k'_{3.69}} N_2 + \text{products} \qquad (3.69)$$

On the other hand, reaction of $(N_2O)^-$ with a second N_2O molecule (3.70) could lead to the eventual formation of two molecules of nitrogen (3.71).

$$(N_2O)^- + N_2O \xrightarrow{k_{3.70}} N_2 + O(N_2O)^- \qquad (3.70)$$

$$O(N_2O)^- \xrightarrow{k_{3.71}} N_2 + \text{products} \qquad (3.71)$$

For such a scheme, the fraction of $(N_2O)^-$ ions undergoing secondary reaction with N_2O, f_{sec}, would be given by (xxxviii).

$$f_{sec} = \frac{k_{3.70}\left[N_2O\right]}{k_{3.70}\left[N_2O\right] + k'_{3.69}} \qquad (xxxviii)$$

The nitrogen yield from a solution containing N_2O and reacting via this mechanism would therefore be given by (xxxix).

$$g(N_2) = G(f.i.)\left(1 + \frac{k_{3.70}\left[N_2O\right]}{k_{3.70}\left[N_2O\right] + k'_{3.69}}\right) \qquad \text{(xxxix)}$$

This expression can be rearranged to give (xl).

$$\frac{1}{(G(N_2) - G(f.i.))} = \frac{1}{G(f.i.)} + \frac{k'_{3.69}}{G(f.i.)\ k_{3.70}\left[N_2O\right]} \qquad \text{(xl)}$$

$G(N_2) - G(f.i.)$ is simply the nitrogen yield in excess of the free ion yield.

A plot of $1/(G(N_2) - G(f.i.))$ versus $1/\left[N_2O\right]$ should be a straight line with intercept $1/G(f.i.)$ and slope $k'_{3.69}/G(f.i.)\ k_{3.70}$. Figure III-14 shows such a plot for the nitrogen yields from N_2O/HMPA solutions of Figure III-3, taking $G(f.i.) = 2.2$. As can be seen, a fairly linear relationship was obtained. From the slope and intercept of a least squares fit of the data, a value of $k_{3.65}/k_{3.70} = 1.2 \pm 0.1 \times 10^{-2}$M was calculated. What this means is that if this is in fact the operative mechanism, then for an HMPA solution containing 1.2×10^{-2}M N_2O, fully half the $(N_2O)^-$ ions undergo secondary ionic reaction to give a second molecule of nitrogen.

iv) Geminate Ion Scavenging Versus Secondary Ionic Reactions

iv.1) In Pure HMPA Radiolysis

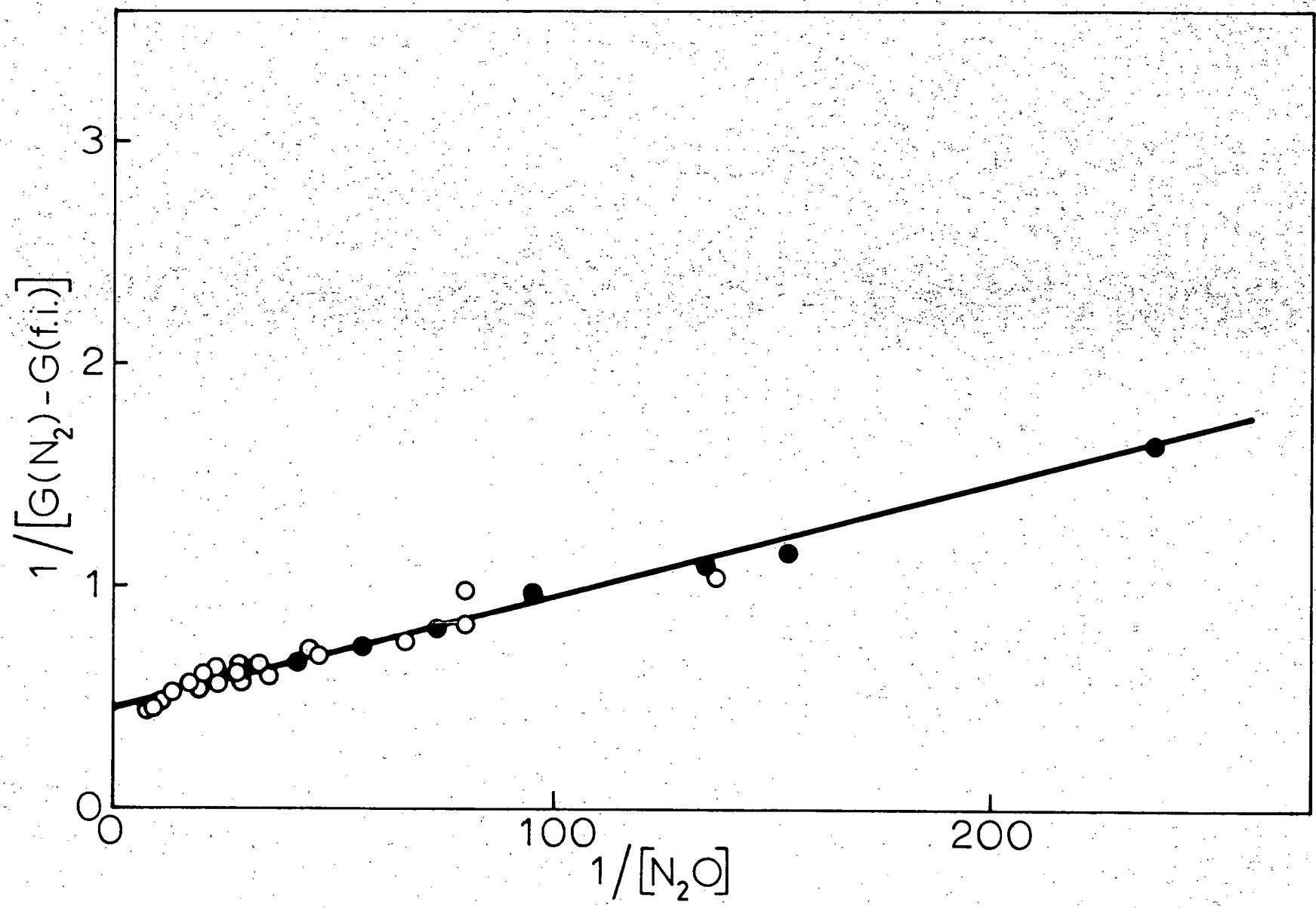

Figure III-14. Plot of the "excess" nitrogen yield from N_2O in HMPA for the data of Figure III-3 utilizing equation (x1).

It is evident that of the many processes which might lead to a nitrogen yield from irradiated solutions of N_2O in HMPA in excess of the free ion yield only two mechanisms are reasonably compatible with the observations. These processes are the reaction of N_2O with:

- Geminate ions
- Secondary N_2O^- ions or one of their decay products

Based on the mechanisms discussed earlier for each of these schemes, the nitrogen yields observed as a function of nitrous oxide concentration would be given by:

- Geminate ion scavenging

$$G(N_2)_{g.i.s.} = G(f.i.) + G(g.i.)\left(1 + \frac{1}{(\alpha_{N_2O}\,[N_2O])^{\frac{1}{2}}}\right) \qquad \text{(xli)}$$

- Secondary ion reaction with $(N_2O)^-$

$$G(N_2)_{s.i.r.} = G(f.i.)\left(1 + \frac{1}{1 + \dfrac{k'_{3.69}}{k_{3.70}\,[N_2O]}}\right) \qquad \text{(xlii)}$$

Theoretical curves for these equations are shown in Figure III-15 which includes the observed nitrogen yields taken from Figure III-3. The dashed line was obtained from the geminate scavenging

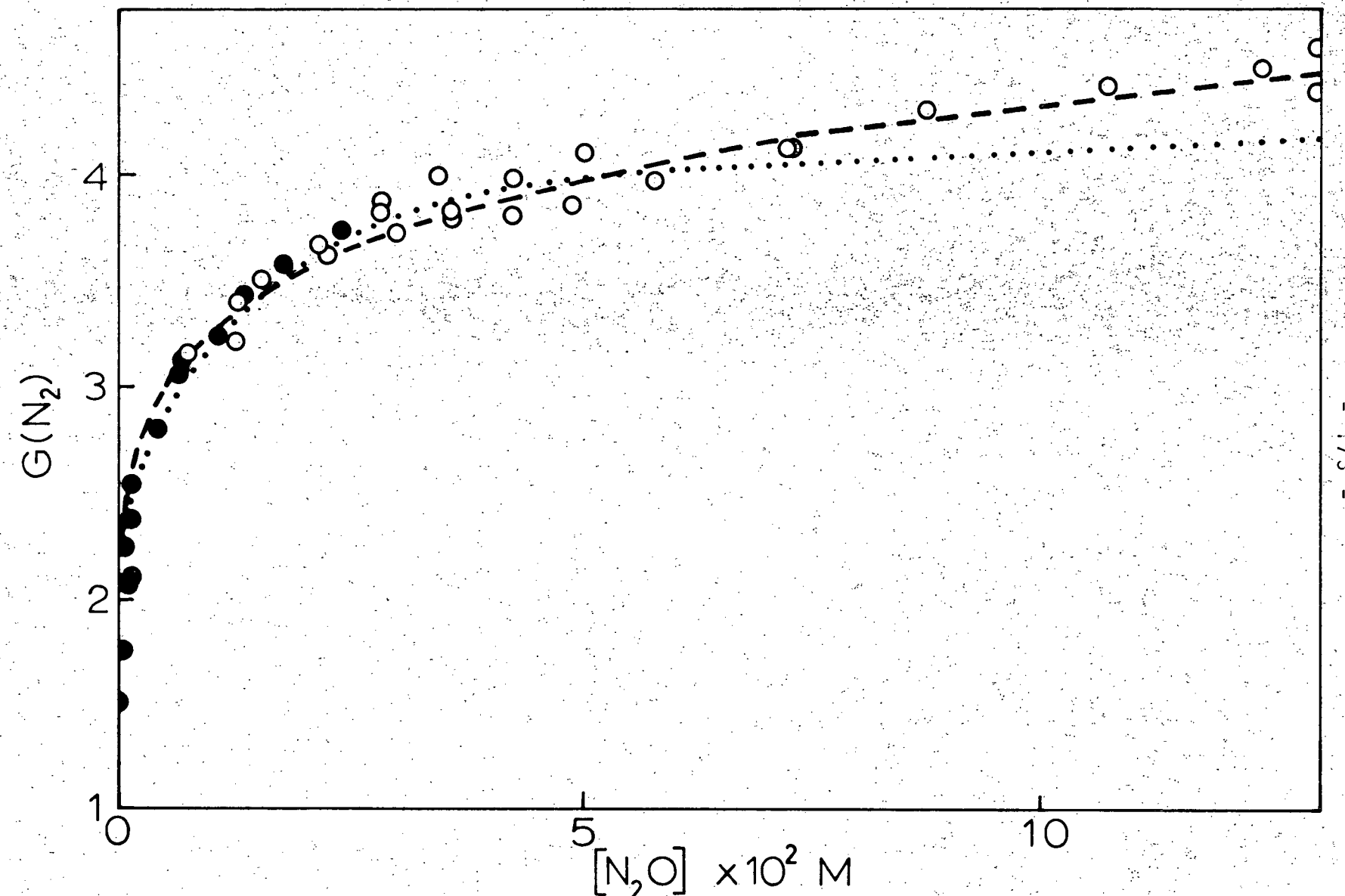

Figure III-15. Theoretical N_2 yield curves resulting from geminate ion scavenging (— — —) and secondary ionic reaction (•••••) considerations. The circles represent actual observed data from Figure III-3.

equation (xli) taking G(f.i.) = 2.2, G(g.i.) = 5.7 and α_{N_2O} = 4.7 M^{-1}. The dotted line was obtained from the secondary ionic reaction equation (xlii) taking G(f.i.) = 2.2 and $k'_{3.69}/k_{3.70}$ = 1.2 X 10^{-2} M^{-1}.

Both functions fit the data fairly well. The secondary ionic curve tends towards a plateau, while the N_2 observed yield continues to increase with N_2O concentration. At very high scavenger concentrations a small contribution from geminate ion scavenging would be anticipated which would account for the deviation. The data from N_2O alone in HMPA thus does not suffice to elucidate the N_2O scavenging mechanism. As pointed out, the addition of other solutes tends to rule out geminate ion scavenging.

e) Radiolysis of Liquid Mixtures

i) Background

It might be expected that radiolysis product yields from a mixture of two liquids would be intermediate between the yields of the pure solvents. Schmidt and Allen,[102] using the clearing field technique, studied a variety of hydrocarbon mixtures and found that indeed, in each case, intermediate free ion yields were obtained.

The ion yield from a mixture will depend mainly upon the electron fraction of the components and perhaps their solvation properties. While it is true that in a mixture additional types

of solvent -- solvent interactions could influence the overall solvating properties, in general, an overall averaging of those properties would tend towards the intermediate yields obtained. Scavenging of the resultant ions on the other hand should be much more dependent on microscopic properties of the mixtures, especially if the two solvents produce "common" primary species (e_s^-, H, $\dot{C}H_3$, etc).

It is proposed that in HMPA, excess N_2 arises as a result of secondary ionic scavenging rather than from geminate ion scavenging. If this is the case, then it was anticipated that a study of the nitrogen yield from mixtures of HMPA and a solvent in which secondary ionic reactions are known <u>not</u> to occur might serve to elucidate the anion scavenging mechanism of nitrous oxide in HMPA.

The yield of scavengeable electrons in water has been measured from studies utilizing many solutes and techniques.[172] The data suggest that nitrogen formation from ionic reactions of nitrous oxide in water does not involve secondary ionic reactions. That is, the nitrogen yields observed were comparable to the scavengeable electron yield determined independently.

ii) <u>HMPA/H_2O Mixtures</u>

Consider the radiolysis of HMPA/H_2O mixtures. If, as is indicated from the results discussed earlier, the free ion yield in HMPA is G(f.i.) = 2.2 and the higher yields of nitrogen arise from secondary ionic reactions, the following model can be

proposed.

For a solution of 0.02M N_2O in water, the nitrogen yield is $G(N_2)_{H_2O} = 3.2$;[7,2] which is accepted as the scavengeable electron yield for a solute at that concentration. Since the electron densities of water and HMPA are nearly equal, the yield of solvated electrons produced by ionizing radiation in HMPA-water mixtures would be given by (xliii):

$$G(e_s^-)_{mix} = G(e_s^-)_{H_2O} \cdot V_{H_2O} + G(e_s^-)_{HMPA} (1 - V_{H_2O}) \qquad \text{(xliii)}$$

where V_{H_2O} is the volume fraction of water in the mixture; $G(e_s^-)_{H_2O}$ and $G(e_s^-)_{HMPA}$ are the solvated electron yields in the pure solvents.

In solutions containing nitrous oxide, the solute scavenges these ionic species to produce nitrogen. The assumption is made that if the scavenging mechanism involves HMPA molecules, more than a single nitrogen molecule could ultimately be produced. If water molecules are involved, it is assumed that only a single N_2 results. These mechanisms are represented by reactions (3.72) and (3.73).

$$e^-_{mix} + N_2O \xrightarrow[H_2O]{k_{3.72}} N_2 + \text{products} \qquad (3.72)$$

$$e^-_{mix} + N_2O \xrightarrow[HMPA]{k_{3.73}} (1 + n)\ N_2 + \text{products} \qquad (3.73)$$

where $n \geq 0.0$ and depends upon the N_2O concentration, even in pure HMPA.

The fraction, f, of electrons that could give rise to more than a single molecule of nitrogen is then given by (xliv):

$$f = \frac{1}{1 + \frac{k_{3.72}\,[H_2O]}{k_{3.73}\,[HMPA]}} \qquad \text{(xliv)}$$

The nitrogen yield from a mixture of HMPA and water containing a fixed N_2O concentration would therefore be given by (xlv):

$$G(N_2)_{mix} = G(e^-)_{mix} \cdot (1 + nf) \qquad \text{(xlv)}$$

Combining equations (xliii) to (xlv) one obtains (xlvi),

$$G(N_2)_{mix} = \left[G(e_s^-)_{H_2O} \cdot V_{H_2O} + G(e_s^-)_{HMPA}\,(1-V_{H_2O})\right] \cdot \left[1 + \frac{n}{1 + \frac{K\,[H_2O]}{[HMPA]}}\right] \qquad \text{(xvli)}$$

where $K = k_{3.72}/k_{3.73}$

For $G(e_s^-)_{H_2O} = 3.2$ and $G(e_s^-)_{HMPA} = 2.2$, equation (xlvi) reduces

to (xlvii):

$$G(N_2)_{mix} = (V_{H_2O} + 2.2)\left(1 + \frac{n}{1 + K\dfrac{[H_2O]}{[HMPA]}}\right) \qquad \text{(xlvii)}$$

For pure HMPA containing 0.02M N_2O a value of $n \sim 0.6$ is indicated from Figure III-3. That is at this concentration $G(N_2) \sim 1.6\ G(f.i.)_{HMPA}$ (assuming $G(f.i.)_{HMPA} = 2.2$). Figure III-16 shows plots of equation (xlvii) for $n = 0.64$ and $K = 10^{-3}$, 10^{-1} and 10^{2}. It can be seen that the general shape of the calculated plots is determined by K, the ratio of the 'rate constants' for the scavenging mechamism. This is logical because K discloses which solvent dominates the overall scavenging scheme thereby determining the extent of possible secondary processes. Also included in the figure are the nitrogen yields of Figure III-7 observed experimentally from $HMPA/H_2O$ mixtures containing 0.02M N_2O in the present study.

Equation (xlvii) indicates a maximum possible value for $G(N_2)_{mix} = (1 + 2.2)(1 + 0.6) = 5.1$. This could be achieved if a trace of HMPA in water made reaction (3.73) dominate over (3.72) so that 1.6 N_2 were formed per e_s^-.

The fact that a maximum is reached at all means that $K << 1$ and implies that HMPA has that effect on water. This then implies that in nearly pure water the process (3.65),

$$N_2O^- \longrightarrow N_2 + O^- \qquad (3.65)$$

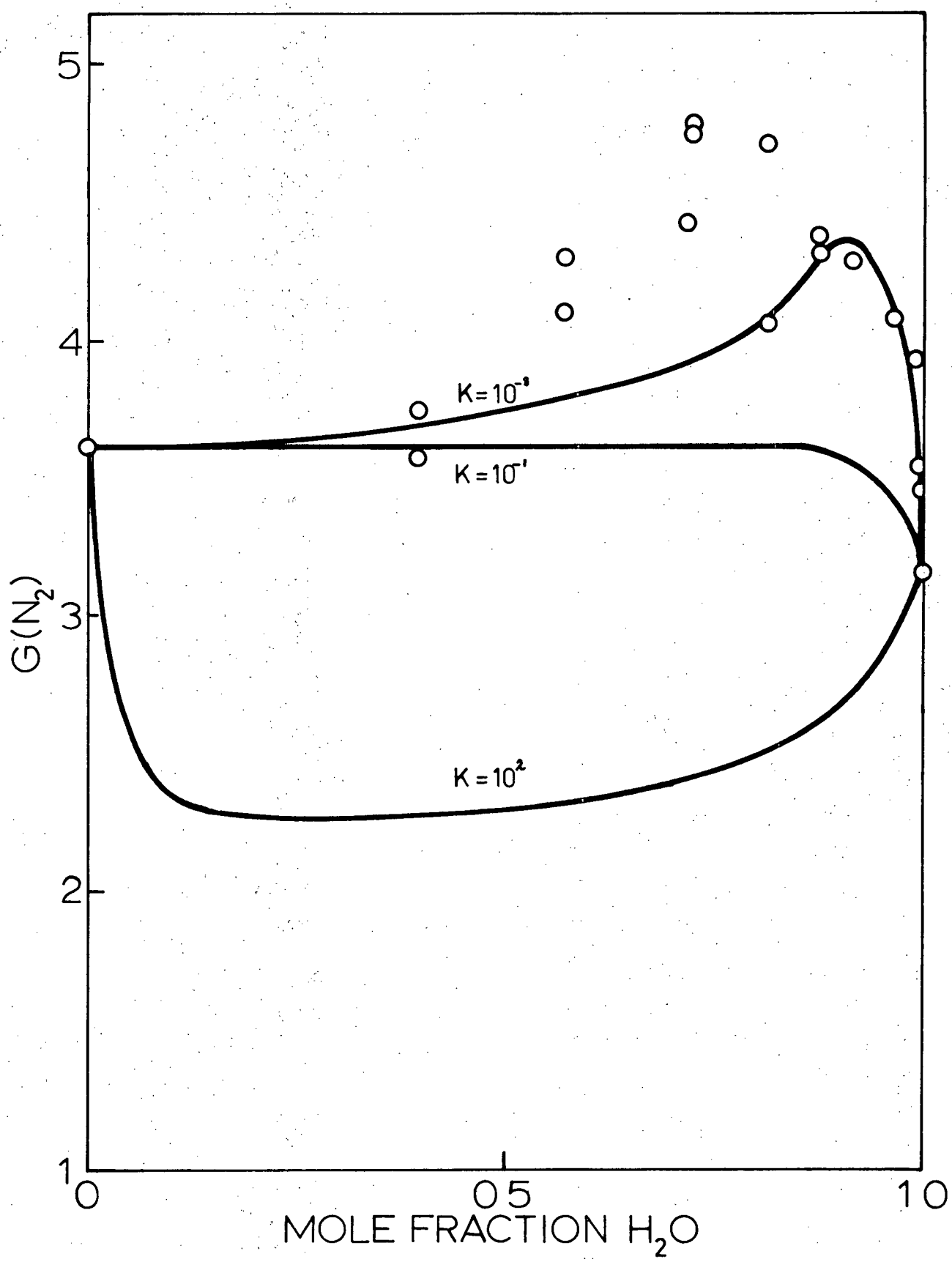

Figure III-16. Computer simulation (lines) and observed nitrogen yields (O) as a function of solution composition from irradiated mixtures of water and HMPA containing 2 X 10^{-2}M N_2O. The curves are explained in the text.

is not very fast or does not simply end there.

The theoretical curve for $K = 10^{-3}$ and $n = 0.64$ represents the best fit to the data from a computer simulation using equation (xlvii). Clearly, the simple overall scheme proposed does not adequately describe the operative mechanism, but further attempts to refine the model would be pure speculation and of little value. Suffice it to say that the N_2 yield data from N_2O in HMPA/H_2O mixtures it consistent with a reaction scheme involving secondary ionic reactions.

Since a constant concentration (0.2M) of N_2O was used in all mixtures, the results point to a second important conclusion. That is, unless the initial radiolytic processes are much different in the mixtures, the observed N_2 yields could <u>not</u> have arisen through geminate ion scavenging processes.

There have been relatively few studies conducted on the radiolysis of liquid mixtures, and fewer still in which N_2O was used as scavenger. The present work appears to be a unique attempt to use mixtures to try to elucidate scavenging mechanisms. Hentz and Scherman[109] studied the radiolysis of dioxane / water mixtures containing N_2O. They concluded that like water, the nitrogen yield corresponded to the solvated electron yield in dioxane.

Now, while they did not examine their N_2 data from dioxane/H_2O mixtures in terms of a function of composition, such considerations are possible from their published data. A plot of dioxane/H_2O data similar to Figure III-16 for the HMPA/H_2O shows N_2 values as a simple linear function of composition --

exactly what one would predict from a mixture of solvents in neither of which secondary ionic reactions are thought to occur.

f) The Nature of the Secondary Ionic Species Leading to N_2 In N_2O Scavenging Studies

Since the experiments had fairly well established that secondary ionic reactions occurred in HMPA containing N_2O, an attempt was made to identify the intermediate species involved. As discussed earlier, electron scavenging by N_2O in liquids almost certainly leads initially to the formation of N_2O^- (3.68). Now, the fate of this N_2O^- ion must be paramount in determining the extent to which ionic reactions lead to excess nitrogen formation. Certainly a lifetime less than the 10^{-4} to 10^{-3} sec attributed to this species in the gas phase[103,121] would be expected. In aqueous systems for example,[173,174,175] there is evidence that N_2O^- is rapidly converted to a hydroxyl radical through proton transfer from solvent (3.66).

$$N_2O^- + H_2O \longrightarrow OH + OH^- + N_2 \qquad (3.66)$$

A half-life less than 3×10^{-6} sec was indicated for this process and Adams[176] estimated a value as low as 1 nsec. Czapski[177] pointed out that O^-_{aq}, rather than N_2O^- (3.74), might in fact be the reactive intermediate species in the aqueous system and that as such might live for perhaps 10^{-9} to 10^{-8} sec before being

converted to a hydroxyl radical (3.75).

$$N_2O^- \xrightarrow{H_2O} N_2 + O_s^- \qquad (3.74)$$

$$O_s^- + H_2O \longrightarrow OH + OH_s^- \qquad (3.75)$$

Zehavi and Rabani[178] conducted a thorough multi-solute study of N_2O saturated aqueous solutions. They presented rather convincing evidence that N_2O^-, O^- and OH were formed in turn from aqueous electrons via reactions (3.68), (3.74) and (3.75) with half-lives of 10, $\leq$ 100, and 7 nsec respectively.

Salmon et al.[179] however, concluded from studies of N_2O and galvinoxyl, Gv, in cyclohexane that N_2O^- has a lifetime $\geq$ 20 μsec in that solvent. They monitored the build-up of the strong optical absorption of the Gv^- anion. From a solution containing 5 X 10^{-5}M galvinoxyl in cyclohexane the presence of 0.1M N_2O had no effect upon the yield of Gv^-, although the kinetics of its formation changed. Now, N_2O is known to be a efficient electron scavenger, therefore, from these solutions where $[N_2O]/[Gv] = 5 \times 10^3$ the electrons would be scavenged by N_2O. Salmon et al. concluded that Gv^- was formed via electron transfer from N_2O (3.76).

$$N_2O^- + Gv \longrightarrow N_2O + Gv^- \qquad (3.76)$$

The fact that Gv^- formation continued for more than 20 μsec was

taken as an indication of the N_2O^- lifetime. On the other hand, the presence of .1 M iodine, another efficient electron scavenger, completely surpressed Gv^- formation.

However, since Salmon et al. did not measure the nitrogen yields from their samples, this author feels that there is no justification for the assignment of N_2O^- as the long-lived intermediate transferring change with Gv. That is, their mechanism implies there should be complete surpression of nitrogen formation from N_2O^- containing solutions in the presence of even small amounts of galvinoxyl. An alternative (and at least equally plausible) explanation for their observations is that galvinoxyl reacted not with N_2O^-, but with some daughter anion arising from the N_2O^- decay mechanism -- possibly O^-, $N_2O_2^-$, O_2^- or some other species -- after N_2 formation. Indeed, Schuler's recent studies on cyclohexane[171] indicate that if secondary ionic reactions of N_2O occur in that system, then they must be extremely rapid.

It was thought that galvinoxyl might prove to be an excellent probe of the N_2O scavenging mechanism in HMPA. The proposed mechanism could be represented by the following simplified scheme (3.77), (3.78), (3.79).

$$e^-_{HMPA} + N_2O \xrightarrow{HMPA/N_2O} N_2O^- \qquad (3.77)$$

$$N_2O^- \xrightarrow{HMPA/N_2O} \longrightarrow N_2 + A^- \qquad (3.78)$$

$$A^- \xrightarrow{HMPA/N_2O} \longrightarrow N_2 + B^- \qquad (3.79)$$

That is, in HMPA solution, nitrous oxide scavenges the electrons to produce N_2O^- which then goes on to produce one or more molecules of nitrogen. Now, consider the effect upon the observed nitrogen yield of the addition of a small amount of galvinoxyl. If galvinoxyl effectively scavenged N_2O^-, nitrogen formation would be totally surpressed. If the A^- anion of the proposed scheme were scavenged, then the nitrogen yield would be reduced to a constant value equal to the electron yield. Finally, if B^- (or some daughter anion) were scavenged by galvinoxyl, the nitrogen yield would be unaffected (or partially reduced). As was shown in Table VII, the addition of 10^{-4}M galvinoxyl to a solution of 1.4×10^{-2}M N_2O in HMPA had little effect upon the nitrous yield. Only when the concentration of galvinoxyl was increased to a level where direct competition between Gv and N_2O for the electrons themselves would be probable did the nitrogen yield drop appreciably. Even then, a plateau value was not observed; the nitrogen yield was simply a function of the solute composition as shown in Figure III-10. It is significant that even in the presence of 0.05M galvinoxyl the nitrogen yield from a solution of 0.12M N_2O in HMPA was $G(N_2) = 2.7$, a value higher than the proposed free ion yield $G(f.i.) = 2.2$. Thus, even at a concentration where galvinoxyl would be competing for electrons directly, there is evidence suggestive of a secondary ionic mechanism of nitrogen formation.

Now, since the galvinoxyl anions, Gv^-, would be neutralized

eventually by the concomitant positive ions produced during the radiolysis, the yield of these ions (or in fact their presence) could not be measured in the present experiments. Capellos and Allen[91] found that the galvinoxyl anion decays on the microsecond timescale in hydrocarbon solvents. However, the experiments with HMPA indicate that either N_2O^- does <u>not</u> transfer an electron to galvinoxyl or else it is too short lived in HMPA to do so. A similar argument would apply to species A^- of reaction (91) which most likely would be O^- or $N_2O_2^-$ in the HMPA system. The evidence, although not strong, suggests that galvinoxyl could interrupt only a later stage of the N_2O scavenging mechanism.

Attempts were made to further define the nature of possible species A^-. The N_2O^- ion might be short lived in HMPA because of decay to an oxide radical anion (3.80).

$$N_2O^- \xrightarrow{\text{HMPA}} O^- + N_2 \qquad (3.80)$$

In this case, secondary nitrogen formation would have arisen from the subsequent reactions of the oxide ion. Now, molecular oxygen is known to react readily with this ion (3.81) to produce the ozonide ion, O_3^- -- a value of $k_{3.81} = 2.6 \times 10^9$ M^{-1} sec^{-1} being reported for the rate constants of aqueous solutions![180]

$$O^- + O_2 \longrightarrow O_3^- \qquad (3.81)$$

Oxygen was added to samples of N_2O in HMPA. If the oxide ion were important in the secondary N_2O scavenging mechanism, one would expect the nitrogen yield to be reduced to a constant value indicative of the electron yield. However, the presence of oxygen, even in large amounts (comparable with the N_2O concentration) had little effect upon the nitrogen yield. This result is somewhat ambiguous, however, because the O^- system may not be quite so straight forward. Beher and Czapski[181] have suggested that the O_3^- ion can dissociate unimolecularily to regenerate the O^- ion (3.81).

$$O_3^- \longrightarrow O_2 + O^- \qquad (3.81)$$

This mechanism was supported by the work of Gall and Dorfman[182] who reported an absolute rate constant $k_{3.81} = 3.3 \times 10^3$ sec^{-1} for this reaction. Therefore, if the ozonide ion had no alternative fate in the HMPA system, regeneration of oxide could produce the observed results. Now, the oxide ion, O^-, also reacts with methanol (3.82) ($k_{3.82} = 5.8 \times 10^8$ M^{-1} sec^{-1})[183]

$$O^- + CH_3OH \xrightarrow{k_{3.82}} CH_2OH + OH^- \qquad (3.82)$$

In the present work, Table VII shows that the presence of 1 M methanol in N_2O solutions of HMPA had no observable effect upon the nitrogen yield. This result taken in conjunction with the oxygen addition data tends to preclude the involvement of oxide ions (reaction 3.80) in the N_2O secondary ionic reaction mechanism

in HMPA radiolysis.

The N_2O^- ion could also be short lived in HMPA because of subsequent reaction with N_2O (3.61).

$$N_2O^- + N_2O \longrightarrow N_2O_2^- + N_2 \qquad (3.61)$$

Recall that the studies on the radiolysis of N_2O in gaseous hydrocarbons gave evidence that CO_2 could scavenge the $N_2O_2^-$ ion (or possibly O^-). Unfortunately there is ample evidence to suggest that in solution, CO_2 may also act as an electron scavenger[184] (3.84).

$$e_s^- + CO_2 \longrightarrow CO_2^- \qquad (3.84)$$

In the present study of HMPA radiolysis, Table VI shows that the nitrogen yield from N_2O solutions was <u>unaffected</u> by the presence of CO_2, even in amounts comparable to N_2O. At first glance, this appears contrary to the other evidence which points to the involvement of $N_2O_2^-$ (or less likely, O^-) ions in the anionic-N_2O scavenging mechanism in HMPA. However, it is significant that CO_2 did not compete for the electrons directly. If CO_2 behaved in HMPA in a way similar to the water or cyclohexane systems cited, then the results necessitates that the electron species (and subsequently O^- or $N_2O_2^-$) be very short-lived in HMPA. Other evidence suggests that this is not the case. One is forced to the conclusion that in HMPA solution,

CO_2 either cannot compete for ionic species on an equal basis with other processes as it does in other media or else the CO_2^- ion readily gives up its excess electron to other solutes. Infelta and Schuler[170] had shown for example that in cyclohexane solution, CO_2^- transfers an electron to CH_3Br. One could further speculate on the source of this ambiguity, but suffice it to say that CO_2 is not suitable as a second solute for attempts to elucidate the N_2O scavenging mechanism in HMPA.

Thus, on the basis of information from N_2O in pure HMPA, H_2O/HMPA mixtures, and solutes of HMPA containing a second solute, some information has been gained about the nature of the electron scavenging mechanism by N_2O in HMPA. The N_2O^- ion formed initially must be short-lived, but probably does not decay to give the oxide ion O^-. The N_2O^- ion reacts with positive ions, solvent molecules or additional N_2O molecules to give a molecule of nitrogen and a product (other than O^-) which may or may not react further with N_2O to produce additional nitrogen. Direct reaction of N_2O^- ions with positive ions (i.e. simple neutralization) is not likely to be of major importance in a system like HMPA where secondary ionic reactions are indicated. Firstly, being uncharged, the species formed from neutralization are unlikely to lead to the subsequent reaction necessary to produce 'secondary' nitrogen molecules. Secondly, even if neutralization occurred at a rate limited only by diffusion, the ions are present at such a low steady state concentration that they would still have lifetimes sufficient to allow effective reaction with added solutes. Indeed, Dainton et al.[180] estimated

a second order rate constant of about 2×10^{12} M^{-1} sec^{-1} for neutralization of N_2O^- in cyclohexane solution. In HMPA the secondary ionic mechanism most likely involves the participation of $N_2O_2^-$ ions at some stage.

Despite the fact that numerous approaches have been tried, the present research has failed to clearly define the mechanism by which N_2O scavenges anionic species produced during steady state γ-radiolysis of HMPA. Consequently, the absolute value of the solvated electron or free ion yield by scavenger methods has not been unequivocally established. It should be noted however that similar ambiguity and uncertainty exists in many systems when scavenging methods are involved.

Recently for example, two groups of investigators studied what was presumably the simplest system of this type -- nitrous oxide in liquid Xenon. Because of the large electron mobility in Xenon (2200 cm^2 V^{-1} sec^{-1})[185] it is likely that the radiolysis would result in a large yield of homogeneously distributed free ions. Rzad and Bakale,[114] basing their arguments on considerable data, convincingly demonstrated the involvement of secondary reactions of N_2O in that system. Robinson and Freeman[115] on the other hand, who were conducting concurrent studies, applied Freeman's diffusion model[146] and proceeded to discuss the same system,equally convincingly,completely in terms of free and geminate electron scavenging.

g) Solutions of Sodium Metal in HMPA

As discussed in some detail in the introduction, many polar solvents have been shown capable of dissolving alkali metals to produce stable solutions. HMPA has been shown to be an excellent solvent for such purposes. The solutions comprise a variety of solvated species which may include solvated electrons, metal ions and atoms, as well as a number of aggregate species. The paramagnetic susceptibility, paramagnetic resonance spectra, optical absorption spectra, and equivalent conductivity of the solutions consistenty indicate that the solvated electron is of paramount importance in those systems. Thus, the dissolution of an alkali metal, M, in a solvent, S, may with reasonable certainty be initially represented by reaction (3.85).

$$M + S \longrightarrow M_s^+ + e_s^- \qquad (3.85)$$

where the subscript, s, denotes solvated species.

Alkali metal solutions of known concentrations are most difficult to prepare. Initial reaction with trace impurities and natural decay during the relatively slow dissolution of bulk metal particles lead to uncertainty in species concentration. The latter problem can be alleviated by transferring the solvent to a vessel containing a prepared metal mirror which dissolves almost instantly. However, such a procedure is not always desirable and Warshawsky[186] has shown that even under "stick" vacuum conditions the distillation of alkali metals in Pyrex

glassware leads to partial decomposition due to reaction with strongly absorbed water molecules. Finally, because of the diversity of species that have been shown to exist in these solutions (possibly in equilibrium with each other) one has little hope in preparing a solution of known composition.

Solutions of alkali metals in HMPA decay slowly to give predominantly the salts of two anions, namely the dimethylamine anion and diamidophosphite anion (3.86)[1]:

$$OP(N(CH_3)_2)_3 + 2M \longrightarrow\longrightarrow (CH_3)_2N^-M^+ + ((CH_3)_2N)_2PO^-M^+ \qquad (3.86)$$

These ions produce the observed orange colouration of the "spent" sodium solutions in the present study. The decay was originally thought to occur via a simple radical-anion mechanism. In view of the now accepted major importance of solvated electrons in these systems, the decay mechanism more likely arises from initial reaction with these species, with radical anions possibly being a reactive intermediate. In HMPA the observed formation of small amounts of hydrogen and methane from decay of the sodium solution suggests that a number of anions and radicals may be formed such as suggested by reactions (3.87) to (3.91).

$$OP(N(CH_3)_2)_3 + e_s^- \xrightarrow{Na^+} \left[OP(N(CH_3)_2)_3^-\right] \qquad (3.87)$$

$$\left[OP(N(CH_3)_2)_3^-\right] \longrightarrow \left[OP(N(CH_3)_2)_2N(CH_3)\bar{C}H_2\right] + \dot{H} \qquad (3.88)$$

$$\xrightarrow{Na^+} OP(N(CH_3)_2)_2\dot{N}CH_3 + \dot{C}H_3 \qquad (3.89)$$

$$\longrightarrow Na^+ \ ^-OP(N(CH_3)_2)_2 + \dot{N}(CH_3)_2 \qquad (3.90)$$

$$\longrightarrow Na^+ \ ^-N(CH_3)_2 + O\dot{P}(N(CH_3)_2)_2 \qquad (3.91)$$

where $\left[OP(N(CH_3)_2)_3^-\right]$ may or may not represent a real species, and the radicals may be stabalized via hydrogen abstraction from HMPA or bimolecular recombination.

The fact that nitrous oxide was efficiently and quantitatively reduced to nitrogen in an excess of the blue solution of sodium in HMPA but completely unaffected by the decayed (orange sodium-salt anion) solution is most significant. It demonstrates that N_2O scavenges an electron species which exhibits an optical absorption in the infra-red region of the spectrum. That is, N_2O was reduced either by solvated electrons themselves or by some solvated species which consists simply of a close association of electrons with sodium ions and/or solvent molecules ($HMPA_s^-$, $(Na^+ \cdot\cdot e^-)_s$, Na_s, Na_s^-, Na_{2s}) -- but was <u>not</u> reduced by sodium cations or any of the anions of decomposed HMPA.

In order to facilitate a more detailed study of the N_2O scavenging mechanism, it was necessary to introduce known amounts of sodium metal to a solution of N_2O in HMPA, water, and mixtures

of the two. In addition, it was necessary to limit the local concentration of solvated species at the point of metal injection so as to allow reactive competition and diffusion by the N_2O solute molecules. These prerequisites were realized through the use of liquid sodium/mercury amalgams. In pure water, where the introduction of pure sodium metal is explosive, the amalgams reacted slowly over a period of hours to produce one-half mole of hydrogen for each mole of sodium atoms (or presumably e^-_{aq}) present. This observation corroborates results previously reported[117] and obeys the accepted stochiometry of reaction (3.92) for which the bimolecular combination rate constant has a reported value $k_{3.92} = 1 \times 10^{10}\ M^{-1}\ sec^{-1}$.[189]

$$e^-_{aq} + e^-_{aq} \xrightarrow{H_2O} H_2 + 2OH^-_{aq} \qquad (3.92)$$

Nitrous oxide, present in water at a concentration of 6×10^{-2}M competed successfully for e^-_{aq} produced upon amalgam dissolution. Hydrogen production was supressed and in its place an equivalent amount of nitrogen obtained. That is, two moles of the reducing species reacted with N_2O to produce a single mole of nitrogen. Shaede and Walker[190] had observed this unusual behavior earlier and attributed the unexpected relationship to inhomogeneity effects. They suggested that the reduction of nitrous oxide in aqueous solution would result in the formation of a hydroxyl radical through protonation of the oxide ion (3.93).

$$e^-_{aq} + N_2O \xrightarrow{H_2O} N_2 + OH + OH^- \qquad (3.93)$$

Reaction is localized at or near the amalgam/water interface which would facilitate the scavenging of a second solvated electron by the hydroxyl radical (3.94).

$$e^-_{aq} + OH \longrightarrow OH^-_{aq} \qquad (3.94)$$

Reaction (3.94) is known to be very fast[37] ($k_{3.94} = 3 \times 10^{10}$ M^{-1} sec^{-1}) and could well account for the observed stoichiometry and absence of molecular oxygen.

It was hoped that the addition of sodium amalgams to solutions of N_2O in HMPA would result in the formation of two moles of nitrogen for each mole of sodium (or solvated electrons) injected. Such a result would provide direct evidence for the secondary ionic scavenging mechanism proposed from the radiolysis experiments. The involvement of the oxide anion, O^-, has been shown most unlikely in the HMPA scheme so that the formation and subsequent reaction of hydroxyl radicals (from reactions analagous to (3.93) and (3.94)) was doubtful. However, as can be seen from the data presented in Table VIII, the addition of sodium amalgam to N_2O/HMPA solutions produced nitrogen yields less than or at best equal to those obtained from the aqueous solutions. In other words, assuming that N_2O scavenges all the reducing species, these results imply that two electrons (or sodium atoms) are required to reduce a single N_2O molecule to N_2 in the amalgam/N_2O/HMPA system. These results are not at all compatible with the radiolysis data and certainly show no evidence of secondary

ionic reactions leading to N_2 formation.

It may be that scavenging reactions on amalgam addition take place totally at the amalgam surface through a unique mechanism and as such do not reflect the properties of the solvent or solutes involved.

One feature of the amalgam experiments that supports this conjecture is the fact that the amalgams were completely stable in pure HMPA, reacting only when N_2O was added. This suggests that solvation energy for electrons in HMPA is small -- certainly less than the stabilization energy provided by the amalgam. Now, such a conclusion is not unreasonable, for as has been stated, HMPA is known to be an extremely poor solvator of anions. Indeed, it came as an unexpected surprise that solvated electrons were at all stable in this solvent. It was noted that when the amalgams were prepared considerable heat was generated, showing the process to be exothermic. The exact nature of the amalgams is unknown. The sodium atoms may be ionized, undissociated or bonded in a Na-Hg compound, although electrical conductivity data[191] on dilute amalgams tends to rule out the former case.

Reaction of N_2O at the amalgam surface could then involve Na atoms directly. In the gas phase, such reaction is known to occur to give Na_2O (3.95).

$$2Na + N_2O \longrightarrow Na_2O + N_2 \qquad (3.95)$$

It is interesting to note that in the gas phase, two Na atoms are

required to reduce a single N_2O molecule.

It was noticed in the present study that N_2O could in fact react with sodium amalgam in the absence of solvent. This, taken with the fact that amalgams were stable in HMPA until N_2O was introduced, strongly suggests that surface reaction also occurred in solution. Possibly then, the unexpectably low N_2 yields from such solution arise from reactions (3.96) and (3.97) in which two Na atoms are required for each N_2O reduced.

$$Na/Hg + N_2O \longrightarrow NaO/Hg + N_2 \qquad (3.96)$$

$$NaO/Hg + Na/Hg \longrightarrow Na_2O/Hg \qquad (3.97)$$

where /Hg refers to species in or at the amalgam surface.

Therefore, while the studies involving sodium metal in HMPA support the general conjecture that N_2O reacts with solvated electrons in HMPA, the data unfortunately cannot further elucidate the exact scavenging mechanism.

C. PULSE RADIOLYSIS STUDIES OF SOLVATED ELECTRONS IN HMPA

As had been anticipated, the steady state gamma radiolysis and sodium metal solution studies showed HMPA to be a very useful medium for investigating solvated electrons. However,

the work suffers a major drawback in that most of the specific conclusions pertaining to the solvated electron come indirectly from observations of reaction products. As a result, a number of ambiguities arose and it has proven difficult to decide in many cases whether the problem originates with a primary species or some reactive intermediate in the product formation scheme.

Scavenger studies indicated that the radiation produced solvated electron in HMPA has a natural lifetime of the order of microseconds -- long enough to be directly observable with modern pulse radiolysis apparatus. Clearly, direct observation of the electron's spectrum and reactions would complement the steady state work very well. It would be particularly valuable to obtain an independent value of the electron yield. Also, observations of the reactions between solvated electrons and scavengers (notably N_2O, acetone and H_2O) might confirm the proposed reaction schemes. The relative importance of geminate ion scavenging in this system might also be resolved from studies using both electron and positive ion scavengers.

The pulse radiolysis facilities at U.B.C. were not suitable for the types of experiments that would give useful information on the HMPA system. Fortunately, an opportunity arose to make use (on a short term basis) of the pulse radiolysis facilities at The Ohio State University in Columbus, Ohio. Those facilities were ideally suited for the particular experiments desired, so arrangements were made for two field trips to that establishment. The knowledge gained about the HMPA system from the steady state

work at U. B. C. facilitated the planning of specific experiments and conditions such that a great deal of useful information could be obtained in the short time available.

The absorption spectra for the wavelength region 300 - 2300 nm obtained in pure HMPA at the end of 5 Krad electron pulses is shown in Figure III-17. HMPA itself exhibits a number of strong absorption bands over this spectral region. These can be seen in Figure III-18 which shows the solvent absorption spectra as measured directly in a radiolysis cell having a 20 mm path length. The transient absorption spectrum of Figure III-17 actually represents the normalized results of several independent series of experiments using cells having optical path lengths of 3 and 20 mm.

The intensity and decay characteristics of this band were studied as a function of wavelength, radiation dose and sample purity. It was revealled that a second species contributed to the absorption below 500 nm. This species, which accounted for the increase in absorbance in the UV region as can be seen in Figure III-17, was much longer lived than the species absorbing in the infra-red. A number of solutes including electron and positive ion scavengers were added to HMPA samples. The effects of these upon the intensity and decay of these bands was investigated. When new absorptions appeared their intensity and decay were monitored. The specific details and results of all these experiments are best presented as their implications are discussed.

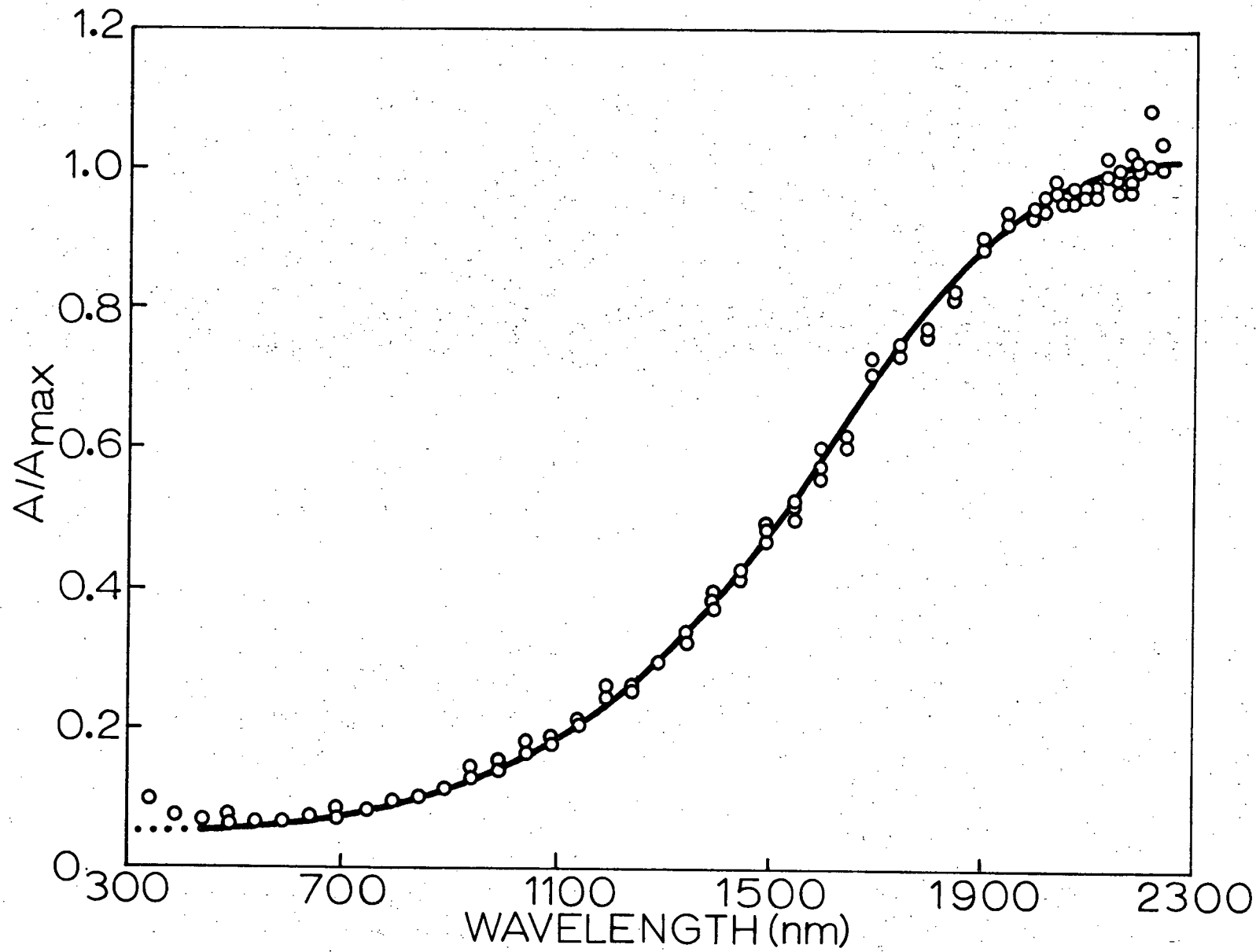

Figure III-17. Transient absorption spectrum in pulse irradiated HMPA. A_{max} represents the absorbance at 2200 nm.

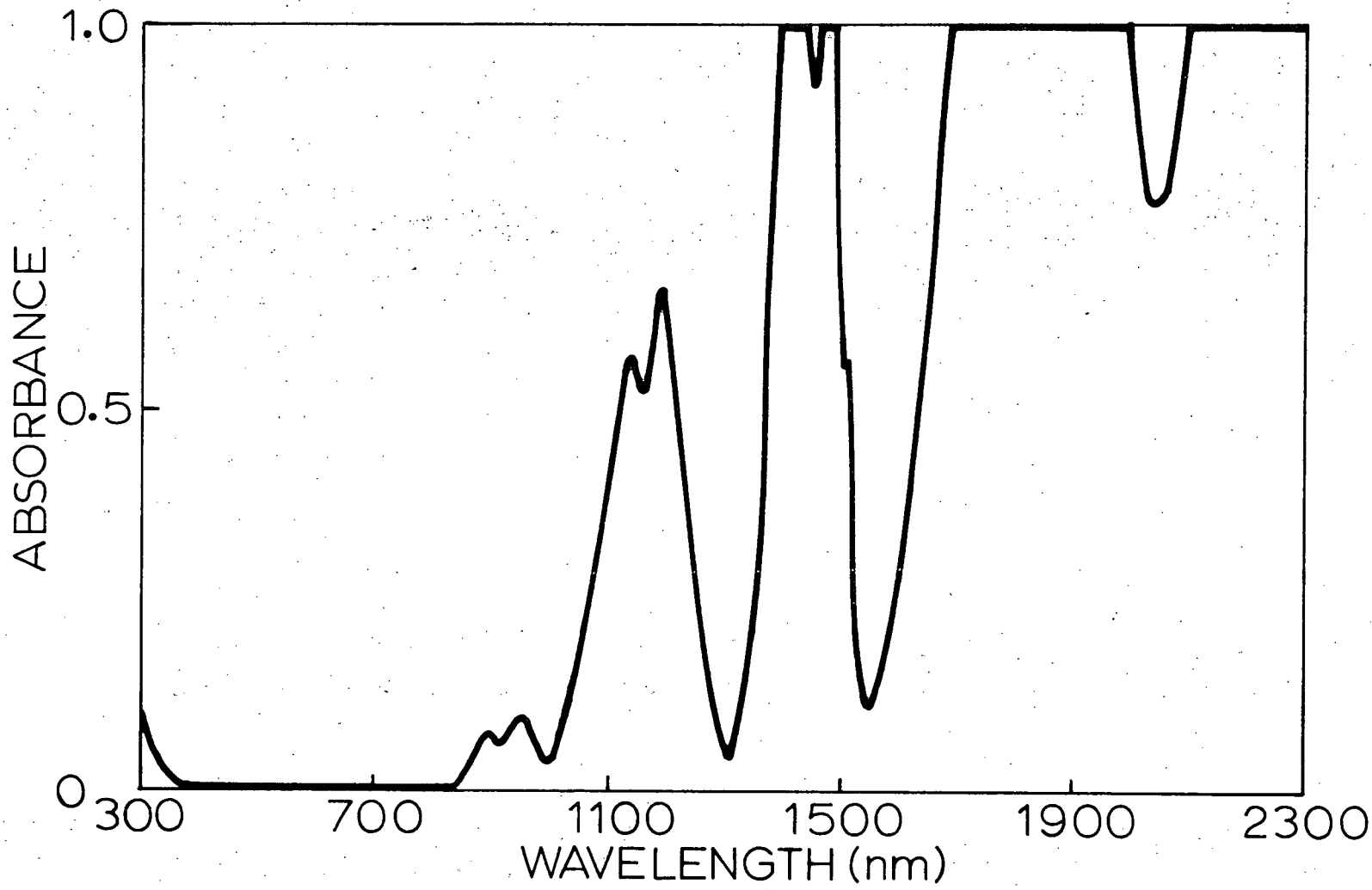

Figure III-18. Absorption spectrum of pure HMPA exhibited in a radiolysis cell having an optical path length of 20 mm.

D. DISCUSSION: PULSE RADIOLYSIS EXPERIMENTS

1. Transient Absorption Spectra

The transient absorption spectrum obtained from the pulse radiolysis of HMPA as shown in Figure III-17 is similar over the wavelength range 1000 - 2300 nm to that attributed by Brooks and Dewald[75] to the solvated electron in solutions of sodium in HMPA. Their spectra exhibits absorptions below 1000 nm attributed to species involving alkali metal cations. No such absorption appears in the present radiolysis study, but when the two spectra are normalized at 1500 nm they correspond very well over the region 1000 nm to 2300 nm (the detection limit for the present study). In addition, the spectrum is in general agreement with two recent studies of the pulse radiolysis of HMPA[193,194] which suggest that absorption band maximum occurs at λ_{max} >1500 nm. As can be seen from Figure III-17, the present study indicates that the absorption maximum is near 2200 nm. However, the intense solvent absorption, the decreased intensity of the analyzing light, and the reduced sensitivity of the photo-diode in this region precluded in unequivocal determination of λ_{max}. Jou et al.[195] have shown empirically that for binary mixtures of ethylenediamine (EDA) with various ethers, λ_{max} changes monotonically between the maxima for the pure liquids. Extrapolation of plots of mixture composition versus band maximum energy to the pure ether case gave excellent agreement with the actual band maximum energy observed from the pure liquid.

The band maxima in pure EDA occurs at 1360 nm. Mixtures of HMPA/EDA would be expected to give maxima between 1360 - 2200 nm -- a region where the photodetection system employed is much more sensitive. Extrapolation of an energy/composition plot to pure HMPA would thus provide a independent estimation of the band maximum for that system. Figure III-19 shows such a plot for HMPA/EDA mixtures. Mixture composition is expressed in terms of both mole and volume fraction. Jou and co-workers used mole fraction in their discussion, but there seems little justification for so doing. For miscible liquids, there are reasons for expecting the composition over which the solvated electron's density is distributed to be given by the volume fractional composition. This conjecture is supported by the superior linearity exhibited by the plot of energy of the mixture maxima verses volume fraction as opposed to mole fraction. When the molecular weights of the components are comparable (as in the Jou experiments) it wouldn't matter which fraction is used.

Extrapolation of Figure III-19 gives a value of λ_{max} = 2150 ± 100 nm for pure HMPA, which is in excellent agreement with the direct measurements.

Dye and co-workers[196] have shown that solvated electron spectra can be mathematically reproduced by a combined Gaussian/Lorentzian function. For a given spectral energy, $\bar{\nu}$, the relative absorbance, $y(\bar{\nu})$, has been found to be well approximated by (xlviii):

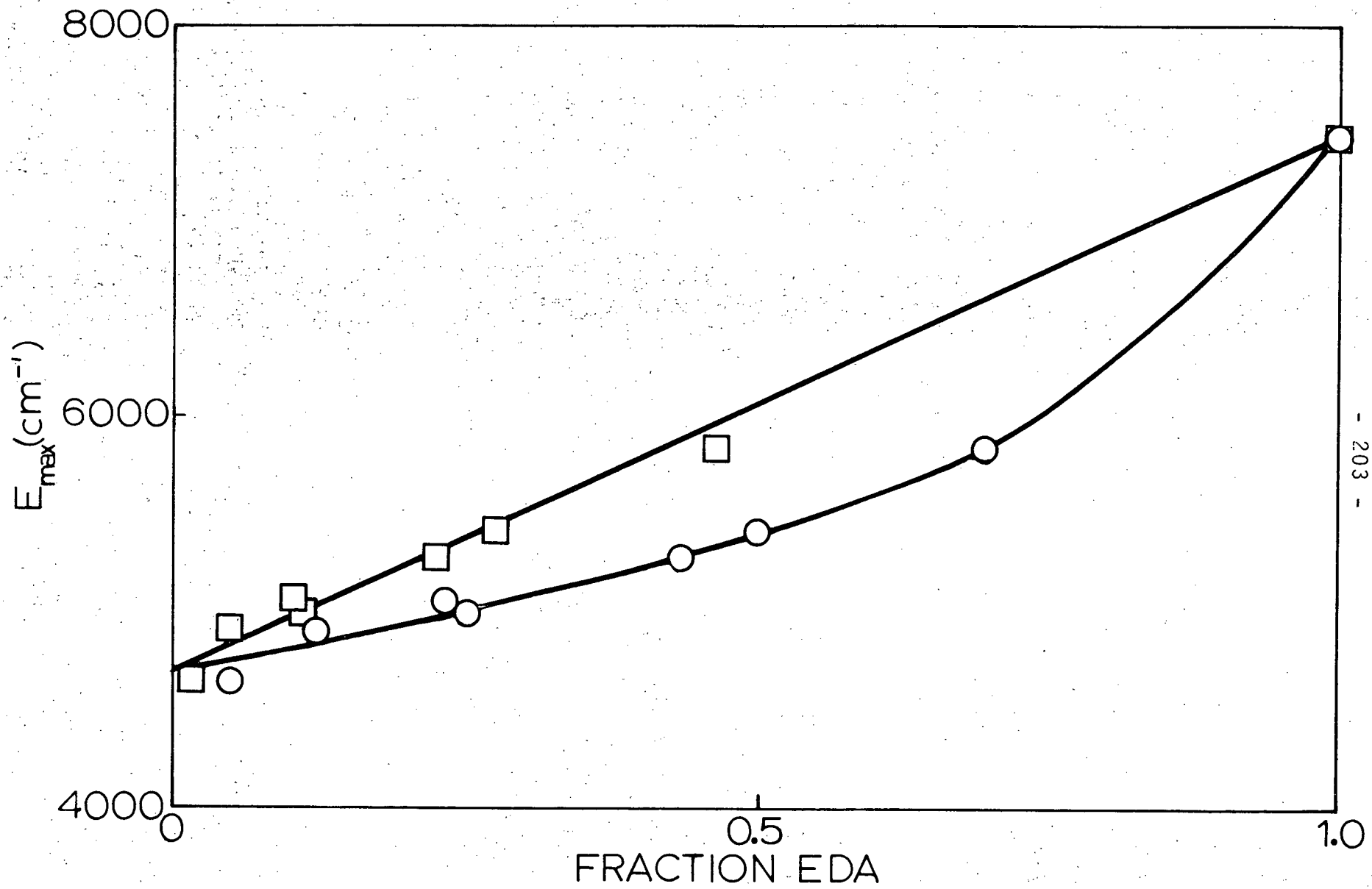

Figure III-19. Absorption maxima for e_s^- in HMPA/EDA mixtures as a function of solution composition expressed as mole (O) and volume (□) fraction.

$$y(\bar{\nu}) = \exp\left[-\frac{\ln 2\,(\bar{\nu}_{max} - \bar{\nu}_i)^2}{G^2}\right] \quad \text{for } \bar{\nu}_i < \bar{\nu}_{max}$$

$$= \frac{L^2}{L^2 + (\bar{\nu}_i - \bar{\nu}_{max})^2} \quad \text{for } \bar{\nu}_i > \bar{\nu}_{max} \qquad \text{(xlviii)}$$

where G and L are half of the independently variable "half-widths" for the Gaussian and Lorentzian functions. $\bar{\nu}_{max}$ is the energy (cm^{-1}) corresponding to the absorption maximum.

Taking $\bar{\nu}_{max}$ = 4550 cm^{-1} (corresponding to λ_{max} = 2200 nm) for the HMPA system, the function was fitted to the data of Figure III-17. The resultant curve is shown along with the data plotted on an energy scale in Figure III-20. Also included in this figure, represented by the filled circles, is data over the region 1000 - 3200 nm taken from the spectrum obtained by Brooks and Dewald[75] for sodium solutions in HMPA.

From this spectral data alone one can with reasonable confidence assign the observed band to the solvated electron in HMPA. As will be detailed later, the behavior of the species responsible for the absorption in the presence of added scavengers corroborates this conclusion.

The half-width of the absorption band in HMPA appears in Figure III-20 to be only 3600 cm^{-1} (0.45 eV) -- a much smaller value than has been generally found in other systems. For instance in the alcohols, amines and ethers, half-widths in the range of 0.7 to 1.5 eV are common. Also, the absorption maximum

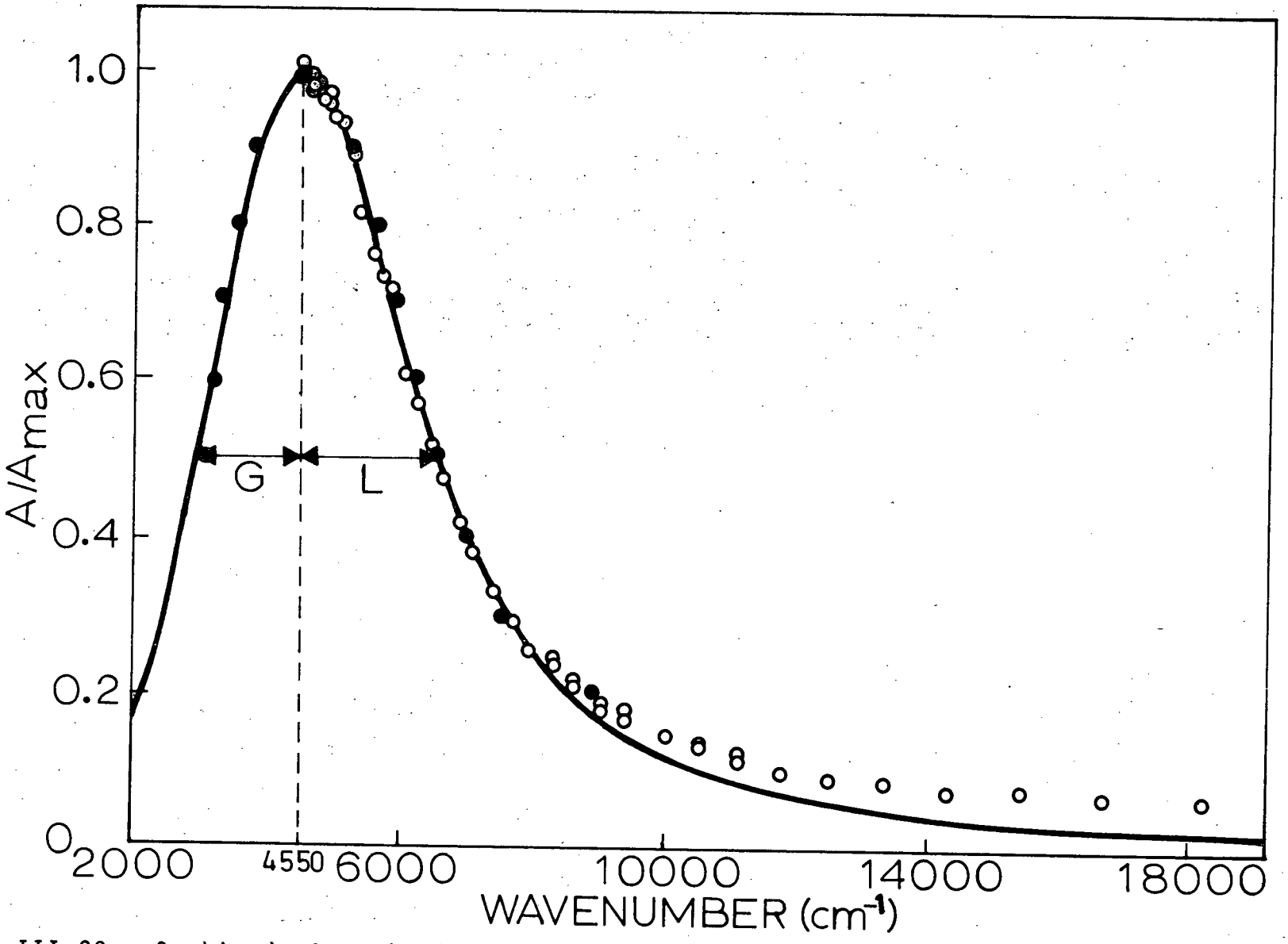

Figure III-20. Combined Gaussion/Lorentzian fit to the spectrum of Figure III-17 plotted on an energy scale. Published data from Na solution in HMPA (●) is included. G and L are explained in the text.

at 2200 nm corresponds to a transition energy of only 0.57 eV. These facts together suggest that solvated electrons are very weakly bound in HMPA, and that the cavities are large and not too dissimilar in size. These results had been anticipated from considerations of the size and nature of the HMPA dipoles. A simple calculation of the smallest cavity possible from a tetrahedral configuration of four HMPA molecules pointing "head-in" indicated a radius of about 5Å. Indeed, taking λ_{max} = 2200 nm, a calculation based on Jortner's cavity continuum model has been made[197] and a value of 4.3 Å for the cavity radius obtained. These values are large in comparison to similar calculations for several alcohols, ethers and amines where radii from 1 - 3 Å were indicated.[198]

2. Molar Absorptivity and Band Oscillator Strength

The absolute intensity of the transient absorption band was measured by converting the solvated electrons to anions of known molar absorptivity. Aromatic hydrocarbons exhibit relatively high electron affinities[199] and they react to produce stable anions which absorb strongly in the visible region of the spectrum. Through electron transfer reactions with a known amount of the dimeric dianion of 1,1-diphenyl ethylene, Gill et al.[200] prepared solutions of the anions of pyrene (Py) and anthracene (An) in tetrahydrofuran (THF). They reported values for the maximum molar absorptivities of 5.0×10^4 M^{-1} cm^{-1} for Py^- at 495 nm and 1.0×10^4 M^{-1} cm^{-1} for An^- at 740 nm respectively.

When pyrene or anthracene were present in pulse irradiated HMPA the electron spectrum was replaced by bands corresponding to the aromatic anions as shown in Figure III-21. In order to verify that these aromatic anions possess equivalent molar absorptivities in HMPA and THF, their spectra in the two systems were compared. Fortunately, the apparatus had been used sometime earlier for a study of pyrene in THF.[201] In Figure III-21, the solid line of the pyrene anion spectra actually represents the spectra obtained in THF, normalized at the band maximum with the HMPA data (circles). The spectra, undoubtedly arising from ($\pi \rightarrow \pi^*$) electronic transitions involving the conjugated aromatic ring system, would not be expected to be greatly influenced by the solvent. The fact that the pyrene anion spectra appear identical in the two solvents supports the idea that equivalent transition states are involved. Thus, since the solvents in question have comparable refractive indices, one can make the reasonable assumption that the oscillator strength for the band is approximately the same in both media. Then, the conclusion is reached that the value for the maximum molar absorptivity of the pyrene anion in THF also applies for that anion in HMPA. An analogous situation most probably holds for the anthracene anion as well.

It should be pointed out that both the aromatic cations[202] and excited aromatic molecules[203] are also known to absorb in the same region of the spectrum as do the aromatic anions. Fortunately, it was easily proven that no such interference had occurred. The relatively long life-times of the absorptions

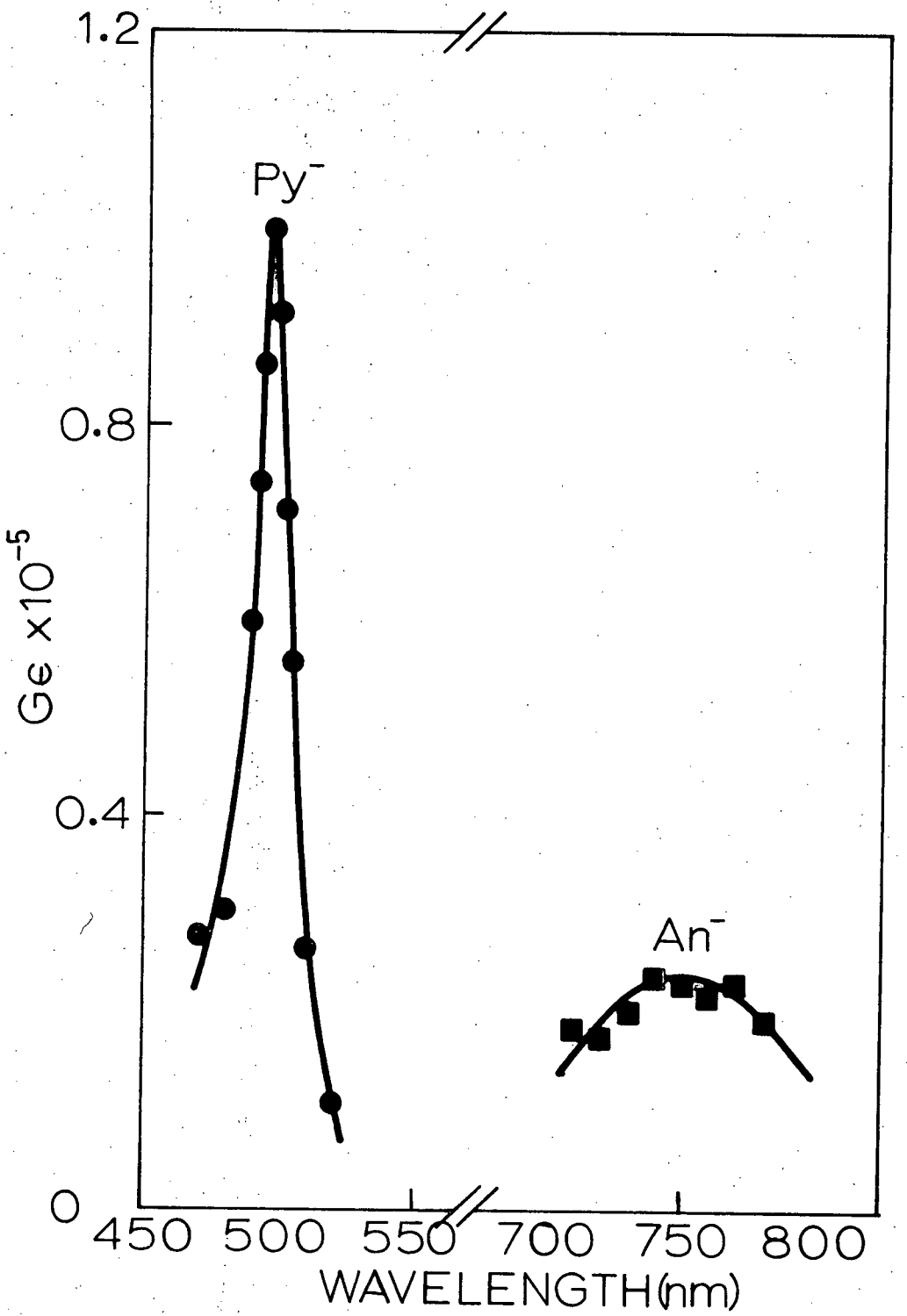

Figure III-21. Radiation produced transients observed at (i) 470 - 520 nm for (2.6 ± 0.1) X 10^{-3}M pyrene and (ii) 710 - 780 nm for (6.3 ± 0.5) X 10^{-4}M anthracene in HMPA. The species are attributed to the aromatic negative ions.

attributed to the aromatic anions precluded any contribution from excited species. In the presence of ∿ 0.1M N_2O (a solute known to scavenge negative but not positive ions) samples containing < 10^{-3}M Py or An, the aromatic anion yield was reduced by more than 95%. This strongly suggests that the aromatic cations Py^+ or An^+ also did not contribute appreciably to the observed absorptions. Further, over the concentration range from 10^{-4} to 10^{-1} M, the yield of aromatic anions in HMPA was found to be essentially independent of solute concentration. On the basis of these considerations it seems reasonable to accept the quantitative conversion of e^-_{HMPA} to the aromatic anions.

The magnitude of the transient absorption at 1000 nm in pulse irradiated pure HMPA was compared with the maximum of the radical anion absorption in the same sample after the addition in vacuo of sufficient amounts of Py or An to ensure complete e^-_{HMPA} scavenging. Table XII shows typical data. The comparisons gave a value for the molar absorptivity for the transient in HMPA at 1000 nm of (4.75 ± 0.4) X 10^3 M^{-1} sec^{-1}. Using the measured ratio of 6.7 ± 0.4 for the absorbance at 2200 nm to that at 1000 nm, the maximum molar absorptivity for the solvated electron in HMPA was calculated to be $\epsilon^{e^-_{HMPA}}_{max}$ = (3.2 ± 0.5) X 10^4 M^{-1} sec^{-1}. This value is substantially larger than that recently reported by Nauta and Van Huis[193] who found $\epsilon^{e^-_{HMPA}}_{max}$ ∿ 1.6 X 10^4 M^{-1} cm^{-1} using biphenyl and anthracene at 10^{-2} to 10^{-1} M. In addition, Mal'tsev and Vannikov's[193] result of $\epsilon^{e^-_{HMPA}}_{1600}$ = 2.8 X 10^3 M^{-1} cm^{-1} based on anthracene at 10^{-3} to 10^{-2} M is only one

TABLE XII Comparison of absorbances in a 20 mm cell of e^-_{HMPA} at 1000 nm with the radical anion maximum after aromatic hydrocarbon addition. For each pair of readings equivalent radiation pulses were used.

Anthracene	Pyrene
$A^{e^-_{HMPA}}_{1000} = 0.365 \pm 0.002$	$A^{e^-_{HMPA}}_{1000} = 0.0325 \pm 0.001$
$A^{An^-}_{740} = 0.172 \pm 0.001$	$A^{Py^-}_{495} = 0.34 \pm 0.01$
$[An] = 6.3 \pm 0.5 \times 10^{-4} M$	$[Py] = 2.6 \pm 0.1 \times 10^{-3} M$
$\epsilon^{An^-}_{740} = 1.0 \times 10^4\ M^{-1}\ cm^{-1}$	$\epsilon^{Py^-}_{495} = 5.0 \times 10^4\ M^{-1}\ cm^{-1}$
calc $\epsilon^{e^-_{HMPA}}_{1000} = 4.71 \pm 0.20 \times 10^3\ M^{-1}\ cm^{-1}$	calc $\epsilon^{e^-_{HMPA}}_{1000} = 4.78 \pm 0.30 \times 10^3\ M^{-1}\ cm^{-1}$

tenth the corresponding value $\epsilon^{e^-}_{1600\,HMPA} = (2.0 \pm 0.2) \times 10^4\ M^{-1}\ cm^{-1}$ found in this work. A possible explanation for the lower values found in the other studies is the fact that they used comparatively long radiation pulses during which a significant fraction of the solvated electrons would have decayed. No indication was given that corrections were made for such decay in those studies. The higher value for the maximum molar absorptivity $\epsilon^{e^-}_{max\,HMPA} = 3.2 \times 10^4\ M^{-1}\ cm^{-1}$ found in this work is supported by a calculation of the oscillator strength for the absorption band.

The oscillator strength of an absorption band, f, is a measure of the probability of electronic transitions occurring. It is a measure of the degree of dipolar oscillation of the electron between orbitals involved in transitions -- the so-called dipole strength of the transitions. The symmetries and multiplicities of states necessarily affect the oscillator strength, but a fully allowed transition has f = 1. It can be shown that[204]

$$f = \frac{2.303\ mc^2}{be^2} F \int \epsilon d\bar{\nu} \qquad \text{(xlix)}$$

where m and e are the mass and charge of an electron, c is the velocity of light, b is the number of solute molecules per cc, and F is a term related to the refractive index, n, of the medium.

Several suggestions have been made as to the appropriate refractive index term to use[205] such as n, n^2, or $9n/(n^2 + 2)^2$. Since there is no general agreement and since each of the expressions usually yields a number close to unity, the term is often omitted. In that case, expression (xlix) reduces to (l).

$$f = 4.32 \times 10^{-9} \int \epsilon d\bar{\nu} \qquad (l)$$

where the integral is simply the area under the total absorption band plotted on an energy scale.

As a first approximation to the IR absorption in HMPA, the Gaussian - Lorentzian function (xlviii) was taken as representative of the electron absorption band. It has been shown[195] that integration of that function leads to the following expression (li) for the enclosed area:

$$y(\bar{\nu})d\bar{\nu} = \left(\frac{\sqrt{\pi}}{2\sqrt{\ln 2}} G + \frac{\pi}{2} L\right) \epsilon_{max}$$

$$= (1.065\ G + 1.571\ L)\ \epsilon_{max} \qquad (li)$$

Values for the half-widths, G and L of 1600 cm^{-1} and 2000 cm^{-1} respectively, were taken from the best fit curve as shown in Figure III-20. Substitution into equation (l) gave a value for the oscillator strength of the solvated electron band in HMPA of $f = 0.7 \pm 0.2$. This large value is in accord with similar determinations for other solvated electron systems[206,207]

and suggests that the value for the maximum molar absorptivity $\epsilon^{e^-}_{max}$HMPA = (3.2 ± 0.5) X 10^4 M^{-1} sec^{-1} obtained in this work is not unreasonable.

Further evidence which tends to corroborate this value for HMPA comes from comparison with the solvated electron spectra reported for other solvents.

To a good approximation,

$$f \alpha \epsilon_{max} \cdot \omega_{1/2} \qquad \text{(1ii)}$$

where $\omega_{1/2}$ is the half band width.

Figure III-22 shows solvated spectra for a number of solvents. Below each curve is the value of $\epsilon_{max} \cdot \omega_{1/2}$ for each spectrum. As can be seen, the value for the solvated electron spectrum in HMPA is comparable to the other systems when the value for $\epsilon^{e^-}_{max}$HMPA found in this work is used.

3. Solvated Electron Yield in HMPA

A particularly useful piece of information that can be learned from a pulse radiolysis experiment is the yield of some absorbing species. If one knows the dosage represented by the radiation pulse and either knows or can ascertain the molar absorptivity of the species in question then the technique has obvious advantages over the indirect methods required in steady-state radiolysis studies. Often the two techniques are

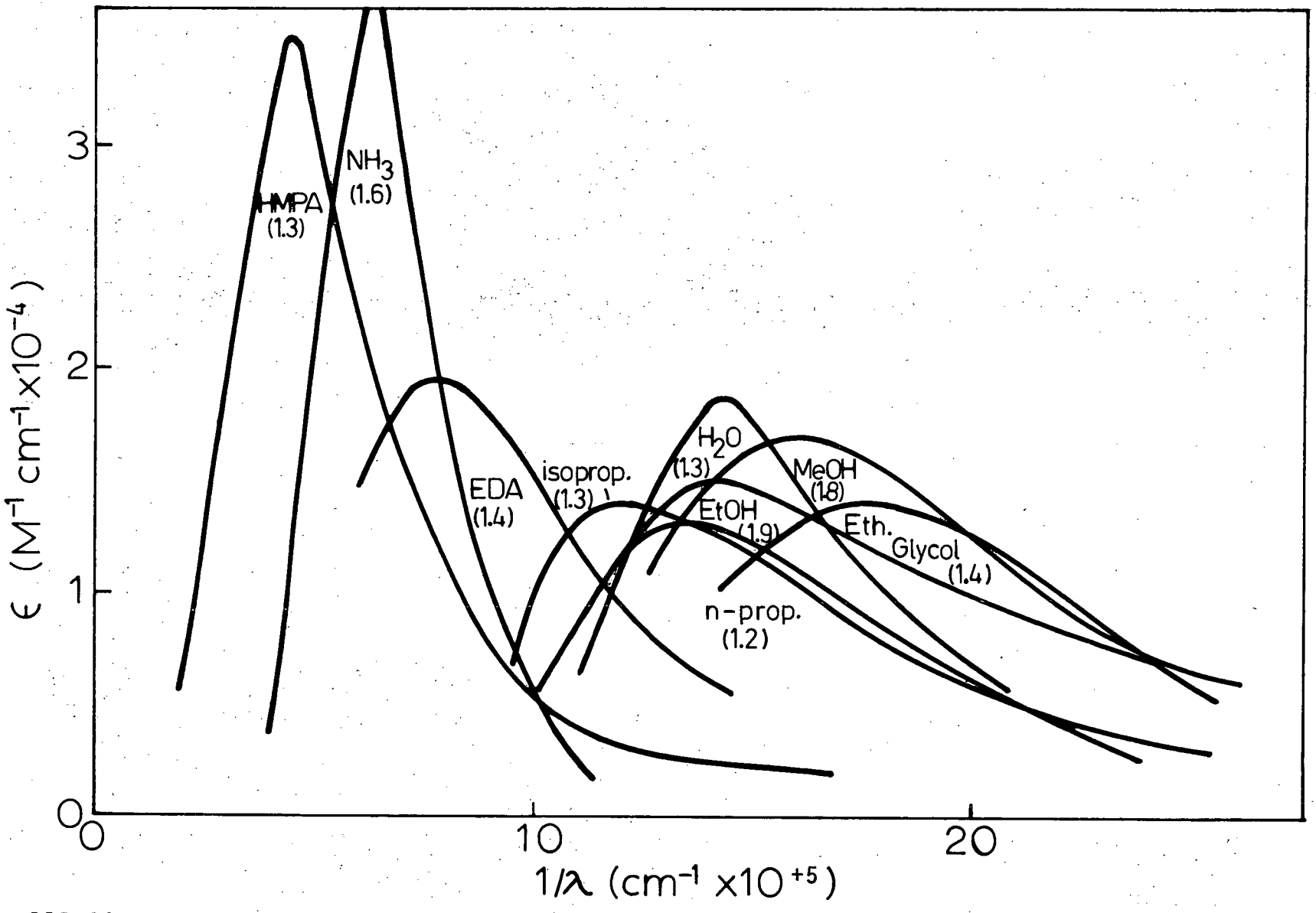

Figure III-22. Oscillator strength comparison for e_s^- in several solvents. The figures in brackets represent values of $\epsilon_{max} \cdot \omega_{1/2}$ X $10^{-5} M^{-1} cm^{-2}$ as explained in the text.

complementary.

In pure HMPA, no fast geminate decay of the solvated electrons could be observed with the fastest available time resolution of 5 ns. This would be expected for a liquid of high dielectric constant because the resulting small Onsager escape radius would lead to very short lifetimes for geminate ion pairs. Thus, it can be reasonably accepted that the absorption observable after 5 ns corresponds almost entirely to free ions -- particularly in light of the fact that the half-life for decay was on the μs timescale.

The yields of the aromatic anions of pyrene and anthracene were determined for various concentrations of those scavengers. Radiation dosimetry was performed under identical accelerator operating conditions and in identical cells using water or KCNS solutions. The electron absorption was completely eliminated from solutions of the aromatic scavengers, so it was assumed that quantitative conversion of free electrons to anions had taken place. As will be shown later in a discussion of the reactions of the solvated electrons, careful examination of the electron decay and aromatic anion build-up from dilute scavenger solutions confirmed this assumed one-to-one correspondence

Table XIII shows the radiation yields of the aromatic anions found for various scavenger concentrations. Based on the data from this table, it is concluded that the free ion or solvated electron yield in HMPA is $G(e^-_{HMPA}) = 2.3 \pm 0.4$.

TABLE XIII Radiation yield of aromatic anions from Anthracene and Pyrene at various concentrations in HMPA for ∿ 1 krad pulses.

	Solute Concentration	Yield
Anthracene	$(6 \pm 2) \times 10^{-5}$M	$G(An^-)$ 1.9 ± 0.4
	$(6.3 \pm 0.5) \times 10^{-4}$M	2.3 ± 0.4
Pyrene	$(3.2 \pm 0.3) \times 10^{-4}$M	$G(Py^-)$ 2.1 ± 0.4
	$(2.6 \pm 0.1) \times 10^{-3}$M	2.3 ± 0.4
	$(1.2 \pm 0.1) \times 10^{-1}$M	2.4 ± 0.4

This yield is in good agreement with the value of 2.4 ± 0.3 measured at about the same time by Nauta and van Huis[194] but twice that reported by Mal'tsev et al.[193] The value is in excellent accord with the value of $G(e^-_{HMPA}) = 2.2 \pm 0.2$ proposed from nitrogen yields from the ^{60}Co steady state radiolysis studies of nitrous oxide solutions in HMPA presented earlier in this Chapter.

4. Kinetics Studies

a) Decay of Primary Species

i) The Solvated Electron

The lifetime of the solvated electron in pure irradiated HMPA was sensitive to sample purification and preparation techniques. Generally, the lifetime initially increased with total absorbed dose per sample, presumably due to the reaction and removal of small amounts of impurities. For a given sample, the electron lifetime was greatly dependent upon the radiation dose per pulse. Typical oscilloscope traces are shown in Figure III-23. By using very low dose pulses ($\sim$ 300 rads) in very carefully deoxygenated samples, first half-lives approaching 50 μsec could be achieved (Figure III-23(a)). For the majority of the experiments reported here, medium dose pulses ($\sim$ 2000 rads) were utilized which gave lifetimes on the order of 5 μsec (Figure III-23(b)). Very large dose pulse ($\sim$ 10,000 rads) gave lifetimes of only about 2 μsec (Figure III-23(c)).

The electron decay data were examined to see if it followed simple 1^{st} or 2^{nd} order kinetics. Figure III-24 shows the results obtained for the data from Figure III-23(a) and (c) -- i.e. for electrons of both long and short lifetimes. As can be seen, the very low dose data curve fits a second order plot over at least the two first half-lives with an apparent bimolecular rate constant of 2.5×10^{10} M^{-1} sec^{-1}. On the other hand, the data from a large dose pulse is nearly linear on a logarithmic plot over the first two half lives with a pseudo-first order constant of about 3×10^{5} sec^{-1}. The latter result is consistent with values reported by the other investigators[193,194] who

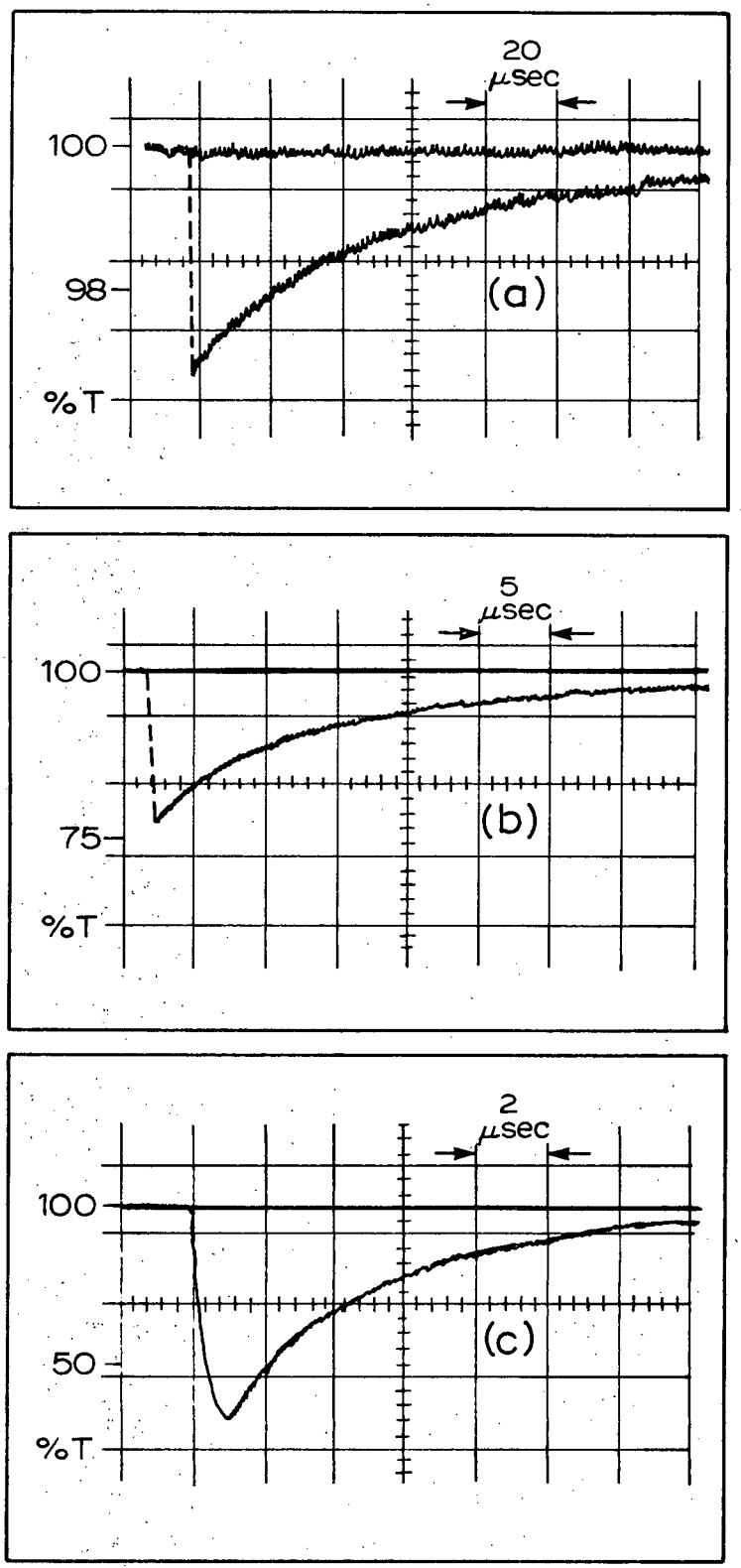

Figure III-23. Lifetime of e^-_{HMPA} as a function of radiation dose per pulse. Doses of (a) 300, (b) 2,000, (c) 10,000 rads gave electron first half-lives of 50, 5 and 2 μsec respectively.

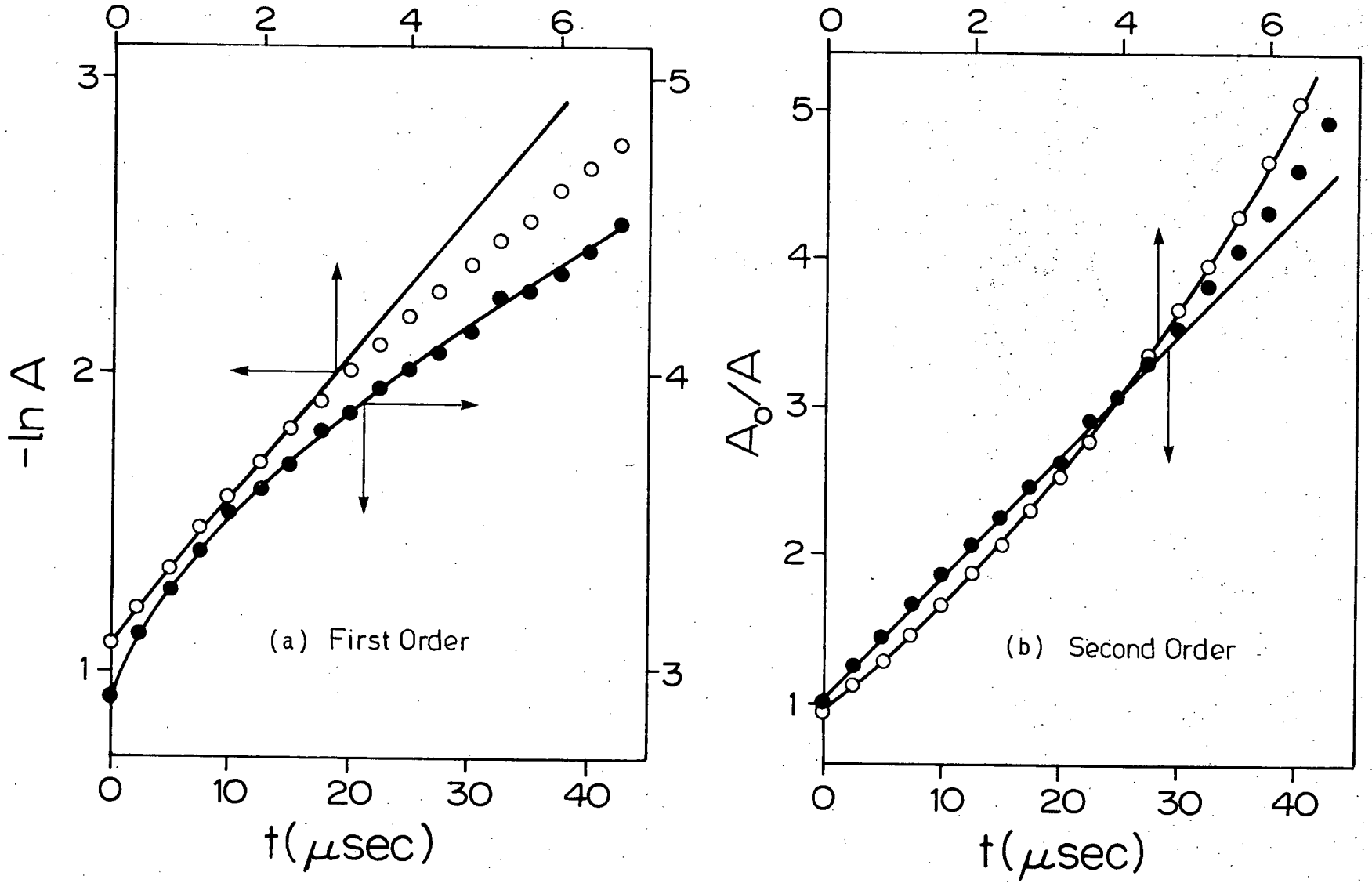

Figure III-24. First (a) and second order (b) plots for the data of Figure III-23 a and c. Data for short-lived electrons (o) and long-lived electrons (●) are shown.

apparently used only large dose pulses. Data from moderate pulses fit neither first nor second order plots. These results suggest that both apparent first and second order process are involved in the decay mechanism, and that the first order component involves reaction of e^-_{HMPA} with radiation produced species.

A method exists for analyzing mixed first and second order decays where the reactant concentration can be monitored.[208] For the electron decay data, the method applies to a mechanism involving a pseudo-first order reaction (3.98) and bimolecular combination (3.99).

$$e^-_{HMPA} + X \xrightarrow{k'_{3.98}} X^- \qquad (3.98)$$

$$e^-_{HMPA} + e^-_{HMPA} \xrightarrow{2k_{3.99}} \text{products} \qquad (3.99)$$

In this case, X represents unspecified impurities, both intrinsic and radiation produced, which are at considerably higher concentration that e^-_{HMPA}.

The method utilizes a plot of $\ln ((A_t + \alpha)/A_t)$ versus time. A_t is the electron absorbance at time t and α is a dimensionless parameter given by equation (liii):

$$\alpha = k'_{3.98}/2k_{3.99} \epsilon l \qquad (liii)$$

where ϵ is the molar absorptivity of the solvated electron

at the wavelength studies and l is the optical path length.

A computer program was written which when given decay data and some arbitrary value for α, calculates through an iterative process the value of α that gives the best least squares fit to the data. The pseudo-first order rate constant is given directly by the slope, m, of the plot of ln $((A_t + \alpha)/A_t)$ versus time:

$$k'_{3.98} = m = \text{slope} \qquad \text{(1iv)}$$

and the bimolecular rate constant, $2k_{3.99}$ from

$$2k_{3.99} = \frac{m \epsilon l}{\alpha} \qquad \text{(1v)}$$

Figure III-25 shows the results of such regression analysis for the electron decay from both the large and small dose cases from Figure III-23. Analyses of this type consistently give values of $2k_{3.99} = (1.9 \pm 0.4) \times 10^{10}$ M^{-1} sec^{-1}; but $k'_{3.98}$ values were found to vary between 7×10^3 and 1×10^5 sec^{-1} depending on pulse dose and sample origin. Table XIV shows typical results for a series of experiments where the dose per pulse varied from 400 to 12,000 rads.

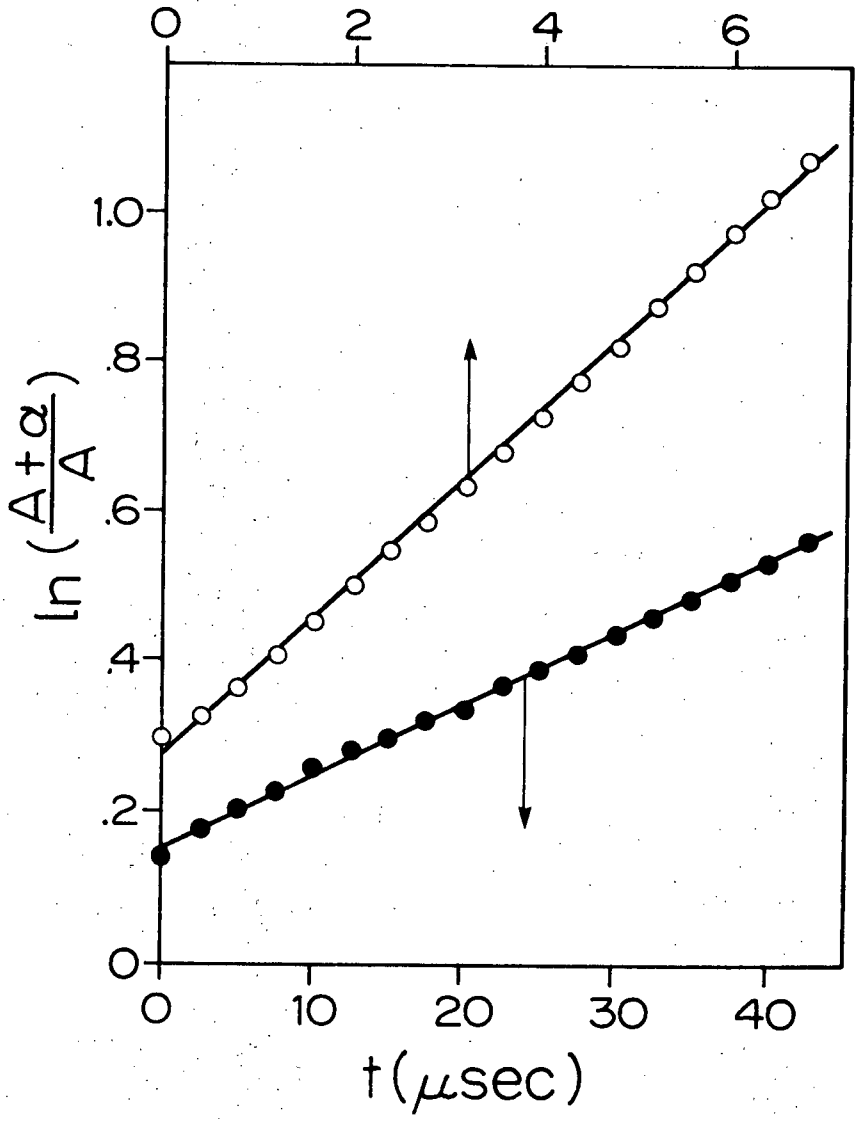

Figure III-25. Mixed first plus second order plot for the data of Figure III-24. The method is explained in the text.

TABLE XIV Kinetic analysis of electron decay data in a sample of HMPA for which the dose per pulse value was varied. The combined first plus second order treatment described in the text was used to calculate the parameters, $k'_{3.98}$ and $2k_{3.99}$.

Dose (rads)	$k'_{3.98}$ ($\times 10^{-4}$ sec^{-1})	$2k_{3.99}$ ($\times 10^{-10}$ M^{-1} sec^{-1})
400	0.96 ± 0.1	2.1 ± 0.2
600	0.96 ± 0.1	2.1 ± 0.2
800	1.6 ± 0.2	1.9 ± 0.2
2,000	3.5 ± 0.4	1.6 ± 0.2
12,000	12.0 ± 1.2	2.0 ± 0.2

Now, the foregoing reaction scheme ignores the neutralization reaction (3.100) that could occur in HMPA.

$$e^-_{HMPA} + S \xrightarrow{k_{3.100}} S^- \qquad (3.100)$$

where S represents the positive counter-ion or some oxidizing radical species formed therefrom.

The computer was programmed to simulate electron decay data from mechanisms involving pseudo-first order decay (3.98) and (A) bimolecular combination (3.99) or (B) bimolecular recombination

(3.100). Figure III-26 shows a typical comparison between an actual observed decay (line) and those simulated from mechanisms (A) (filled circles) and (B) (open circles) taking $k_{3.98} = 3 \times 10^3\ M^{-1}\ sec^{-1}$; $2k_{3.99} = 2 \times 10^{10}\ M^{-1}\ sec^{-1}$; and $k_{3.100} = 2.5 \times 10^{10}\ M^{-1}\ sec^{-1}$. No doubt other mechanisms are also possible, but one can conclude that electron decay via reactions (3.98), (3.99) and/or (3.100) is entirely consistent with the data.

That a single species contributed to the absorption over the wavelength range from 500 to 2300 nm was confirmed from kinetic studies. Within experimental error the decay characteristics of transient absorptions over this region were identical and the band has been attributed to the solvated electron in HMPA. This kinetic consistency also prevailed in the presence of a number of solutes which exhibited varying decrees of reactivity towards the transient.

ii) The UV Absorbing Species

Below 500 nm, as noted previously;[194] at least one other species contributes to the absorption. This is evidenced by the fact that after the infra-red electron absorption in pure irradiated HMPA had decayed, some absorption persisted at wavelengths shorter than 500 nm. Indeed, this second species had a lifetime on the order of 100 μsec. The UV absorption band was much weaker than that found in the infra-red, suggesting that either this longer-lived species was produced with a

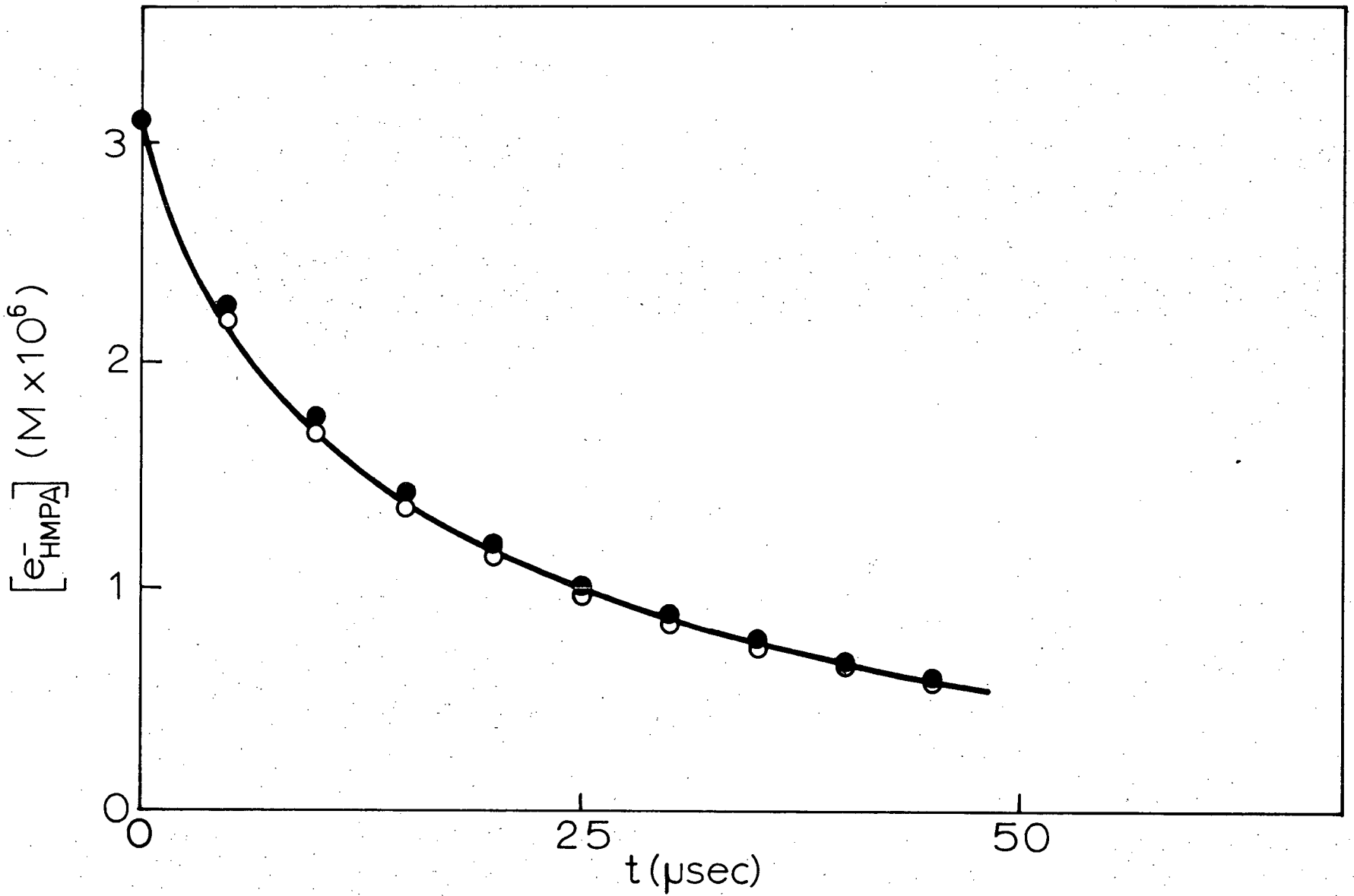

Figure III-26. Simulation of the electron decay at 1000 nm in HMPA (——) by means of mechanisms involving bimolecular combination (●) and bimolecular recombination (○).

correspondingly lower yield or else it possessed a smaller molar absorptivity at the wavelengths studied. The figure would tend to support the latter idea for, as can be seen in Figure III-17, it is very possible that only the low energy tail of the absorption band was being monitored.

Now, the experimental apparatus was not designed for, nor well suited to,the study of transient species which absorb only in the ultra violet region of the spectrum. Consequently, quantitative studies of this second species -- particularly kinetic analyses -- were cumbersome and subject to gross uncertainties. In addition to the problem of intense solvent absorption, observations in that region were complicated by the presence of Cerenkov radiation emission and the possible photolysis of species in the cell by the analyzing light beam. Also, the electron band may have contributed significantly to the absorbance in the UV region. By monitoring the electron decay in the infra-red, one could determine the nature of the electron decay then subtract the appropriate contribution from the UV decay. However, it proved difficult to determine the exact proportionality between the electron absorptivity for the two regions. In any event, the resulting "corrected" UV decay data must then contain a correspondingly greater uncertainty.

A further complication arose because of the much longer lifetime of the UV species. Recall that the analyzing light source was operated in a pulsed mode so as to increase its intensity. Such operation restricted the time period over which reactions could be studied to a few hundred μsec. Resorting to

a steady-state mode of lamp operation would have facilitated longer timescale studies, but the resulting enormous loss in the signal-to-noise ratio would render results more ambiguous.

The contribution of the solvated electrons to the UV absorption could be eliminated through the addition of electron scavengers such as nitrous oxide or oxygen. Under those conditons, an absorption in the UV region persisted with a lifetime of the same order of that found in the pure system. However, one could not be certain that the yield of reactivity of the UV species was unaffected under those conditions. In addition, most solutes produced new absorptions in the UV or visible regions which masked the absorption being studied.

The presence of electron scavengers in the system had little observable effect on the UV species. Certainly, its lifetime was not significantly altered. As will be detailed, there is evidence that the transient reacted to some extent with the solvated electrons of the system. These facts tend to suggest that the species may in fact be the primary oxidizing species, S. This species would be expected to be either the solvated positive counter ion, $HMPA_s^+$, or else one of its decay products -- possibly some radical species. Cooper[117] for example, has identified a band centered at 550 nm as the positive ion in irradiated dimethylsulphoxide (DMSO). DMSO, also being a polar aprotic solvent, is similar to HMPA in reactivity and many of its properties. Also, Simic and Hayon[210] have shown that radicals and radical anions of many amides exhibit absorption maxima below 300 nm.

Low concentrations of water or methanol, both known to react with positive ions, had no effect on the UV species. However, the scavenging reactions of both water (3.101) and methanol (3.102) are known to occur via proton transfer from the positive ion.

$$H_2O + RH^+ \longrightarrow R + H_3O^+ \qquad (3.101)$$

$$CH_3OH + RH^+ \longrightarrow R + CH_3OH_2 \qquad (3.102)$$

Because of the exceptionally aprotic nature of HMPA, the failure of the UV species to react with methanol or water does not rule out the possibility of it being the positive ion. The species was also unreactive towards dissolved hydrogen gas. Strongly oxidizing radical species react with hydrogen (305),

$$R + H_2 \longrightarrow RH + H \qquad (305)$$

and the fact that the UV species did not, does tend to rule out the likelihood of it being of this nature.

iii) Reaction Between Transient Species

That the two transient species reacted together was demonstrated by a series of experiments conducted with a sample of HMPA containing a small amount of some unknown electron

scavenging impurity. Figure III-27 details the pertinent transient absorptions observed at 1000 nm (a,b,c,) and 350 nm (d,e,f,). After the first irradiation pulse the electron, monitored at 1000 nm, decayed rapidly (a) because of reaction with dissolved impurity. The first half-life was only 3 μsec in that case and the electron absorption totally unobservable 50 μsec after the pulse. With each succeeding pulse, the electron lifetime increased as the trace impurity concentration decreased. After five pulses, the first half-life had doubled to about 6 μsec, (b). The electron absorption was again absent after 50 μsec suggesting that its decay still involved a significant first order component. Following 30 pulses, the first half-life for the electron had not significantly increased, (c), but its decay characteristics had changed. A significant absorption remained 50 μsec after the pulse, indicating that first order components to the decay were negligible after that period.

It is interesting to compare this with that behavior of the UV absorbing species (d,e,f,) monitored at 350 nm from a parallel series of experiments. Those results were obtained after the small (1 ml) volume of liquid that had been "purified" by irradiation was mixed with the bulk of the solution (50 ml) and replaced with a fresh sample containing the trace impurity. Figure III-27 (d,e,f,) show the decays observed for the UV species under similar conditions to those described for the electron decay studies. Because the UV species is longer lived, the timescale is increased four-fold in those diagrams. Contrary to the

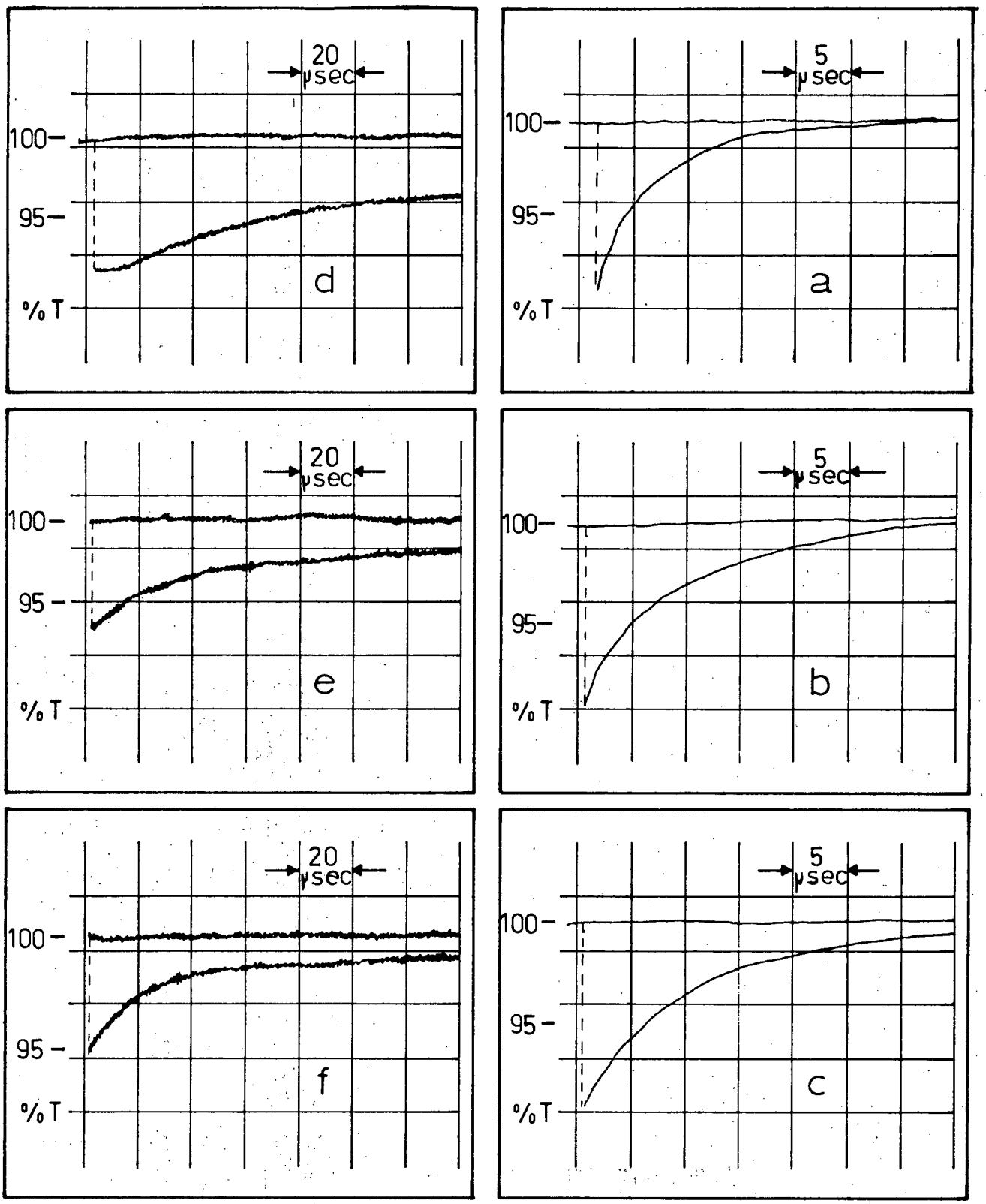

Figure III-27. Interaction between e^-_{HMPA} observed at 1000 nm (a,b,c) and the UV species at 350 nm (d,e,f), as a function of sample purity. The various effects on decays are explained in the text.

electron case, removal of the trace impurity resulted in acceleration of the decay of the UV absorbing species. After the first pulse the UV species had a first half-life of about 90 μsec (d). After 5 and 30 pulses this value had decreased to ∿ 45 μsec and 20 μsec respectively. In addition, the decay in those latter cases clearly occurred via at least two processes on vastly different timescales. In the latter experiment the fast decay of the UV species corresponded very well to the electron decay. On a qualitative basis, these observations are consistent with a mechanism in which the two transients react with each other in competition with other species.

Attempts to establish a feasible reaction scheme and thereby obtain qualitative information about such reactions, however, proved fruitless. Undoubtedly the large uncertainties associated with the UV species absorption is responsible for the difficulties.

iv) Electron Decay in Irradiated Sodium Metal Solution

In an attempt to further elucidate the mechanism for the electron decay, some experiments were performed on the pulse radiolysis of blue solutions of Na metal dissolved in HMPA. These solutions contained substantial (but unknown) concentrations of solvated electrons and possibly other ionic species. Figure III-28 shows a typical oscilloscope trace at 750 nm obtained when such a solution was subjected to two radiation pulses, about 30 seconds apart.

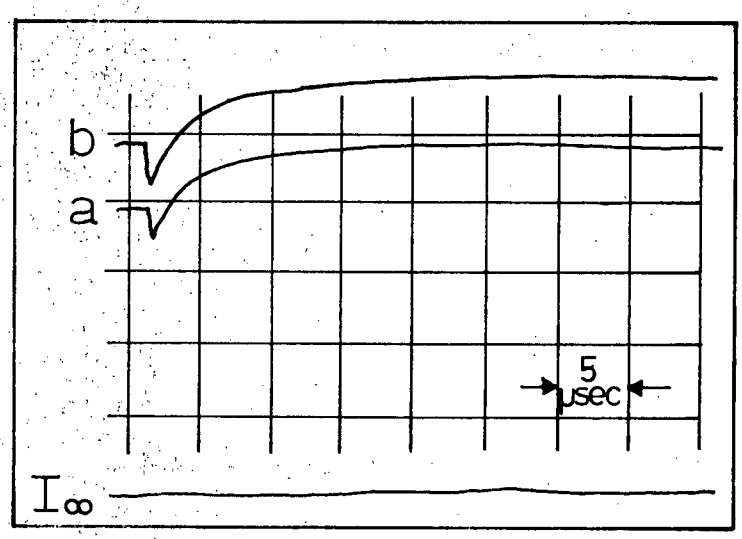

Figure III-28. Effect of electron pulses on a solution of Na in HMPA at 750 nm. The second pulse, b, followed 30 sec after the first and showed that the pulses gave an initial increase in e^-_{HMPA} concentration but a net permanent loss of the species. Similar results were found at 1550 nm.

As can be seen, each radiation pulse initially created additional solvated electrons but the overall processes led to a net loss in concentration of e^-_{HMPA}. The loss was comparable in magnitude to the radiation yield of solvated electrons. Furthermore, the loss was permanent as evidenced by the fact that 30 seconds later, just prior to the second radiation pulse, the residual concentration of e^-_{HMPA} had remained at the lower value.

If the electron species formed via radiation induced ionization and sodium metal dissolution are identical, then electron decay through bimolecular combination (3.99) can be ruled out as an important step in this system.

$$e^-_{HMPA} + e^-_{HMPA} \longrightarrow \text{products} \qquad (3.99)$$

Even if such a reaction involved an equilibrium with some dimeric $(e_2)^{2-}_{HMPA}$ species, the observations could not be reconciled. It is significant that neutralization recombination reaction between electrons and the co-produced positive ions could not account for the net loss in e^-_{HMPA}. In order that the charge balance be preserved, these two species must be produced in equal yield during radiolysis, therefore, the initial and final concentrations of e^-_{HMPA} would have been the same. Since the stable Na solutions obviously cannot contain impurities which react with e^-_{HMPA}, one must conclude that other radiation produced species, such as free radicals, contribute to the electron decay. Recall that this conclusion had been proposed to account for the dependence of the electron decay on the radiation dose per pulse.

b) Behavior of Transient Species in the Presence of Added Solutes

i) Electron Scavengers

i.1) Pyrene and Anthracene

As has been discussed previously, the aromatic hydrocarbons pyrene (Py) and anthracene (An) react with the reducing species in HMPA to yield the aromatic anions. The reactions appeared to

be very fast -- the electron decay being complete in ns for solutions containing moderate concentrations (> 10^{-3}M) of the aromatic scavengers.

The reaction between solvated electrons and anthracene was studied by preparing a sample containing only (6 ± 2) X 10^{-5}M anthracene in HMPA. Upon irradiation, both the electron decay at 1000 nm and the corresponding anthracene anion build-up at 740 nm could be observed.

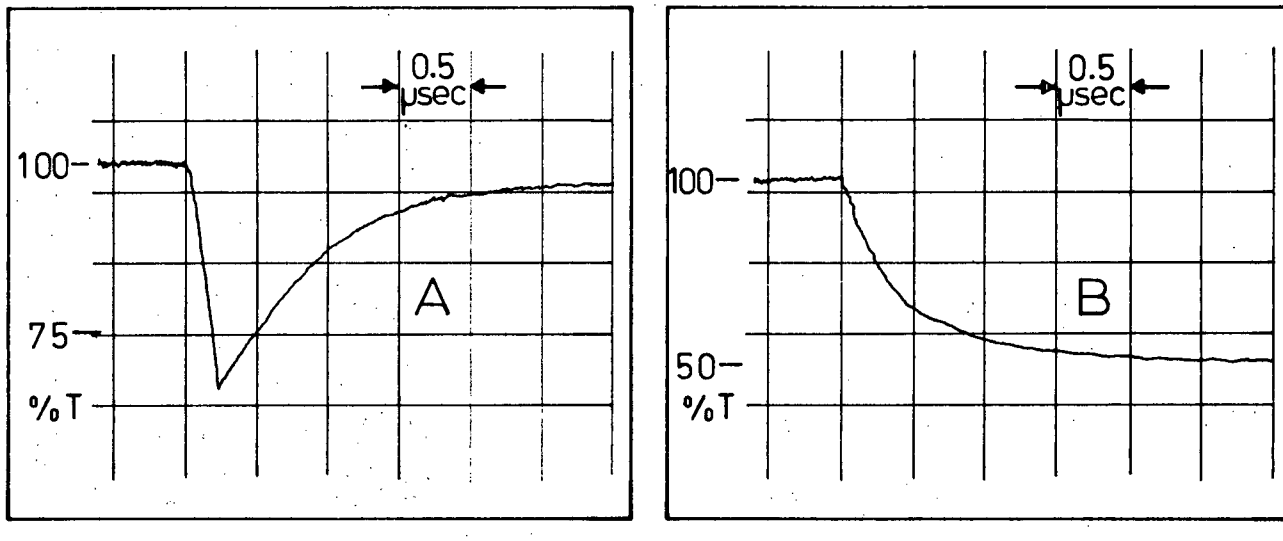

Figure III-29. Decay of e^-_{HMPA} absorption at 1000 nm (A) and simultaneous build-up of An^- absorption at 740 nm (B) in a solution of (6 ± 2) X 10^{-5}M anthracene in HMPA following a 200 ns radiation pulse.

Figure III-29(a) shows the accelerated electron decay, monitored at 1000 nm. Initially, the aromatic anion is absent and thus does not mask the electron decay. The aromatic anion is much longer lived than the electron, so its maximum contribution

to the absorption at 1000 nm is given by the steady non-zero absorbance at long time (in this case t > 2 μsec). Since this absorption represented less than 5% of the initial electron absorption, and since its contribution would actually be much smaller during the initial stages of the electron decay, it was ignored in the kinetic analysis of the data. On the other hand, as shown in Figure III-17, the solvated electron in HMPA absorption band encompasses the whole of the visible spectrum. Thus, the build-up of the anthracene anion, monitored at 740 nm, shown in Figure III-29(b) contains a significant contribution from solvated electrons. The problem is compounded by the fact that electron absorption is largest initially when the anthracene anion component is small. However, the contribution by the electron to the total absorbance at 740 nm is determined simply from the corresponding values observed at 1000 nm, multiplied by the ratio of the electron extinction coefficients at these two wavelengths. From Figure III-17 the ratio is found to be:

$$\epsilon^{e^-}_{740\,HMPA} \;/\; \epsilon^{e^-}_{1000\,HMPA} = 0.56 \qquad \text{(1vi)}$$

Even at (6 ± 2) X 10^{-5}M concentration, the anthracene concentration would be about ten times that expected for solvated electrons produced in HMPA by a 200 ns pulse. Therefore, bimolecular reaction between those species would be expected to appear as a pseudo-first order process. Figure III-30 shows first order plots for the electron decay at 1000 nm and the

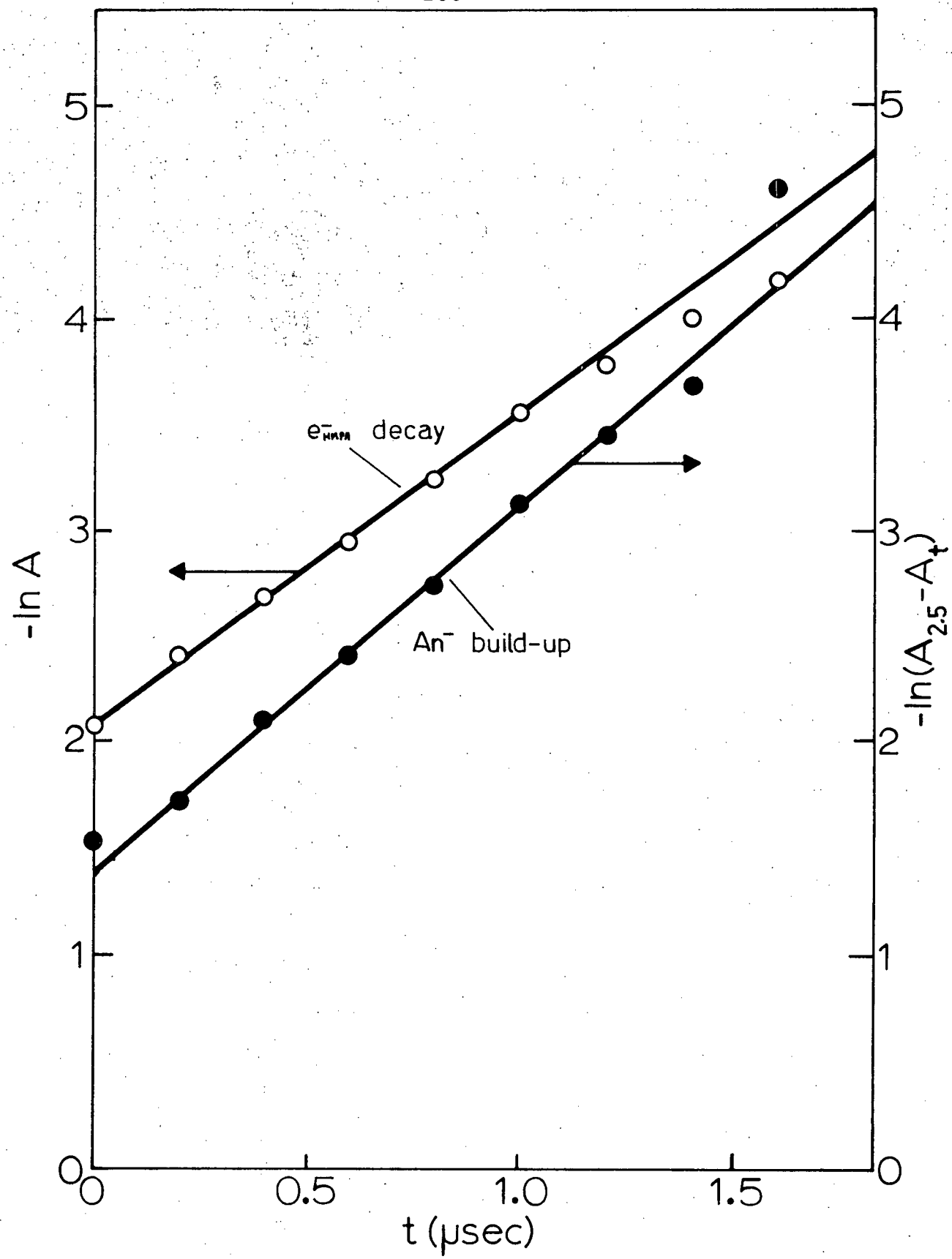

Figure III-30. First order kinetic plots for the e^-_{HMPA} decay at 1000 nm (O) and the "corrected" anthracene anion absorption build-up at 740 nm (●) from an irradiated solution of (6 ± 2) X 10^{-5}M An in HMPA.

"corrected" anthracene anion build-up at 740 nm. As expected, the electron decay deviated from first order behavior at long times ($t > 1.5$ μsec) because of a small but significant contribution to the total absorption by anthracene at that point. For the An^- build-up, the plot is $\ln (A_{2.5} - A_t)$ against time, where $A_{2.5}$ is the absorbance 2.5 μsec after the pulse (plateau value) and A_t is the absorbance at time t, corrected for the electron contribution.

It is most significant that the two plots exhibit nearly identical slopes. That is, from the slopes one calculates pseudo-first order rate constants for the electron decay and anion build-up of $(1.5 \pm 0.2) \times 10^6$ sec^{-1} and $(1.7 \pm 0.2) \times 10^6$ sec^{-1} respectively. This result affords rather convincing evidence that the solvated electron in HMPA reacts on a one-to-one basis with anthracene molecules to produce one singly charged anion (3.103).

$$e^-_{HMPA} + An \xrightarrow{k_{3.103}} An^- \qquad (3.103)$$

Combining the pseudo-first order rate constants with the concentration of anthracene present ($(6 \pm 2) \times 10^{-5}$M) one calculates the rate constant for reaction (3.103) to be $k_{3.103} = (3 \pm 1) \times 10^{10}$ M^{-1} sec^{-1}.

Similar behavior was found for solutions of pyrene in HMPA. However, the electron and Py^- absorptions appeared to mutually interfer to a greater extent making analysis more difficult.

Also, the lowest concentration studied, (3.2 ± 0.3) X 10^{-4}M Py, resulted in the electron decay and Py^- build-up being too fast to be studied in detail. To a first approximation, the scavenging reaction between pyrene and solvated electrons (3.104) occurs at a rate comparable to that measured for anthracene.

$$e^-_{HMPA} + Py \longrightarrow Py^- \qquad (3.104)$$

The aromatic anions were remarkably long-lived in HMPA. Figure III-31 shows the decay of the absorption of (a) An^- at 740 nm and (b) Py^- at 495 nm.

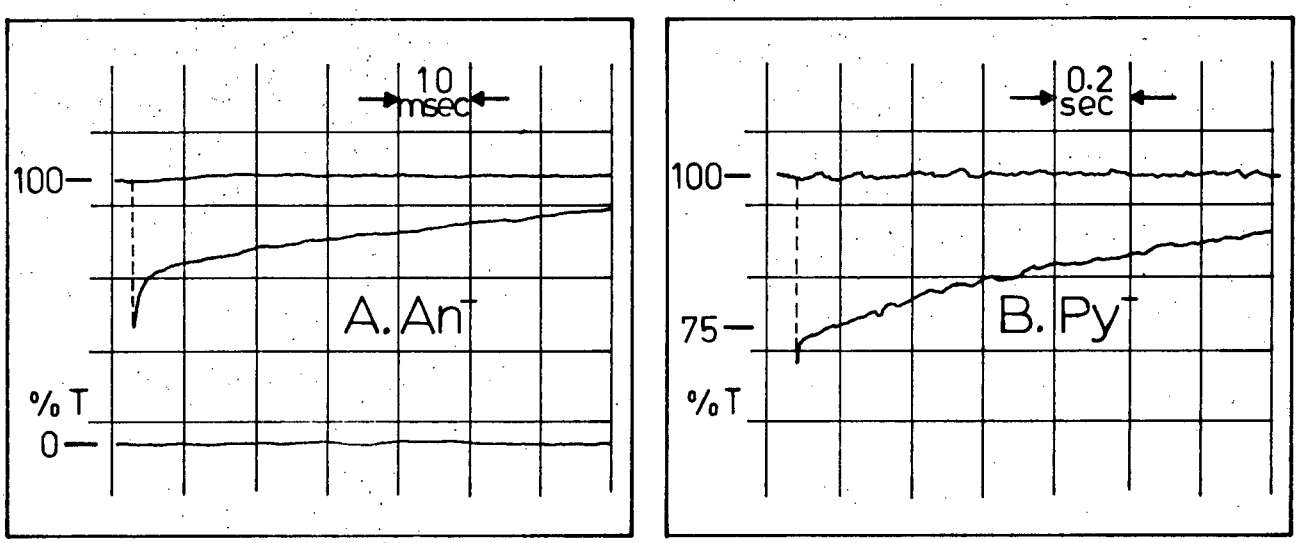

Figure III-31. Decay of aromatic anions produced via electron scavenging in irradiated HMPA. (A) An^- at 740 nm from (6 ± 2) X 10^{-5}M An in HMPA. (B) Py^- at 495 nm from (3.2 ± 0.3) X 10^{-4}M Py in HMPA.

It can be seen that these decays are complex as each clearly exhibits two distinct decay regions. Such behavior could arise from the formation and subsequent decay of a dimeric aromatic species or possibly some neutralization complex. In any case, electron scavenging by An or Py in HMPA leads to the formation of absorbing species with lifetimes approaching seconds.

Small amounts of the electron scavenger nitrous oxide were added to samples of anthracene or pyrene in HMPA. Upon irradiation, the initial yield of aromatic anions was substantially decreased -- but the decay rate of An^- or Py^- was essentially unchanged. These findings are consistent with there being a competition between N_2O and the hydrocarbons for solvated electrons. It further implies that there is no charge exchange between An^- (or Py^-) and N_2O or between $[N_2O^-]$ and An (or Py). By contrast, the presence of oxygen in a Py solution affected both the yield of Py^- and its rate of decay. In that case, the Py^- decay was greatly accelerated, suggesting that O_2 reacted with the aromatic anion (3.105).

$$Py^- + O_2 \longrightarrow Py + O_2^- \qquad (3.105)$$

Since the aromatic hydrocarbons produced observable transient species upon reaction with solvated electrons, they provided a means whereby the possible involvement of geminate ion scavenging could be studied directly. The scavenging rate of anthracene (and presumably pyrene) has been shown to be fast enough that one would expect that at high concentration the aromatic hydro-

carbons could compete effectively with geminate recombination for the electrons. If such were the case, one would anticipate the following behavior. As the concentration of An or Py was increased from the normal scavenger level (10^{-5} to 10^{-3}M) to say 10^{-1}M one would expect to see a corresponding increase in the initial anion yield -- due to geminate electron scavenging (3.106).

$$\left[\text{HMPA} + \ldots e^-_{\text{HMPA}}\right] + \text{Py} \longrightarrow \left[\text{HMPA} + \ldots \text{Py}^-\right] \qquad (3.106)$$

However, as a result of the strong coulombic attraction of the nearby positive ion, this extra absorbing anion would almost certainly itself undergo a rapid geminate neutralization reaction (3.107), resulting in a decreased absorbance.

$$\left[\text{HMPA} + \ldots \text{Py}^-\right] \longrightarrow \left[\text{HMPA} - \text{Py}\right] \qquad (3.107)$$

Jou[208] has observed just such behavior in tetrahydrofuron (THF) solution, where the rate constant for the electron scavenging reaction is $(1.2 \pm 0.2) \times 10^{11}$ M^{-1} sec^{-1}. Irradiation of THF containing up to 3×10^{-4}M pyrene gave results similar to those reported here for HMPA. At higher Py concentrations Jou found an increased initial Py^- yield that decayed rapidly (over ns) to the lower value at which point the much slower decay prevailed.

No such evidence was found in HMPA. Recall from Table XVI

that from a sample containing (1.2 ± 0.1) X 10^{-1}M pyrene in HMPA the initial Py^- yield was $G(Py^-)$ = 2.4 ± 0.4. This value is not significantly higher than that observed from solutions containing orders of magnitude less pyrene. Also, at the fastest timescale observable (5 ns), no fast decay of Py^- could be detected. These findings tend to rule out the involvement of geminate electron reactions the scavenging processes in irradiated HMPA.

Because of its limited solubility in HMPA, anthracene could not be used at a high enough concentration to provide corroborating evidence.

i.2) Nitrous Oxide

Nitrous oxide, N_2O, was used extensively as an electron scavenger in the steady state gamma radiolysis studies. As has been discussed, those experiments indicated that the scavenging reaction (3.68) was rapid and led ultimately to the production of molecular nitrogen.

$$e^-_{HMPA} + N_2O \xrightarrow{k_{3.68}} (N_2O^-) \longrightarrow N_2 + \text{other products} \qquad (3.68)$$

It was thus imperative that the pulse radiolysis work include experiments to directly confirm that N_2O scavenges e^-_{HMPA} and if possible to measure the rate of such a reaction.

Figure III-32 shows typical fast time scale oscilloscope

traces obtained at 1000 nm upon irradiation (a) of pure HMPA and (b) containing (7.9 ± 0.2) X 10^{-4}M N_2O.

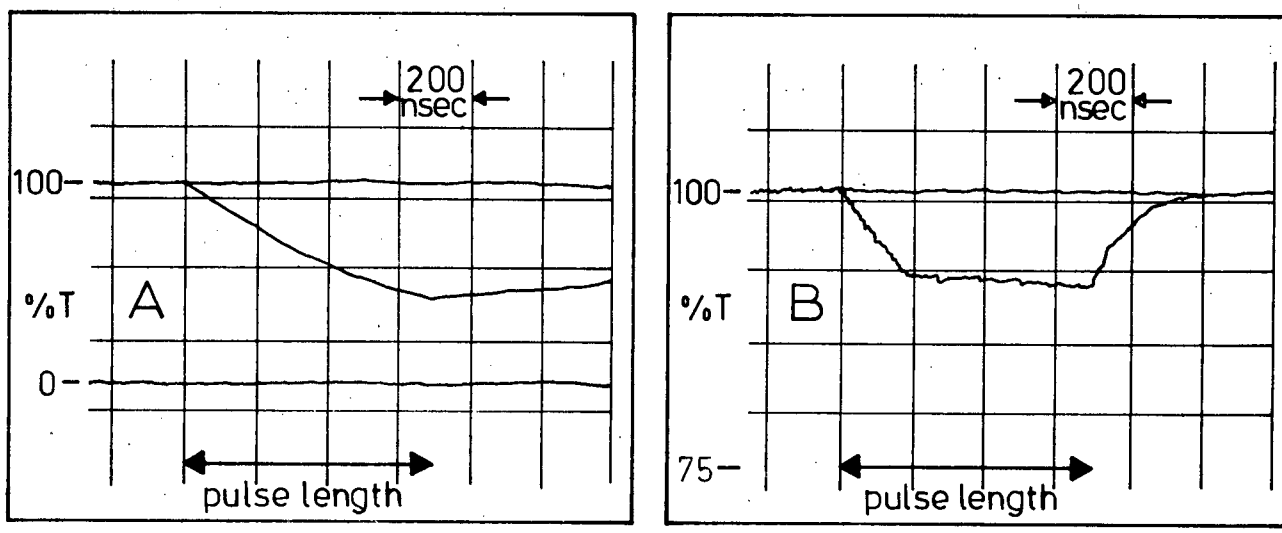

Figure III-32. Typical fast time scale oscilloscope traces obtained at 1000 nm following 700 nsec radiation pulses in pure HMPA (A) and HMPA containing (7.9 ± 0.2) X 10^{-4}M N_2O (B).

As can be clearly seen in the figure, the electron decay was greatly accelerated in the presence of N_2O. Figure III-33 is a first order plot of the electron decay in the presence of N_2O (from Figure III-32(b)) in which the end of the pulse is taken as time zero. Within the uncertainty of the data, the plot is linear, and from the slope, a pseudo-first order rate constant equal to (1.1 ± 0.3) X 10^7 sec^{-1} was obtained. For $[N_2O]$ = (7.9 ± 0.2) X 10^{-4}M, this corresponds to a bimolecular rate constant $k_{3.68}$ = (1.4 ± 0.4) X 10^{10} M^{-1} sec^{-1} for the reaction between N_2O and e^-_{HMPA} (3.68).

Figure III-32 shows that the build-up of the solvated

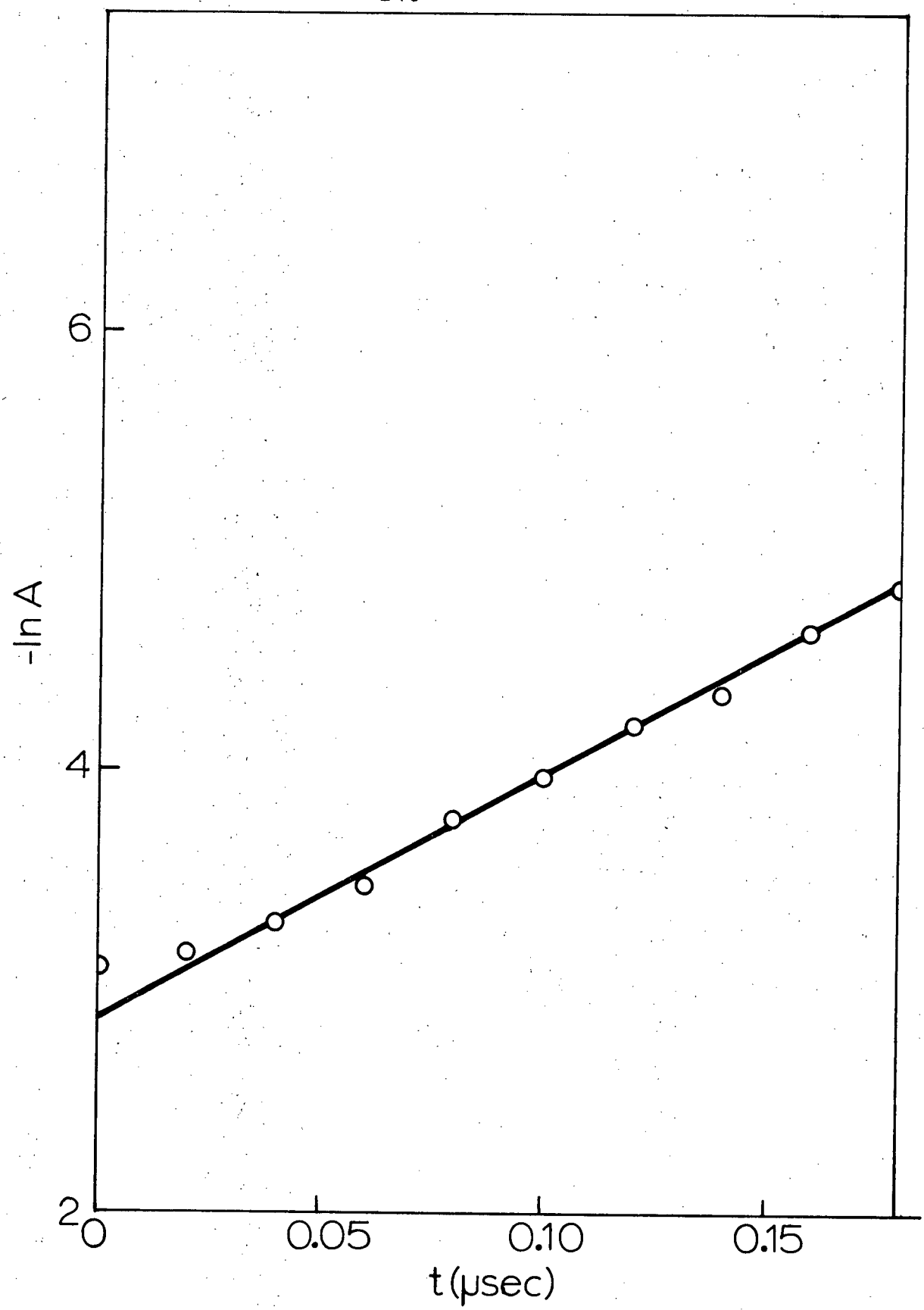

Figure III-33. First order kinetic plot for rapid e^-_{HMPA} decay in the presence of (7.9 ± 0.2) X 10^{-4}M N_2O from Figure III-32(b). Time zero corresponds to the end of the radiation pulse.

electron concentration is very different in the presence and absence of N_2O. In Figure III-34 the data are plotted in absorbance units. As a consequence of the fact that the radiation pulses were essentially square waves (Figure II-12), the electron absorbance increased steadily throughout the duration of the pulse. That is, the rate of formation of solvated electrons was a constant, K:

$$\frac{de^-_{HMPA}}{dt} = \frac{d(A/\epsilon l)}{dt} = K \qquad (lvii)$$

where A is the electron absorbance, ϵ is its molar absorptivity at the wavelength studies and l is the optical path length.

Now, in the presence of N_2O, the electron decay is greatly accelerated through reaction (3.68). The result is that during the radiation pulse a point is reached where the rates of electron formation and decay are equal and electron absorbance remains constant -- at a so-called steady state value, $A_{s.s.}$. Under those conditions,

$$k_{3.68} = \frac{dA}{dt} \times \frac{1}{A_{s.s.}[N_2O]} \qquad (lviii)$$

Substitution of the appropriate values from Figure III-34 into (lviii) gives $k_{3.68} = (1.5 \pm 0.2) \times 10^{10}\ M^{-1}\ sec^{-1}$ as the rate constant for scavenging of solvated electrons by nitrous oxide

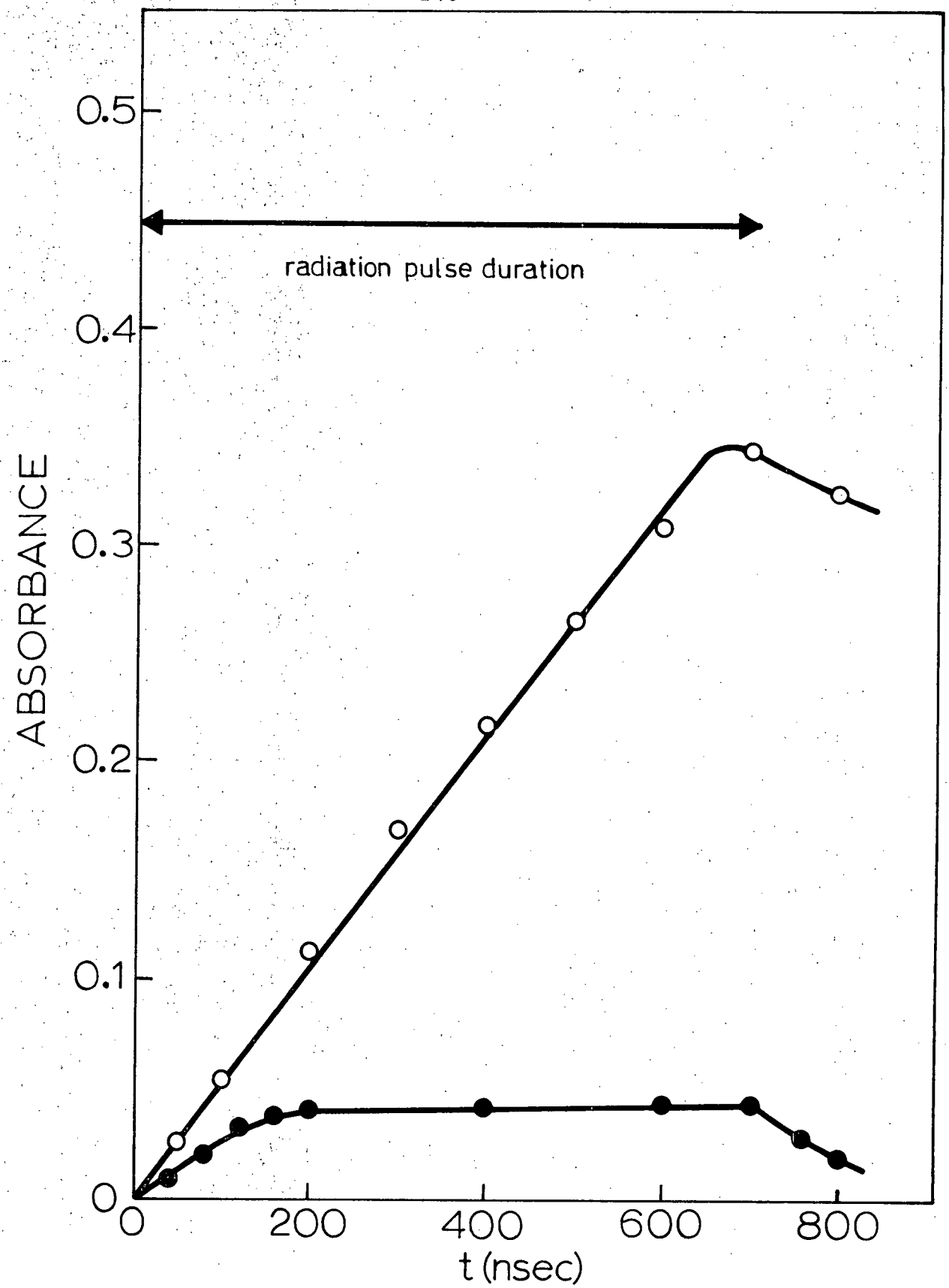

Figure III-34. Build-up of e^-_{HMPA} absorbance at 1000 nm during 700 nsec "square" radiation pulses of Figure III-32. In pure HMPA (O) rate of formation was constant, $dA/dt = (5.2 \pm 0.1) \times 10^5 sec^{-1}$. For HMPA containing $(7.9 \pm 0.2) \times 10^{-4}$M N_2O (●) a steady state absorbance $A_{s.s.} = 0.044 \pm 0.002$ was reached.

in HMPA. This result is in excellent agreement with that obtained directly from the electron decay and therefore lends credence to that value; but, since it was not obtained completely independently, does not confirm its precision.

The rate constant for the corresponding reaction in water is 0.56×10^{10} M^{-1} sec^{-1}.[37] The higher rate in HMPA is understandable in terms of the very weak solvation energy of the electron in HMPA and possibly its higher electron mobility.

i.3) Oxygen

Oxygen appears to react rapidly (and expectedly) with e^-_{HMPA} as evidenced by the fact that when irradiated HMPA was exposed to air at one atm pressure the electron absorbance was greatly reduced and short-lived.

i.4) Acetone

Another proven electron scavenger, acetone, had been used in the steady state ^{60}Co radiolysis studies of HMPA -- usually in conjunction with N_2O. Under these conditions, it was expected that acetone would scavenge electrons (3.107) in competition with nitrous oxide (3.68) with the result being a lower yield of nitrogen from the latter reaction.

$$e^-_{HMPA} + CH_3COCH_3 \longrightarrow (CH_3COCH_3)^- \qquad (3.107)$$

$$e^-_{HMPA} + N_2O \longrightarrow N_2 + \text{products} \qquad (3.68)$$

In point of fact however, the nitrogen yield was found to be increased in those studies. The ambiguity was attributed to a charge transfer reaction (3.43) between the acetone anion and N_2O.

$$(CH_3COCH_3)^- + N_2O \longrightarrow N_2 + \text{products} \qquad (3.43)$$

In that case, the increased nitrogen yield would simply be a reflection of the increased total scavenger concentration.

In order to confirm these suspicions, a series of pulse radiolysis experiments were conducted. As can be seen from Table XV, the initial electron yield in irradiated HMPA (as measured from the absorbance at 1550 nm immediately following the electron pulse) was considerably lower in the presence of acetone. In the case of a solution containing (1.6 ± 0.2) X 10^{-1}M acetone, the decrease amounted to 96%.

A new broad transient absorption appeared in the visible region of the spectrum from irradiated solutions of HMPA containing acetone. Figure III-35 shows the spectra observed between 400 and 2050 nm from a solution containing (1.6 ± 0.2) X 10^{-2}M acetone. Spectra present immediately after, and 2 μsec after, the radiation pulse are given. The absorption from about 1300 nm to 2050 nm is assigned to the solvated electron. The electron spectra would also contribute to some extent below 1300 nm

TABLE XV Effect of acetone on the electron absorbance at 1550 nm in irradiated HMPA.

[Ac]	A_o Relative Initial Absorbance @ 1550 nm	Percentage Decrease in A_o From Pure HMPA	First Half-Life (e^-_{HMPA}) (μsec)
0	0.708 ± 0.010	0	2.3 ± 0.2
$(3.2 \pm 0.5) \times 10^{-2}$M	0.135 ± 0.005	81%	2.2 ± 0.2
$(1.6 \pm 0.2) \times 10^{-1}$M	0.031 ± 0.003	96%	1.5 ± 0.4

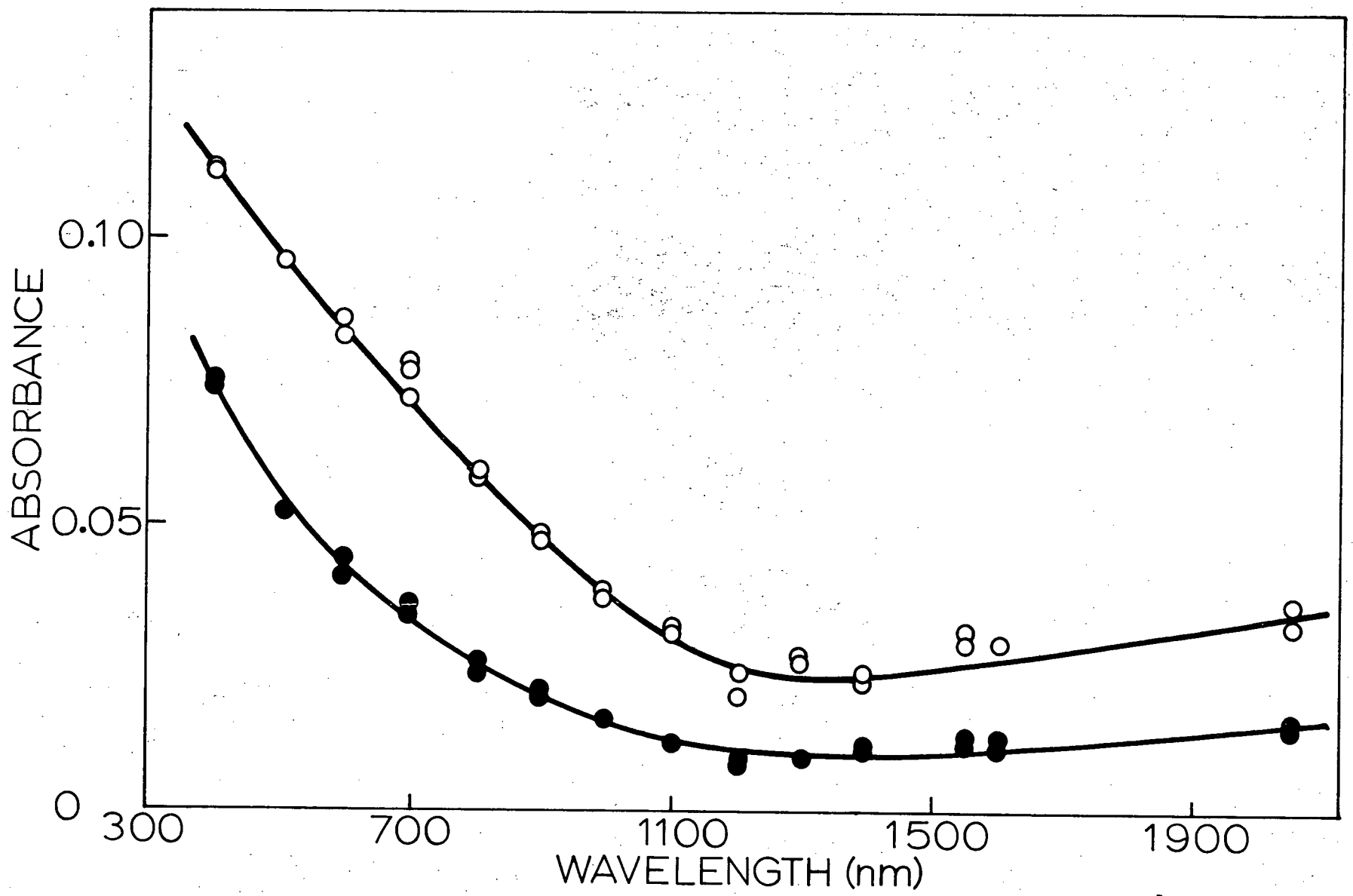

Figure III-35. Spectra obtained in irradiated HMPA containing (1.6 ± 0.2) X 10^{-1}M acetone immediately (O) and 2 μsec (●) after the pulse.

but the major increase in the visible and UV regions is attributed to the product of reaction (3.107), perhaps to the acetone anion, $(CH_3COCH_3)^-$. Vidyathi[137] has observed an absorption due to this anion or its protonated radical in water, and has reported that its absorption maximum occurs below 250 nm.

It should be noted that the electron spectra persisted 2 μsec after the pulse. The significance of this fact is more evident from the data in Table XV. The table shows that while the initial electron absorbance was greatly reduced in the presence of acetone, the electron decay following the pulse was essentially unaffected. These facts imply that acetone does not in fact scavenge solvated electrons in HMPA but rather attacks the precursor of that species, e^- (3.108).

$$\text{HMPA} \xrightarrow{\sim\sim\sim} [e^-] + \text{products} \qquad (3.14)$$

$$[e^-] \longrightarrow e_s^- \qquad (3.23)$$

$$[e^-] + CH_3COCH_3 \longrightarrow (CH_3COCH_3)^- \qquad (3.108)$$

This proposition is supported by evidence found by investigating the solvated electron formation during the radiation pulse in both the presence and absence of acetone. Figure III-36 shows the build-ups observed at 1550 nm. Note that in both pure HMPA and in the presence of $(3.2 \pm 0.5) \times 10^{-2}$M acetone the electron

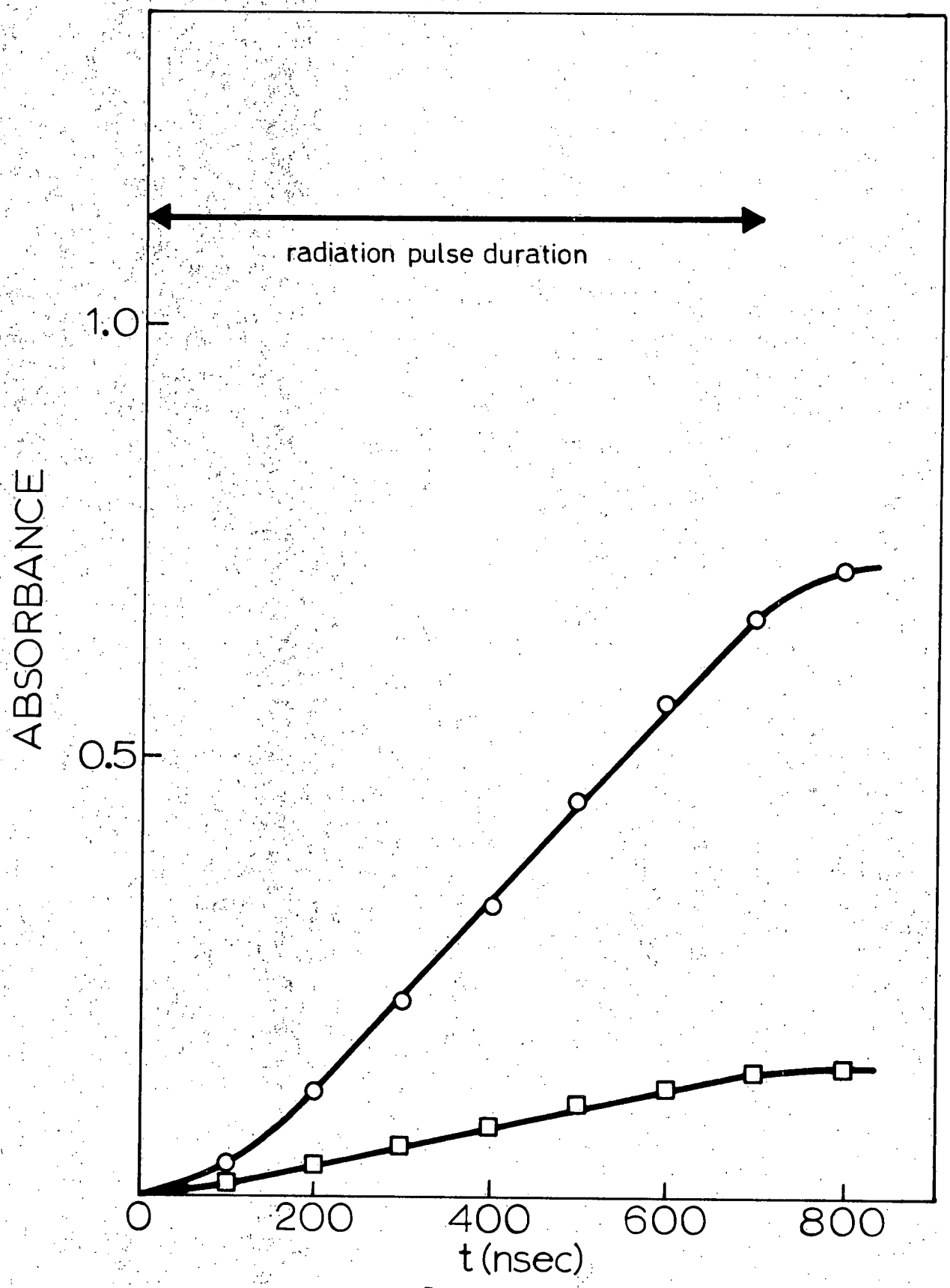

Figure III-36. Build-up of e^-_{HMPA} absorbance at 1550 nm in irradiated samples of HMPA (○) and HMPA containing (3.2 ± 0.5) X 10^{-2}M acetone (□).

absorbance build-up was linear, with $\frac{dA}{dt}$ = (1.1 ± 0.1) X 10^6 sec^{-1} and (2.1 ± 0.1) X 10^5 sec^{-1} respectively. That is, in the presence of (3.2 ± 0.5) X 10^{-2}M acetone the rate of solvated electron formation was one-fifth that in pure HMPA. Since such a decreased rate would itself account for the 80% drop in electron concentration at pulse end between the samples, reaction between acetone and e^-_{HMPA} is <u>not</u> indicated. Instead, acetone appears to scavenge four-fifths of the solvated electron precursors in that case.

Contrast these results with those from a sample containing a fifty-fold lower concentration of N_2O ((7.9 ± 0.2) X 10^{-4}M) in HMPA. In that case also, the electron absorbance was similarly reduced at the pulse end (by 87%) but during the pulse the electron concentration had quickly reached a constant (steady-state) value. Clearly different processes were operative for the two scavengers.

The presence of (7.9 ± 0.2) X 10^{-4}M N_2O in a solution of (3.2 ± 0.5) X 10^{-2}M acetone in HMPA resulted in the near total removal of all absorptions at 1000 nm. This observation confirms the earlier conjecture that N_2O reacted with the anionic acetone species in HMPA (3.43).

$$(CH_3COCH_3)^- + N_2O \xrightarrow{k_{3.43}} \text{products} \qquad (3.43)$$

Based on a crude "steady-state" calculation, the present experiment puts a lower limit for the rate constant of $k_{3.43} \geq 10^9$ M^{-1} sec^{-1} for the reaction between N_2O and Ac^-.

ii) Positive Ion Scavengers

ii.1) Water and Methanol

As might be expected, even large concentrations of water or methanol had little effect on the solvated electron absorption in HMPA. These molecules are known to scavenge positive ions through proton transfer reactions. An upper limit for the rate constant for bimolecular combination with e^-_{HMPA}, $k < 10^5\ M^{-1}\ sec^{-1}$ was established from solutions containing up to 4M water and up to 2M methanol. Most likely, that limit is governed by impurity levels in those solutes.

ii.2) Bromide Ions

ii.2i) Yield of Oxidizing Species

Irradiation of HMPA samples containing bromide ions resulted in an increase in both the yield and lifetime of solvated electrons. For example, from 0.14M LiBr or 0.17M NaBr, the electron yield was 35% greater than from pure HMPA alone. In addition, a new transient absorption with $\lambda_{max} \sim$ 360 nm was observed on irradiation of the bromide solutions. The transient spectra can be seen in Figure III-37.

This new visible band was similar to that reported by Grossweiner and Matheson[209] from photolyzed aqueous bromide solutions. They attributed the absorption to the dibromide

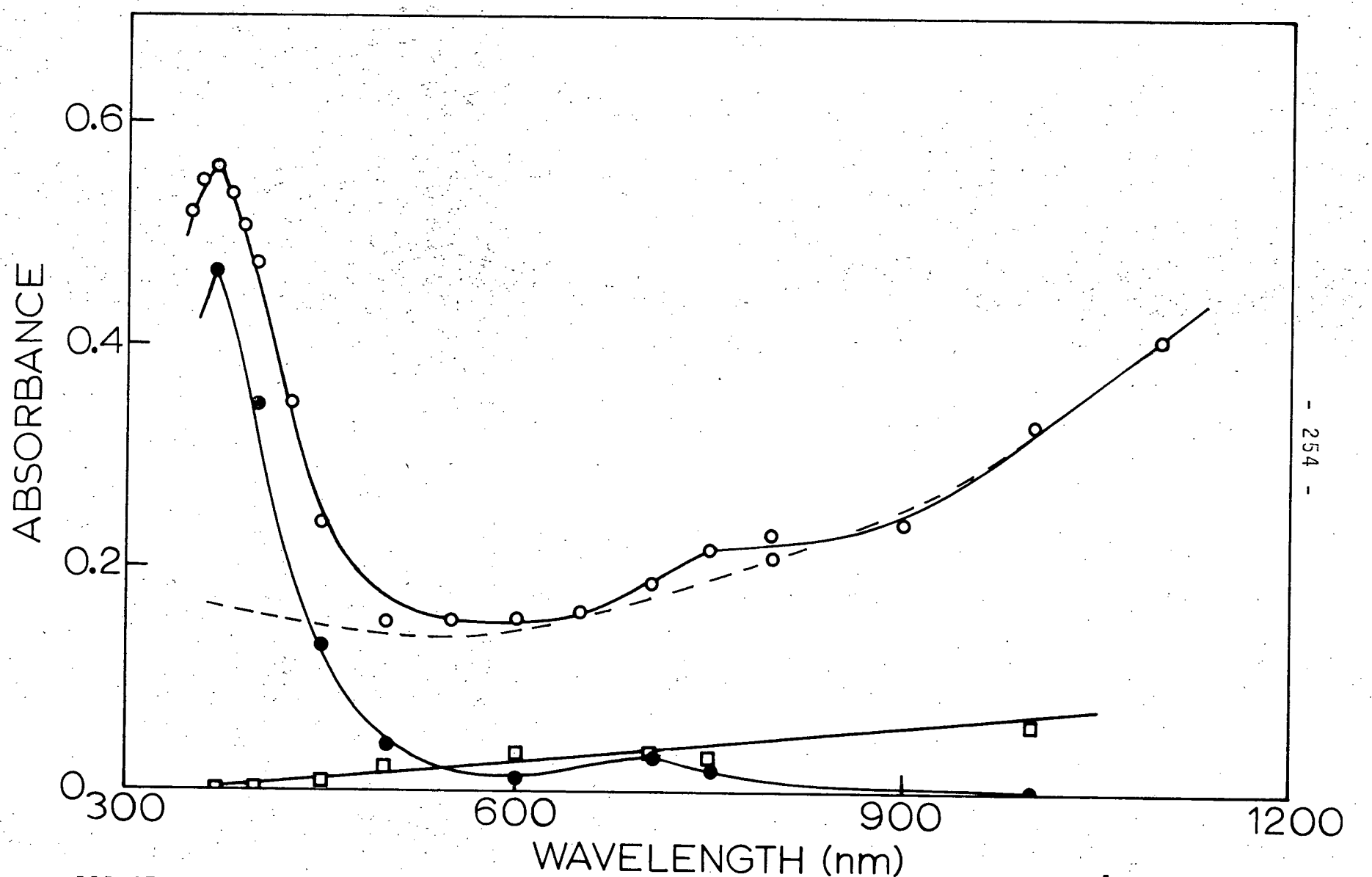

Figure III-37. Spectra obtained in irradiated HMPA containing (2.0 ± 0.2) X 10^{-1} M LiBr (o), compared to pure HMPA (— — —). Also shown are the long-lived transient observed on the addition of (1.3 ± 0.1) X 10^{-3} M N_2O (●) and the short-lived e^-_{HMPA} contribution from that solution (□).

anion, Br_2^-. Subsequently, that species has been observed and identified in a number of pulse radiolysis studies.[211]

Many investigators concluded that Br_2^- ions arise from the scavenging of positive ions by Br^- (3.109, 3.110).

$$Br^- + S^+ \longrightarrow Br + S \qquad (3.109)$$

$$Br + Br^- \longrightarrow Br_2^- \qquad (3.110)$$

Such processes were proposed to account for an observed increase in solvated electron yield from irradiated solutions of Br^- ions in ethanol and methanol.[212] That is, they suggest that positive ion scavenging leads to a decrease in neutralization processes (3.111).

$$\left[ROH^+, e^-\right] + Br^- \longrightarrow \left[ROH, Br, e^-\right] \qquad (3.111)$$

The observed increase in e^-_{HMPA} yield and lifetime in HMPA containing large concentrations of Br^- has two important consequences on that system. Firstly, it supports the postulate the neutralization with positive ions contributes to the complex electron decay mechanism. Secondly, the results indicate some involvement of geminate ion scavenging in HMPA.

If large concentrations of Br^- ions can scavenge positive geminate ions in irradiated HMPA, then they would be expected to have scavenged all free positive ions in the process. Since such reaction leads to an observable product, Br_2^-, it should be

possible to measure the positive free ion yield. This would give another independent measure of the solvated electron yield if one assumes a one-to-one correspondence between those species. From the measured dosimetry and the absorbance at 360 nm for a 0.14M LiBr solution in HMPA, one calculates $G(Br_2^-) \epsilon_{max}^{Br_2^-} = (2.1 \pm 0.1) \times 10^4\ M^{-1}\ cm^{-1}$ molecule $(100\ ev)^{-1}$.

A problem arises as to whether or not the absorbance at 360 nm from this solution arises solely from Br_2^- anions. In pure HMPA, studies indicated that e^-_{HMPA} and at least one other species, S, (which may be the positive ion or its derivative) also absorb at 360 nm. Assuming that both species contribute in the bromide solution and based on extrapolation and comparison with the electron absorbance at 1000 nm one finds that the contribution from Br_2^- is reduced to $(1.2 \pm 0.1) \times 10^4$. If only one of the other two species contributes to the absorbance at 360 nm, this value becomes $(1.5 \pm 0.1) \times 10^4$ or $(1.7 \pm 0.1) \times 10^4$ for the electron and UV species respectively.

Unfortunately, the Br_2^- species itself completely masked the region over which the UV species was observable in those experiments. Thus it was impossible to further define its contribution to the absorbance by direct means. The solvated electron and dibromide anion decays occurred over comparable timescales, so that their relative components could not be resolved directly either. Nitrous oxide at $(1.3 \pm 0.1) \times 10^{-3}$M concentration was introduced into a sample containing $(2.0 \pm 0.2) \times 10^{-1}$M LiBr. Figure III-38 depicts a series of normalized oscilloscope traces observed at various wavelengths between 360

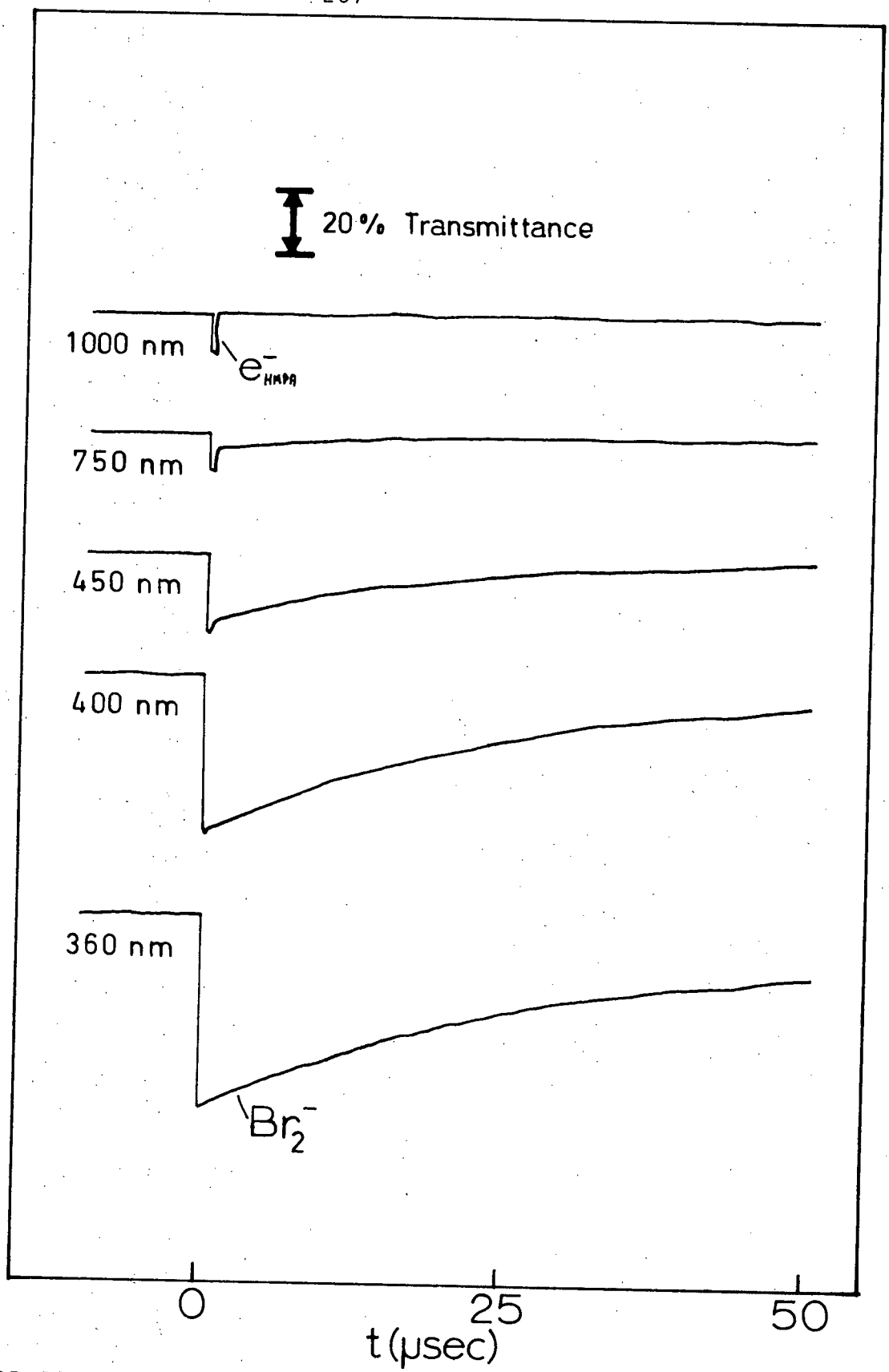

Figure III-38. Normalized oscilloscope traces showing the relative contributions of e^-_{HMPA} and Br^- at various wavelengths from the irradiation of a solution of HMPA containing (2.0 ± 0.2) X 10^{-1}M LiBr and (1.3 ± 0.1) X 10^{-3}M N_2O.

and 1000 nm. Under these conditions, the electron absorption was greatly reduced and very short lived, while that of the Br_2^- ion was nearly unaffected. Thus the effect of N_2O addition was to facilitate the resolution of the two absorbing species over this wavelength region. Shortening the electron lifetime in this way had its price however, for the initial electron yield was reduced to a steady-state value only one-sixth that found in the original, making accurate resolution difficult. The most striking and obvious conclusion that one reaches from these data is that the electron does not contribute to the absorbance below 400 nm and therefore cannot interfere with the Br_2^- absorption at 360 nm. However, as can be seen in Figure III-37 the presence of N_2O resulted in a decrease in the Br_2^- maximum at 360 nm. These results are not compatible. Therefore, unfortunately, the huge range in the $G\epsilon$ value for Br_2^- from $(1.2 \pm 0.1) \times 10^4$ to $(2.1 \pm 0.1) \times 10^4$ could not be definitively narrowed down.

A second major controversy which adversely affects the uncertainty of a Br_2^- yield calculation is that regarding the magnitude of the maximum molar absorptivity of the dibromide anion, $\epsilon_{360}^{Br_2^-}$. Values have been reported in the literature[211,213,214] for this constant ranging from 8200 to 12000 M^{-1} cm^{-1} in aqueous solution. Thus, the present study gives a value for the yield of dibromide ions from 0.14M LiBr in HMPA, $G(Br_2^-) = 1.8 \pm 0.8$. This value which should be equivalent to the positive ion yield is much lower than the corresponding electron yield, $G(e^-_{HMPA}) = 3.1 \pm 0.4$, in the same solution. Certainly it is

significantly larger than the increase in the electron yield caused by the presence of Br^-.

It is possible that the oxidizing species in HMPA have rapid alternative decay paths and thus are not all scavenged by 0.14M Br^- ions. For example, from a solution containing $(6 \pm 2) \times 10^{-4}$M LiBr, the Br_2^- yield was only 3 or 4 percent that of the 0.14M solution. From $(1.7 \pm 0.3) \times 10^{-2}$M LiBr, the yield of Br_2^- was about half that of the more concentrated solution, but all the absorbance grew-in during the radiation pulse and was certainly complete in a microsecond. These findings support the idea that the positive ions have alternate fates which renders them relatively unreactive. This possibility could explain why the aromatic anions Py^- and An^- were so long lived in HMPA. Indeed -- such a mechanism might well be the major contributing factor responsible for the large yield of stable solvated electrons found in irradiated HMPA.

ii.2.ii) Kinetic Considerations

As mentioned, in the presence of 0.14M LiBr, the solvated electron decay was diminished. The first half-life increased from 3.5 μsec to 5.0 μsec. Table XVI gives the results obtained from first plus second order regression analyses of the electron decay under the two conditions. As one would expect, bromide ions had no effect on the apparent first order portion of the electron decay. The calculated second order component of its decay however was halved. This is attributed to the

removal by bromide ions of positive ions that would otherwise neutralize solvated electrons.

TABLE XVI Results of first plus second order regression analyses for the electron decay at 1000 nm in pure HMPA and the same sample containing 0.14M LiBr.

Sample	$k'_{e^-_{HMPA}}$ - Calculated First Order Component of e_s^- decay (sec^{-1})	$k''_{e^-_{HMPA}}$ - Calculated Second Order Component of e_s^- decay (M^{-1} sec^{-1})
pure HMPA	$(1.2 \pm 0.1) \times 10^5$	$(2.0 \pm 0.1) \times 10^{10}$
0.14M LiBr	$(1.1 \pm 0.1) \times 10^5$	$(8.6 \pm 0.1) \times 10^9$

The dibromide anion decay proved to be much simpler than that of the electron. In Figure III-39 the Br_2^- decay at 360 nm from the same 0.14M LiBr solution (open circles) was found to conform to a second order plot. From the slope, one obtains a second order rate constant, $k_{Br_2^-} = (8.6 \pm 0.1) \times 10^5 \epsilon_{360}^{Br_2^-}$ M^{-1} sec^{-1}. Taking $\epsilon_{Br_2^-}^{360} = (1.0 \pm 0.2) \times 10^4$ M^{-1} cm^{-1} one calculates a second order rate constant for the Br_2^- decay,

$$k_{Br_2^-} = (8.5 \pm 1.5) \times 10^9 \ M^{-1} \ sec^{-1}$$

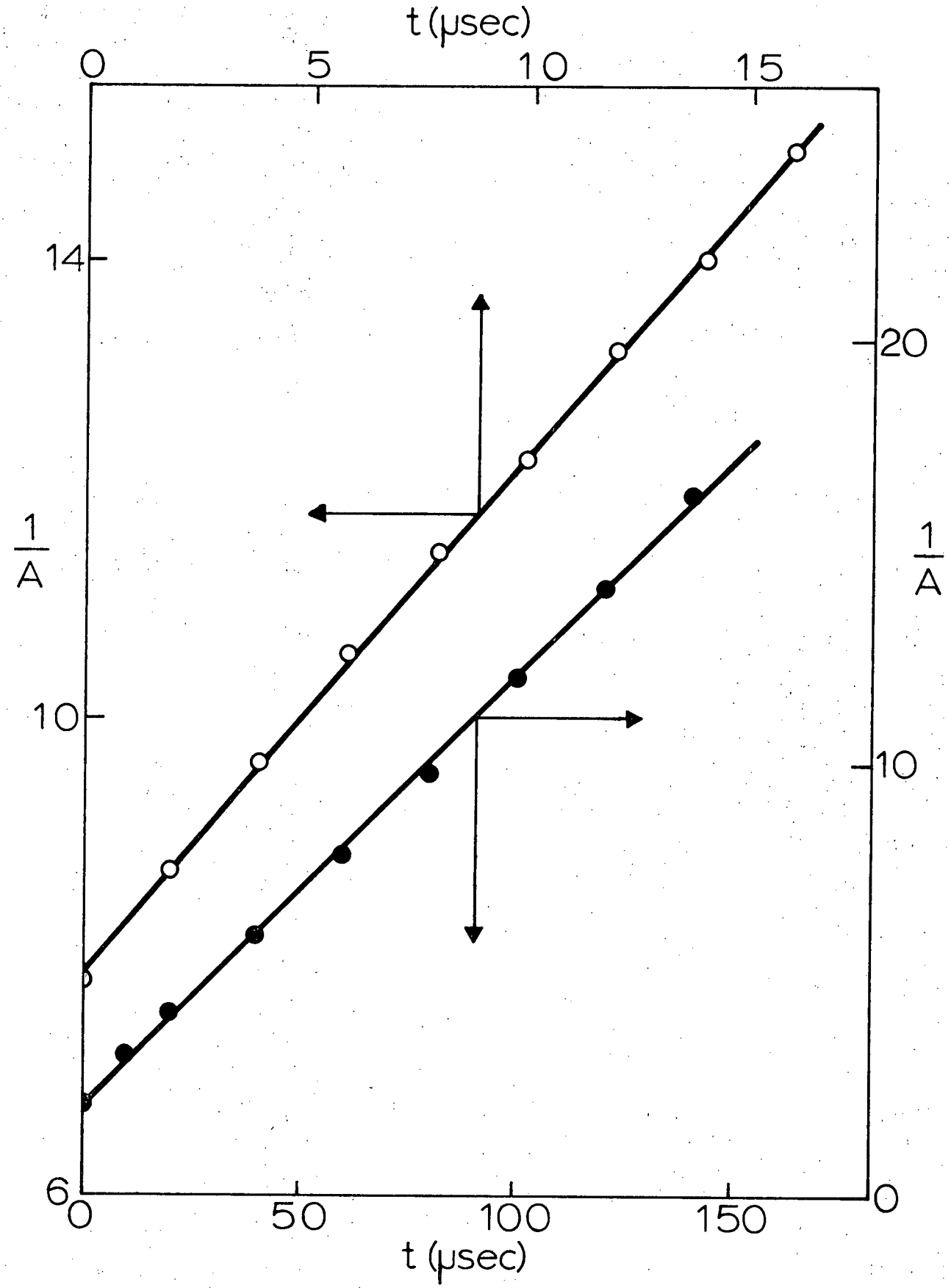

Figure III-39. Second order kinetic plots for the decay of the Br_2^- absorption at 360 nm in irradiated HMPA containing (0.17 ±0.03) M LiBr. Decay was examined over both short (O) and long time scales (●).

Comparing this value with that obtained for the second order component of the electron decay,

$$k''_{e_s^-} = (8.6 \pm 0.1) \times 10^9 \ M^{-1} \ sec^{-1}$$

it suggests that these species in fact react together (3.111).

$$Br_2^- + e^-_{HMPA} \xrightarrow{k_{3.111}} 2Br^- \qquad (3.111)$$

Such a reaction has been proposed to occur in aqueous solution[211c] a value for the bimolecular rate constant $k = (1.3 \pm 0.5) \times 10^{10}$ M^{-1} sec^{-1} being reported.

It should be remembered that about half of the electron absorption decay occurs simutaneously via first order processes. Therefore, if reaction (3.111) is the dominant decay process for dibromide ions, about half the Br_2^- absorption would remain when the electron absorption had disappeared. This was found to be so for the 0.14M LiBr solution.

From a solution containing $(2.0 \pm 0.2) \times 10^{-1}$M LiBr, the Br_2^- decay was monitored over a time period of 150 μsec by using the analyzing lamp in its steady DC mode. This allowed investigation of the Br_2^- decay after e^-_{HMPA} had completely decayed. As can be seen in the plot of Figure III-39, the slow Br_2^- decay (filled circles) also followed second order kinetics with an apparent bimolecular rate constant $k = (4.0 \pm 1.2) \times 10^9$ M^{-1} cm^{-1}. In aqueous solution a simple bimolecular combination reaction (3.112) has been proposed with $k_{3.112}$ on the order of (2 to 3) X

10^9 M^{-1} sec^{-1};[211b]

$$Br_2^- + Br_2^- \xrightarrow{k_{3.112}} Br_3^- + Br^- \qquad (3.112)$$

The tribromide anion is reported to absorb below 300 nm;[211a] an inaccessible region in the present study of HMPA because of strong solvent absorption.

The removal of solvated electrons through the addition of N_2O would be expected to surpress reaction (3.111) and thereby extend the lifetime of Br_2^- ions -- particularly over the first 10 - 20 μsec. However, the first half-life period of 18 μsec for 0.14M LiBr in HMPA was reduced to 14 μsec and 13 μsec in the presence of N_2O at (1.3 ± 0.1) X 10^{-3}M and (1.3 ± 0.1) X 10^{-2}M respectively. While it is possible that some impurity could have been introduced along with the N_2O, these results would tend to suggest that Br_2^- reacts with N_2O^- or some other species formed from it ($N_2O_2^-$, O^-, O_2^-, etc.). Such reaction might well surpress secondary ionic reactions of N_2O to such an extent so as to account for the only marginal increase in nitrogen yield from nitrous oxide solutions of HMPA in the presence of bromide ions. Thus, while the solvated electron yield increased up to 35% through geminate positive ion scavenging by Br^-, the increase was not necessarily reflected in the nitrogen yield from N_2O.

ii.2.iii) Na^- Spectrum

For solutions containing NaBr, the spectrum was studied carefully over the wavelength region 700 to 1000 nm. In both sodium metal solution studies and other pulse radiolysis investigations,[193] a strong absorption attributed to Na^- has been reported. The end of pulse spectrum from 0.17M NaBr in HMPA was essentially identical to that from pure HMPA. However, some 30 μsec after the radiation pulse when ~97% of the solvated electrons had decayed, there was some evidence of an absorption band with a maximum in the region of 750 nm. The absorption was very weak and probably amounted to less than 5% of the initial electron absorption in this region. Certainly the data does not indicate the presence of a significant absorption due to some anionic sodium species. Rather, this small contribution is probably associated with the Br_2^- anion. Rabani[211e] has reported a second absorption at 700 nm from aqueous LiBr solutions and attributed it to Br_2^-. Indeed, a closer look at the Br_2^- spectrum from $(2.0 \pm 0.2) \times 10^{-1}$M LiBr solution in HMPA where e^-_{HMPA} had been removed by N_2O (Figure III-37) reveals the presence of such a peak in the present work.

E. Summary

This investigation has provided a wealth of information about the rather remarkable phenomenon of the solvated electron in HMPA. The experiments were designed in such a way so as

to thoroughly probe that curious and complex system through the use of several investigative techniques.

As predicted, solvated electrons proved to be sufficiently long-lived in HMPA so as to be positively identified from their spectra, behavior and reactivity with a host of solutes. The radiolysis yield, $G(e^-_{HMPA}) = 2.2 \pm 0.2$ established from two quite different radiolysis techniques; the nature and optical properties of the absorption spectrum; and the diversity of the kinetic behavior attributed to the solvated electron in HMPA are completely compatible with the extraordinary properties of that solvent. There is ample evidence to support the supposition that solvated electrons in HMPA do not undergo fast geminate decay and therefore the observed yield does in fact represent the free-ion yield.

Taken in toto, the results strongly support the important conclusion that the high nitrogen yields observed from steady-state studies involving the use of nitrous oxide as electron scavenger arise from secondary ionic processes. Perhaps as a consequence of some of the unusual properties of HMPA, a number of such unique findings (particularly involving added solutes) were obtained. It may well be that some of the innovative approaches taken in this work may be applicable to other solvent systems where ambiguities exist.

In any event, while far from being completely definitive, this work does present a very consistent and reasonably comprehensive picture of the nature, yield, stability and reactivity of solvated electrons in HMPA.

REFERENCES

1. (a) H. Normant, Angew. Chem. Internat. Edit., 6 1046(1967). (b) H. Normant, Russian Chemical Reviews, 39 457(1970).
2. G. Fraenkel, S. H. Ellis, D. T. Dix, J. Amer. Chem. Soc., 87 1406(1965).
3. W. Weyl, Ann. Phys., 121 601(1864).
4. C. A. Kraus, J. Amer. Chem. Soc., 30 1323(1908).
5. R. A. Ogg, J. Amer. Chem. Soc., 68 155(1946); Phys. Rev., 69 668(1946).
6. W. L. Jolly, "Progress in Inorganic Chemistry", vol. I, Interscience, New York, 1959.
7. W. N. Lipscomb, J. Chem. Phys., 21 52(1953).
8. C. A. Kraus, J. Amer. Chem. Soc., 36 864(1914).
9. E. Arnold, A. Patterson Jr., J. Chem. Phys., 41 3098(1964).
10. J. L. Dye, Scientific American, Feb., 1967, page 77.
11. W. L. Jolly, C. J. Hallada, M. Gold, "Solutions Métal - Ammoniac", Physiochem Prop., Colloq. Weyl, 174 (1963).
12. R. A. Stairs, J. Chem. Phys., 27 1431(1957).
13. R. L. Potter, R. G. Shores, J. L. Dye, J. Chem. Phys., 35 1907(1961).
14. D. A. Copeland, N. R. Kestner, J. Jortner, J. Chem. Phys., 53 1189(1970).
15. J. Logan, N. R. Kestner, J. Phys. Chem., 76 2738(1972).
16. P. F. Rusch, J. J. Lagowski, J. Phys. Chem., 77 1311(1973).
17. H. Aulich, B. Baron, P. Delahay, R. Lugo, J. Chem. Phys., 58 4439(1972).

18. R. F. Pohler, J. C. Thompson, J. Chem. Phys., 40 1449(1964).

19. R. D. Nasby, J. C. Thompson, J. Chem. Phys., 53 109(1970).

20. C. A. Hutchison Jr., R. C. Pastor, J. Chem. Phys., 21 1959, (1953).

21. E. Hustler, Ann. Physik., 33 477(1938).

22. E. Becker, R. H. Lindquist, B. J. Alder, J. Chem. Phys., 25 971(1956).

23. L. R. Dalton, J. D. Rynbrandt, E. M. Hansen, J. L. Dye, J. Chem. Phys., 44 3969(1966).

24. E. Arnold, A. Patterson Jr., J. Chem. Phys., 41 3089(1964).

25. S. Golden, C. Guttman, T. R. Tuttle Jr., J. Chem. Phys., 44 3791(1966).

26. (a) M. T. Lok, F. J. Tehan, J. L. Dye, J. Phys. Chem., 76 2975(1972) and ref. (2) to (5) therein.

(b) K. Bar-Eli, G. Gabor, J. Phys. Chem., 77 323(1973) and ref. (1) therein.

27. I. Hurley, T. R. Tuttle Jr., S. Golden, J. Chem. Phys., 48 2818(1968) and refs. (1) to (8) therein.

28. J. Eloranta, J. Linschitz, J. Chem. Phys., 38 2214(1963).

29. M. Ottolenghi, K. Bar-Eli, H. Linschitz, T. R. Tuttle Jr., J. Chem. Phys., 40 3729(1964).

30. M. G. DeBracker, J. L. Dye, J. Phys. Chem., 75 3092(1971).

31. S. Mantalon, S. Golden, M. Ottolenghi, J. Phys. Chem., 73 3098(1969).

32. G. Gabor, K. Bar-Eli, J. Phys. Chem., 75 286(1971).

33. R. Catterall, M. C. R. Symons, J. W. Tipping, J. Chem. Soc. (A) 1234(1967).

34. K. D. Vos, J. L. Dye, J. Chem. Phys., 38 2033(1963).

35. K. Bar-Eli, T. R. Tuttle Jr., J. Chem. Phys., 40 2508(1964).

36. E. A. Shaede, D. C. Walker, "The Alkali Metals", Sp. publication #22, The Chem. Soc. (London), 277(1966).

37. M. Anbar, P. Neta, Int. J. Appl. Radiat. Isotopes, 18 493(1967).

38. G. Hughes, R. J. Roach, Chem. Comm., 600(1965).

39. J. J. Weiss, Ann. Rev. Phys. Chem., 4 (1953).

40. G. Stein, Disc. Farad. Soc., 12 227(1952).

41. R. L. Platzman, N. A. S. - N. R. C. Reports, 305 22(1953).

42. J. H. Baxendale, G. Hughes, Z. Physik. Chem., 14 323(1958).

43. E. Hayon, J. J. Weiss, 2nd Proc. Intern. Conf. Peaceful Uses At. Energy, Geneva, 29 80(1959).

44. N. F. Barr, A. O. Allen, J. Phys. Chem., 63 928(1959).

45. G. Czapski, H. A. Schwarz, J. Phys. Chem., 66 471(1962).

46. E. J. Hart, J. W. Boag, J. Amer. Chem. Soc., 84 4090(1962).

47. J. W. T. Spinks, R. J. Woods, "An Introduction to Radiation Chemistry", John Wiley and Son, Inc., New York, N. Y., 1964, Ch. 3.

48. M. S. Matheson, L. M. Dorfman, "Pulse Radiolysis", M. I. T. Press, Cambridge, Mass., 1969, page 14, 15.

49. A. Kuppermann, "The Chemical and Biological Action of Radiations", Vol. 5, 87 (1961).

50. A. H. Samuel, J. L. Magee, J. Chem. Phys., 21 1080(1953).

51. (a) A. O. Allen, H. A. Schwarz, Proc. Second Intern. Conf. Peaceful Uses Atomic Energy, United Nations, Geneva, 29 30(1958).

51. (b) M. Lefort and X. Tarrago, J. Phys. Chem., 63 833(1959).

52. E. J. Hart, Survey of Progress in Chemistry, 5 129(1969).

53. J. H. Baxendale, Radiat. Res. Suppl., 4 139(1964).

54. R. M. Minday, L. D. Schmidt, H. T. Davis, J. Phys. Chem., 76 442(1972).

55. D. C. Walker, Can. J. Chem., 44 2226(1966).

56. D. C. Walker, Can. J. Chem., 45 807(1967).

57. R. A. Ogg, Phys. Rev., 69 668(1946).

58. (a) J. Jortner, J. Chem. Phys., 30 839(1959).
(b) J. Jortner, Radn. Res. Suppl., 4 24(1964).
(c) S. Pekar, J. Phys. (U.S.S.R.), 10 341(1946).
(d) L. Landau, Sov. Phys., 3 664(1933).

59. K. Fueki, J. Chem. Phys., 49 765(1968).

60. D. A. Copeland, N. R. Kestner, J. Jortner, J. Chem. Phys., 53 1189(1970).

61. (a) M. Natori, T. Watanabe, J. Phys. Soc. Jap., 21 1573(1966).
(b) K. Fueki, D. F. Feng, L. Kevan, J. Phys. Chem., 74 1976(1970).
(c) M. Tachiya, Y. Tabata, K. Oshima, J. Phys. Chem., 77 263(1973).
(d) K. Fueki, D. F. Feng, L. Kevan, J. Amer. Chem. Soc., 95 1398(1973).

62. Z. D. Draganic, I. G. Draganic, J. Phys. Chem., 76 2733(1972).

63. (a) T. Sawai, W. H. Hamill, J. Chem. Phys., 52 3843(1970).
(b) T. Sawai, W. H. Hamill, J. Phys. Chem., 74 3914(1970).

64. E. Peled, G. Czapski, J. Phys. Chem., 75 3626(1971).

65. K. D. Asmus, J. M. Warman, R. H. Schuler, J. Phys. Chem., 74 246(1970).

66. R. Schiller, Current Topics in Rad'n. Res., 6 3(1970).

67. L. Onsager, Phys. Rev., 54 554(1938).

68. (a) G. R. Freeman, J. M. Fayadh, J. Chem. Phys., 43 86(1965).
(b) E. Hayon, J. Chem. Phys., 53 2353(1970).
(c) R. Hentz, G. Kenney-Wallace, J. Phys. Chem., 78 514(1974).

69. L. M. Dorfman, Amer. Chem. Soc., Adv. Chem. Ser., 50 36(1965).

70. M. C. Sauer Jr., S. Arai, L. M. Dorfman, J. Chem. Phys., 42 708(1965).

71. S. Arai, M. C. Sauer Jr., J. Chem. Phys., 44 2297(1966).

72. J. L. Dye, M. G. Debacker, L. M. Dorfman, J. Chem. Phys., 52 6251(1970).

73. T. J. Kemp, G. A. Salmon, P. Wardman in "Pulse Radiolysis", M. Ebert, J. P. Keene, A. J. Swallow, and J. H. Baxendale, Ed. Academic Press, London, 1965, pages 247 - 257.

74. L. B. Magnusson, J. T. Richards, J. K. Thomas, Int. J. Radiat. Phys. Chem., 3 295(1971).

75. A. V. Vannikov, V. S. Marevtsev, Int. J. Radiat. Phys. Chem., 5 453(1973).

76. J. M. Brooks, R. R. Dewald, J. Phys. Chem., 72 2655(1968).

77. R. Catterall, L. P. Stodulski, M. C. R. Symons, J. Chem. Soc. (A), 437(1968).

78. (a) G. Dodin, J. E. Dubois, J. Phys. Chem., 77 2483(1973).
(b) H. W. Sternberg, R. E. Markby, I. Wender, D. M. Mohilner, J. Amer. Chem. Soc., 89 186(1967).

79. N. M. Alpatova, A. D. Grishina, Elecktrokhimiya, 7 853(1971).

80. G. J. Flynn, B. Sc. Thesis, The University of British Columbia, 1969.

81. Ref. 47, pages 106 - 112.

82. (a) L. M. Dorfman, F. Y. Jou, R. Wageman, Ber. Bunsen-Gesell. Phys. Chem., 75 681(1971).

(b) F. Y. Jou, L. M. Dorfman, J. Chem. Phys., 58 4715(1973).

83. G. E. Adams, J. W. Boag, B. D. Michael, Proc. Chem. Soc., 411(1964).

84. G. E. Adams, J. W. Boag, J. Currant, B. D. Michael, "Pulse Radiolysis", M. Ebert et al., Ed. Acad. Press, Inc, New York, N. Y., 1965 page 117.

85. J. H. Baxendale, P. L. T. Bevan, D. A. Scott, Trans. Faraday Soc., 64 2389(1968).

86. (a) D. Behar, P. L. T. Bevan, G. Scholes, Chem. Comm., 1486(1971).

(b) D. Behar, P. L. T. Bevan, G. Scholes, J. Phys. Chem., 76 1537(1972).

87. E. J. Hart, M. Anbar, In "The Hydrated Electron", Wiley, N. Y., 1970, page 42.

88. M. S. Kharasch, B. S. Joshi, J. Org. Che., 22 1435(1957).

89. R. E. Buckles, J. P. Yuk, A. I. Popov, J. Amer. Chem. Soc., 74 4379(1952).

90. L. J. Andrews, R. M. Keefer, Adv. in Inorg. & Radiochem., 3 91(1961).

91. C. Capellos, A. O. Allen, J. Phys. Chem., 74 840(1970).

92. J. Rabani, J. Amer. Chem. Soc., 84 868(1962).

93. H. Seki, M. Imamura, J. Phys. Chem., 71 870(1967).

94. F. Busi, G. R. Freeman, J. Phys. Chem., 75 2560(1971).

95. G. Czapski, J. Jortner, Nature, 188 50(1960).

96. J. T. Allan, C. M. Beck, J. Amer. Chem. Soc., 86 1483(1964).

97. R. A. Holroyd, in "Fundamental Processes in Radiation Chemistry", Ed. P. Ausloos, Interscience, N. Y., 1968, page 413.

98. E. Hayon, J. Chem. Phys., 53 2353(1970).

99. M. G. Robinson, G. R. Freeman, J. Chem. Phys., 55 5644(1971).

100. K. Horacek, G. R. Freeman, J. Chem. Phys., 53 4486(1970).

101. S. J. Rzad, K. M. Bansal, J. Phys. Chem., 76 2374(1972).

102. W. F. Schmidt, A. O. Allen, J. Chem. Phys., 52 2345(1970).

103. J. M. Warman, K. D. Asmus, R. H. Schuler, Adv. Chem., Ser., 82 25(1968).

104. S. Sato, R. Yugeta, K. Shinsaka, T. Terao, Bull. Chem. Soc. Jap., 39 156(1966).

105. K. N. Jha, G. R. Freeman, J. Chem. Phys., 48 5480(1968).

106. S. M. S. Akhtar, G. R. Freeman, J. Phys. Chem., 75 2756(1971).

107. J. C. Russell, G. R. Freeman, J. Phys. Chem., 73 808(1968).

108. K. M. Bansal, S. J. Rzad, J. Phys. Chem., 74 2888(1970).

109. R. R. Hentz, W. V. Sherman, J. Phys. Chem., 72 2635(1968).

110. F. Kiss, J. Teply, Int. J. Radiat. Phys. Chem., 3 503(1971).

111. D. A. Head, D. C. Walker, Nature, 207 517(1965).

112. E. J. Hart, Survey of Progr. in Chem., 5 129(1969).

113. F. S. Dainton, S. R. Logan, Trans. Farad. Soc., 61 715(1965).

114. S. J. Rzad, G. Bakale, J. Phys. Chem., 77 1176(1973).

115. M. G. Robinson, G. R. Freeman, Can. J. Chem., 51 650(1973).

116. D. A. Head, D. C. Walker, Can. J. Chem., 48 1657(1970).

117. T. K. Cooper, D. C. Walker, Can. J. Chem., 49 2248(1971).

118. E. A. Shaede, Ph. D. Thesis, U. B. C., 1971.

119. J. M. Warman, J. Phys. Chem., 71 4066(1967).

120. G. G. Meisels, J. Chem. Phys., 41 51(1964).

121. W. J. Holtslander, G. R. Freeman, Can. J. Chem., 45 1661(1967).

122. K. G. McLaren, Int. J. Radiat. Phys. Chem., 2 123(1970).

123. M. G. Bailey, R. S. Dixon, Can. J. Chem., 49 2909(1971).

124. S. Sato, Bull. Chem. Soc. Japan, 41 304(1968) and ref. (1) therein.

125. G. R. A. Johnston, J. M. Warman, Nature, 203 73(1964).

126. F. T. Jones, T. J. Sworski, J. Phys. Chem., 70 1546(1966).

127. S. Takao, Y. Hatano, S. Shida, J. Phys. Chem., 75 3178(1971).

128. M. G. Robinson, G. R. Freeman, J. Phys. Chem., 72 1394(1968).

129. J. C. Russell, G. R. Freeman, J. Chem. Phys., 48 90(1968).

130. R. A. Holroyd, J. Phys. Chem., 72 759(1968).

131. R. May, Ph. D. Thesis, University of Leeds 1971, page 132.

132. Sir Frederick Dainton, F. R. S., T. Morrow, G. A. Salmon, G. F. Thompson, Proc. R. Soc. Lond. A, 328 457(1972).

133. J. H. Baxendale, M. A. J. Rodgers, J. Phys. Chem., 72 3849 (1968).

134. E. A. Rojo, R. R. Hentz, J. Phys. Chem., 69 3024(1965).

135. J. H. Baxendale, J. Mayer, Chem. Phys. Lett., 17 458(1972).

136. E. J. Hart, S. Gordon, J. K. Thomas, J. Phys. Chem., 68 1271(1964).

137. S. K. Vidyarthi, Ph. D. Thesis, U. B. C., 1973.

138. S. A. Chaudhri, K.-D. Asmus, J. Phys. Chem., 76 26(1972).

139. C. E. Burchill, G. P. Wollner, Can. J. Chem., 50 1751(1972).

140. T. K. Cooper, Ph. D. Thesis, U. B. C. 1972, page 116.

141. A. H. Samuel, J. L. Magee, J. Chem. Phys., 21 1080(1953).

142. S. Khorana, W. H. Hamill, J. Phys. Chem., 75 3081(1971).

143. (a) S. Arai, A. Kira, M. Imamura, J. Phys. Chem., 74 2102(1970).

(b) M. M. Fisher, W. H. Hamill, J. Phys. Chem., 77 171(1973).

144. J. M. Warman, K.-D. Asmus, R. H. Schuler, Adv. Chem. Ser., 82 25(1968).

145. J. W. Buchanan, F. Williams, J. Chem. Phys., 44 4377(1966).

146. G. R. Freeman, J. Chem. Phys., 46 2822(1967).

147. A. Hummel, J. Chem. Phys., 48 3268(1968).

148. S. Sato, T. Terao, M. Kono, S. Shida, Bull. Chem. Soc. Japan, 40 1818(1967).

149. F. Williams, J. Amer. Chem. Soc., 86 3954(1964).

150. G. C. Abell, K. Funabashi, J. Chem. Phys., 58 1079(1973).

151. R. K. Wolff, M. J. Bronskill, J. W. Hunt, J. Chem. Phys., 53 4211(1970).

152. K. Watanabe, T. Nakayama, J. Mottl, J. Quant. Spectr. Radiative Transfer, 2 369(1962).

153. S. J. Rzad, R. H. Schuler, A. Hummel, J. Chem. Phys., 51 1369(1969).

154. W. E. Wentworth, E. Chen, R. Freeman, J. Chem. Phys., 55 2075(1971).

155. A. V. Phelps, R. E. Voshall, J. Chem. Phys., 49 3246(1968).

156. J. M. Warman, R. W. Fessenden, J. Chem. Phys., 49 4718(1968).

157. J. F. Paulson, J. Chem. Phys., 52 959(1970).

158. J. F. Paulson, J. Chem. Phys., 52 963(1970).

159. J. L. Moruzzi, A. V. Phelps, J. Chem. Phys., 45 4617(1966).

160. J. F. Paulson, Adv. Chem., 58 28(1966).

161. J. L. Moruzzi, J. T. Dakin, J. Chem. Phys., 49 5000(1968).

162. J. Schaefer, J. M. S. Henis, J. Chem. Phys., 49 5377(1968).

163. E. E. Ferguson, Advan. Electron. Electron Phys., 24 23 (1968).

164. G. R. A. Johnson, J. L. Redpath, Trans. Farad. Soc., 66 861(1970).

165. W. A. Seddon, M. J. Young, Can. J. Chem., 48 393(1970).

166. W. A. Seddon, J. W. Fletcher, F. C. Sopchyshyn, Can. J. Chem., 51 1123(1973).

167. S. J. Rzad, J. M. Warman, J. Phys. Chem., 72 3013(1968).

168. W. J. Holtslander, G. R. Freeman, J. Phys. Chem., 71 2562(1967).

169. S. Hirokami, S. Shishido, S. Sato, Bull. Chem. Soc. Japan, 44 1511(1971).

170. P. P. Infelta, C. H. Schuler, J. Phys. Cehm., 76 987(1972).

171. P. O. Infelta, R. H. Schuler, Int. J. Radiat. Phys. Chem., 5 41(1973).

172. G. V. Buxton, Radiation Res. Rev., 1 209(1968).

173. M. S. Matheson, W. A. Mulac, J. L. Weeks, J. Rabani, J. Phys. Chem., 70 2092(1966).

174. J. Rabani, M. S. Matheson, J. Phys. Chem., 70 761(1966).

175. K. H. Schmidt, S. M. Ander, J. Phys. Chem., 73 2846(1969).

176. G. E. Adams, "Radiation Research", G. Silini, Ed. North-Holland Publishing Co., Amsterdam, 1967, page 195.

177. G. Czapski, "Radiation Chemistry of Aqueous Systems", G. Stein, E. The Weizman Sc. Press, Jerusalem, 1968, page 229.

178. D. Zehavi, J. Rabani, J. Phys. Chem., 75 1738(1971).

179. Sir Frederick Dainton, P. O'Neill, G. A. Salmon, J. Chem. Soc., Chem. Comm., 510(1972).

180. G. E. Adams, J. W. Boag, B. D. Michael, Nature, 205 898(1965).

181. D. Behar, G. Czapski, Israel J. Chem., 6 43(1968).

182. B. Gall, L. M. Dorfman, J. Amer. Chem. Soc., 91 2199(1969).

183. R. Wander, B. Gall, L. M. Dorfman, J. Phys. Chem., 1819 (1970).

184. (a) P. M. Johnson, A. C. Albrecht, J. Chem. Phys., 44 1845(1966).

(b) S. Gordon, E. J. Hart, M. S. Matheson, J. Rabani, J. K. Thomas, Disc. Farad. Soc., 36 193(1963).

(c) N. H. Sagert, Can. J. Chem., 46 336(1968).

(d) B. A. Thrush, Progr. Reaction Kinetics, 3 63(1965).

185. L. S. Miller, S. Howe, W. E. Spear, Phys. Reo., 166 871 (1968).

186. I. Warshawsky, J. Inorg. Nucl. Chem., 25 601(1963).

187. G. Huges, R. J. Roach, Chem. Comm., 600(1965).

188. E. J. Kirschke, W. L. Jolly, Inorg. Chem., 6 855(1967).

189. L. M. Dorfman, I. A. Taub, J. Amer. Chem. Soc., 85 2370(1963).

190. E. A. Shaede, D. C. Walker, "The Alkali Metals", Sp. Publication #22, The Chem. Soc., 277(1967).

191. Mellor, "Comprehensive Treatise on Inorganic and Theoretical Chemistry", J. Wiley and Sons, 1961, Vol. 2, Suppl. 2.

192. C. E. H. Bawn, A. G. Evans, Trans. Farad. Soc., 33 1571(1937).

193. (a) E. I. Mal'tsev, A. V. Vannikov, N. A. Boch, Radiat. Effects, 11 79(1971).

193. (b) E. I. Mal'tsev, A. V. Vannikov, Dokl. Akad. Nauk. SSSR, 200 379(1971).

194. E. Nauta, C. van Huis, J. Chem. Soc. Farad. I, 647(1972).

195. (a) L. M. Dorfman, F. Y. Jou, R. Wageman, Ber. Bunsen-Gesell. Phys. Chem., 75 681(1971).
(b) F. U. Jou, L. M. Dorfman, J. Chem. Phys., 58 4715(1973).

196. J. L. Dye, M. G. Debacker, L. M. Dorfman, J. Chem. Phys., 52 6251(1970).

197. F. Y. Jou, private communication.

198. D. C. Walker, N. V. Klassen, H. A. Gillis, Chem. Phys. Lett., 10 636(1971).

199. J. Jagur-Grodzinski, M. Feld, S. L. Yang, M. Szwarc, J. Phys. Chem., 69 628(1965).

200. D. Gill, J. Jagur-Grodzinski, M. Szwarc, Trans Farad. Soc., 60 1424(1964).

201. E. A. Shaede, private communication of unpublished results.

202. T. Shida, W. H. Hamill, J. Chem. Phys., 44 4372(1966).

203. C. R. Goldschmidt, M. Ottolenghi, J. Phys. Chem., 74 2041(1970).

204. "Modern Coordiantion Chemistry", J. Lewis, R. G. Wilkins Ed. Interscience, New York, N. Y., (1960), page 276.

205. E. J. Land, Trans. Farad. Soc., 67 1908(1971).

206. E. J. Hart, M. Anbar, In "The Hydrated Electron", Wiley, N. Y., 1970, page 40.

207. R. K. Quinn, J. J. Lagowski, J. Phys. Chem., 73 2326(1969).

208. F. Y. Jou, Ph.D. Thesis, The Ohio State University, Columbus, Ohio, page 77 - 80.

209. L. I. Grossweiner, M. S. Matheson, J. Chem. Phys., 23 2443(1955)

210. M. Simic, E. Hayon, J. Phys. Chem., 77 996(1973).

211. (a) B. Cercek, M. Ebert, J. P. Keene, A. J. Swallow, Science, 145 919(1964).

(b) B. Cereck, M. Ebert, C. W. Gilbert, A. J. Swallow, "Pulse Radiolysis", Acad. Press, Inc., New York, 1965, page 83.

(c) M. S. Matheson, W. A. Mulac, J. L. Weeks, J. Rabani, J. Phys. Chem., 70 2092(1966).

(d) D. Behar, J. Phys. Chem., 76 1815(1972).

(e) D. Zehavi, J. Rabani, J. Phys. Chem., 76 312(1972).

212. S. Arai, A. Kira, M. Imamura, J. Phys. Chem., 74 2102(1970).

213. H. C. Sutton, G. E. Adams, J. W. Boag, B. D. Michael, In "Pulse Radiolysis", Ed. M. Ebert et al., Acad. Press, 1965, page 61.

214. B. Cereck, Int. J. Radiat. Phys. Chem., 4 25(1972).